

# **DESIGN, DEVELOPMENT AND EVALUATION OF NANOSUSPENSIONS FOR ENHANCEMENT OF ORAL BIOAVAILABILITY OF POORLY SOLUBLE DRUGS**

A Thesis submitted to Gujarat Technological University

for the Award of

**Doctor of Philosophy**

in

**Pharmacy**

By

**Ms. Jalpa Shantilal Paun**

[Enrollment No. 119997290038]

Under supervision of

**Dr. Hemraj M. Tank**



**GUJARAT TECHNOLOGICAL UNIVERSITY  
AHMEDABAD**

**March – 2018**

# **DESIGN, DEVELOPMENT AND EVALUATION OF NANOSUSPENSIONS FOR ENHANCEMENT OF ORAL BIOAVAILABILITY OF POORLY SOLUBLE DRUGS**

A Thesis submitted to Gujarat Technological University

for the Award of

**Doctor of Philosophy**

in

**Pharmacy**

By

**Ms. Jalpa Shantilal Paun**

[Enrollment No. 119997290038]

Under supervision of

**Dr. Hemraj M. Tank**



**GUJARAT TECHNOLOGICAL UNIVERSITY  
AHMEDABAD**

**March – 2018**

**© Jalpa Shantilal Paun**

## DECLARATION

I declare the thesis entitled, “**Design, Development and Evaluation of Nanosuspensions for Enhancement of Oral Bioavailability of Poorly Soluble Drugs**” submitted by me for the degree of Doctor of Philosophy is the record of research work carried out by me during the period from **September 2011** to **April 2017** under the supervision of **Dr. Hemraj M. Tank** and this has not formed the basis for the award of any degree, diploma, associateship, fellowship, titles in this or any other University or other institution of higher learning.

I further declare that the material obtained from other sources has been duly acknowledged in the thesis. I shall be solely responsible for any plagiarism or other irregularities if noticed in the thesis.

Signature of the Research Scholar: .....Date: .....

Name of Research Scholar: **Ms. Jalpa Shantilal Paun**

Place: **Ahmedabad**

## CERTIFICATE

I certify that the work incorporated in the thesis, “**Design, Development and Evaluation of Nanosuspensions for Enhancement of Oral Bioavailability of Poorly Soluble Drugs**” submitted by **Kum. Jalpa Shantilal Paun** was carried out by the candidate under my supervision/guidance. To the best of my knowledge: (i) the candidate has not submitted the same research work to any other institution for any Degree/Diploma, Associateship, Fellowship or other similar titles (ii) the thesis submitted is a record of original research work done by the Research Scholar during the period of study under my supervision, and (iii) the thesis represents independent research work on the part of the Research Scholar.

Signature of Supervisor: ..... Date: .....

Name of Supervisor: **Dr. Hemraj M. Tank**

Place: **Ahmedabad**

## Originality Report Certificate

It is certified that Ph.D. Thesis titled, “**Design, Development and Evaluation of Nanosuspensions for Enhancement of Oral Bioavailability of Poorly Soluble Drugs**” by **Ms. Jalpa Shantilal Paun** has been examined by us. We undertake the following:

- a. The thesis has significant new work/knowledge as compared already published or are under consideration to be published elsewhere. No sentence, equation, diagram, table, paragraph or section has been copied verbatim from previous work unless it is placed under quotation marks and duly referenced.
- b. The work presented is original and own work of the author (i.e. there is no plagiarism). No ideas, processes, results or words of others have been presented as Author own work.
- c. There is no fabrication of data or results which have been compiled/ analyzed.
- d. There is no falsification by manipulating research materials, equipment or processes, or changing or omitting data or results such that the research is not accurately represented in the research record.
- e. The thesis has been checked using < **Turnitin** > (copy of originality report attached) and found within limits as per GTU Plagiarism Policy and instructions issued from time to time (i.e. permitted similarity index  $\leq 25\%$ ).

Signature of the Research Scholar: ..... Date: .....

Name of Research Scholar: **Ms. Jalpa Shantilal Paun**

Place: **Ahmedabad**

Signature of Supervisor: ..... Date: .....

Name of Supervisor: **Dr. H.M. Tank**

Place: **Ahmedabad**

# REPORT OF SIMILARITY DOWNLOADED FROM "TURNITIN" DATABASE

DESIGN, DEVELOPMENT AND EVALUATION OF  
NANOSUSPENSIONS FOR ENHANCEMENT OF ORAL  
BIOAVAILABILITY OF POORLY SOLUBLE DRUGS

## ORIGINALITY REPORT

<b>%21</b> SIMILARITY INDEX	<b>%20</b> INTERNET SOURCES	<b>%12</b> PUBLICATIONS	<b>%7</b> STUDENT PAPERS
--------------------------------	--------------------------------	----------------------------	-----------------------------

## PRIMARY SOURCES

<b>1</b>	<b>banglajol.info</b> Internet Source	<b>%3</b>
<b>2</b>	<b>etheses.saurashtrauniversity.edu</b> Internet Source	<b>%3</b>
<b>3</b>	<b>gnu.inflibnet.ac.in</b> Internet Source	<b>%2</b>
<b>4</b>	<b>Submitted to Jawaharlal Nehru Technological University</b> Student Paper	<b>%2</b>
<b>5</b>	<b>www.science.gov</b> Internet Source	<b>%1</b>
<b>6</b>	<b>Thakkar, Hetal Paresh. "Development and characterization of nanosuspensions of olmesartan medoxomil for bioavailability enhancement", Journal of Pharmacy &amp; Bioallied Sciences/09764879, 20110701</b> Publication	<b>%1</b>

[Ms. Jalpa S. Paun]

[Dr. H.M. Tank]

<b>7</b>	<b>Submitted to Cranfield University</b> Student Paper	% <b>1</b>
<b>8</b>	<b>jpbscience.com</b> Internet Source	% <b>1</b>
<b>9</b>	<b>Miao, Yanfei, Guoguang Chen, Lili Ren, and Pingkai Ouyang. "Preparation and evaluation of ziprasidone-phospholipid complex from sustained-release pellet formulation with enhanced bioavailability and no food effect", Journal of Pharmacy and Pharmacology, 2016.</b> Publication	% <b>1</b>
<b>10</b>	<b>www.jpsr.pharmainfo.in</b> Internet Source	% <b>1</b>
<b>11</b>	<b>Submitted to Pacific University</b> Student Paper	% <b>1</b>
<b>12</b>	<b>www.iajpr.com</b> Internet Source	% <b>1</b>
<b>13</b>	<b>www.bioline.org.br</b> Internet Source	% <b>1</b>
<b>14</b>	<b>ijpsr.com</b> Internet Source	% <b>1</b>
<b>15</b>	<b>hypertension-highbloodpressure.com</b> Internet Source	% <b>1</b>
<b>16</b>	<b>www.gmpua.com</b> Internet Source	% <b>1</b>

[Ms. Jalpa S. Paun]

[Dr. H.M. Tank]



<b>17</b>	<a href="http://www.scribd.com">www.scribd.com</a> Internet Source	% 1
<b>18</b>	<a href="http://www.eurekaselect.com">www.eurekaselect.com</a> Internet Source	% 1
<b>19</b>	<a href="http://www.omicsonline.org">www.omicsonline.org</a> Internet Source	% 1

EXCLUDE QUOTES ON  
EXCLUDE BIBLIOGRAPHY ON

EXCLUDE MATCHES < 1%

**[Ms. Jalpa S. Paun]**

**[Dr. H. M. Tank]**

## **Ph.D. Thesis Non-Exclusive License to GUJARAT TECHNOLOGICAL UNIVERSITY**

In consideration of being a Ph.D. Research Scholar at GTU and in the interests of the facilitation of research at GTU and elsewhere, I, **Ms. Jalpa Shantilal Paun** having **Enrollment No. 119997290038** hereby grant a non-exclusive, royalty-free and perpetual license to GTU on the following terms:

- a) GTU is permitted to archive, reproduce and distribute my thesis, in whole or in part, and/or my abstract, in whole or in part (referred to collectively as the “Work”) anywhere in the world, for non-commercial purposes, in all forms of media;
- b) GTU is permitted to authorize, sub-lease, sub-contract or procure any of the acts mentioned in paragraph (a);
- c) GTU is authorized to submit the Work at any National / International Library, under the authority of their “Thesis Non-Exclusive License”;
- d) The Universal Copyright Notice (©) shall appear on all copies made under the authority of this license;
- e) I undertake to submit my thesis, through my University, to any Library and Archives. Any abstract submitted with the thesis will be considered to form part of the thesis.
- f) I represent that my thesis is my original work, does not infringe any rights of others, including privacy rights, and that I have the right to make the grant conferred by this non-exclusive license.

- g) If third party copyrighted material was included in my thesis for which, under the terms of the Copyright Act, written permission from the copyright owners is required, I have obtained such permission from the copyright owners to do the acts mentioned in paragraph (a) above for the full term of copyright protection.
- h) I retain copyright ownership and moral rights in my thesis and may deal with the copyright in my thesis, in any way consistent with rights granted by me to my University in this non-exclusive license.
- i) I further promise to inform any person to whom I may hereafter assign or license my copyright in my thesis of the rights granted by me to my University in this non-exclusive license.
- j) I am aware of and agree to accept the conditions and regulations of Ph.D. including all policy matters related to authorship and plagiarism.

Signature of the Research Scholar: \_\_\_\_\_

Name of Research Scholar: **Ms. Jalpa Shantilal Paun**

Date: \_\_\_\_\_

Place: **Ahmedabad**

Signature of Supervisor: \_\_\_\_\_

Name of Supervisor: **Dr. H.M. Tank**

Date: \_\_\_\_\_

Place: **Ahmedabad**

Seal:

## Thesis Approval Form

The viva-voice of the PhD Thesis submitted by **Kum. Jalpa Shantilal Paun** (Enrollment No. 119997290038) entitled, “**Design, Development and Evaluation of Nanosuspensions for Enhancement of Oral Bioavailability of Poorly Soluble Drugs**” was conducted on ..... (day and date) at Gujarat Technological University.

**(Please tick any one of the following options)**

- The performance of the candidate was satisfactory. We recommend that he/she be awarded the Ph.D. degree.
- Any further modifications in research work recommended by the panel after 3 months from the date of first viva-voice upon request of the Supervisor or request of Independent Research Scholar after which viva-voice can be re-conducted by the same panel again.

- The performance of the candidate was unsatisfactory. We recommend that he/she should not be awarded the Ph.D. degree.

-----  
Name and Signature of Supervisor with Seal

-----  
1) (External Examiner 1) Name and Signature

-----  
2) (External Examiner 2) Name and Signature

-----  
3) (External Examiner 3) Name and Signature

# **DESIGN, DEVELOPMENT AND EVALUATION OF NANOSUSPENSIONS FOR ENHANCEMENT OF ORAL BIOAVAILABILITY OF POORLY SOLUBLE DRUGS**

Submitted by

**Ms. Jalpa Shantilal Paun**

[Enrollment No. 119997290038]

Under supervision of

**Dr. Hemraj M. Tank**

## **ABSTRACT**

A drug which belongs to BCS class-II has poor oral bioavailability due to its limited aqueous solubility. Antihypertensive agents (candesartan cilexetil and telmisartan), as well as atypical antipsychotic agent (ziprasidone hydrochloride monohydrate) which belongs to BCS class-II and has poor water solubility, dissolution, and poor bioavailability, were selected as drug candidates for the research work. In this study, an attempt was made to develop stable nanosuspensions to enhance oral bioavailability of selected drugs. Analytical methods were developed for selected drugs for the estimation of the drug in formulations and plasma too. Gratis samples of selected drugs and stabilizers were received and subjected to identification and compatibility study by FTIR and DSC. Based on solubility from different solvents and their combinations, methanol was identified as solvent and water as an antisolvent. Nanosuspensions were prepared using a precipitation-ultrasonication method using suitable stabilizers. Developed products were lyophilized using mannitol as a cryo-protectant. Various formulation parameters like amount of drug, amount of stabilizers, the solvent to antisolvent volume ratio as well as process parameters like the effect of stirring speed, sonication time etc. were screened by Plackett-Burman design to identify key factors producing maximum effect on quality of nanosuspension. Maximum impact producing two factors were considered for further study to optimize the formulation by  $3^2$  factorial design. The optimized formulations of selected drugs were

evaluated by various parameters like particle size and size distribution, polydispersity index, zeta potential, solubility and *in-vitro* dissolution study. The residual solvent analysis was done using gas chromatography. Scanning electron microscopy was performed to study the surface topology of selected drugs and optimized formulations. Optimized formulations were subjected to accelerated stability study according to ICH guidelines. A bioavailability study was also carried out to compare optimized nanosuspensions with available marketed preparations. The developed products were stable for six months storage at  $25^{\circ}\text{C} \pm 2^{\circ}\text{C}$  and  $60\% \pm 5\%$  RH condition. The developed products exhibited improved bio-availability as compared to marketed formulations.



**DEDICATED**  
**IN THE LOTUS FEET OF**  
**MAA SARASWATI**

## ***Acknowledgment***

*“Gratitude makes sense of our past, brings peace for today and creates a vision for tomorrow”*

I take this privilege and pleasure to acknowledge the contributions of many individuals who have been inspirational and supportive throughout my work undertaken and endowed me with the most precious knowledge to see success in my endeavor.

At this amenity of successful completion of this research work, I have deeply obliged to **‘MAA SARASWATI’**, for having bestowed on me the ability to discharge my duties thoroughly in her endeavour and with whose showers of blessings, this task was ventured without any hindrances.

I avail this opportunity to express my deepest sense of gratitude with profound respect towards my beloved and revered preceptor and Guide **Dr. H. M. Tank**, Principal, Atmiya Institute of Pharmacy, Rajkot, whose masterly suggestions and ablest guidance at every stage inspired me and gave me considerable impetus not only to accomplish this milestone but in all aspects. His untiring energy propelled the research work to completion. I am thankful to him for being my persistent source of inspiration throughout my career.

I sincerely convey my obligations to both DPC members of my research work, **Dr. R. K. Parikh**, Ex. HOD, Department of Pharmaceutics, L. M. College of Pharmacy, Ahmedabad and **Dr. M. M. Patel**, Principal, Shree Swaminarayan Sanskar Pharmacy College, Zundal, who helped me throughout my research work. Their positive flow of knowledge made the research journey very smooth. With a deep sense of pleasure, I am thankful to them for continuous advice and their precious remarks.



A special mention has to be given to **Dr. J. R. Chavda**, Principal, B. K. Mody Government Pharmacy College, Rajkot for all the facilities provided to carry out the work.

I owe a special thanks to **Dr. M. M. Soniwala**, Associate Professor, Department of Pharmaceutics, B. K. Mody Govt. Pharmacy College, Rajkot for his endless support as well as timely and accurate suggestions. I am also grateful for his motivation, encouragement to carry out the work enthusiastically at college.

I am sincerely thankful to my colleagues **Dr. Sandeep Nathwani, Dr. Suuny Shah, Dr. Ramesh Parmar, Dr. Dipen Bhimani, Dr. Chetan Borkhataria, Mr. Kalpesh Patel, Ms. Neelam Rathod, Dr. Ravi Manek, Dr. Devang Sheth, Dr. Nilesh Patel** and all other faculty members of B. K. Mody Govt. Pharmacy College, Rajkot for sharing their knowledge and advice regarding my research work.

I would like to thank the librarian **Mr. N. P. Joshi** for his co-operation. I would also thank all the lab assistants and nonteaching staff of B. K. Mody Govt. Pharmacy College, Rajkot for extending their assistance.

Also special thanks to my friends Jagruti Vaghela, Arti Bagda, Rachana Rajani, Resa Parmar, Khyati Shah, Daya Chothani, Mayuri Thumar, Urvi Chotaliya and Khyati Parekh for their unique way of friendship and affection. Their everlasting friendship is a boon for my life.

I convey my gratitude to **Dr. Mihir Raval** (HOD) and his team of Department of Pharmaceutical Sciences, Saurashtra University, Rajkot, for their valuable support to carry out my analytical study at their organization.

I extend my thanks to **Mr. Pinakin**, NFDD, Saurashtra University, Rajkot and **Mr. Rohit**, Junagadh Agricultural University, Junagadh for their support in sample analysis of my research work.

I am very much thankful to **Alembic Pharmaceuticals Ltd., Vadodara, Amneal Pharmaceuticals, Ahmedabad** and **Astron Research Centre, Ahmedabad** for providing gift samples for the research work.

I am thankful to **Gujarat Council on Science and Technology (GUJCOST), Department of Science and Technology**, Government of Gujarat for funding the research work under **Minor Research Project—2014-15**.

The belief of my parents, **Mrs. Veenaben S. Paun** and **Mr. Shantilal R. Paun**, in me always inspired and persuaded me in all my endeavours throughout. It is because of their pain taking efforts, I have reached up to this position. I pay due regards to them for their hard work, sacrifice, devotion, and blessings led me on this path. I am very thankful to my little brother **Vrushank** and sister **Charmi** for their support, boundless sacrifice, and love.

I owe my gratitude to all those well-wishers who directly or indirectly or in one or the other way have inspired, encouraged and helped me to pursue the path of success along with my life.

Thanks to one and all....

***Jalpa S. Paun***

## TABLE OF CONTENTS

SR. NO.	TITLE	PAGE. NO.
<b>CHAPTER - 1 – INTRODUCTION</b>		
1.1	Introduction to bioavailability	2
1.2	History of bioavailability	3
1.3	Factors affecting bioavailability	4
1.4	Approaches for improvement of bioavailability	5
1.5	Nanosuspension	6
1.6	Profiles of selected drugs	28
1.7	Profile of excipients	39
1.8	Aim and objectives	43
1.9	References	45
<b>CHAPTER - 2 - REVIEW OF LITERATURE</b>		
2.1	Review of literature on bioavailability enhancement by nanosuspension	56
2.2	Review of literature on the preparation of nanosuspension by precipitation method	62
2.3	Review of literature on bioavailability enhancement of candesartan cilexetil	68
2.4	Review of literature on bioavailability enhancement of telmisartan	70
2.5	Review of literature on bioavailability enhancement of ziprasidone hydrochloride	73
2.6	Review of patents related to selected project work	75
2.7	References	76
<b>CHAPTER - 3 – EXPERIMENTAL</b>		
3.1	List of materials used for the study	83
3.2	List of equipments used for the study	84
3.3	Scanning and calibration curve preparation of selected drugs	84
3.4	Selection of solvent and antisolvent	88
3.5	Preparation of nanosuspension by the antisolvent precipitation-ultrasonication method	88

3.6	Lyophilization of nanosuspension	88
3.7	Selection of stabilizer	89
3.8	Drug-excipient compatibility study	89
3.9	Plackett-Burman design	90
3.10	Optimization of other preliminary parameters	90
3.11	Factorial design for optimization of key parameters	91
3.12	Checkpoint analysis	92
3.13	Evaluation of nanosuspensions	92
3.14	Bioavailability study	96
3.15	References	104
<b>CHAPTER - 4 – RESULT AND DISCUSSION</b>		
<b>4A</b>	<b>Results and discussion of candesartan cilexetil nanosuspension</b>	108
4A.1	Scanning and calibration curve preparation	108
4A.2	Selection of solvent and antisolvent	112
4A.3	Selection of stabilizer	112
4A.4	Drug-excipient compatibility study	114
4A.5	Plackett - Burman design	116
4A.6	Optimization of other preliminary parameters	118
4A.7	3 <sup>2</sup> factorial design	120
4A.8	Statistical analysis	121
4A.9	Contour plots	123
4A.10	Surface plots	124
4A.11	Optimization of candesartan cilexetil nanosuspension by desirability function of Minitab17.0	125
4A.12	Checkpoint cum optimized batch analysis	126
4A.13	Checkpoint batch cum optimized batch validation	126
4A.14	Evaluation of optimized batch of candesartan cilexetil nanosuspension	127
4A.15	Bioavailability Study	131
4A.16	Conclusion	135

<b>4B</b>	<b>Results and discussion of telmisartan nanosuspension</b>	137
4B.1	Scanning and calibration curve preparation	137
4B.2	Selection of solvent and antisolvent	141
4B.3	Selection of stabilizer	141
4B.4	Drug-excipient compatibility study	142
4B.5	Plackett - Burman design	145
4B.6	Optimization of other preliminary parameters	147
4B.7	3 <sup>2</sup> factorial design	149
4B.8	Statistical analysis	150
4B.9	Contour plots	152
4B.10	Surface plots	153
4B.11	Optimization of telmisartan nanosuspension by desirability function of minitab17.0	154
4B.12	Checkpoint cum optimized batch analysis	155
4B.13	Checkpoint batch cum optimized batch validation	155
4B.14	Evaluation of optimized batch of telmisartan nanosuspension	156
4B.15	Bioavailability study	160
4B.16	Conclusion	164
<b>4C</b>	<b>Results and discussion of ziprasidone hydrochloride nanosuspension</b>	165
4C.1	Scanning and calibration curve preparation	165
4C.2	Selection of solvent and antisolvent	169
4C.3	Selection of stabilizer	169
4C.4	Drug-excipient compatibility study	171
4C.5	Plackett - Burman design	173
4C.6	Optimization of other preliminary parameters	176
4C.7	3 <sup>2</sup> factorial design	177
4C.8	Statistical analysis	179
4C.9	Contour plots	182
4C.10	Surface plots	183
4C.11	Optimization of ziprasidone hydrochloride nanosuspension by desirability function of Minitab17.0	184
4C.12	Checkpoint cum optimized batch analysis	185

4C.13	Checkpoint batch cum optimized batch validation	186
4C.14	Evaluation of optimized batch of ziprasidone hydrochloride nanosuspension	186
4C.15	Bioavailability study	190
4C.16	Conclusion	194
4C.17	References	195
<b>CHAPTER – 5 SUMMARY AND CONCLUSION</b>		
	Summary and conclusion	199
	Bibliography	203
<b>APPENDICES</b>		
	Appendix A - IAEC Approval letter	207
	Appendix B - GUJCOST Minor Research Project Sanction Letter	208
	Appendix C - List of Publications	209
	Appendix D - Poster Presentation of Research Work in National Level Seminar	213

## LIST OF ABBREVIATIONS

Abbreviation	Full form
Abs	Absorbance
ANDA	Abbreviated new drug application
ANOVA	Analysis of variance
API	Active pharmaceutical ingredient
AR	Analytical reagent
AUC	Area under curve
BCS	Biopharmaceutical classification system
BP	British Pharmacopoeia
CC	Candesartan cilexetil
CCNS	Candesartan cilexetil nanosuspension
cm <sup>-1</sup>	Centimeter inverse
Conc.	Concentration
CPR	Cumulative percentage release
DF	Degree of freedom
DMF	Dimethylformamide
DSC	Differential scanning calorimetry
Ed.	Edition
EPN	Evaporative precipitation of nanosuspension
Eq.	Equation
FbD	Formulation by design
FDA	Food and drug administration
FDAMA	Food and drug administration modernization act
Fm	Full model
FTIR	Fourier transform infrared spectroscopy
GC-HS	Gas chromatography headspace sampler
GIT	Gastrointestinal tract
gm	Gram
GRAS	Generally regard as safe
HPH	High-pressure homogenization
HPLC	High-performance liquid chromatography
HPMC	Hydroxypropyl methylcellulose
HPMCAS	Hydroxypropyl methylcellulose acetate succinate
HP-β-CD	Hydroxypropyl- β-cyclodextrin

---

h	Hour
ICH	International conference on harmonization
IIG	Inactive ingredient guide
IP	Indian pharmacopoeia
ISTD	Internal standard
IUPAC	International Union of pure and applied chemistry
JP	Japanese pharmacopoeia
LCMS	Liquid chromatography-mass spectroscopy
LD	Laser diffractometry
M	Molarity
MA	Melt agglomeration
MEKC	Micellar electrokinetic chromatography
mg	Milligram
min	Minute
ml	Millilitre
MM	Media Milling
MPS	Mean particle size
MS	Mean square
mV	Millivolt
NaCMC	Sodium carboxymethyl cellulose
NDA	New drug application
NF	National formulary
nm	Nanometre
No.	Number
NS	Nanosuspension
PCA	Precipitation with the compressed antisolvent process
PCS	Photon correlation spectroscopy
PDI	Polydispersity index
PEG	Polyethylene glycol
ppm	Parts per million
PTFE	Polytetrafluoroethylene
PVA	Polyvinyl alcohol
PVP K-30	Polyvinylpyrrolidone K-30
PXRD	Powder x-ray diffraction
R <sup>2</sup>	Regression coefficient
RESS	Rapid expansion of supercritical solution

---



---

RH	Relative humidity
RPM	Rotation per minute
SCF	Supercritical fluid
SD	Solid dispersion
SD	Standard deviation
SDD	Spray-dried dispersion
SDS	Sodium dodecyl sulfate
SE	Solvent evaporation
SEDDS	Self-emulsifying drug delivery system
SEM	Scanning electron microscopy
SGF	Simulated gastric fluid
SNCD	Solid nanocrystalline dispersion
SNEDDS	Self-nano emulsifying drug delivery system
SPIP	<i>in-situ</i> single pass perfusion
SS	Saturation solubility
SS	Sum of square
TGA	Thermal gravimetric analysis
TM	Telmisartan
TMNS	Telmisartan nanosuspension
UK	United Kingdom
USA	United States of America
USP	Unites States Pharmacopoeia
UV	Ultraviolet
ZH	Ziprasidone hydrochloride
ZHNS	Ziprasidone hydrochloride nanosuspension
ZP	Zeta potential

**LIST OF SYMBOLS**

°C	Degree Celsius
%	Percentage
µm	Micrometer
k	1000
kV	Kilovolt
<	Less than
$\lambda_{\max}$	Absorbance maxima
$\Delta G_{\text{tro}}$	Gibbs free energy
$V_d$	Volume of distribution
$C_{\max}$	Maximum plasma concentration
$T_{\max}$	Time required for maximum plasma concentration
$T_{1/2}$	Terminal half-life
$K_E$	Elimination rate constant
$K_a$	Absorption rate constant
mV	Millivolt
% w/v	Percentage weight by volume

## LIST OF TABLES

TABLE NO.	TABLE TITLE	PAGE NO.
1.1	Formulation consideration for nanosuspension	9
1.2	Currently marketed pharmaceutical products based on nanotechnology	28
1.3	Marketed formulations of candesartan cilexetil	32
1.4	Marketed formulations of telmisartan	35
1.5	Marketed formulations of ziprasidone hydrochloride	38
3.1	List of materials used for the study	83
3.2	List of equipments used for the study	84
3.3	Dissolution conditions for nanosuspensions	93
3.4	Dosing details for bioavailability study	97
4.1	Calibration curve data of candesartan cilexetil in methanol	109
4.2	Calibration curve data of candesartan cilexetil in 0.05 M phosphate buffer, pH 6.5 containing 0.7% v/v polysorbate 20	111
4.3	Results of selection of solvents for CCNS	112
4.4	Formulating and processing parameters for selection of stabilizer for CCNS	113
4.5	Results for selection of stabilizer for CCNS	113
4.6	Comparison of characteristic bands between candesartan cilexetil and its physical mixture.	115
4.7	Layout and observed responses of Plackett - Burman design batches for CCNS	117
4.8	Results of optimization of other preliminary parameters for CCNS	119
4.9	Layout and observed responses of 3 <sup>2</sup> factorial design for CCNS	120
4.10	Other evaluation parameters of factorial batches of CCNS	121
4.11	Results of regression analysis of mean particle size for CCNS	121
4.12	Results of regression analysis of saturation solubility for CCNS	122
4.13	ANOVA for a full model for CCNS	122

4.14	Formulation and process parameters for an optimized batch of CCNS	126
4.15	The composition of checkpoint batch cum optimized batch of CCNS	127
4.16	Comparison of calculated data with experimental data of CCNS	127
4.17	Evaluation parameters of an optimized batch of CCNS	129
4.18	Results of accelerated stability study of CCNS	131
4.19	Results of bioavailability study of candesartan cilexetil nanosuspension and marketed formulation	132
4.20	Results of pharmacokinetic parameters of candesartan cilexetil nanosuspension and marketed formulation	133
4.21	Calibration curve data of telmisartan in methanol	138
4.22	Calibration curve data of telmisartan in phosphate buffer, pH 7.5	140
4.23	Results of selection of solvents for TMNS	141
4.24	Formulating and processing parameters for selection of stabilizer for TMNS	141
4.25	Results for selection of stabilizer for TMNS	142
4.26	Comparison of characteristic bands between telmisartan and its physical mixture	144
4.27	Layout and observed responses of Plackett - Burman design batches for TMNS	146
4.28	Results of optimization of other preliminary parameters for TMNS	148
4.29	Layout and observed responses of 3 <sup>2</sup> factorial design for TMNS	149
4.30	Other evaluation parameters of factorial batches of TMNS	150
4.31	Results of regression analysis of mean particle size for TMNS	150
4.32	Results of regression analysis of saturation solubility for TMNS	151
4.33	ANOVA for full model for TMNS	151
4.34	Formulation and process parameters for an optimized batch of TMNS	155
4.35	The composition of checkpoint batch cum optimized batch of TMNS	155
4.36	Comparison of calculated data with experimental data of	155

	TMNS	
4.37	Evaluation parameters of an optimized batch of TMNS	158
4.38	Results of accelerated stability study of TMNS	160
4.39	Results of bioavailability study of telmisartan nanosuspension and marketed formulation	160
4.40	Results of pharmacokinetic parameters of telmisartan nanosuspension and marketed formulation	162
4.41	Calibration curve data of ziprasidone hydrochloride in methanol	166
4.42	Calibration curve data of ziprasidone hydrochloride in 0.05M sodium phosphate buffer, pH 7.5	168
4.43	Results of selection of solvents for ZHNS	169
4.44	Formulating and processing parameters for selection of stabilizer for ZHNS	170
4.45	Results for selection of stabilizer for ZHNS	170
4.46	Comparison of characteristic bands between ziprasidone hydrochloride and its physical mixture	172
4.47	Layout and observed responses of Plackett - Burman design batches for ZHNS	174
4.48	Results of optimization of other preliminary parameters for ZHNS	177
4.49	Layout and observed responses of 3 <sup>2</sup> factorial design for ZHNS	178
4.50	Other evaluation parameters of factorial batches of ZHNS	178
4.51	Results of regression analysis of mean particle size for ZHNS	179
4.52	Results of regression analysis of saturation solubility for ZHNS	179
4.53	Results of regression analysis of CPR at 15 min for ZHNS	180
4.54	ANOVA for a full model for ZHNS	181
4.55	Formulation and process parameters for an optimized batch of ZHNS	185
4.56	The composition of checkpoint batch cum optimized batch of ZHNS	186
4.57	Comparison of calculated data with experimental data of ZHNS	186
4.58	Evaluation parameters of an optimized batch of ZHNS	188

4.59	Results of accelerated stability study of ZHNS	190
4.60	Results of bioavailability study of ziprasidone hydrochloride nanosuspension and marketed formulation	191
4.61	Results of pharmacokinetic parameters of ziprasidone hydrochloride nanosuspension and marketed formulation	192

## LIST OF FIGURES

FIGURE NO.	FIGURE TITLE	PAGE NO.
1.1	Approaches for improvement of bioavailability	6
1.2	Chemical structure candesartan cilexetil	29
1.3	Chemical structure telmisartan	32
1.4	Chemical structure of ziprasidone hydrochloride	35
1.5	Structural formula of polyvinyl alcohol	39
1.6	Structural formula of PVP K-30	40
1.7	Structural formula of sodium lauryl sulfate	41
1.8	Structural formula of poloxamer	42
4.1	Scanning of candesartan cilexetil in methanol	109
4.2	Calibration curve of candesartan cilexetil in methanol	110
4.3	Scanning of candesartan cilexetil in 0.05 M phosphate buffer, pH 6.5 containing 0.7% v/v polysorbate 20	110
4.4	Calibration curve of candesartan cilexetil in 0.05 M phosphate buffer, pH 6.5 containing 0.7% v/v polysorbate 20	111
4.5	FT-IR spectra of [A] Candesartan cilexetil, [B] PVP K-30 and [C] Physical mixture of candesartan cilexetil and PVP K-30	114
4.6	DSC thermograms of [A] Candesartan cilexetil [B] PVP K-30 [C] Physical mixture of candesartan cilexetil and PVP K-30 [D] Lyophilized nanosuspension of candesartan cilexetil	116
4.7	Pareto chart of the effect of independent variables on saturation solubility of CCNS	118
4.8	Pareto chart of the effect of independent variables on the mean particle size of CCNS	118
4.9	Contour plot of CCNS for effect on [A] Mean particle size and [B] Saturation solubility	124
4.10	Response surface plot of CCNS for effect on [A] Mean particle size and [B] Saturation solubility	125
4.11	Optimized plot of factorial design form Minitab 17 for CCNS	126
4.12	Particle size graph for CCNS	128
4.13	Comparison of <i>in-vitro</i> dissolution of candesartan cilexetil nanosuspension with marketed formulation	129
4.14	Scanning electron microscopy of [A] Candesartan cilexetil	130

	[B] CCNS	
4.15	Gas chromatograph of methanol in lyophilized candesartan cilexetil nanosuspension	131
4.16	Plasma concentration vs. time profile of candesartan cilexetil nanosuspension and marketed formulation	133
4.17	Scanning of telmisartan in methanol	137
4.18	Calibration curve of telmisartan in methanol	138
4.19	Scanning of telmisartan in phosphate buffer, pH 7.5	139
4.20	Calibration curve of telmisartan in phosphate buffer, pH 7.5	140
4.21	FT-IR spectra of [A] Telmisartan, [B] Poloxamer 407 and [C] Physical mixture of telmisartan and poloxamer 407	143
4.22	DSC thermograms of [A] Telmisartan [B] Poloxamer 407 [C] Physical mixture of telmisartan and poloxamer 407 [D] Lyophilized nanosuspension of telmisartan	145
4.23	Pareto chart of the effect of independent variables on saturation solubility of TMNS	147
4.24	Pareto chart of the effect of independent variables on the mean particle size of TMNS	147
4.25	Contour plot of TMNS for effect on [A] Mean particle size and [B] Saturation solubility	153
4.26	Response surface plot of TMNS for effect on [A] Mean particle size and [B] Saturation solubility	154
4.27	Optimized plot of factorial design form Minitab 17 for TMNS	154
4.28	Particle size graph for TMNS	156
4.29	Comparison of <i>in-vitro</i> dissolution of telmisartan nanosuspension with marketed formulation	157
4.30	Scanning electron microscopy of [A] Telmisartan [B] TMNS	158
4.31	Gas chromatograph of methanol in lyophilized telmisartan nanosuspension	159
4.32	Plasma concentration vs. time profile of telmisartan nanosuspension and marketed formulation	161
4.33	Scanning of ziprasidone hydrochloride in methanol	165
4.34	Calibration curve of ziprasidone hydrochloride in methanol	166
4.35	Scanning of ziprasidone hydrochloride in 0.05 M sodium phosphate buffer, pH 7.5 containing 2% SDS	167
4.36	Calibration curve of ziprasidone hydrochloride in 0.05M sodium phosphate buffer, pH 7.5 containing 2% SDS	168



4.37	FT-IR spectra of [A] Ziprasidone hydrochloride, [B] Poloxamer 407 and [C] Physical mixture of ziprasidone hydrochloride and poloxamer 407	171
4.38	DSC thermograms of [A] Ziprasidone hydrochloride [B] Poloxamer 407 [C] Physical mixture of ziprasidone hydrochloride and poloxamer 407 [D] Lyophilized nanosuspension of ziprasidone hydrochloride	173
4.39	Pareto chart of the effect of independent variables on saturation solubility of ZHNS	175
4.40	Pareto chart of the effect of independent variables on the mean particle size of ZHNS	175
4.41	Contour plot of ZHNS for effect on [A] Mean particle size, [B] Saturation solubility and [C] CPR at 15 mins	183
4.42	Response surface plot of ZHNS for effect on [A] Mean particle size, [B] Saturation solubility and [C] CPR at 15 mins.	184
4.43	The optimized plot of factorial design form Minitab 17 for ZHNS	185
4.44	Particle size graph for ZHNS	187
4.45	Comparison of <i>in-vitro</i> dissolution of ziprasidone hydrochloride nanosuspension with marketed formulation	188
4.46	Scanning electron microscopy of [A] Ziprasidone hydrochloride and [B] ZHNS	189
4.47	Gas chromatograph of methanol in lyophilized ziprasidone hydrochloride nanosuspension	190
4.48	Serum concentration vs. time profile of ziprasidone hydrochloride nanosuspension and marketed formulation	192

**LIST OF APPENDICES**

Appendix A	IAEC Approval letter
Appendix B	GUJCOST Minor Research Project Sanction Letter
Appendix C	List of Publications
Appendix D	Poster Presentation of Research work in National Level Seminar

# **INTRODUCTION**



# CHAPTER – 1

## Introduction

### 1.1 Introduction to Bioavailability

Bioavailability is defined as the rate and extent to which the active ingredient is absorbed from a drug product and becomes available at the site of action [1]. From a pharmacokinetic perspective, bioavailability data for a given formulation provide an estimate of the relative fraction of the orally administered dose that is absorbed into the systemic circulation when compared to the bioavailability data for a solution, suspension or intravenous dosage form. In addition, bioavailability studies provide other useful pharmacokinetic information related to distribution, elimination, effects of nutrients on the absorption of the drug, dose proportionality, and linearity in the pharmacokinetics of the active and inactive moieties.

Bioavailability data can also provide information indirectly about the properties of a drug substance before entry into the systemic circulation, such as permeability and the influence of pre-systemic enzymes and/or transporters. Bioavailability of a drug is largely determined by the properties of the dosage form, rather than by the drug's physicochemical properties, which determines absorption potential. Differences in bioavailability among formulations of a given drug can have clinical significance; thus, knowing whether drug formulations are equivalent is essential.

Poorly water-soluble drugs are increasingly becoming a problem in terms of obtaining satisfactory dissolution within the gastrointestinal tract that is necessary for good oral bioavailability. It is not only existing drugs that cause problems but it is the challenge to

ensure that new drugs are not only active pharmacologically but have enough solubility to ensure fast enough dissolution at the site of administration, often the gastrointestinal tract [2].

## **1.2 History of bioavailability[3]**

The study of absorption of an exogenously administered compound (sodium iodide) can be traced back to 1912. The concept of bioavailability, however, was not introduced until 1945. Oser et al. studied the relative absorption of vitamins from pharmaceutical products and referred to such relative absorption as physiological bioavailability. In recent years, generic drug products, which are those manufactured by generic drug companies or the innovator companies themselves, have become very popular. Bioavailability/bioequivalence studies are of particular interest to the innovator and the generic drug companies in the following ways.

First, for the approval of a generic drug product, the FDA usually does not require a regular new drug application (NDA) submission, which demonstrates the efficacy, safety and benefit-risk of the drug product, if the generic drug companies can provide the evidence of bioequivalence between the generic drug products and the innovator drug product through bioavailability and bioequivalence studies in a so-called abbreviated new drug application (ANDA).

Second, when a new formulation of a drug product is developed, the FDA requires that a bioavailability study is conducted to assess its bioequivalence to the standard (or reference) marketed formulation of the drug product. Thus, bioavailability studies are important because an NDA submission includes the results from phases 1-3 clinical trials, which are very time to consume and costly to obtain. Finally, under the Food and Drug Administration Modernization Act (FDAMA) passed by the U.S. Congress in 1997, after the approval, depending on the magnitudes of changes in components and composition or method of manufacture, the FDA may require the evidence of bioequivalence between the pre- and post-change products under NDA or post-change generic product with the reference list product under ANDA.

The concept of bioavailability and bioequivalence became a public issue in the late 1960s because of the concern that a generic drug product might not be as bioavailable as that manufactured by the innovator. These concerns arose from clinical observations in humans

together with the ability to quantify minute quantities of the drug in biological fluids. This initiated not only a period of four decades of extremely active scientific research and development in bioavailability and bioequivalence but also started the process and formulation of the current regulatory requirements for approval of generic drug products. Spanning from the early 1970s to date, the research and development of bioavailability and bioequivalence can be roughly divided into four phases.

- The first phase is from the early 1970s to 1984 when the U.S. Congress passed the Drug Price Competition and Patent Term Restoration Act that authorized to approve generic drug products through bioavailability and bioequivalence studies.
- The second phase begins from 1984 to 1992 after the issue of the U.S. FDA guidance entitled Statistical Procedures for Bioequivalence Studies Using a Standard Two-Treatment Crossover Design in 1992, which provides the sponsors a guidance as to how the data should be analyzed and presented in an ANDA submission for bioequivalence review.
- The concept of population and individual bioequivalence for addressing drug interchangeability in terms of drug prescribability and drug switchability and their corresponding statistical methods has been discussed in the third phase since 1992.
- The fourth phase starts at the dawn of the twenty-first century when based on the fruit of research conducted in the last 30 years of the twentieth century, the FDA issued and implemented the new guidance on general considerations and statistical approaches to bioavailability and bioequivalence studies.

### **1.3 Factors affecting bioavailability**

Low bioavailability is most common with oral dosage forms of poorly water-soluble, slowly absorbed drugs. Solid drugs need to dissolve before they are exposed to be absorbed. If the drug does not dissolve readily or cannot penetrate the epithelial membrane (e.g. if it is highly ionized and polar), time at the absorption site may be insufficient. In such cases, bioavailability tends to be highly variable as well as low [4]. Age, sex, physical activity, genetic phenotype, stress, disorders (e.g. achlorhydria, malabsorption syndromes), or previous GI surgery (e.g. bariatric surgery) can also affect drug bioavailability.

#### 1.4 Approaches for improvement of bioavailability

Improvement of bioavailability of poorly water-soluble drug remains one of the most challenging aspects of drug development. By many estimates up to 40% of new chemical entities discovered by the pharmaceutical industry today are poorly water compounds [5].

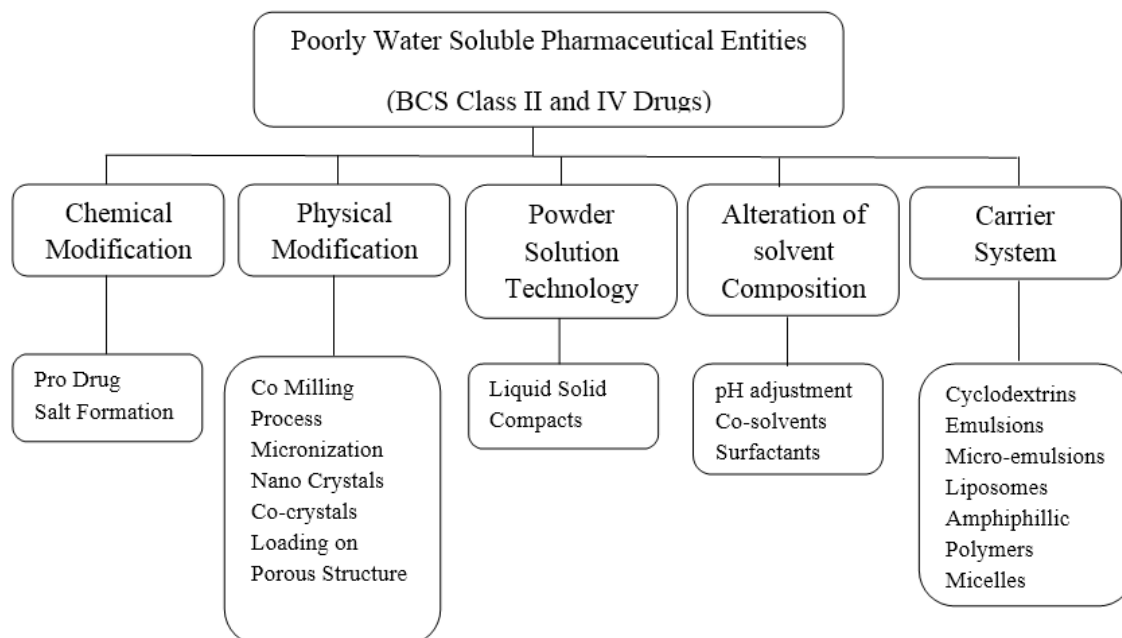
Together with the permeability, the solubility behavior of a drug is a key determinant of its bioavailability. There have always been certain drugs for which solubility has presented a challenge to the development of a suitable formulation for oral administration. Examples are griseofulvin, digoxin, phenytoin, sulphathiazole etc. With the recent arrival of high throughput screening of potential therapeutic agents, the number of poorly soluble drug candidates has risen sharply and the formulation of poorly soluble compounds for delivery now presents one of the most frequent and greatest challenges to formulation scientists in the pharmaceutical industry.

Consideration of the modified Noyes-Whitney equation provides some hints as to how the dissolution rate of even very poorly soluble compounds might be improved to minimize the limitations on oral availability [6]. The main possibilities for improving dissolution according to this analysis are:

- To increase the surface area available for dissolution by decreasing the particle size of the solid compound,
- By optimizing the wetting characteristics of the compound surface,
- To decrease the diffusion layer thickness,
- To ensure sink conditions for dissolution and,
- To improve the apparent solubility of the drug under physiologically relevant conditions. [7]

A fundamental step in the solubilization of drug compound is the selection of an appropriate salt form, or for liquid drugs, adjustment of pH of the solution. Traditional approaches to drug solubilization include either chemical or mechanical modification of the drug molecule, or physically altering the macromolecular characteristics of aggregated drug particles.

Improvement of bioavailability can be obtained by following measures:



**FIGURE 1.1: Approaches for improvement of bioavailability [8]**

### 1.5 Nanosuspension

Nevertheless, pharmacokinetic studies of BCS class – II drugs showed that they have a low oral bioavailability, which may be due to the poor water solubility of the drug. There are many classical pharmaceutical ways to improve drug dissolution rates such as dissolution in aqueous mixtures with an organic solvent [9], the formation of  $\beta$ -cyclodextrin complexes [10], solid dispersions [11] and drug salt form [12].

During last 20 years a new technology, reducing drug particle size, has been developed to increase drug dissolution rate. According to Noyes–Whitney equation, drugs with smaller particle size have enlarged surface areas which lead to increase dissolution velocity. Higher the dissolution rate together with the resulting higher concentration gradient between the gastrointestinal lumen and systemic circulation could further increase oral bioavailability of drugs [13]. Nanosuspension is a submicron colloidal dispersion of drug particles which are stabilized by surfactants. A pharmaceutical nanosuspension is defined as very finely dispersed solid drug particles in an aqueous vehicle for oral, topical, parenteral or pulmonary administration. The particle size distribution of the solid particles in nanosuspensions is usually less than one micron with an average particle size ranging between 200 and 600 nm [14]. In nanosuspension technology, the drug is maintained in the required crystalline state with reduced particle size, leading to an increased dissolution rate



and therefore improved bioavailability. An increase in the dissolution rate of micronized particles (particle size  $< 10 \mu\text{m}$ ) is related to an increase in the surface area and consequently the dissolution velocity. Nanosized particles can increase solution velocity and saturation solubility because of the vapor pressure effect. In addition; the diffusional distance on the surface of drug nanoparticles is decreased, thus leading to an increased concentration gradient. Increase in surface area, as well as concentration gradient, leading to a much more pronounced increase in the dissolution velocity as compared to a micronized product. Another possible explanation for the increased saturation solubility is the creation of high energy surfaces when disrupting the more or less ideal drug microcrystals to nanoparticles. Dissolution experiments can be performed to quantify the increase in the saturation solubility of a drug when formulated into a nanosuspension [15].

The stability of the particles obtained in the nanosuspension is attributed to their uniform particle size which is created by various manufacturing processes. The absence of particles with large differences in their size in nanosuspensions prevents the existence of different saturation solubilities and concentration gradients; consequently preventing the Oswald ripening effect. Ostwald ripening is responsible for crystal growth and subsequently formation of micro-particles. It is caused by a difference in dissolution pressure/saturation solubility between small and large particles. Molecules diffuse from the higher concentration area around small particles which have higher saturation solubility to an area around larger particles possessing a lower drug concentration. This leads to the formation of a supersaturated solution around the large particles and consequently to drug crystallization and growth of the large particles.

### **1.5.1 Advantages of nanosuspensions**

The major advantages of nanosuspension technology are: [16]

- Provides ease of manufacture and scale-up for large-scale production,
- Long-term physical stability due to the presence of stabilizers,
- Oral administration of nanosuspensions provide rapid onset, reduced fed/fasted ratio and improved bioavailability,
- Rapid dissolution and tissue targeting can be achieved by IV route of administration,
- Reduction in tissue irritation in case of subcutaneous/intramuscular administration,

- Higher bioavailability in case of ocular administration and inhalation delivery,
- Drugs with high log P value can be formulated as nanosuspensions to increase the bioavailability of such drugs,
- Improvement in biological performance due to high dissolution rate and saturation solubility of the drug,
- Nanosuspensions can be incorporated in tablets, pellets, hydrogels, and suppositories are suitable for various routes of administration,
- The flexibility offered in the modification of surface properties and particle size, and ease of postproduction processing of nanosuspensions enables them to be incorporated in various dosage forms for various routes of administration, thus proving their versatility.

### **1.5.2 Interesting special features of nanosuspensions [17]**

- Increase in saturation solubility and consequently an increase in the dissolution rate of the drug.
- Increase in adhesive nature, thus resulting in enhanced bioavailability.
- Increasing the amorphous fraction in the particles, leading to a potential change in the crystalline structure and higher solubility.
- The absence of Ostwald ripening, producing physical long-term stability as an aqueous suspension.
- The possibility of surface-modification of nanosuspensions for site-specific delivery.

### **1.5.3 Criteria for selection of a drug for nanosuspensions**

Nanosuspension can be prepared for the API that is having either of the following characteristics: [18]

- Water-insoluble but which are soluble in oil (high log P) **OR** API are insoluble in both water and oils
- Drugs with a reduced tendency of the crystal to dissolve, regardless of the solvent
- API with a very large dose

### 1.5.4 Formulation of nanosuspension [19]

**TABLE 1.1: Formulation consideration for nanosuspension**

Excipients	Function	Examples
Stabilizers	Wet the drug particles thoroughly, prevent Ostwald's ripening and agglomeration of nanosuspensions, providing a steric or ionic barrier	Soya Lecithins, Poloxamers 188/407, Polysorbate 80, HPMC E-15/E-50, PVP K-25/K-30
Co-surfactants	Influence phase behavior when microemulsions are used to formulate nanosuspensions	Bile salts, Dipotassium Glycyrrhizinate, Transcutol, Ethanol, Isopropanol
Organic solvent	Pharmaceutically acceptable less hazardous solvent for preparation of formulation.	Methanol, Ethanol, Chloroform, Isopropanol, Ethyl acetate, Ethyl formate, Butyl lactate, Triacetin, Propylene carbonate, Benzyl alcohol.
Other additives	According to the requirement of the route of administration or the properties of the drug moiety	Buffers, Salts, Polyols, Osmogens, Cryoprotectant etc.

### 1.5.5 Methods of preparation for nanosuspensions

#### (A) Milling techniques (Nanocrystals or Nanosystems)

##### i) Media milling:

Media milling is a technique used to prepare nanosuspensions [13,14][19,20]. Nanocrystal is a patent protected technology in which, the drug nanoparticles are obtained by subjecting the drug to media milling. High energy and shear forces generated as a result of impaction of the milling media with the drug provide the necessary energy input to disintegrate the micro-particulate drug into nanosized particles. In the media milling process, the milling chamber is charged with the milling media, water or a suitable buffer, drug and stabilizer. Then the milling media or pearls are rotated at a very high shear rate. The major concern with this method is the residues of milling media remaining in the finished product could be problematic for administration [19].

Nanosuspensions are produced by using high-shear media mills or pearl mills. The mill consists of a milling chamber, milling shaft, and a recirculation chamber. An aqueous suspension of the drug is then fed into the mill containing small grinding balls/pearls. As

these balls rotate at a very high shear rate under controlled temperature, they fly through the grinding jar interior and impact against the sample on the opposite grinding jar wall. The combined forces of friction and impact produce a high degree of particle size reduction. The milling media or balls are made of a ceramic-sintered aluminum oxide or zirconium oxide or highly cross-linked polystyrene resin with high abrasion resistance. Planetary ball mill is one example of the equipment that can be used to achieve a grind size below 0.1  $\mu\text{m}$ .

**ii) Dry co-grinding:**

Nanosuspensions prepared by high-pressure homogenization and media milling using pearl-ball mill are wet-grinding processes. Recently, nanosuspensions can be obtained by dry milling techniques. Successful work in preparing stable nanosuspensions using dry-grinding of poorly soluble drugs with soluble polymers and copolymers after dispersing in a liquid media has been reported [21–23].

The colloidal particles formation of many poorly water-soluble drugs; griseofulvin, glibenclamide, and nifedipine were obtained by grinding with polyvinylpyrrolidone (PVP) and sodium dodecyl sulfate (SDS). Many soluble polymers and copolymers such as PVP, polyethylene glycol (PEG), hydroxypropyl methylcellulose (HPMC) and cyclodextrin derivatives have been used [24–26]. Physicochemical properties and dissolution of poorly water-soluble drugs were improved by co-grinding because of an improvement in the surface polarity and transformation from a crystalline to an amorphous drug [27,28]. Dry co-grinding can be carried out easily and economically and can be conducted without organic solvents. The co-grinding technique can reduce particles to the submicron level and a stable amorphous solid can be obtained.

**Advantages**

- Media milling is applicable to the drugs that are poorly soluble in both aqueous and organic media.
- Very dilute as well as highly concentrated nanosuspensions can be prepared by handling 1 mg/ml to 400 mg/ml drug quantity.
- Nanosize distribution of final nanosized products.

**Disadvantages**

- Nanosuspensions contaminated with materials eroded from balls may be problematic when it is used for long therapy. (Wet milling technique)
- The media milling technique is time-consuming.
- Some fractions of particles are in the micrometer range.
- Scale up is not easy due to mill size and weight.

**(B) High-Pressure Homogenization****i) Homogenization in Aqueous media (Dissocubes)**

Homogenization involves the forcing of the suspension under pressure through a valve having a narrow aperture. Dissocube technology was developed by Muller et al. in which, the suspension of the drug is made to pass through a small orifice that results in a reduction of the static pressure below the boiling pressure of water, which leads to boiling of water and formation of gas bubbles. When the suspension leaves the gap and normal air pressure is reached again, the bubbles shrink and the surrounding part containing the drug particles rushes to the center and in the process colloids, causing a reduction in the particle size. Most of the cases require multiple passes or cycles through the homogenizer, which depends on the hardness of drug, the desired mean particle size, and the required homogeneity.

Atovaquone nanosuspensions was prepared using Dissocubes technique [29]. To produce a nanosuspension with a higher concentration of solids, it is preferred to start homogenization with very fine drug particles, which can be accomplished by pre-milling.

**ii) Homogenization in Non-Aqueous Media (Nanopure)**

Nanopure is the technology in which suspension is homogenized in water-free media or water mixtures [30]. In the Dissocubes technology, the cavitation is the determining factor of the process. But, in contrast to water, oils and oily fatty acids have very low vapor pressure and a high boiling point. Hence, the drop of static pressure will not be sufficient enough to initiate cavitation. Patents covering disintegration of polymeric material by high-pressure homogenization mention that higher temperatures of about 80°C promoted disintegration, which cannot be used for thermolabile compounds. In nanopure technology, the drug suspensions in the non-aqueous media were homogenized at 0°C or even below

---

the freezing point and hence are called "deep-freeze" homogenization. The results obtained were comparable to Dissocubes and hence can be used effectively for thermolabile substances at milder conditions.

### **Advantages**

- Drugs that are poorly soluble in both aqueous and organic media can be easily formulated into nanosuspensions.
- Ease of scale-up and little batch-to-batch variation [31]
- Narrow size distribution of the nanoparticulate drug present in the final product [32]
- Allows aseptic production of nanosuspensions for parenteral administration.
- Flexibility in handling the drug quantity, ranging from 1 to 400 mg.ml<sup>-1</sup>, thus enabling formulation of very dilute as well as highly concentrated nanosuspensions

### **Disadvantages**

- Prerequisite of micronized drug particles.
- Prerequisite of suspension formation using high-speed mixers before subjecting it to homogenization.

### **(C) Precipitation Method**

Using a precipitation technique, the drug is dissolved in an organic solvent and this solution is mixed with a miscible antisolvent. In water-solvent mixture the solubility is low and the drug precipitates. Mixing processes vary considerably. Precipitation has also been coupled with high shear processing. The nanoedge process (is a registered trademark of Baxter International Inc. and its subsidiaries) relies on the precipitation of friable materials for subsequent fragmentation under conditions of high shear and/or thermal energy [33].

### **Nanoedge**

The basic principles of Nanoedge are the same as that of precipitation and homogenization. A combination of these techniques results in smaller particle size and better stability in a shorter time. The major drawback of the precipitation technique, such as crystal growth and long-term stability, can be resolved using the Nanoedge technology. Rapid addition of a drug solution to an antisolvent leads to sudden super-saturation of the mixed solution and

generation of fine crystalline or amorphous solids. Precipitation of an amorphous material may be favored at high super-saturation when the solubility of the amorphous state is exceeded. The success of drug nanosuspensions prepared by precipitation techniques has been reported [33–36].

In this technique, the precipitated suspension is further homogenized, leading to a reduction in particle size and avoiding crystal growth. Precipitation is performed in water using water-miscible solvents such as methanol, ethanol, and isopropanol. It is desirable to remove those solvents completely, although they can be tolerated to a certain extent in the formulation. For an effective production of nanosuspensions using the Nanoedge technology, an evaporation step can be included to provide a solvent-free modified starting material followed by high-pressure homogenization.

#### **(D) Nanojet Technology**

This technique, called opposite stream or nanojet technology, uses a chamber where a stream of suspension is divided into two or more parts, which collide with each other at high pressure. The high shear force produced during the process results in particle size reduction. Equipment using this principle includes the M110L and M110S micro-fluidizers (Microfluidics).

The major disadvantage of this technique is the high number of passes through the micro-fluidizer and the product obtained contains a relatively larger fraction of micro-particles.

#### **(E) Emulsions as Templates**

Apart from the use of emulsions as a drug delivery vehicle, they can also be used as templates to produce nanosuspensions. The use of emulsions as templates is applicable for those drugs that are soluble in either volatile organic solvent or partially water-miscible solvent. Such solvents can be used as the dispersed phase of the emulsion. There are two ways of fabricating drug nanosuspensions by the emulsification method. In the first method, an organic solvent or mixture of solvents loaded with the drug is dispersed in the aqueous phase containing suitable surfactants to form an emulsion. The organic phase is then evaporated under reduced pressure so that the drug particles precipitate instantaneously to form a nanosuspension stabilized by surfactants. Since one particle is formed in each emulsion droplet, it is possible to control the particle size of the

nanosuspension by controlling the size of the emulsion. Optimizing the surfactant composition increases the intake of the organic phase and ultimately the drug loading in the emulsion. Originally, organic solvents such as methylene chloride and chloroform were used [37].

However, environmental hazards and human safety concerns about residual solvents have limited their use in routine manufacturing processes. Relatively safer solvents such as ethyl acetate and ethyl formate can still be considered for use [38,39].

The emulsion is formed by the conventional method and the drug nanosuspension is obtained by just diluting the emulsion. Dilution of the emulsion with water causes complete diffusion of the internal phase into the external phase, leading to the instantaneous formation of a nanosuspension. The nanosuspension thus formed has to be made free of the internal phase and surfactants by means of di-ultrafiltration in order to make it suitable for administration. However, if all the ingredients that are used for the production of the nanosuspension are present in a concentration acceptable for the desired route of administration, then simple centrifugation or ultracentrifugation is sufficient to separate the nanosuspension.

### **Advantages**

- Use of specialized equipment is not necessary.
- Particle size can easily be controlled by controlling the size of the emulsion droplet.
- Ease of scale-up if the formulation is optimized properly.

### **Disadvantages**

- Drugs that are poorly soluble in both aqueous and organic media cannot be formulated by this technique.
- Safety concerns because of the use of hazardous solvents in the process.
- Need for di-ultrafiltration for purification of the drug nanosuspension, which may render the process costly.
- The high amount of surfactant/stabilizer is required as compared to the production techniques described earlier.

The production of drug nanosuspensions from emulsion templates has been successfully applied to the poorly water soluble and poorly bioavailable anti-cancer drug mitotane,

---



where a significant improvement in the dissolution rate of the drug (a five-fold increase) as compared to the commercial product was observed [40].

#### **(F) Microemulsions as Templates**

Microemulsions are thermodynamically stable and iso-tropically clear dispersions of two immiscible liquids, such as oil and water, stabilized by an interfacial film of surfactant and co-surfactant [41].

Their advantages, such as high drug solubilization, long shelf life and ease of manufacture, making them an ideal drug delivery vehicle. Recently, the use of microemulsions as templates for the production of solid lipid nanoparticles [42] and polymeric nanoparticles [43] has been described. Taking advantage of the microemulsion structure, one can use microemulsions even for the production of nanosuspensions [44]. The drug can be either loaded in the internal phase or preformed microemulsions can be saturated with the drug by intimate mixing. The suitable dilution of the microemulsion yields the drug nanosuspension by the mechanism described earlier. The influence of the amount and ratio of surfactant to co-surfactant on the uptake of internal phase and on the globule size of the microemulsion should be investigated and optimized in order to achieve the desired drug loading. The nanosuspension thus formed has to be made free of the internal phase and surfactants by means of di-ultrafiltration in order to make it suitable for administration. However, if all the ingredients that are used for the production of the nanosuspension are present in a concentration acceptable for the desired route of administration, then simple centrifugation or ultracentrifugation is sufficient to separate the nanosuspension. The advantages and disadvantages are the same as for emulsion templates. The only added advantage is the need for less energy input for the production of nanosuspensions by virtue of microemulsions.

#### **(G) Supercritical Fluid Method**

Supercritical fluid technology can be used to produce nanoparticles from drug solutions. The various methods attempted are a rapid expansion of supercritical solution process (RESS), supercritical antisolvent process and precipitation with the compressed antisolvent process (PCA). The RESS involves expansion of the drug solution in supercritical fluid through a nozzle, which leads to loss of solvent power of the supercritical fluid resulting in precipitation of the drug as fine particles. In the PCA method, the drug solution is atomized

into a chamber containing compressed CO<sub>2</sub>. As the solvent is removed, the solution gets supersaturated and thus precipitates as fine crystals. The supercritical antisolvent process uses a supercritical fluid in which a drug is poorly soluble and a solvent for the drug that is also miscible with the supercritical fluid. The drug solution is injected into the supercritical fluid and the solvent gets extracted by the supercritical fluid and the drug solution gets supersaturated. The drug is then precipitated as fine crystals. The disadvantages of the above methods are use of hazardous solvents and use of high proportions of surfactants and stabilizers as compared with other techniques, particle nucleation overgrowth due to transient high super-saturation, which may also result in the development of an amorphous form or another undesired polymorph [45].

### **1.5.6 Post-production processing**

Post-production processing of nanosuspensions becomes essential when the drug candidate is highly susceptible to hydrolytic cleavage or chemical degradation. Processing may also be required when the best possible stabilizer is not able to stabilize the nanosuspension for a longer period of time or there are acceptability restrictions with respect to the desired route. Considering these aspects, techniques such as lyophilization or spray drying may be employed to produce a dry powder of nano-sized drug particles. The rational selection has to be made in these unit operations considering the drug properties and economic aspects [19].

### **1.5.7 Characterization of nanosuspension**

#### **(A) Mean particle size and particle size distribution**

The mean particle size and particle size distribution are important characterization parameters as they influence the saturation solubility, dissolution velocity, physical stability as well as biological performance of nanosuspensions. It has been indicated that saturation solubility and dissolution velocity show considerable variation with the changing particle size of the drug [15]. Photon correlation spectroscopy (PCS) can be used for rapid and accurate determination of the mean particle diameter of nanosuspensions. Moreover, PCS can even be used for determining the width of the particle size distribution (polydispersity index, PDI). The PDI is an important parameter that governs the physical stability of nanosuspensions and should be as low as possible for the long-term stability of nanosuspensions. A PDI value of 0.1– 0.25 indicates a fairly narrow size distribution

---

whereas a PDI value greater than 0.5 indicates a very broad distribution. No logarithmic normal distribution can definitely be attributed to such a high PDI value. Although PCS is a versatile technique, because of its low measuring range (3 nm to 3  $\mu\text{m}$ ) it becomes difficult to determine the possibility of contamination of the nanosuspension by microparticulate drugs (having a particle size greater than 3  $\mu\text{m}$ ). Hence, in addition to PCS analysis, laser diffractometry (LD) analysis of nanosuspensions should be carried out in order to detect as well as quantify the drug micro-particles that might have been generated during the production process.

Various methods are available for particle size measurement [46]. Laser diffractometry yields a volume size distribution and can be used to measure particles ranging from 0.05–80  $\mu\text{m}$  and in certain instruments particle sizes up to 2000  $\mu\text{m}$  can be measured. The typical LD characterization includes determination of diameter 50% LD<sub>50</sub> and diameter 99% LD<sub>99</sub> values, which indicate that either 50 or 99% of the particles are below the indicated size. The LD analysis becomes critical for nanosuspensions that are meant for parenteral and pulmonary delivery. Even if the nanosuspension contains a small number of particles greater than 5–6  $\mu\text{m}$ , there could be a possibility of capillary blockade or emboli formation, as the size of the smallest blood capillary is 5–6  $\mu\text{m}$ . It should be noted that the particle size data of a nanosuspension obtained by LD and PCS analysis are not identical as LD data are volume based and the PCS mean diameter is the light intensity weighted size. The PCS mean diameter and the 50 or 99% diameter from the LD analysis are likely to differ, with LD data generally exhibiting higher values. The nanosuspensions can be suitably diluted with deionized water before carrying out PCS or LD analysis.

### **(B) Crystalline state and particle morphology**

The assessment of the crystalline state and particle morphology together helps in understanding the polymorphic or morphological changes that a drug might undergo when subjected to nano-sizing. Additionally, when nanosuspensions are prepared drug particles in an amorphous state are likely to be generated. Hence, it is essential to investigate the extent of amorphous drug nanoparticles generated during the production of nanosuspensions. The changes in the physical state of the drug particles as well as the extent of the amorphous fraction can be determined by X-ray diffraction analysis [31,32] and can be supplemented by differential scanning calorimetry [47]. In order to get an actual idea of particle morphology, scanning electron microscopy is preferred [32].

**(C) Particle charge (zeta potential)**

The particle charge is of importance in the study of the stability of the suspensions. Usually, the zeta potential of more than  $\pm 40\text{mV}$  will be considered to be required for the stabilization of the dispersions. For electrostatically stabilized nanosuspension a minimum zeta potential of  $\pm 30\text{mV}$  is required and in case of combined steric and electrostatic stabilization it should be a minimum of  $\pm 20\text{mV}$  of zeta potential is required. Surface charges can arise from (i) ionization of the particle surface or (ii) adsorption of ions (such as surfactants) onto the surface. Typically, the surface charge is assessed through measurements of the zeta potential. Zeta potential is the potential at the hydrodynamic shear plane and can be determined from the particle mobility under an applied electric field [48]. The mobility will depend on the effective charge on the surface. Zeta potential is also a function of electrolyte concentration.

**(D) Solubility study**

The solubility can also define as the ability of one substance to form a solution with another substance. The substance to be dissolved is called as solute and the dissolving fluid in which the solute dissolve is called as a solvent, which together forms a solution. The main advantage associated with the nanosuspensions is improved saturation solubility. This is studied in different physiological solutions at different pH. Kelvin equation and the Ostwald-Freundlich equations can explain the increase in saturation solubility. Determination of this parameter is used to assess *in vivo* performance of the formulation also [49].

The Kelvin equation (Eq. 1.1) is originally used to describe the vapor pressure over a curved surface of a liquid droplet in gas; it is also applicable to explain the relationship between the dissolution pressure and the curvature of the solid particles in liquid:

$$\ln\left(\frac{Pr}{P\infty}\right) = \frac{2\gamma Mr}{rRT\rho} \quad \text{Eq... (1.1)}$$

Where,  $Pr$  = Dissolution pressure of a particle with the radius  $r$ ,

$P\infty$  = Dissolution pressure of an infinitely large particle,

$\gamma$  = Surface tension,

$R$  = Gas constant,

$T$  = Absolute temperature,

$r$  = Radius of the particle,

$M_r$  = Molecular weight,

$\rho$  = Density of the particle.

According to the Kelvin equation, the dissolution pressure increases with increasing curvature, which means decreasing particle size. The curvature is enormous when the particle size is in the nanometer range; then a large dissolution pressure can be achieved leading to a shift of the equilibrium toward dissolution.

The Ostwald–Freundlich (Eq. 1.2) directly describes the relationship between the saturation solubility of the drug and the particle size:

$$\text{Log} \frac{C_s}{C_\alpha} = \frac{2\sigma V}{2.303RT\rho r} \quad \text{Eq... (1.2)}$$

Where,  $C_s$  = Saturation solubility,

$C_\alpha$  = Solubility of the solid consisting of large particles,

$\sigma$  = Interfacial tension of substance,

$V$  = Molar volume of the particle material,

$R$  = Gas constant,

$T$  = Absolute temperature,

$\rho$  = Density of the solid,

$r$  = Radius.

It is obvious that the saturation solubility ( $C_s$ ) of the drug increases with a decrease of particle size ( $r$ ). However, this effect is pronounced for materials that have a mean particle size of less than 2  $\mu\text{m}$ . [50]

### (E) *In-vitro* drug release study

Drug release rate may be defined as the amount of drug substance that goes in the solution per unit time under standard conditions of liquid/solid interface, temperature and solvent composition. It can be considered as a specific type of certain heterogeneous reaction in which a mass transfer results as a net effect between escape and deposition of solute molecules at a solid surface [51].

As such, drug release from nano-sized dosage forms can be assessed using one of the following three categories, namely, sample and separate (SS), continuous flow (CF), and dialysis membrane (DM) methods. More recently, apparatus that combine the principles of

either the SS and DM or CF and DM have also been reported. A few novel methods that use voltammetry, turbidimetry and so forth are discussed. For each of these methods, a brief description is provided along with adaptations, additional considerations, advantages, and disadvantages.

- **Sample and Separate:** In the SS method, the nanoparticulate dosage form is introduced into the release media that is maintained at a constant temperature, after which drug release is assessed by a sampling of the release media (filtrate or supernatant) or the nanoparticles. From literature, there are several adaptations to the SS method, with differences noted in set-up, container size, mode of agitation, and sampling techniques. Commonly reported set-ups include USP I (basket), USP II (paddle), or vials and generally depend on the volume of release media used in the *in-vitro* release study. For instance, vials were used when the volume of release media was small (1–15 mL) and *in-vitro* release vessels were employed with larger volumes (600–900 mL).
- **Continuous Flow:** In the CF method, drug release from the nanoparticulate dosage form is monitored using the USP IV apparatus (flow-through cell) or a modification thereof. Drug release occurs as a result of buffer or media constantly circulating through a column containing the immobilized dosage form and is monitored by collecting the eluent at periodic intervals.
- **Dialysis Method:** Of all the methods used to assess drug release from nano-sized dosage forms, the dialysis method (DM) is the most versatile and popular. In this method, physical separation of the dosage forms is achieved by usage of a dialysis membrane which allows for ease of sampling at periodic intervals. As with the other methods, several adaptations of the DM have been reported in the literature with key differences in set-up, container size and molecular weight cut-off (MWCO). Of the variety of DM set-ups used, the most commonly cited is the dialysis bag (regular dialysis), other adaptations being the reverse dialysis and side-by-side dialysis set-up.
- **Combination Methods:** A few publications have modified the set-ups used in the SS, CF and DM methods to evaluate drug release from nano-sized dosage forms. In most of these reports, the set-up of the SS method is combined with a dialyzer to allow ease

of sampling. In other publications, the DM and the CF set-up is used to assess *in vitro* release from nanoparticles [52].

#### **(F) Stability of Nanosuspensions**

Stability of the suspensions is dependent on particle size. As the particle size reduces to the nanosize the surface energy of the particles will be increased and they tend to agglomerate. So stabilizers are used which decreases the chances of Ostwald ripening effect and improving the stability of the suspension by providing a steric or ionic barrier. Typical examples of stabilizers used in nanosuspensions are cellulosic, poloxamer, polysorbates, lecithin, polyoleate and povidones etc [53].

#### **(G) Bioavailability study**

Direct and indirect methods are used to assess the drug bioavailability. The design of the bioavailability study depends on the objectives of the study, the ability to analyze the drug (and metabolites) in biological fluids, the pharmacodynamics of the drug substance, and the route of drug administration and the nature of the drug product. Pharmacokinetic or pharmacodynamic parameters, as well as clinical observations and *in-vivo* studies, may be used to determine drug bioavailability from a drug or drug product. The various approaches to bioavailability studies are summarized as follows: [54]

#### **Plasma drug concentration studies**

Measurement of drug concentrations in blood, plasma, or serum after drug administration is the most direct and objective method to determine systemic drug availability. By appropriate blood sampling, an accurate description of the plasma drug concentrations vs. time profile of the therapeutically active drug substance(s) can be obtained using a validated drug assay. In plasma drug concentrations studies, the following three important parameters are measured:

- **Peak plasma concentration ( $C_{max}$ ):** The peak plasma concentration ( $C_{max}$ ) is the maximum plasma drug concentration obtained after oral administration of the drug. The size of the dose administered influences the blood level concentration and  $C_{max}$ . For many drugs, a relationship is found between the pharmacodynamic drug effect and the plasma drug concentration.  $C_{max}$  provides indications that the drug is sufficiently systemically absorbed to provide a therapeutic response. In addition,  $C_{max}$  also provides

warning of possible toxic levels of the drug.  $C_{\max}$  is usually expressed in terms of concentration in relation to a specific volume of blood, serum, or plasma (e.g.  $\mu\text{g/ml}$  or  $\text{ng/ml}$ , etc.). [55]

- **Time of peak plasma concentration ( $T_{\max}$ ):** The time of peak plasma concentration ( $T_{\max}$ ) corresponds to the time required to reach maximum drug concentration after drug administration. This parameter reflects the rate of drug absorption from a formulation. At  $T_{\max}$ , peak drug absorption occurs and the rate of absorption exactly equals the rate of drug elimination. Drug absorption still occurs after  $T_{\max}$  is reached, but at a slower rate. When comparing drug products,  $T_{\max}$  can be used as an approximate indication of the rate of drug absorption. [56]
- **Area under the plasma drug concentration vs. time curve (AUC):** The area under curve (AUC) is the total area under the biological fluid (serum, plasma, blood, etc.) concentration of the drug vs. time curve between time  $T = 0$  and time  $T = t$ , preferably  $T = \infty$ , which is determined by a numerical integration procedure, such as ‘trapezoidal rule’. According to the trapezoidal rule, the area between drug concentration-time curves can be estimated through the assumption that the AUC can be represented as a series of trapezoids. The total AUC would be the sum of the areas of the individual trapezoids.

$$\text{Area of each trapezoid} = 1/2 (C_{n-1} + C_n) (t_n - t_{n-1}) \quad \text{Eq...}(1.3)$$

Where,  $C_n$  is the drug concentration in blood, plasma, or serum at time  $t_n$ . The AUC is dependent on the total quantity of the available drug,  $FD_0$ , divided by the elimination rate constant,  $k$ , and the apparent volume of distribution,  $V_D$ .

$$[\text{AUC}]_0^{\infty} = \int_0^{\infty} C_p dt$$

$$[\text{AUC}]_0^{\infty} = FD_0 / \text{clearance} = FD_0 / kV_D \quad \text{Eq...}(1.4)$$

Where,  $F$  is the fraction of dose absorbed,  $D_0$  is the dose,  $k$  is the elimination rate constant,  $V_D$  is the apparent volume of distribution,  $C_p$  is the plasma concentration and the units for AUC are  $\mu\text{g}\cdot\text{hr/ml}$ . [57]



**Urinary drug excretion method:**

Urinary drug excretion data is an indirect method for estimating bioavailability. The drug must be excreted in significant quantities as unchanged drug in the urine, timely urine samples must be collected, and the total amount of urinary drug excreted must be determined. In urinary drug excretion data, the cumulative amount of drug excreted in the urine ( $D_U^\infty$ ) is measured for further *in-vivo* studies.

**1.5.8 Applications of nanosuspensions in drug delivery****(A) Parenteral administration**

From the formulation perspective, nanosuspensions meet almost all the requirements of an ideal drug delivery system for the parenteral route. Since the drug particles are directly nanosized, it becomes easy to process almost all drugs for parenteral administration. Hence, nanosuspensions enable significant improvement in the parenterally tolerable dose of the drug, leading to a reduction in the cost of the therapy and also improved therapeutic performance. The maximum tolerable dose of paclitaxel nanosuspension was found to be three times higher than the currently marketed Taxol, which uses Cremophore EL and ethanol to solubilize the drug [58].

Nanosuspensions can be administered via different parenteral administration routes ranging from intra-articular via intra-peritoneal to intravenous injection. For administration by the parenteral route, the drug either has to be solubilized or has particle/globule size below 5  $\mu\text{m}$  to avoid capillary blockage. In this regard, liposomes are much more tolerable and versatile in terms of parenteral delivery. However, they often suffer from problems such as physical instability, high manufacturing cost and difficulties in scale-up. Nanosuspensions would be able to solve the problems mentioned above. In addition, nanosuspensions have been found to increase the efficacy of parenterally administered drugs [30].

**(B) Oral administration**

The oral route is the preferred route for drug delivery because of its numerous well-known advantages. The efficacy or performance of the orally administered drug generally depends on its solubility and absorption through the gastrointestinal tract. Hence, a drug candidate that exhibits poor aqueous solubility and/or dissolution rate limited absorption is believed

---

to possess slow and/or highly variable oral bioavailability. Danazol is poorly bioavailable gonadotropin inhibitor, showed a drastic improvement in bioavailability when administered as a nanosuspension as compared to the commercial danazol macrosuspension Danocrine. Danazol nanosuspension led to an absolute bioavailability of 82.3%, whereas the marketed danazol suspension Danocrine was 5.2% bioavailable [13].

Nanosizing of drugs can lead to a dramatic increase in their oral absorption and subsequent bioavailability. Improved bioavailability can be explained by the adhesiveness of drug nanoparticles to the mucosa, the increased saturation solubility leading to an increased concentration gradient between gastrointestinal tract lumen and blood as well as the increased dissolution velocity of the drug. Aqueous nanosuspension can be used directly in a liquid dosage form and a dry dosage form such as a tablet or hard gelatin capsule with pellets. The aqueous nanosuspension can be used directly in the granulation process or as a wetting agent for preparing the extrusion mass pellets. A similar process has been reported for incorporating solid lipid nanoparticles into pellets. Granulates can also be produced by spray drying of nanosuspensions [30].

### **(C) Ophthalmic drug delivery**

Nanosuspensions could prove to be vital for drugs that exhibit poor solubility in lachrymal fluids. Suspensions offer advantages such as prolonged residence time in a cul-de-sac, which is desirable for most ocular diseases for effective treatment and avoidance of high tonicity created by water-soluble drugs. Their actual performance depends on the intrinsic solubility of the drug in lachrymal fluids. Thus the intrinsic dissolution rate of the drug in lachrymal fluids controls its release and ocular bioavailability. However, the intrinsic dissolution rate of the drug will vary because of the constant inflow and outflow of lachrymal fluids. One example of a nanosuspension intended for ophthalmic controlled delivery was developed as a polymeric nanosuspension of Acyclovir [59]. This nanosuspension is successfully prepared using Eudragit RS100 by a quasi-emulsion and solvent diffusion method. Nanosuspensions of glucocorticoid drugs; hydrocortisone, prednisolone, and dexamethasone enhance rate, drug absorption and increase the duration of drug action [60]. To achieve sustained release of the drug for a stipulated time period, nanosuspensions can be incorporated in a suitable hydro-gel base or mucoadhesive base or even in ocular inserts. The bio-erodible, as well as water-soluble/permeable polymers possessing ocular tolerability[61], could be used to sustain the release of the medication.

The polymeric nanosuspension of flurbiprofen has been successfully formulated using acrylate polymers such as Eudragit RS 100 and Eudragit RL 100[62][63][64]. The polymeric nanosuspensions have been characterized for drug loading, particle size, zeta potential, *in-vitro* drug release, ocular tolerability and *in-vivo* biological performance. The designed polymeric nanosuspensions indicated superior *in-vivo* performance over the existing marketed formulations and could sustain drug release for 24 h. The scope of this strategy could be extended by using various polymers with ocular tolerability.

#### **(D) Pulmonary drug delivery**

Nanosuspensions may prove to be an ideal approach for delivering drugs that exhibit poor solubility in pulmonary secretions. Currently, such drugs are delivered as suspension aerosols or as dry powders by means of dry powder inhalers. The drugs used in suspension aerosols and dry powder inhalers are often jet milled and have particle sizes of microns.

Because of the micro-particulate nature and wide particle size distribution of the drug moiety present in suspension aerosols and dry powder inhalers, some disadvantages are encountered: like limited diffusion and dissolution of the drug at the site of action, rapid clearance of the drug from the lungs, less residence time for the drugs, unwanted deposition of the drug particles in pharynx and mouth [65,66].

The ability of nanosuspensions to offer quick onset of action initially and then controlled the release of the active moiety is highly beneficial and is required for most pulmonary diseases. Moreover, as nanosuspensions generally contain a very low fraction of micro-particulate drug, they prevent unwanted deposition of particles in the mouth and pharynx, leading to decreased local and systemic side-effects of the drug. Additionally, because of the nano-particulate nature and uniform size distribution of nanosuspensions, it is very likely that in each aerosol droplet at least one drug nanoparticle is contained, leading to even distribution of the drug in the lungs as compared to the micro-particulate form of the drug. In conventional suspension aerosols, many droplets are drug-free and others are highly loaded with the drug, leading to uneven delivery and distribution of the drug in the lungs. Nanosuspensions could be used in all available types of the nebulizer. However, the extent of influence exerted by the nebulizer type as well as the nebulization process on the particle size of nanosuspensions should be ascertained.

**(E) Bioavailability enhancement**

A drug with poor solubility or permeability in gastrointestinal tract leads to poor oral bioavailability. Nanosuspension resolves the problem of poor bioavailability by solving the problem of poor solubility and poor permeability across the membranes. Dissolution rate was increased in diclofenac when formulated in nanosuspension form from 25% to 50% in SGF and H<sub>2</sub>O while in case of SIF it was increased from 10% to 35% as compared to coarse suspension [67]. Bioavailability of poorly soluble, a COX-2 inhibitor, celecoxib was improved using a nanosuspension formulation. The crystalline nanosized celecoxib alone or in tablet showed a dramatic increase of dissolution rate and extent compared to a micronized tablet. Spironolactone and budesonide are poorly soluble drugs. The higher flux contributes to the higher bioavailability of nanosuspension formulation. The bioavailability of poorly soluble fenofibrate following oral administration was increased compared to the suspensions of micronized fenofibrate [68].

A significant difference ( $p < 0.05$ ) was observed between the fluxes from saturated solution vs. nanosuspension at all concentrations of surfactant. Oral administration of micronized Amphotericin B does not show any significant effect. However, administration in nanosuspension form showed a significant reduction ( $P < 0.5\%$ ) of the liver parasite load by 28.6%, it indicates that the nanosuspension of Amphotericin B has a high systemic effect and superior oral uptake in nanosuspension form [69].

The poor oral bioavailability of the drug may be due to poor solubility, poor permeability or poor stability in the gastrointestinal tract (GIT). Nanosuspensions resolve the problem of poor bioavailability by solving the twin problems of poor solubility and poor permeability across the membrane. Bioavailability of poorly soluble oleanolic acid, a hepatoprotective agent, was improved using a nanosuspension formulation. The therapeutic effect was significantly enhanced, which indicated higher bioavailability. This was due to the faster dissolution (90% in 20 min) of the lyophilized nanosuspension powder when compared with the dissolution from a coarse powder (15% in 20 min) [30].

**(F) Target drug delivery**

Nanosuspensions can also be used for targeted delivery as their surface properties and *in-vivo* behavior can easily be altered by changing either the stabilizer or the milieu. Their versatility, ease of scale-up and commercial product enable the development of

---

commercially viable nanosuspensions for targeted delivery. The engineering of stealth nanosuspensions by using various surface coatings for active or passive targeting of the desired site is the future of targeted drug delivery systems. Targeting of *Cryptosporidium parvum*, the organism responsible for cryptosporidiosis was achieved by using surface modified mucoadhesive nanosuspensions of buparvaquone [70,71].

Similarly, conditions such as pulmonary aspergillosis can easily be targeted by using suitable drug candidates, such as Amphotericin B, in the form of pulmonary nanosuspensions instead of using stealth liposomes [72].

Nanosuspensions can also be used for targeting their surface properties and changing of the stabilizer can easily alter the *in vivo* behavior. The drug will be uptaken by the mononuclear phagocytic system to allow regional-specific delivery. This can be used for targeting anti-mycobacterial, fungal or leishmanial drugs to the macrophages if the infectious pathogen is persisting intra-cellularly [73].

#### **(G) Topical formulations**

Drug nanoparticles can be incorporated into creams and water-free ointments. The nanocrystalline form leads to an increased saturation solubility of the drug in the topical dosage form, thus enhancing the diffusion of the drug into the skin [74–78].

#### **(H) Mucoadhesion of the nanoparticles**

Nanosuspension containing drug nanoparticles orally diffuse into the liquid media and rapidly encounter the mucosal surface. The particles are immobilized at the intestinal surface by an adhesion mechanism referred to as "bioadhesion." From this moment on, the concentrated suspension acts as a reservoir of particles and an adsorption process takes place very rapidly. The direct contact of the particles with the intestinal cells through a bioadhesive phase is the first step before particle absorption [66]. The adhesiveness of the nanosuspensions not only helps to improve bioavailability but also improves targeting of the parasites persisting in the GIT.

### **1.5.9 Marketed formulations based on nanosuspension**

All the products based on nanosuspension have been approved by the FDA from the year 2000 on. A remarkable point is that all commercial products are intended for oral delivery.

---

This is an illustration of the general preference of the oral route since it avoids the pain and discomfort associated with injections and is more attractive from a marketing and patient compliance perspective. Finally, the major advantage of nanocrystals for oral delivery is generally regarded as being on the increased specific surface area of the particles. However, EMEND<sup>®</sup> and Triglide<sup>™</sup> are formulated as nanosuspension to reduce fed/fasted variability [79].

**TABLE 1.2: Currently marketed pharmaceutical products based on nanotechnology[80]**

Product	Drug Compound	Company	Manufacturing Technique	Technology
RAPAMUNE <sup>®</sup>	Sirolimus	Wyeth	MM*	Elan Nanocrystals <sup>®</sup>
EMEND <sup>®</sup>	Aprepitant	Merck	MM*	Elan Nanocrystals <sup>®</sup>
TriCor <sup>®</sup>	Fenofibrate	Abbott	MM*	Elan Nanocrystals <sup>®</sup>
MEGACE <sup>®</sup> ES	Megestrol Acetate	PAR Pharmaceuticals	MM*	Elan Nanocrystals <sup>®</sup>
Avinza <sup>®</sup>	Morphine Sulphate	King Pharmaceutical	MM*	Elan Nanocrystals <sup>®</sup>
Focalin <sup>®</sup> XR	Dexmethylphenidate Hydrochloride	Novartis	MM*	Elan Nanocrystals <sup>®</sup>
Ritalin <sup>®</sup> LA	Methylphenidate Hydrochloride	Novartis	MM*	Elan Nanocrystals <sup>®</sup>
Zanaflex Capsules <sup>™</sup>	Tizanidine Hydrochloride	Acorda	MM*	Elan Nanocrystals <sup>®</sup>
Triglide <sup>™</sup>	Fenofibrate	First Horizon Pharmaceutical	HPH <sup>#</sup>	SkyePharmaIDD <sup>®</sup> - P Technology

\*MM - Media Milling, # HPH - High-Pressure Homogenisation

### 1.5.10 Conclusion

Nanotechnology is an incredible field of the medicine. Since solubility is a crucial factor for drug effectiveness, it is a challenging task to formulate any poorly soluble drug in the industry in conventional dosage forms. Nano-technique is simple; fewer requirements of excipients are there for the formulation of dosage form design. Attractive features, such as reduction of particles size up to submicron level lead to a significant increase in dissolution velocity as well as saturation solubility. Improved bio-adhesiveness, versatility in surface modification and ease of post-production processing has widened the applications of nanosuspensions for various routes. Nanosuspension technology can be combined with traditional dosage forms: tablets, capsules, pellets and also can be used for parenteral

products. Production techniques such as media milling and high-pressure homogenization have been successfully employed for the large-scale production of nanosuspensions. The advances in production methodologies using emulsions or microemulsions as templates and precipitation method have provided still simpler approaches for production but with limitations. Further investigation in this regard is still essential. Some of the patented commercially productive technologies have been reviewed and if the patent period ends for such techniques there would be a revolutionary advancement in the formulation of poorly water-soluble drugs.

## 1.6 Profiles of selected drugs

### 1.6A Candesartan Cilexetil BP/USP

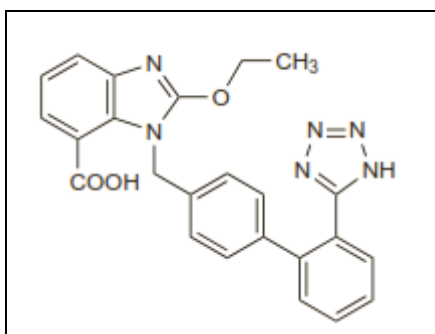
**1.6A.1 Molecular formula** [81]:  $C_{33}H_{34}N_6O_6$

**1.6A.2 Molecular weight** [81]: 610.66g/mol

**1.6A.3 Chemical name** [82]

It is ester prodrug hydrolyzed *in-vivo* to the active carboxylic acid. Cyclohexyl carbonate ester of (±)-1-hydroxyethyl 2-ethoxy-1-[p-(o-1H-tetrazole-5-yl-phenyl) benzyl]-7-benzimidazole carboxylate.

**1.6A.4 Chemical structure** [83]



**FIGURE 1.2: Chemical structure of candesartan cilexetil**

**1.6A.5 Description** [81]

It is colorless crystal obtained from ethanol-water with melting point 163°C. It is white to off-white powder.

**1.6A.6 Solubility** [81]

It is practically insoluble in water, sparingly soluble in methanol

**1.6A.7 Category** [81]

Angiotensin-II receptor antagonists

**1.6A.8 Indication** [81]

It is indicated for hypertension; heart failure with impaired left the ventricular systolic function in conjunction with an ACE inhibitor, or when ACE inhibitors are not tolerated.

**1.6A.9 Dose** [83]

**Hypertension**, initially 8 mg (hepatic impairment 2 mg, renal impairment or intravascular volume depletion 4 mg) once daily, increased if necessary at intervals of 4 weeks to maximum up to 32 mg once daily; usual maintenance dose 8 mg once daily.

**Heart failure**, initially 4 mg once daily, increased at intervals of at least 2 weeks to 'target' dose of 32 mg once daily or to the maximum tolerated dose.

**1.6A.10 Pharmacokinetics** [84]

- **Absorption:** Candesartan cilexetil is an ester prodrug that is hydrolyzed during absorption from the gastrointestinal tract to the active form candesartan.
- **Bioavailability:** The absolute bioavailability for candesartan is about 40% when candesartan cilexetil is given as a solution and about 14% when given as tablets.
- **T<sub>max</sub>:** Peak plasma concentrations of candesartan occur about 3 to 4 hours after oral doses as tablets.
- **Plasma protein binding:** Candesartan is more than 99% bound to plasma proteins.
- **Excretion:** It is excreted in urine and bile mainly as unchanged drug and a few inactive metabolites.
- **Terminal elimination half-life:** about 9 hours.
- Candesartan is not removed by hemodialysis.



**1.6A.11 Adverse effects**

Vertigo, headache; very rarely nausea, hepatitis, blood disorders, hyponatremia, back pain, arthralgia, myalgia, rash, urticaria, pruritus. Adverse effects of candesartan have been reported to be usually mild and transient, and include dizziness, headache, and dose-related orthostatic hypotension. Impaired renal function and rarely, rash, urticaria, pruritus, angioedema and raised liver enzyme values may occur. Candesartan appears less likely than ACE inhibitors to cause a cough. Other adverse effects that have been reported with angiotensin-II receptor antagonists include respiratory-tract disorders, back pain, gastrointestinal disturbances, fatigue, and neutropenia. Rhabdomyolysis has been reported rarely.

**1.6A.12 Uses and administration [85–92]**

Candesartan is an angiotensin-II receptor antagonist with anti-hypertensive activity mainly due to selective blockade of AT<sub>1</sub> receptors and the consequently reduced pressure effect of angiotensin-II. It is used in the management of hypertension, particularly in patients who develop a cough with ACE inhibitors and to reduce the risk of stroke in patients with left ventricular hypertrophy and in the treatment of diabetic nephropathy. It has also been tried in heart failure and in myocardial infarction. The maximum hypotensive effect is achieved in about 3 to 6 weeks after starting treatment.

Candesartan is given orally as the ester prodrug candesartan cilexetil. The onset of anti-hypertensive action occurs about 2 hours after a dose and the maximum effect is achieved within about 4 weeks of starting therapy. In the management of hypertension, the usual initial dose of candesartan cilexetil is 8 mg once daily in the UK or 16 mg once daily in the USA. The dose should be adjusted according to response; the usual maintenance dose is 8 mg once daily, but doses up to 32 mg daily, as a single dose or in 2 divided doses, may be used. Lower initial doses should be considered in patients with intravascular volume depletion; in the UK an initial dose of 4 mg once daily is suggested. Patients with a renal or hepatic impairment may also require lower initial doses. In heart failure, candesartan cilexetil is given in an initial dose of 4 mg once daily; the dose should be doubled at intervals of not less than two weeks up to 32 mg once daily if tolerated.

## 1.6A.13 Marketed formulations

Table 1.3: Marketed formulations of candesartan cilexetil

Drug Name	Brand Name	Dosage Form	Company Name	Dose of Drug
Candesartan Cilexetil	Creanz 16	Tablet	Sava Medica Pvt. Ltd.	16 mg
	Atacand	Tablet	AstraZeneca Pharmaceuticals	4 mg / 8 mg / 16 mg
	Candelong	Tablet	Micro Cardicare	4 mg / 8 mg / 16 mg
	Candesar	Tablet	Ranbaxy	4 mg / 8 mg
	Candestan	Tablet	Medley	4 mg / 8 mg
	Cantar	Tablet	Dr. Reddy's	4 mg / 8 mg
	Ipsita	Tablet	Bal Pharma	4 mg / 8 mg / 16 mg

## 1.6B Telmisartan BP/USP

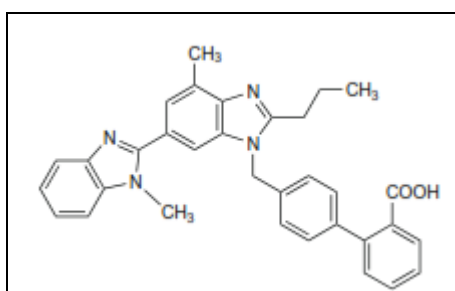
1.6B.1 Molecular formula [93]:  $C_{33}H_{30}N_4O_2$ 

1.6B.2 Molecular weight [93]: 514.62 gm/mol

1.6B.3 Chemical name [94]

Chemically Telmisartan is 4'-[(1,4'-Dimethyl-2'-propyl[2,6'-bi-1H-benzimidazol]-1'yl)methyl][1,1'-biphenyl]-2-carboxylic acid; 4'-[[4-methyl-6-(1-methyl-2-benzimidazolyl)-2-propyl-1-benzimidazolyl] methyl]-2- biphenyl carboxylic acid.

1.6B.4 Chemical structure [95]



FIGRUE 1.3: Chemical structure of telmisartan

**1.6B.5 Description** [93]

It is a white or slightly yellowish, crystalline powder. It exhibits polymorphism. It has a melting range of 261-263°C.

**1.6B.6 Solubility** [93]

It is practically insoluble in water (pH 3-9), sparingly soluble in strong acid (except insoluble hydrochloric acid), soluble in strong base. It shows slight solubility in methyl alcohol and it is sparingly soluble in dichloromethane.

**1.6B.7 Category** [93]

Angiotensin- II receptor antagonists

**1.6B.8 Indication** [95]

It is indicated for hypertension.

**1.6B.9 Dose** [95]

40 mg once daily (but 20 mg may be sufficient), increased if necessary after at least 4 weeks, to maximum 80 mg once daily.

**1.6B.10 Pharmacokinetics** [96]

- **Absorption:** Telmisartan is rapidly absorbed from the gastrointestinal tract;
- **Bioavailability:** The absolute oral bioavailability is dose-dependent and is about 42% after a 40-mg dose and 58% after a 160-mg dose.
- **T<sub>max</sub>:** Peak plasma concentration of telmisartan is reached about 0.5 to 1 hour after an oral dose.
- **Plasma protein binding:** Telmisartan is over 99% bound to plasma proteins.
- **Excretion:** It is excreted almost entirely in the feces via bile, mainly as unchanged drug.
- **Terminal elimination half-life:** about 24 hours for telmisartan.

**1.6B.11 Adverse effects and precautions [97][98]**

Gastro-intestinal disturbances; chest pain; influenza-like symptoms including pharyngitis and sinusitis; urinary tract infection; arthralgia, myalgia, back pain, leg cramps; eczema; less commonly dry mouth, flatulence, anxiety, vertigo, tendinitis-like symptoms, abnormal vision, increased sweating; rarely bradycardia, tachycardia, dyspnoea, insomnia, depression, blood disorders, increase in uric acid, eosinophilia, rash and pruritus; syncope and asthenia also reported.

Adverse effects of telmisartan have been reported to be usually mild and transient, and include dizziness, headache, and dose-related orthostatic hypotension. Hypotension may occur particularly in patients with volume depletion (for example those who have received high dose diuretics). Impaired renal function and rarely, rash, urticaria, pruritus, angioedema and raised liver enzyme values may occur. Hyperkalaemia, myalgia, and arthralgia have been reported. Telmisartan appears less likely than ACE inhibitors to cause a cough. Other adverse effects that have been reported with angiotensin-II receptor antagonists include respiratory-tract disorders, back pain, gastrointestinal disturbances, fatigue, and neutropenia. Rhabdomyolysis has been reported rarely. Telmisartan should be used with caution in patients with hepatic impairment or biliary obstruction.

**1.6B.12 Uses and administration [99–104]**

Telmisartan is an angiotensin-II receptor antagonist with anti-hypertensive activity mainly due to selective blockade of AT<sub>1</sub> receptors and the consequently reduced pressure effect of angiotensin-II. It is used in the management of hypertension, particularly in patients who develop a cough with ACE inhibitors and to reduce the risk of stroke in patients with left ventricular hypertrophy and in the treatment of diabetic nephropathy. It has also been tried in heart failure and in myocardial infarction. The maximum hypotensive effect is achieved in about 3 to 6 weeks after starting treatment.

Telmisartan is given orally. After a dose, the hypotensive effect peaks within 3 hours and persists for at least 24 hours. The maximum hypotensive effect occurs within about 4 to 8 weeks after starting therapy. In hypertension, telmisartan is given in an initial dose of 40 mg once daily. This may be increased, if necessary, to a maximum dose of 80 mg once daily. Lower doses should be considered in patients with hepatic or renal impairment.

## 1.6B.13 Marketed formulations

TABLE 1.4: Marketed formulations of telmisartan

Drug Name	Brand Name	Dosage Form	Company Name	Dose of Drug
Telmisartan	Inditel	Tablet	Zydus Cadila	40 mg / 80 mg
	A2B	Tablet	Fidelity	40 mg
	Adcom	Tablet	Intel Pharma	40 mg
	Angitel	Tablet	Molekule	40 mg / 80 mg
	Anzitel	Tablet	Essweil	40 mg
	Arbitel	Tablet	Micro Cardicare	20 mg / 40 mg
	Astel	Tablet	AS Pharma	20 mg / 40 mg

## 1.6C Ziprasidone Hydrochloride Monohydrate BP/USP

1.6C.1 Molecular formula [105]:  $C_{21}H_{22}Cl_2N_4OS \cdot H_2O$

1.6C.2 Molecular weight [105]: 467.4 gm/mol

1.6C.3 Chemical name [105]:

Ziprasidone hydrochloride monohydrate is chemically 5-[2-[4-(1, 2-Benzisothiazol-3-yl) piperazin-1-yl] ethyl]-6-chloro-1, 3-dihydro-2H-indol-2-one hydrochloride monohydrate.

1.6C.4 Chemical structure [106]:

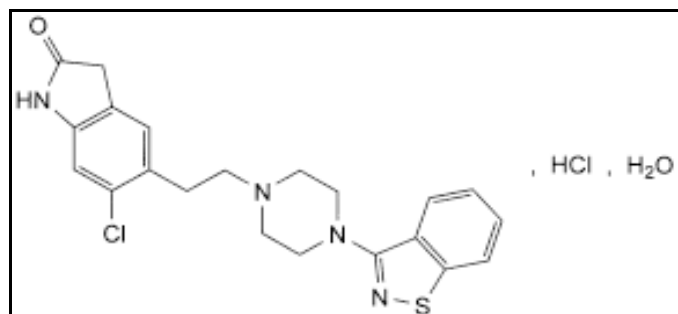


FIGURE 1.4: Chemical structure of ziprasidone hydrochloride monohydrate

1.6C.5 Description [105]

It is a white or slightly pink powder. It shows polymorphism.

**1.6C.6 Solubility** [105]

It is practically insoluble in water, slightly soluble in methanol and in methylene chloride

**1.6C.7 Category** [105]

It is an atypical antipsychotic drug.

**1.6C.8 Indication** [106]

It is indicated for the treatment of schizophrenia, as monotherapy for the acute treatment of bipolar manic or mixed episodes and as an adjunct to lithium or valproate for the maintenance treatment of bipolar disorder.

**1.6C.9 Dose** [107]

It is administered at an initial daily dose of 20 mg twice daily with food. In some patients, daily dosage may subsequently be adjusted on the basis of individual clinical status up to 80 mg twice daily.

**1.6C.10 Pharmacokinetics** [107–109]

- **Absorption:** Ziprasidone is well absorbed from the gastrointestinal tract with peak plasma concentrations being reached 6 to 8 hours after oral doses. The presence of food may double the absorption. Following intramuscular injection, peak plasma concentrations are reached within 1 hour.
- **Plasma protein binding:** It is about 99%.
- **Metabolism:** Ziprasidone is extensively metabolized by aldehyde oxidase (about 66% of a dose) and by the cytochrome P450 isoenzyme CYP3A4.
- **Terminal elimination half-life:** It has been reported to be about 7 hours after oral dosage and about 2 to 5 hours after intramuscular dosage.
- **Excretion:** Ziprasidone is excreted mainly as metabolites in the feces (about 66%) and urine (about 20%); less than 5% of a dose appears as unchanged drug.

**1.6C.11 Adverse effects and precautions**

Frequent adverse effects of ziprasidone include somnolence, rash or urticaria, gastrointestinal disturbances, dizziness, flu-like symptoms, hypertension, headache,

---

agitation, confusion, and dyspnoea. Orthostatic hypotension may be a problem, particularly when starting treatment.

Ziprasidone may increase prolactin levels and weight gain has also been noted. Sexual dysfunction has been reported infrequently. Extrapyramidal symptoms may occur and tardive dyskinesia may develop with prolonged use. There have also been infrequent or rare cases of cholestatic jaundice, hepatitis, seizures and blood dyscrasias including leucopenia and thrombocytopenia, and hyperlipidemia. Hyperglycemia occurs uncommonly with ziprasidone. Clinical monitoring for hyperglycemia has been recommended, especially in patients with, or at risk of, developing diabetes.

Ziprasidone has been associated with dose-related prolongation of the QT interval. Because of this and the consequent danger of life-threatening arrhythmias such as torsade de pointes and sudden death, its use is contraindicated in patients with a history of QT prolongation or cardiac arrhythmias, with recent acute myocardial infarction, or with decompensated heart failure. Baseline serum potassium and magnesium screening should be performed in patients who are at risk of significant electrolyte disturbances and hypokalemia or hypomagnesemia should be corrected before starting ziprasidone therapy. Serum electrolytes should be monitored in patients who start diuretic therapy during ziprasidone treatment.

Ziprasidone should be used with caution in patients with a history of seizures or in conditions that lower the seizure threshold, cardiovascular or cerebrovascular disease, or conditions which predispose to hypotension. Since intramuscular injections are formulated with cyclodextrin, which is cleared by renal filtration, the manufacturer recommends caution in patients with renal impairment. Ziprasidone may affect the performance of skilled tasks including driving.

### **3.12 Uses and administration**

Ziprasidone is an atypical antipsychotic reported to have an affinity for adrenergic ( $\alpha_1$ ), histamine ( $H_1$ ) and serotonin ( $5-HT_2$ ) receptors as well as dopamine ( $D_2$ ) receptors. It is used for the treatment of schizophrenia and in acute manic or mixed episodes associated with bipolar disorder. Ziprasidone is given by mouth usually as the hydrochloride; it is also given parenterally as the mesilate. Doses are expressed in terms of the base; ziprasidone

hydrochloride 11.3 mg or ziprasidone mesylate 13.6 mg are each equivalents to about 10 mg of ziprasidone.

For the treatment of **schizophrenia**, ziprasidone hydrochloride is given in an initial oral dose of 20 mg twice daily with food. Doses may be increased if necessary at intervals of not less than 2 days up to 80 mg twice daily. For maintenance, doses as low as 20 mg twice daily may be effective.

For acute agitation in patients with schizophrenia, ziprasidone may be given as the mesilate by intramuscular injection. The recommended dose is 10 to 20 mg as required, up to a maximum of 40 mg daily for 3 consecutive days. Doses of 10 mg may be given every 2 hours and doses of 20 mg may be given every 4 hours. Patients should be switched to oral therapy as soon as possible.

For the treatment of **mania**, ziprasidone hydrochloride is given in an initial oral dose of 40 mg twice daily with food. The dose should be increased to 60 or 80 mg twice daily on the second day of treatment and subsequently adjusted according to tolerance.

### 1.6C.13 Marketed formulations

**TABLE 1.5: Marketed formulations of ziprasidone hydrochloride**

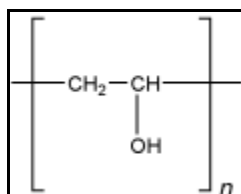
Drug Name	Brand Name	Dosage Form	Company Name	Dose of Drug
Ziprasidone Hydrochloride	Zipsydon	Capsules	Sun Pharma	20 mg /40 mg / 60 mg/ 80 mg
	Geodon	Capsules	Pfizer	20 mg /40 mg / 60 mg/ 80 mg
	Ziprasidone Hydrochloride Capsules	Capsules	Apotex Worldwide	60 mg



## 1.7 Profile of excipients

### 1.7A Polyvinyl Alcohol USP [110]

#### 1.7A.1 Structural formula



**FIGURE 1.5: Structural formula of polyvinyl alcohol**

#### 1.7A.2 Description

Polyvinyl alcohol occurs as an odorless, white to cream-colored granular powder.

#### 1.7A.3 Functional category

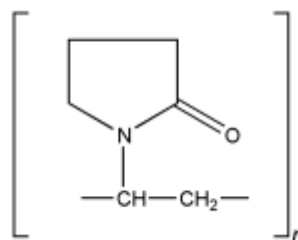
Coating agent, lubricant, stabilizing agent, viscosity-increasing agent.

#### 1.7A.4 Applications in pharmaceutical formulation or technology

- It is used as a stabilizing agent for emulsions (0.25–3.0% w/v).
- Polyvinyl alcohol is also used as a viscosity-increasing agent for viscous formulations such as ophthalmic products.
- It is used in artificial tears and contact lens solutions for lubrication purposes, in sustained release formulations for oral administration, and in transdermal patches.
- Polyvinyl alcohol may be made into microspheres when mixed with a glutaraldehyde solution.

#### 1.7A.5 Regulatory status

- It is included in the FDA Inactive Ingredients Guide, in non-parenteral medicines licensed in the UK and in the Canadian List of Acceptable Non-medicinal Ingredients.

**1.7B Povidone USP/BP/JP (PVP K-30) [111]****1.7B.1 Structural formula****FIGURE 1.6: Structural formula of PVP K-30****1.7B.2 Description**

Povidone occurs as a fine, white to creamy-white colored, odorless or almost odorless, hygroscopic powder. Povidones with *K*-values equal to or lower than 30 are manufactured by spray-drying and occur as spheres.

**1.7B.3 Functional category**

Disintegrant, dissolution aid, suspending agent, tablet binder.

**1.7B.4 Applications in pharmaceutical formulation or technology**

- Although povidone is used in a variety of pharmaceutical formulations, it is primarily used in solid dosage forms. In tableting, povidone solutions are used as binders in wet-granulation processes. Povidone is also added to powder blends in the dry form and granulated *in-situ* by the addition of water, alcohol or hydro-alcoholic solutions. Povidone is used as a solubilizer in oral and parenteral formulations and has been shown to enhance dissolution of poorly soluble drugs from solid-dosage forms. Povidone solutions may also be used as coating agents.
- Povidone is additionally used as a suspending, stabilizing, or viscosity-increasing agent in a number of topical and oral suspensions and solutions. The solubility of a number of poorly soluble active drugs may be increased by mixing with povidone.
- Special grades of pyrogen-free povidone are available and have been used in parenteral formulations.

### 1.7B.5 Regulatory status

- It is included in the FDA Inactive Ingredients Guide, in non-parenteral medicines licensed in the UK, in the Canadian List of Acceptable Non-medicinal Ingredients.

## 1.7C Sodium Lauryl Sulphate USP/BP/JP [112]

### 1.7C.1 Structural formula

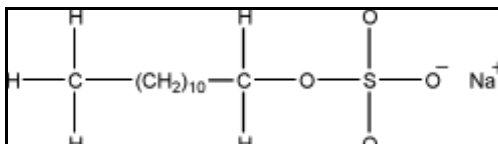


FIGURE 1.7: Structural formula of sodium lauryl sulfate

### 1.7C.2 Description

Sodium lauryl sulfate consists of white or cream to pale yellow-colored crystals, flakes, or powder having a smooth feel, a soapy, bitter taste, and a faint odor of fatty substances.

### 1.7C.3 Functional category

Anionic surfactant, detergent, emulsifying agent, skin penetrant, tablet and capsule lubricant, wetting agent.

### 1.7C.4 Applications in pharmaceutical formulation or technology

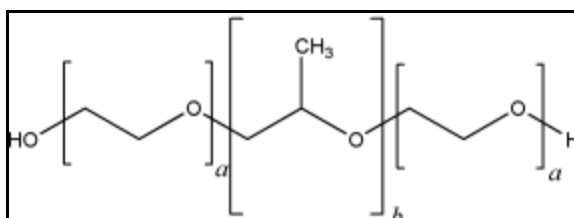
- Sodium lauryl sulfate is an anionic surfactant employed in a wide range of non-parenteral pharmaceutical formulations and cosmetics.
- It is a detergent and wetting agent effective in both alkaline and acidic conditions.
- In recent years it has found application in analytical electrophoretic techniques: SDS (sodium dodecyl sulfate) polyacrylamide gel electrophoresis is one of the more widely used techniques for the analysis of proteins, and sodium lauryl sulfate has been used to enhance the selectivity of micellar electrokinetic chromatography (MEKC).

### 1.7C.5 Regulatory status

GRAS listed, also included in the FDA Inactive Ingredients Guide, in non-parenteral medicines licensed in the UK, in the Canadian List of Acceptable Non-medicinal Ingredients.

## 1.7D Poloxamer USPNF/BP (Poloxamer 188 and Poloxamer 407)[113]

### 1.7D.1 Structural formula



**FIGURE 1.8: Structural formula of poloxamer**

### 1.7D.2 Description

Poloxamers generally occur as white, waxy, free-flowing prilled granules, or as cast solids. They are practically odorless and tasteless.

### 1.7D.3 Functional category

Dispersing agent, emulsifying and co-emulsifying agent, solubilizing agent, tablet lubricant, wetting agent.

### 1.7C.4 Applications in pharmaceutical formulation or technology

- Poloxamers are non-ionic polyoxyethylene–polyoxypropylene copolymers used primarily in pharmaceutical formulations as emulsifying or solubilizing agents.
- The polyoxyethylene segment is hydrophilic while the polyoxypropylene segment is hydrophobic. All of the poloxamers are chemically similar in composition, differing only in the relative amounts of propylene and ethylene oxides added during manufacture. Their physical and surface-active properties vary over a wide range and a number of different types are commercially available.
- Poloxamers are used as emulsifying agents in intravenous fat emulsions, and as solubilizing and stabilizing agents to maintain the clarity of elixirs and syrups.

- Poloxamers may also be used as wetting agents; in ointments, suppository bases, and gels and as tablet binders and coatings.
- Poloxamer 188 has also been used as an emulsifying agent for fluorocarbons used as artificial blood substitutes and in the preparation of solid-dispersion systems. More recently, poloxamers have found use in drug-delivery systems.
- Therapeutically, poloxamer 188 is administered orally as a wetting agent and stool lubricant in the treatment of constipation. It is usually used in combination with a laxative such as danthron.
- Poloxamers may also be used therapeutically as wetting agents in eye-drop formulations, in the treatment of kidney stones, and as skin-wound cleansers. Poloxamer 407 is used in solutions for contact lens care.

#### **1.7D.5 Regulatory status**

- Included in the FDA Inactive Ingredients Guide, in non-parenteral medicines licensed in the UK, in the Canadian List of Acceptable Non-medicinal Ingredients.

### **1.8 Aim and objectives**

Bioavailability enhancement is nowadays a great challenge to the pharmaceutical industries. The drug specifically from BCS class II and IV are always considered to have a dissolution rate limited bioavailability. Various approaches have been used to enhance the rate of dissolution of such types of drugs in order to get better bioavailability.

Nanosuspension is one of those approaches which can tremendously enhance the effective surface area of drug particles as well as shows vapor pressure effect and thereby increases the rate of dissolution and hence bioavailability.

Telmisartan and candesartan cilexetil, antihypertensive agents - angiotensin II inhibitors as well as ziprasidone hydrochloride monohydrate, an atypical antipsychotic drug are BCS class II drugs which are poorly soluble in water. Hence, dissolution is a rate-limiting step for enhancement of bioavailability of selected drugs. Reported bioavailability of candesartan cilexetil, telmisartan and ziprasidone hydrochloride is 40%, 42%, 60% respectively.

Various techniques like liposomes, microemulsions, solid-dispersions and inclusion complexes using cyclodextrins have been utilized for improving the dissolution characteristics of BCS class-II drugs, but the application of novel drug delivery strategy for improving their dissolution characteristics is still lacking. Hence there is a need for the development of a drug delivery strategy applicable to BCS class-II drugs for improving dissolution characteristics. Novel drug delivery strategies such as nanosuspensions could be studied for dissolution enhancement of such drugs. A nanosuspension is a submicron colloidal dispersion of drug particles which are stabilized by stabilizers.

Hence, the aim of present work is to prepare lyophilized nanosuspension of poorly water-soluble drugs by antisolvent precipitation – ultrasonication method. For convenience in handling dosage form, the lyophilized product shall be converted to the solid unit dosage form.

### 1.8.1 Complete hierarchy of work

- Preformulation study of selected drugs. eg. drug - excipient compatibility study
- Scanning and calibration curve preparation of selected drugs.
- Selection of solvents and stabilizer for the formulation of nanosuspension.
- Preparation of nanosuspension by antisolvent precipitation followed by ultrasonication technique from selected drugs.
- Identification of key factors affecting the formulation of nanosuspension by Plackett-Burman design of experiments.
- Optimization of nanosuspension formulation by 3<sup>2</sup> factorial design.
- Characterization of developed nanosuspension formulation by various physicochemical parameters as well as analytical techniques.
- Study of *in-vitro* drug release profile of optimized formulation and comparison of it with un-milled suspension and marketed formulation.
- Performance of accelerated stability studies of the optimized formulation according to ICH guidelines.
- Performance of bioavailability study of optimized formulation and comparison with the marketed formulation.
- Bioavailability and dose reduction calculation of selected drugs by converting into nanosuspension to have the same effect as of marketed formulation.

### 1.9 References

1. Makoid CM, Vuchetich PJ, Banakar UV (1999) *Basic Pharmacokinetics*. 1<sup>st</sup> Edition. The Virtual University Press.
2. Aulton ME (2007) *Pharmaceutics - The Science and Dosage Form Design*. 2<sup>nd</sup> Edition. Churchill Livingstone, New York.
3. Chow SC and Liu JP (2009) *Design and Analysis of Bioavailability and Bioequivalence Studies*. 3<sup>rd</sup> Edition. CRC Press, Taylor and Francis Group, Boca Raton.
4. Russell TL, Berardi RR, Burnet JL, O'Sullivan TL, Wagner JG and Dressman JB, 1994, pH-related changes in the absorption of Dipyridamole in the elderly, *Pharmaceutical Research*, 11(1), 136-143, ISSN: 1573-904X.
5. Lipinski CA, 2001, Avoiding investment in doomed drugs, is poor solubility an industry-wide problem? *Current Drug Discovery*, 4, 17-19.
6. Noyes AA, Whitney WR, 1897, The rate of solution of solid substances in their own solutions, *Journal of American Chemical Society*, 19, 930-934, ISSN: 0002-7863.
7. Galia E, Nicolaidis E, Horter D, Lobenberg R, Reppas C and Dressman JB, 1998, Evaluation of various dissolution media for predicting in vivo performance of class I and II drugs, *Pharmaceutical Research*, 15(5), 698-705, ISSN: 1573-904X.
8. Sravana Lakshmi M, Srivalli Kumari P, and Rajeev Kumar T, 2012, A Novel Approach for Improvement of Solubility and Bioavailability of Poorly Soluble Drugs: Lquisolid Compact Technique, *International Journal of Research in Pharmaceutical and Biomedical Sciences*, 3(4), 1621-1632, ISSN: 2229-3701.
9. Stovall DM, Givens C, Keown S, Hoover KR, Barnes R, Harris C, Lozano J, Nguyen M, Rodriguez E, Acree WE and Abraham MH, 2005, Solubility of crystalline nonelectrolyte solutes in organic solvents: mathematical correlation of 4-chloro-3-nitrobenzoic acid and 2-chloro-5-nitrobenzoic acid solubilities with the Abraham solvation parameter model, *Physics and Chemistry of Liquids*, 43, 351-360, ISSN: 0031-9104.
10. Makhlof A, Miyazaki Y, Tozuka Y and Takeuchi H, 2008, Cyclodextrins as stabilizers for the preparation of drug nanocrystals by the emulsion solvent diffusion method, *International Journal of Pharmaceutics*, 357(1-2), 280-285, ISSN: 0378-5173.
11. Park YJ (2014) *Revaprazan-containing solid dispersion and process for the preparation thereof*, European Patent EP 2101737B1.

12. Tao T, Zhao Y, Wu J and Zhou B, 2009, Preparation and evaluation of Itraconazole dihydrochloride for the solubility and dissolution rate enhancement, *International Journal of Pharmaceutics*, 367(1-2), 109–114, ISSN: 0378-5173.
13. Liversidge GG and Conzentino P, 1995, Drug particle size reduction for decreasing gastric irritancy and enhancing absorption of naproxen in rats, *International Journal of Pharmaceutics*, 125(2), 309–313, ISSN: 0378-5173.
14. Muller RH, Jacobs C and Kayser O (2000) *Nanosuspensions for the formulation of poorly soluble drugs*. In: F Nielloud, G Marti- Mestres (ed). *Pharmaceutical emulsion and suspension*, Marcel Dekker, New York, pp. 383-407.
15. Müller RH and Peters K, 1998, Nanosuspensions for the formulation of poorly soluble drug I: Preparation by size reduction technique, *International Journal of Pharmaceutics*, 160(2), 229-237, ISSN: 0378-5173.
16. Nagaraju P, Krishnachaithanya K, Srinivas VDN and Padma SVN, 2010, Nanosuspensions: Promising Drug Delivery Systems, *International Journal of Pharmaceutical Sciences and Nanotechnology*, 2(4), 679-684, ISSN: 0974-3278.
17. Dhiman S and Thakur GS, 2011, Nanosuspension: A recent approach for nano drug delivery system, *International Journal of Current Pharmaceutical Research*, 3(4), 96-101, ISSN: 0975-7066.
18. Chandra A, Soni RK, Sharma U and Jain SK, 2013, Nanosuspension: an Overview, *Journal of Drug Delivery and Therapeutics*, 3(6), 162-167, ISSN: 2250-1177.
19. Patravale VB, Date AA, and Kulkarni RM, 2004, Nanosuspension: a promising drug delivery strategy, *Journal of Pharmacy and Pharmacology*, 56(7), 827-840, ISSN: 2042-7158.
20. Rabinow BE, 2004, Nanosuspensions in drug delivery, *Nature Reviews Drug Discovery*, 3, 785-796, ISSN: 1474-1776.
21. Wongmekiat A, Tozuka Y, Oguchi T and Yamamoto K, 2002, Formation of fine drug particles by co-grinding with cyclodextrin. I. the use of  $\beta$ -cyclodextrin anhydrate and hydrate, *Pharmaceutical Research*, 19(12), 1867-1872, ISSN: 1573-904X.
22. Itoh K, Pongpeerapat A, Tozuka Y, Oguchi T and Yamamoto K, 2003, Nanoparticle formation of poorly water-soluble drugs from ternary ground mixtures with PVP and SDS, *Chemical and Pharmaceutical Bulletin*, 51(2), 171-174, ISSN: 1347-5223.
23. Mura P, Cirri M, Faucci MT, Ginès-Dorado JM and Bettinetti GP, 2002, Investigation of the effects of grinding and co-grinding on physicochemical properties of glisentide, *Journal of Pharmaceutical and Biomedical Analysis*, 30(2), 227-237, ISSN: 0731-7085.



24. Mura P, Faucci MT, and Bettinetti GP, 2001, The influence of polyvinylpyrrolidone on naproxen complexation with hydroxyl propyl- $\beta$ -cyclodextrin, *European Journal of Pharmaceutical Sciences*, 13(2), 187-194, ISSN: 0928-0987.
25. Otsuka M and Matsuda Y, 1995, Effect of co-grinding with various kinds of surfactants on the dissolution behavior of phenytoin, *Journal of Pharmaceutical Sciences*, 84(12), 1434-1437, ISSN: 1520-6017.
26. Sugimoto M, Okagaki T, Narisawa S, Koida Y and Nakajima K, 1998, Improvement of dissolution characteristics and bioavailability of poorly water-soluble drugs by novel co-grinding method using water-soluble polymer, *International Journal of Pharmaceutics*, 160(1), 11-19, ISSN: 0378-5173.
27. Yonemochi E, Kitahara S, Maeda S, Yamamura S, Oguchi T and Yamamoto K, 1999, Physicochemical properties of amorphous clarithromycin obtained by grinding and spray drying, *European Journal of Pharmaceutical Sciences*, 7(4), 331-338, ISSN: 0928-0987.
28. Watanabe T, Ohno I, Wakiyama N, Kusai A and Senna M, 2002, Stabilization of amorphous indomethacin by co-grinding in a ternary mixture, *International Journal of Pharmaceutics*, 241(1), 103-111, ISSN: 0378-5173.
29. Scholer N, Krause K, Kayser O, Muller RH, Borner K, Hahn H and Liesenfeld O, 2001, Atovaquone nanosuspensions show an excellent therapeutic effect in a new murine model of reactivated toxoplasmosis, *Antimicrobial Agents Chemotherapy*, 45(6), 1771–1779, ISSN: 1098-6596.
30. Venkatesh T, Reddy AK, Maheswari JU, Dalith MD and Kumar CKA, 2011, Nanosuspensions: Ideal approach for the drug delivery of poorly water-soluble drugs, *Der Pharmacia Lettre*, 3(2), 203-213, ISSN: 0975-508X.
31. Muller RH, Bohm BHL and Grau J (2000) Nanosuspensions: a formulation approach for poorly soluble and poorly bioavailable drugs. In D. Wise (Ed.) *Handbook of pharmaceutical controlled release technology*, Marcel Dekker Inc., New York, pp. 345- 357.
32. Jahnke S (1998) The theory of high-pressure homogenization. In: Muller RH, Benita S, Bohm BHL, *Emulsions and nanosuspensions for the formulation of poorly soluble drugs*, Medpharm Scientific Publishers, Stuttgart, pp. 177–200.
33. Kipp JE, Wong JCT, Doty MJ and Rebbeck CL (2003) *Microprecipitation method for preparing submicron suspensions*, US Patent 6607784.

34. Zili Z, Sfar S and Fessi H, 2005, Preparation and characterization of poly- $\epsilon$ -caprolactone nanoparticles containing griseofulvin, *International Journal of Pharmaceutics*, 294(1-2), 261-267, ISSN: 0378-5173.
35. Patel VR and Agrawal YK, 2011, Nanosuspension: An approach to enhance the solubility of drugs, *Journal of Advanced Pharmaceutical Technology and Research*, 2(2), 81-87, ISSN: 0976-2094.
36. Zhang X, Xia Q, and Gu N, 2006, Preparation of all-trans retinoic acid nanosuspensions using a modified precipitation method, *Drug Development and Industrial Pharmacy*, 32(7), 857-863, ISSN: 1520-5762.
37. Bodmeier R, McGinity JM, 1998, Solvent selection in the preparation of poly (DL-lactide) microspheres prepared by a solvent evaporation method, *International Journal of Pharmaceutics*, 43(1-2), 179–186, ISSN: 0378-5173.
38. Sah H, 1997, Microencapsulation technique using ethyl acetate as a dispersed solvent: effects on its extraction rate on the characteristics of PLGA microspheres, *Journal of Controlled Release*, 47(3), 233–245, ISSN: 0168-3659.
39. Sah H, 2000, Ethyl formate–alternative dispersed solvent useful in preparing PLGA microspheres, *International Journal of Pharmaceutics*, 195(1-2), 103–113, ISSN: 0378-5173
40. Trotta M, Gallarate M, Pattarino F and Morel S, 2001, Emulsions containing partially water-miscible solvents for the preparation of drug nanosuspensions, *Journal of Controlled Release*, 76(1-2), 119–128, ISSN: 0168-3659.
41. Eccleston GM (1992) Microemulsions. In: Swarbrick S, Boylan CJ, (eds) *Encyclopedia of pharmaceutical technology*, Vol.9, Marcel Dekker Inc., New York, pp 375–421.
42. C. Francesco and L. Francesco, 2011, New Methods for Lipid Nanoparticles Preparation, *Recent Patents on Drug Delivery and Formulation*, 5(3), 201-213, ISSN: 2212-4039.
43. Watnasirichaikul S, Rades T, Tucker IG and Davies NM, 2002, Effects of formulation variables on characteristics of poly (ethyl cyanoacrylates) nanocapsules prepared from w/o micro-emulsions, *International Journal of Pharmaceutics*, 235(1-2), 237– 246, ISSN: 0378-5173.
44. Trotta M, Gallarate M, Carlotti ME and Morel S, 2003, Preparation of Griseofulvin nanoparticles from water-dilutable microemulsions, *International Journal of Pharmaceutics*, 254(2), 235–242, ISSN: 0378-5173.

45. Kamble VA, Jagdale DM and Kadam VJ, 2010, Nanosuspension a novel drug delivery system, *International Journal of Pharma Biological Sciences*, 1(4), 352-360, ISSN: 0975-6299.
46. Allen T (2004) *Particle Size Measurement*, 5<sup>th</sup> Edition, Springer, London.
47. Shanthakumar TR, Prakash S, Basavraj RM, Ramesh M, Kant R, Venkatesh P, Rao K, Singh S and Srinivas NR (2004) 'Comparative pharmacokinetic data of DRF-4367 using nanosuspension and HP- $\beta$ -CD formulation', *Proceedings of the International Symposium on Advances in Technology and Business Potential of New Drug Delivery Systems*, Mumbai, pp. 75.
48. Hunter RJ (2001) *Foundations of Colloid Science*. 2<sup>nd</sup> Edition, Oxford University Press, New York.
49. Banavath H, Sivaramaraju K, Tahiransari MD, Sajidali MD and Pattnaik G, 2010, Nanosuspension: an attempt to enhance bioavailability of poorly soluble drugs, *International Journal of Pharmaceutical Sciences and Research*, 1(9), 1-11, ISSN: 0975-8232.
50. Gao L, Zhang D, and Chen M, 2008, Drug nanocrystals for the formulation of poorly soluble drugs and its application as a potential drug delivery system, *Journal of Nanoparticulate Research*, 10(5), 845-862, ISSN: 1388-0764.
51. Prasanna L and Giddam AK, 2010, Nanosuspension technology: A review, *International Journal of Pharmacy and Pharmaceutical Sciences*, 2(4), 35-40, ISSN: 0975 – 1491.
52. D'Souza S, 2014, A review of *in-vitro* drug release test methods for nano-sized dosage forms, *Advances in Pharmaceutics*, Volume 2014, 1-12, ISSN: 2314-775X.
53. Blunk T, Hochstrasser DF, Sanchez JC and Muller BW, 1993, Colloidal carriers for intravenous drug targeting: Plasma protein adsorption patterns on surface-modified latex particles evaluated by two-dimensional polyacrylamide gel electrophoresis, *Electrophoresis*, 14(12), 1382–1387, ISSN: 1522-2683.
54. Faiyazuddin M, Ahmad S, Mustafa G, Ahmad FJ and Shakeel F, 2010, Bioanalytical approaches, bioavailability assessment, and bioequivalence study for waiver drugs: *In-vivo* and *in-vitro* perspective, *Clinical Research and Regulatory Affairs*, 27(2), 1–10, ISSN: 1060-1333.
55. Shargel L and Yu ABC (2005) *Applied biopharmaceutics and pharmacokinetics*, 5<sup>th</sup> Edition, McGraw-Hill Companies Inc; New York, USA.

56. Blum HH and Schug BS, 1999, The biopharmaceutics classification system (BCS): class III drugs better candidates for BA/BE waiver? *European Journal of Pharmaceutical Sciences*, 9(2), 117–121, ISSN: 0928-0987.
57. Ansel HC (1985) *Introduction to pharmaceutical dosage forms*. Philadelphia, PA: Lea and Febiger.
58. Merisko LE, Sarpotdar P, Bruno J, Hajj S, Wei L, Peltier N, Rake J, Shaw JM, Pugh S, Polin L, Jones J, Corbett T, Cooper E and Liversidge GG, 1996, Formulation and anti-tumor activity evaluation of nanocrystalline suspensions of poorly soluble anti-cancer drugs, *Pharmaceutical Research*, 13(2), 272–278, ISSN: 1573-904X.
59. Dandagi P, Kerur S, Mastiholimath V, Gadad A and Kulkarni A, 2009, Polymeric ocular nanosuspension for controlled release of acyclovir: *in-vitro* release and ocular distribution, *Iranian Journal of Pharmaceutical Research*, 8(2), 79-86, ISSN: 1735-0328.
60. Kassem MA, Abdul Rahman AA, Ghorab MM, Ahmed MB and Khalil RM, 2007, Nanosuspension as an ophthalmic delivery system for certain glucocorticoid drugs, *International Journal of Pharmaceutics*, 340(1-2), 126-33, ISSN: 0378-5173.
61. Pignatello R, Bucolo C, Spedaliere G, Maltese A and Puglisi G, 2002a, Flurbiprofen-loaded acrylate polymer nanosuspensions for ophthalmic application, *Biomaterials*, 23(15), 3247–3255, ISSN: 0142-9612.
62. Bucolo C, Maltese A, Puglisi G and Pignatello R, 2002, Enhanced ocular anti-inflammatory activity of ibuprofen carried by Eudragit RS100 nanoparticle suspension, *Ophthalmic Research*, 34(5), 319–323, ISSN: 0030-3747.
63. Pignatello R, Bucolo C, Ferrara P, Maltese A, Puleo A and Puglisi G, 2002b, Eudragit RS100 nanosuspensions for the ophthalmic controlled delivery of ibuprofen, *European Journal of Pharmaceutical Sciences*, 16(1-2), 53–61, ISSN: 0928-0987.
64. Pignatello R, Bucolo C and Puglisi G, 2002c, Ocular tolerability of Eudragit RS100 and RL100 nanosuspensions as a carrier for ophthalmic controlled delivery, *Journal of Pharmaceutical Sciences*, 91(12), 2636–2641, ISSN: 0928-0987.
65. Jacobs C and Muller RH, 2002b, Production and characterization of a budesonide nanosuspension for pulmonary administration, *Pharmaceutical Research*, 19(2), 189–194, ISSN: 1573-904X.
66. Ponchel G, Montisci MJ, Dembri A, Durrer C and Duchene D, 1997, Mucoadhesion of colloidal particulate systems in the gastrointestinal tract, *European Journal of Pharmaceutics and Biopharmaceutics*, 44(1), 25–31, ISSN: 0939-641.

67. Francesco L, Chiara S, Guido E, Francesc M, Giaime M and Anna MF, 2009, Diclofenac nanosuspensions. Influence of preparation procedure and crystal form on drug dissolution behavior, *International Journal of Pharmaceutics*, 373(1-2), 124–132, ISSN: 0378-5173.
68. Hanafy A, Spahn-Langguth HG, Vergnault G, Grenier P, Tubic Grozdanis M, Lenhardt T and Langguth P, 2007, Pharmacokinetic evaluation of oral fenofibrate nanosuspension and SLN in comparison to the conventional suspension of micronized drug, *Advanced Drug Delivery Reviews*, 59(6), 419 - 426, ISSN: 0169-409X.
69. Kayser O, Olbrich C, Yardley V, Kinderlen AF and Croft SL, 2003, Formulation of amphotericin B as nanosuspension for oral administration, *International Journal of Pharmaceutics*, 254(1), 73–75, ISSN: 0378-5173.
70. Muller RH and Jacobs C, 2002, Buparvaquone mucoadhesive nanosuspension: preparation, optimization and long-term stability, *International Journal of Pharmaceutics*, 237(1-2), 151-161, ISSN: 0378-5173.
71. Kayser O, 2001, A new approach for targeting to *Cryptosporidium parvum* using mucoadhesive nanosuspensions: research and applications, *International Journal of Pharmaceutics*, 214(1-2), 83-85, ISSN: 0378-5173.
72. Kohno S, Otsubo T, Tanaka E, Maruyama K and Hara K, 1997, Amphotericin B encapsulated in polyethylene glycol immune-liposomes for infectious diseases, *Advanced Drug Delivery Reviews*, 24(2-3), 325-329, ISSN: 0169-409X.
73. Kayser O, Lemke A and Hernandez TN, 2005, The impact of Nanobiotechnology on the development of new drug delivery systems, *Current Pharmaceutical Biotechnology*, 6(1), 3-5, ISSN: 1873-4316.
74. Muller RH, Bohm BHL, and Grau MJ, 1999, Nanosuspensions- Formulations for poorly soluble drugs with poor bioavailability / 2nd communication: Stability, biopharmaceutical aspects, possible drug forms and registration aspects, *Die Pharmazeutische Industrie*, 61(12), 175-178, ISSN: 0031-711X.
75. Shim J, Kang HS, Park WS, Han SH, Kim J and Chang IS, 2004, Transdermal delivery of minoxidil with block copolymer nanoparticles, *Journal of Controlled Release*, 97(3), 477-484, ISSN: 0168-3659.
76. Kohli AK and Alpar HO, 2004, Potential use of nanoparticles for transcutaneous vaccine delivery: Effect of particle size and charge, *International Journal of Pharmaceutics*, 275(1-2), 13-17, ISSN: 0378-5173.
-

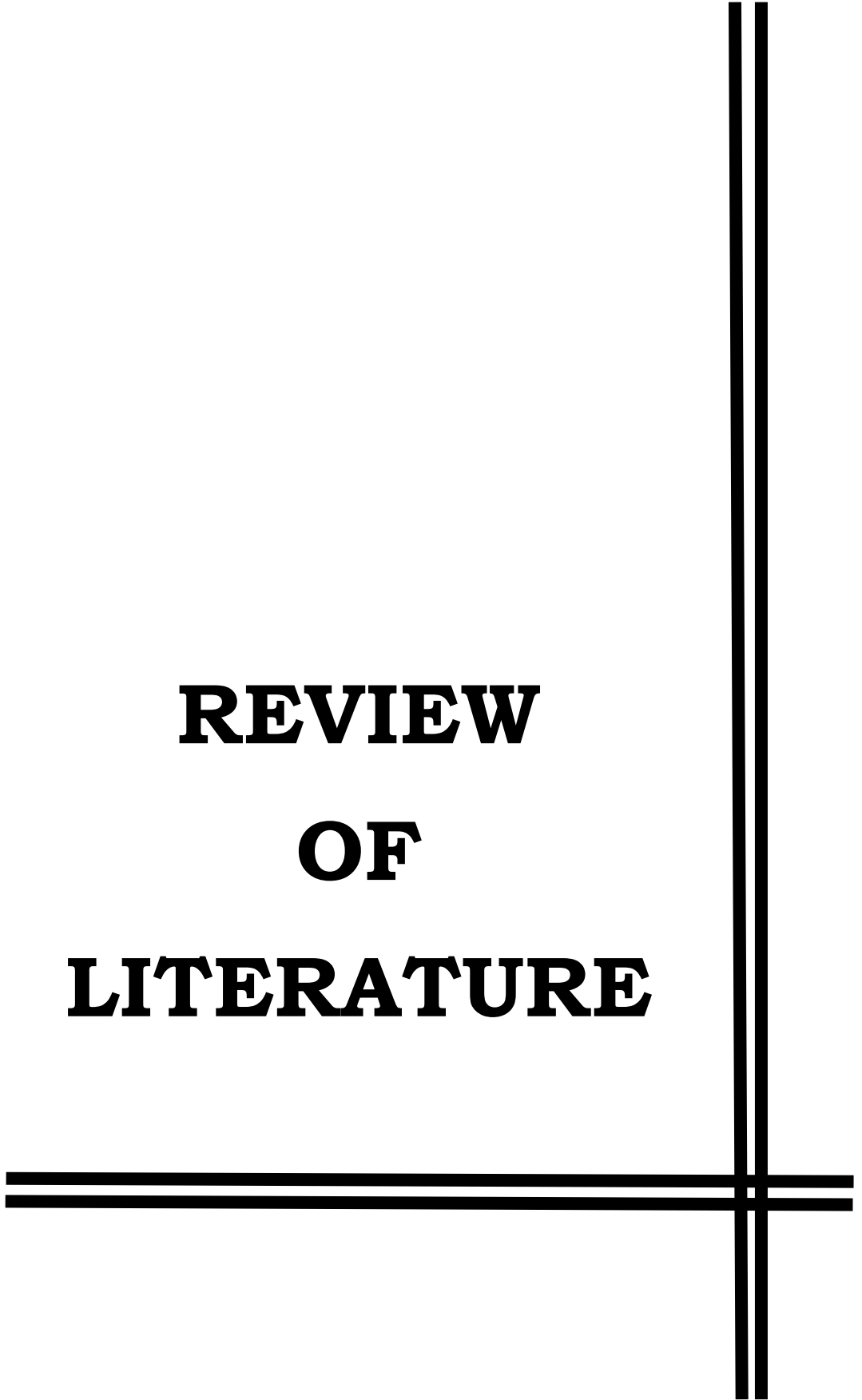
77. Yamaguchi Y, Nagasawa T, Nakamura N, Takenaga M, Mizoguchi M, Kawai SI, Mizushima Y and Igarashi R, 2005, Successful treatment of photo-damaged skin of nano-scale at RA particles using a novel transdermal delivery, *Journal of Controlled Release*, 104(1), 29-40, ISSN: 0168-3659.
78. Chen X, Lo CY-L, Sarkari M, Williams III RO and Johnston KP, 2006, Ketoprofen nanoparticle gels formed by evaporative precipitation into an aqueous solution, *AIChE Journal*, 52(7), 2428-2435, ISSN: 1547-5905.
79. Eerdenbrugh BV, Mooter GV, and Augustijns P, 2008, Top-down production of drug nanocrystals: Nanosuspension stabilization, miniaturization, and transformation into solid products, *International Journal of Pharmaceutics*, 364(1), 64-75.
80. Mauludin R (2008) Nanosuspension of poorly soluble drugs for oral administration. Ph.D. Thesis. The Free University of Berlin.
81. Anonymous (2015) Candesartan Cilexetil. In: *British Pharmacopoeia*, Vol. 1, British Pharmacopoeia Commission Office, MHRA, London, pp. 393-395
82. Budvari S (1996) Candesartan Cilexetil. In: O' Neil MJ, Heckelman PE, Koch CB, Roman KJ, Kenny Cm and D'Arecca MR (Editors) *The Merck Index – An encyclopedia of chemicals, drugs and biological*, 14<sup>th</sup> Edition, Merck Research Laboratory, Division of Merck and Co., Inc., Whitehouse Station, New Jersey, pp. 283-284.
83. Sweetman SC (2009) Candesartan Cilexetil. In: *Martindale - The Complete Drug Reference*, 36<sup>th</sup> Edition, Pharmaceutical Press, London, pp. 1238-1239.
84. Gleiter CH, Morike KE, 2002, Clinical pharmacokinetics of Candesartan, *Clinical Pharmacokinetics*, 41(1), 7–17, ISSN: 1179-1926.
85. Sever P, Menard J, 1997, Angiotensin II antagonism refined: candesartan cilexetil, *Journal of Human Hypertension*, 11 (suppl 2), S1–S95, ISSN: 1476-5527.
86. McClellan KJ and Goa KL, 1998, Candesartan cilexetil: a review of its use in essential hypertension, *Drugs*, 56(5), 847–69, ISSN: 1179-1950.
87. Stoukides CA, McVoy HJ, Kaul AF, 1999, Candesartan cilexetil: an angiotensin II receptor blocker, *The Annals of Pharmacotherapy*, 33(12), 1287–1298, ISSN: 1542-6270.
88. See S and Stirling AL, 2000, Candesartan cilexetil: an angiotensin II-receptor blocker, *American Journal of Health-System Pharmacy*, 57(8), 739–46, ISSN: 1535-2900.
89. Easthope SE and Jarvis B, 2002, Candesartan cilexetil: an update of its use in essential hypertension, *Drugs*, 62(8), 1253–1287, ISSN: 1179-1950.
-

90. Fenton C and Scott LJ, 2005, Candesartan cilexetil: a review of its use in the management of chronic heart failure, *Drugs*, 65(4), 537–58, ISSN: 1179-1950.
91. McKelvie RS, 2006, Candesartan for the management of heart failure: more than an alternative, *Expert Opinion on Pharmacotherapy*, 7(14), 1945–1956, ISSN: 1465-6566.
92. Meredith PA, 2007, Candesartan cilexetil—a review of effects on cardiovascular complications in hypertension and chronic heart failure, *Current Medical Research and Opinion*, 23(7), 1693–1705, ISSN: 1473-4877.
93. Anonymous (2015) Telmisartan. In: *British Pharmacopoeia*, Vol. 2, British Pharmacopoeia Commission Office, MHRA, London, pp. 979-980.
94. Budvari S (1996) Telmisartan. In: O'Neil MJ, Heckelman PE, Koch CB, Roman KJ, Kenny Cm and D'Arecca MR (Editors) *The Merck Index – An encyclopedia of chemicals, drugs and biological*, 14<sup>th</sup> Edition, Merck Research Laboratory, Division of Merck and Co., Inc., Whitehouse Station, New Jersey, pp. 1569.
95. Sweetman SC (2009) Telmisartan. In: *Martindale - The Complete Drug Reference*, 36<sup>th</sup> Edition, Pharmaceutical Press, London, pp. 1409.
96. Stangier J, Schmid J, Turck D, Switek H, Verhagen A, Peeters PA, vanMarle SP, Tamminga WJ, Sollie FA and Jonkman JH, 2000, Absorption, metabolism, and excretion of intravenously and orally administered [<sup>14</sup>C] telmisartan in healthy volunteers, *Journal of Clinical Pharmacology*, 40(1), 1312–22, ISSN: 1552-4604.
97. Mazzolai L and Burnier M, 1999, Comparative safety and tolerability of angiotensin II receptor antagonists, *Drug Safety*, 21(1), 23–33, ISSN: 1179-1942.
98. Michel MC, Bohner H, Koster J, Schafers R and Heemann U, 2004, Safety of telmisartan in patients with arterial hypertension: an open-label observational study, *Drug Safety*, 27(5), 335–44, ISSN: 1179-1942.
99. McClellan KJ and Markham A, 1998, Telmisartan, *Drugs*, 56(6), 1039–44, ISSN: 1179-1950.
100. Sharpe M, Jarvis B, and Goa KL, 2001, Telmisartan: a review of its use in hypertension, *Drugs*, 61(10), 1501–29, ISSN: 1179-1950.
101. Battershill AJ and Scott LJ, 2006, Telmisartan: a review of its use in the management of hypertension, *Drugs*, 66(1), 51–83, ISSN: 1179-1950.
102. Gosse P, 2006, A review of telmisartan in the treatment of hypertension: blood pressure control in the early morning hours, *Vascular Health and Risk Management*, 2(3), 195–201, ISSN: 1176-6344.

103. Yamagishi S, Nakamura K and Matsui T, 2007, The potential utility of telmisartan, an angiotensin II type 1 receptor blocker with peroxisome proliferator-activated receptor  $\gamma$ (PPAR- $\gamma$ )-modulating activity for the treatment of cardiometabolic disorders, *Current Molecular Medicine*, 7(5), 463–469, ISSN: 1875-5666.
104. Francischetti EA, Celoria BM, Francischetti A and Genelhu VA, 2008, Treatment of hypertension in individuals with the cardiometabolic syndrome: the role of an angiotensin II receptor blocker, telmisartan. *Expert Review of Cardiovascular Therapy*, 6(3), 289–303, ISSN: 1477-9072.
105. Anonymous, (2015) Ziprasidone Hydrochloride. In: *British Pharmacopoeia*, Vol. 2, British Pharmacopoeia Commission Office, MHRA, London, pp. 1209-1210.
106. Sweetman SC (2009) Ziprasidone Hydrochloride. In: *Martindale - The Complete Drug Reference*, 36<sup>th</sup> Edition, Pharmaceutical Press, London, pp. 1036-1037.
107. Aweeka F, Jayasekara D, Horton M, Swan S, Lambrecht L, Wilner KD, Sherwood J, Anziano RJ, Smolarek TA and Turncliff RZ, 2000, The pharmacokinetics of ziprasidone in subjects with normal and impaired renal function, *British Journal of Clinical Pharmacology*, 49 (suppl 1), 27S–33S, ISSN: 1365-2125.
108. Miceli JJ, Wilner KD, Swan SK, Tensfeldt TG, 2005, Pharmacokinetics, safety, and tolerability of intramuscular Ziprasidone in healthy volunteers. *Journal of Clinical Pharmacology*, 45(6), 620–30, ISSN: 1552-4604.
109. Preskorn SH, 2005, Pharmacokinetics and therapeutics of acute intramuscular Ziprasidone, *Clinical Pharmacokinetics*, 44(11), 1117–1133, ISSN: 1179-1926.
110. Rowe RC (2009) Polyvinyl alcohol, In: Rowe RC, Sheskey PJ and Quinn ME (Eds). *Pharmaceutical Excipients*, 6<sup>th</sup> Edition, Pharmaceutical Press, London, pp. 564-565.
111. Rowe RC (2009) Povidone, In: Rowe RC, Sheskey PJ and Quinn ME (Eds). *Pharmaceutical Excipients*, 6<sup>th</sup> Edition, Pharmaceutical Press, London, pp. 581-585.
112. Rowe RC (2009) Sodium Lauryl Sulphate, In: Rowe RC, Sheskey PJ and Quinn ME (Eds). *Pharmaceutical Excipients*, 6<sup>th</sup> Edition, Pharmaceutical Press, London, pp. 651-653.
113. Rowe RC (2009) Poloxamer, In: Rowe RC, Sheskey PJ and Quinn ME (Eds). *Pharmaceutical Excipients*, 6<sup>th</sup> Edition, Pharmaceutical Press, London, pp. 506-509.



**REVIEW  
OF  
LITERATURE**



## CHAPTER - 2

### Review of Literature

#### 2.1 Review of literature on bioavailability enhancement by nanosuspension

**Arunkumar N et al (2010)** [114] prepared nanosuspensions of a poorly soluble atorvastatin calcium in order to enhance its dissolution and oral bioavailability. Nanosuspensions were prepared by antisolvent precipitation followed by sonication technique. They were characterized by thermal gravimetric analysis (TGA), differential scanning calorimetry (DSC), powder x-ray diffraction (PXRD), solubility, dissolution and *in-vivo* bioavailability studies. The absence of atorvastatin peaks in PXRD profiles of nanosuspensions suggested the transformation of the crystalline drug into an amorphous form. TGA examination suggested that the drug was converted into anhydrous form from the original tri-hydrate form. DSC curves also complimented the result obtained by TGA and PXRD. The effect of particle size was found to be significant on the saturation solubility of the drug. The *in-vitro* drug release studies showed a significant increase in the dissolution rate of nanosuspensions as compared with the pure drug. Bioavailability studies have shown a nearly 3-fold increase in the AUC for the nanosuspensions as opposed to the pure drug.

**Patel GV et al (2014)** [115] developed nanosuspension (NS) of efavirenz (EFV) and investigated its potential in enhancing the oral bioavailability of EFV. EFNNS was prepared using the media milling technique. The Box – Behnken design was used for

optimization of the factors affecting EFVNS. Sodium lauryl sulfate and PVP K-30 were used to stabilize the NS. Freeze-dried NS was completely re-dispersed with double-distilled filtered water. Mean particle size and zeta potential of the optimized NS were found to be  $320.4 \pm 3.62$  nm and  $-32.8 \pm 0.4$  mV, respectively. X-ray diffraction and differential scanning calorimetric analysis indicated no phase transitions. Rate and extent of drug dissolution in the dissolution medium for NS was significantly higher compared to the marketed formulation. The parallel artificial membrane permeability assay indicated that NS successfully enhanced the permeation of EFV. Results of *in-situ* absorption studies showed a significant difference in absorption parameters such as  $K_a$ ,  $t_{1/2}$  and uptake percentages between lyophilized NS and marketed formulation of EFV. Oral bioavailability of EFV in rabbits resulting from NS was increased by 2.19-fold compared to the marketed formulation. Thus, it can be concluded that NS formulation of EFV can provide improved oral bioavailability due to enhanced solubility, dissolution velocity, permeability and hence absorption.

**Wahlstrom JL et al (2007)** [116] developed a nanosuspension formulation of 1,3-Dicyclohexylurea (DCU) to support oral, intravenous bolus and intravenous infusion dosing. Use of the nanosuspension formulation maintained DCU free plasma levels above the soluble epoxide hydrolase (sEH)  $IC_{50}$  and demonstrated that the application of formulation technology can accelerate the *in-vivo* evaluation of new targets by enabling pharmacodynamics studies of poorly soluble compounds. The use of nanoparticle parenteral drug delivery systems for oral, IV injection and IV infusion of tool compounds to reach desired exposures allowed to obtain reliable and critical data for early decision making early in the discovery process without large investment by utilizing less-than-ideal, prototype compounds for target validation.

**Zhao J et al (2016)** [117] improved the oral bioavailability of Lacidipine (LCDP) by applying nanosuspension technology prepared by a hybrid method of micro-precipitation and high-pressure homogenization. The effects of the production parameters (shearing rate and time, the stabilizers and their concentrations, homogenization pressure and a number of cycles) were investigated to optimize the preparation process. *In-vitro* characterizations (X-ray powder diffraction, differential scanning calorimetry, scanning electron microscopy and dissolution measurement) were carried out and an oral pharmacokinetic study was performed in beagle dogs. LCDP was transformed into an amorphous state using the

preparation process, and the mean particle size was about  $714.0 \pm 12.7$  nm. The dissolution rate of LCDP nanosuspensions was faster than that of physical mixtures but slower than that of Lacipil® (the commercial tablet). Regarding the *in-vivo* pharmacokinetics, the key pharmacokinetic parameters ( $C_{\max}$  and  $AUC_{0 \rightarrow \infty}$ ) of the nanosuspensions were statistically significantly higher than those of both the commercial tablet and physical mixtures. So, this is an efficient drug delivery strategy to facilitate the oral administration of LCDP by using nanosuspension technology and should be generally applicable to many poorly water-soluble drugs with dissolution rate-limited absorption.

**Anju Raju et al (2014)** [118] prepared and characterized nevirapine nanosuspensions so as to improve the dissolution rate of nevirapine. The low solubility of nevirapine leads to a decrease and variable oral bioavailability. Nanosuspension can overcome the oral bioavailability problem of nevirapine. Nevirapine nanosuspensions were prepared using nanoedge method. The suspensions were stabilized using surfactants Lutrol F127 or Poloxamer 407 and hydroxypropyl methylcellulose. The nanosuspension was characterized by particle size, polydispersity index, crystalline state, particle morphology, *in-vitro* drug release and pharmacokinetics in rats after oral administration. The results supported the claim for the preparation of nanosuspensions with enhanced solubility and bioavailability.

**Xia D et al (2010)** [119] prepared nanosuspension by the precipitation–ultrasonication method. The effects of five important process parameters, i.e. the concentration of polyvinyl alcohol in the antisolvent, the concentration of nitrendipine in the organic phase, the precipitation temperature, the power input and the time length of ultrasonication on the particle size of nanosuspensions were investigated systematically and the optimal values were 0.15%, 30 mg/ml, below 3°C, 400 W, and 15 min, respectively. The particle size and zeta potential of nanocrystals were 209 nm ( $\pm 9$  nm) and -13.9 mV ( $\pm 1.9$  mV), respectively. The morphology of nanocrystals was found to be flaky in shape by scanning electron microscopy (SEM) observation. The X-ray powder diffraction (XRPD) and differential scanning calorimetry (DSC) analysis indicated that there was no substantial crystalline change in the nanocrystals compared with raw crystals. The *in-vitro* dissolution rate of nitrendipine was significantly increased by reducing the particle size. The *in-vivo* test demonstrated that the  $C_{\max}$  and AUC values of nanosuspension in rats were approximately 6.1-fold and 5.0-fold greater than that of commercial tablets, respectively.

**Liu D et al (2012)** [120] prepared carvedilol (CAR) nanosuspensions using antisolvent precipitation–ultrasonication technique to improve its dissolution rate and oral bioavailability.  $\alpha$ -tocopherol succinate (VES) was first used as a co-stabilizer to enhance the stability of the nanosuspension. The optimal values of the precipitation temperature, power inputs and time length of ultrasonication were selected as 10°C, 400 W, and 15 mins respectively. Response surface methodology based on central composite design was utilized to evaluate the formulation factors that affect the size of nanosuspensions. The optimized formulation showed a mean size of 212±12 nm and a zeta potential of -42±3 mV. Scanning electron microscopy indicated that the nanosuspensions were flaky-shaped. Powder X-ray diffraction and differential scanning calorimetry analysis confirmed that the nanoparticles were in the amorphous state. Fourier transform infrared analysis demonstrated that the reaction between CAR and VES is probably due to hydrogen bonding. The nanosuspension was physically stable at 25°C for 1 week, which allows it to be further processing such as drying. The dissolution rate of the nanosuspensions was markedly enhanced by reducing the size. The *in-vivo* test demonstrated that the  $C_{max}$  and AUC values of nanosuspensions were approximately 3.3- and 2.9-fold greater than that of the commercial tablets, respectively.

**Sahu BP et al (2014)** [121] formulated nanosuspension of furosemide to enhance its oral bioavailability by increasing its dissolution in the stomach where it has better permeability. The nanosuspensions were prepared by precipitation with ultrasonication method. Polyvinyl acetate was used for sterically stabilizing the nanosuspensions. The diffusing drug concentration and stabilizer were used as the independent variables and the particle size, polydispersity index and drug release were selected as dependent variables and characterized. The effect of nanoprecipitation on the enhancement of oral bioavailability of furosemide nanosuspension was studied by *in-vitro* dissolution and *in-vivo* absorption studies in rats and compared to pure drug. The *in-vivo* studies on rats indicated a significant increase in the oral absorption of furosemide in the nanosuspension compared to pure drug. The  $AUC_{0\rightarrow24}$  and  $C_{max}$  values of nanosuspension were approximately 1.38- and 1.68 -fold greater than that of pure drug, respectively. The improved oral bioavailability and pharmacodynamic effect of furosemide may be due to the improved dissolution of furosemide in the simulated gastric fluid which results in enhanced oral systemic absorption of furosemide from stomach region where it has better permeability.

**Thadkala K et al (2014)** [122] investigated for better and stable amorphous ezetimibe nanosuspensions for oral bioavailability enhancement. Nanosuspensions of ezetimibe were prepared by solvent-antisolvent precipitation technique using a surfactant, tween 80 as a stabilizer. Nanosuspension preparation was optimized for particle size by investigating two factors that are, solvent: antisolvent ratio and surfactant concentration, at three levels. The formulations were characterized for particle size, surface morphology, crystallinity, zeta potential, saturation solubility, *in-vitro* drug release and *in-vivo* drug absorption. Nanosuspensions were smooth and spherical. The X-ray powdered diffraction and differential scanning calorimetry results indicated that the antisolvent precipitation method led to the amorphization of ezetimibe. Ezetimibe nanosuspensions increased the saturation solubility to an extent of 4-times. The  $C_{max}$  with ezetimibe nanosuspension was approximately 3-fold higher when compared with that of ezetimibe conventional suspensions administered orally.

**Bhalekar MR et al (2014)** [123] formulated and characterized nanosuspensions of acyclovir to increase the oral bioavailability. Nanosuspensions were prepared by the precipitation-ultrasonication method and the effects of important process parameters i.e., precipitation temperature, stirring speed, endpoint temperature of probe sonicator, energy input and sonication time were investigated systematically. The optimal nanosuspension (particle size 274 nm) was obtained at values of 4°C, 10,000 RPM, 30°C, 600 Watt and 20 mins respectively. The nanosuspension was lyophilized using different matrix formers and sucrose (100% w/w to the drug) was found to prevent agglomeration and particle size upon reconstitution was found to be 353 nm. The lyophilized nanocrystals appeared flaky in scanning electron microscopy images, the X-ray powder diffraction and differential scanning calorimetry analysis showed the nanoparticles to be in the crystalline state. *Ex-vivo* permeation study for calculating absorption rate and *in-vivo* bioavailability area under the curve both showed a three-fold increase over marketed suspension.

**Natarajan J et al (2013)** [124] prepared olanzapine nanosuspension using solvent diffusion followed by sonication technique. The nanosuspension was characterized for particle size distribution, polydispersity index, zeta potential, crystallinity study (DSC), *in-vitro* dissolution release profile and pharmacokinetic studies. The average size of the nanoparticles in F6 was 122.2 nm. Saturation solubility of an optimized batch of nanosuspension and the plain drug was found to be 2851.3±6.3 µg/ml and 251.3±6.1

$\mu\text{g/ml}$ , respectively. *In-vitro* cumulative drug release from the nanosuspension was 83.54% at 45 min when compared to pure drug 22.91% and in freeze-dried nanosuspension 92.67%. Pharmacokinetic studies in rats indicated that  $\text{AUC}_{(0 \rightarrow \infty)}$  was increased and clearance was decreased when olanzapine nanosuspensions were administered orally compared with that of olanzapine suspension which in turn 2 folds increased bioavailability. The enhanced relative bioavailability by the formulation might be attributed to oral bioavailability can be attributed to the adhesiveness of the drug nanosuspension, increased surface area (due to a reduction in particle size), increased saturation solubility, leading to an increased concentration gradient between the gastrointestinal tract lumen and blood, and increased dissolution velocity. This enhancement in bioavailability will lead to a subsequent reduction in drug dose, rendering the therapy cost-effective and obliterating any undue drug dumping in the body.

**Sawant KK et al (2016)** [125] developed nanosuspensions (NS) of Cefdinir (CEF) by the media milling technique using zirconium oxide beads as the milling media to improve its oral bioavailability. The particle size and zeta potential were found to be  $224.2 \pm 2.7 \text{ nm}$  and  $-15.7 \pm 1.9 \text{ mV}$ , respectively. Saturation solubility of NS was found to be  $1985.3 \pm 10.2 \mu\text{g/ml}$  which was 5.64 times higher than pure drug ( $352.2 \pm 6.5 \mu\text{g/ml}$ ). The DSC thermograms and XRD patterns indicated that there was no interaction between drug and excipients and that the crystallinity of CEF remained unchanged after media milling process. Results of *in-vitro* release studies and *ex-vivo* permeation studies showed improved drug release of  $88.21 \pm 2.90\%$  and  $83.11 \pm 2.14\%$ , respectively, from NS after 24h as compared to drug release of  $54.09 \pm 2.54$  and  $48.21 \pm 1.27\%$ , respectively, from the marketed suspension (Adcef). *In-vivo* studies in rats demonstrated a 3-fold increase in oral bioavailability from the NS in comparison to marketed suspension.

**Patel Y et al (2014)** [126] prepared nanosuspension of cefuroxime axetil for improving its solubility and thereby its bioavailability. Cefuroxime axetil nanosuspensions were prepared by the media milling technique using zirconium oxide beads. The particle size of the drug was drastically reduced to  $221.2 \pm 0.26 \text{ nm}$  from  $5 \mu\text{m}$  after nanosizing. Saturation solubility achieved was  $2387 \pm 3.35 \mu\text{g/ml}$  which was 16 times more than the bulk drug. DSC thermograms confirmed the non-interference of excipients on the drug particles. *In-vivo* diffusion studies showed  $94.17 \pm 5.689\%$  drug release from nanosuspension as against  $62.34 \pm 1.139\%$  release from plain Cefuroxime axetil suspension in 24 hours. Similarly, for

*ex-vivo studies*,  $57.52 \pm 1.159\%$  was released from plain cefuroxime axetil suspension in comparison to  $85.58 \pm 3.12\%$  for nanosuspension in 24 hours. *In-vivo* studies in rats demonstrated a two times increase in oral bioavailability from the nanosuspension in comparison to the marketed formulation. Therefore, nanosuspension which exhibited improved solubility, dissolution and absorption could be a better option as a delivery system compared to the present oral suspension formulation.

## **2.2 Review of literature on the preparation of nanosuspension by precipitation method**

**Nagajyothi N et al (2014)** [127] formulated nanosuspension of pitavastatin by precipitation method to improve its dissolution characteristics. Pitavastatin was dissolved in a methanol at room temperature. This was poured into water containing different amount of  $\beta$ -cyclodextrin and tween 80 maintained at room temperature and subsequently stirred on magnetic stirrer to allow the volatile solvent to evaporate. The prepared nanosuspension were evaluated by differential scanning calorimetry (DSC), zeta potential analysis, scanning electron microscopy, fourier transform infrared spectroscopy, saturation solubility, and *in-vitro* drug release studies. DSC curve obtained confirmed the transfer of drug crystalline form to amorphous form. Solubility studies and *in-vitro* drug release studies showed that the prepared nanosuspension has increased solubility and dissolution rate compared to pure drug. The technology is easy to scale up and requires less sophistication, the method can be extended to various poorly water-soluble drugs.

**Shah SMH et al (2016)** [128] optimized the processes and experimental conditions for fabrication of stable artemisinin (ART) nanosuspension using precipitation ultrasonication approach with subsequent enhanced dissolution rate compared to raw and micronized ART. The effect of important parameters including concentrations of stabilizer solution using polyvinyl alcohol (PVA), ultrasonication power inputs, length of ultrasonication and effect of temperature were systematically investigated for fabrication of stable ART nanosuspension. The optimized parameters to produce ART nanocrystals with smaller particle sizes were found to be 0.15% of PVA, at 200 Watt ultrasonic power input over 15 minutes of ultra-sonication at 4°C temperature. The average particle size and polydispersity index for ART nanosuspension were found to be  $98.77 \pm 1.5$  nm and  $0.186 \pm 0.01$  respectively. The crystallinity of the processed ART particles was confirmed using DSC and PXRD. Physical stability studies conducted for 30 days at different storage



temperatures which include 4, 25 and 40°C demonstrated that nanosuspensions stored at 4°C and 25°C were most stable compared to the samples stored at 40°C. The ART nanosuspension showed significantly ( $P < 0.05$ ) increased (87 fold) in dissolution rate of the produced nanocrystals compared to the micronized and raw ART which include 97%, 70%, and 10.5% respectively after 60 minutes.

**Shinde S et al (2014)** [129] prepared and characterized lornoxicam nanosuspensions to enhance the dissolution rate of the drug. Nanosuspensions were prepared by the precipitation–ultrasonication method. The particle size and zeta potential of nanospray dried powder were 213nm and  $-20\text{mV}$ , respectively. The morphology of nanocrystals was found to be spherical in shape by scanning electron microscopy (SEM) observation. The X-ray powder diffraction (XRPD) and differential scanning calorimetry (DSC) analysis indicated that there was no substantial crystalline change in the nanocrystals compared with the pure drug. The *in-vitro* dissolution rate of lornoxicam was significantly increased by reducing the particle size. The amorphous lornoxicam nanoparticles showed dramatic improvement in rate as well as the extent of *in-vitro* drug dissolution. The improvement can be attributed to amorphization and surface area, reduced particle size and decreased diffusion layer thickness. Spray drying process produced dry nanosuspension with high stability compared to liquid formulation.

**Sahu BP et al (2014)** [130] worked to enhance the oral bioavailability of furosemide by preparation of nanosuspensions by nanoprecipitation with sonication using dimethyl sulfoxide (DMSO) as a solvent and water as an antisolvent (NA). The prepared nanosuspensions were sterically stabilized with polyvinyl acetate (PVA). These were characterized by particle size, zeta potential, polydispersity index, scanning electron microscopy (SEM), differential scanning calorimetry (DSC), X-ray diffraction (XRD) pattern and drug release behavior. The average particle size of furosemide nanoparticles was found to be in the range of 150-300 nm. The particle size varied with an increase in the concentration of drug and stabilizer. The preparations showed negative zeta potential and polydispersity index in the range of  $0.3 \pm 0.1$ . DSC and XRD studies indicated that the crystalline furosemide was converted to amorphous form upon precipitation into nanoparticles. The saturation solubility of prepared furosemide nanoparticles markedly increased compared to the original drug in the simulated gastric fluid. The release profiles of nanosuspension formulation showed up to 81.2% release in 4 h. It may be concluded

that the nanoprecipitation with ultrasonication have potential to formulate homogenous nanosuspensions with uniform sized amorphous nanoparticles of furosemide. It was concluded that polyvinyl acetate can be used as a suitable steric stabilizer to prepare stable furosemide nanosuspensions. The enhanced saturation solubility in simulated gastric fluid leads to enhanced absorption of furosemide.

**Agarwal V et al (2014)** [131] prepared and optimized esomeprazole nanosuspension to enhance drug dissolution rate. Esomeprazole nanosuspensions were prepared by an evaporative precipitation-ultrasonication method using poloxamer 188 and poloxamer 407 as stabilizers. Formulation and process variables (concentration of stabilizers and drug, power input and duration of ultrasonication) affecting the characteristics of nanosuspensions were optimized. The nanosuspensions were characterized by particle size, shape, zeta potential, stability and *in-vitro* drug release study. For optimization of esomeprazole nanosuspension, the effect of some important parameters, including concentration of poloxamer 188, concentration of esomeprazole, precipitation temperature, duration of ultrasonication and power input, on particle size was investigated and the optimal values were 0.4% w/v, 3.5 mg/ml, 4°C, 20 mins and 60 W, respectively. Particle size was in the range of 125 - 184 nm with good zeta potential (15.9 - 25.5 mV). The *in-vitro* dissolution rate of esomeprazole was enhanced 4-fold (100% in 60 mins) compared with crude esomeprazole (24% in 60 min), and this was due to a decrease in particle size. The stability results indicated that nano-formulations stored at 4°C for two months showed maximum stability. The results indicated the suitability of the evaporative-precipitation-ultrasonication method for preparation of nanosuspensions of poorly soluble drugs with improved *in-vitro* dissolution rate, thus potentially capable of enhancing fast onset of therapeutic activity and bioavailability.

**Singh C et al (2015)** [132] enhanced the dissolution rate of a poorly water-soluble drug cefpodoxime proxetil by nanosuspension formation using a precipitation method. Cefpodoxime proxetil (CP), a semisynthetic  $\beta$ -lactam antibiotic of cephalosporin class belonging to BCS class IV with poor solubility and poor permeability is the ideal drug candidate with limited oral bioavailability when orally administered. The selected parameter of nanosuspension such as the concentration of drug, solvent-anti solvent volume ratio was varied so as obtain nanoparticle within the size range less than 1 $\mu$ m. Characterization of the Cefpodoxime proxetil of nanoparticle was carried out on the basis

of scanning electron microscopy (SEM), X-ray diffraction (XRD), FTIR spectrum, particle size, zeta potential and dissolution profile. Results signified that the combination of the lowest concentration of stabilizer HPMC E50 (0.1% w/v) with low stirring speed (800 rpm) tends to achieves smallest particle size 755.6 nm and -22.6 mV respectively. FTIR spectra are shown, that no chemical incompatibility between drug and polymer exist. The *in-vitro* drug release (%) cumulative profile of cefpodoxime proxetil nanosuspension was significantly higher (94%) as compared to marketed preparation (54%) in simulated intestinal fluid (pH 6.8).

**Kakran M et al (2015)** [133] developed nanoparticles by evaporative precipitation of nanosuspension (EPN) of poorly water-soluble drugs, namely silymarin (SLM), hesperetin (HSP) and glibenclamide (GLB), with the aim of improving their rate of dissolution. The original drugs and EPN prepared drug nanoparticles were characterized by scanning electron microscopy (SEM), differential scanning calorimetry (DSC) and dissolution test. The particle sizes were found to be influenced by the drug concentration and the solvent to antisolvent ratio. The smallest average particle sizes obtained were 350 nm for SLM, 450 nm for HSP and 120 nm for GLB. The DSC study suggested that the crystallinity of nanosuspension prepared drug nanoparticles was lower than the original drug. The dissolution rate of nanosuspension prepared drug nanoparticles markedly increased as compared to the original drug. The dissolution rate was increased up to 95% for SLM nanoparticles, up to 90% for HSP and up to almost 100% for the GLB nanoparticles fabricated. From this study, it was be concluded that the evaporative precipitation nanosuspension is an effective method to fabricate drug nanoparticles with enhanced dissolution rate.

**Esfandi EH et al (2014)** [134] investigated series of nanosuspensions containing Clarithromycin (CLM) and stabilizers such as HPMC, NaCMC, Polysorbate 80, poloxamer 188 and polyvinyl alcohol in various ratios using sono-precipitation method. Briefly, CLM was dissolved in acid solution and the pH of the solution was raised under sonication and the effects of different stabilizers on the particle size of nanoparticles were evaluated. Characterization of nanoparticles in terms of size, polydispersity index, zeta potential, differential scanning calorimetry and dissolution studies were performed. Antimicrobial activity of CLM nanosuspension was compared with coarse powder by using an agar well diffusion method. The results showed that HPMC was more efficient in size reduction of

particles and presence of HPMC E5 with a ratio of 3:5 to CLM in formulation led to developing the stable nanosuspension with a particle size of 340 nm. The obtained nanosuspension successfully showed enhanced dissolution rate and antimicrobial activity.

**Zhang X et al (2006)** [36] prepared All-Trans Retinoic Acid (ATRA) nanosuspensions with a modified precipitation method. The ATRA solution in acetone was injected into the pure water by an air compressor under the action of ultrasonication. Photon correlation spectroscopy results showed that the mean particle size of ATRA nanoparticles in nanosuspensions reduced from 337 nm to 155 nm as the injection velocity increased and the polydispersity index was 0.45–0.50. The morphology of ATRA nanoparticles varied with the different concentration of ATRA solution in acetone. ATRA nanoparticles showed an amorphous state and stable for 6 months. It could be concluded that this modified precipitation method could produce stable and controllable ATRA nanosuspension to a certain extent, thus benefit from higher saturation solubility.

**Ghasemian E et al (2015)** [135] formulated and characterize cefixime nanosuspensions in order to enhance the dissolution rate and solubility of this drug. Nanosuspensions were prepared using sono-precipitation method and the effects of surfactant type, surfactant and solid content, sonication power input, and interval of acid addition on the yield and particle size of nanosuspensions was investigated. Particle size and yield of the optimal nanosuspension formulation were  $266\pm 10$  nm and  $35\pm 2\%$ , respectively. Scanning electron microscopy (SEM) results showed a nearly spherical morphology of cefixime nanoparticles. Thermal analysis indicated that there was a partially crystalline structure in the nanoparticles and *in-vitro* dissolution rate of the drug was significantly increased by the reduction in particles size. Sono-precipitation was shown to be a successful method to produce cefixime nanosuspensions and the optimum conditions of the process were introduced.

**Zhang Z et al (2012)** [136] enhanced the dissolution rate by preparing Irbesartan (IBS) nanocomposite particles via antisolvent precipitation combined with a spray drying process. Four pharmaceutically acceptable excipients, including three different polymers and one charged surfactant, were evaluated as stabilizers to control the particle size and to prevent the agglomeration of particles. The experiment results indicated that PVP combined with sodium dodecyl sulfate (SDS) significantly decreased the particle size and enhanced the stability of drug nanoparticles. As a result, finally obtained stable IBS

nanoparticles, with an average size of approximately 55 nm. In the dissolution test, the IBS nanocomposite particles showed a significantly enhanced dissolution rate and 100% of the drug dissolved within 20 min. In contrast, the physical mixture with the same recipe as the IBS nanocomposite particles and the raw IBS reached only 8% and 40% of drug dissolved in 20 min respectively and both of them did not dissolve completely, even after 120 min.

**Suthar AK et al (2011)** [137] investigated promising methods of nanoparticle engineering for the formulation of poorly water-soluble drug compounds to enhance *in-vitro* dissolution and oral bioavailability of poorly water-soluble Raloxifene Hydrochloride (RH) by preparing stable nanoparticles. Mechanism of dissolution enhancement was also investigated. Nanoparticles were produced by combining the antisolvent precipitation and high-pressure homogenization (HPH) approaches in the presence of HPMC E5 and SDS (2:1, w/w). Then the nanosuspensions were converted into dry powders by spray-drying. The effect of process variables on particle size and physical state of the drug were investigated. The physicochemical properties of raw RH and nanoparticles were characterized by Scanning Electron Microscopy (SEM). The images of SEM indicated spherical RH nanoparticles. Nanoparticles showed good dissolution profile. The process by combining the antisolvent precipitation under sonication and HPH was producing small, uniform and stable nanoparticles which markedly enhanced dissolution rate.

**Vishnu Priya P et al (2016)** [138] prepared oral nanosuspensions of Irbesartan which is an angiotensin II receptor antagonist used mainly for the treatment of hypertension, in order to overcome bioavailability problems, to reduce dose-dependent side effects and frequency of administration. Nanosuspension containing the drug was prepared by precipitation method using combinations of polymers (such as PVP K-15, Tween 80, SLS and Poloxamer F127). The oral nanosuspension was evaluated for various physical and biological parameters, drug content uniformity, entrapment efficiency, scanning electron microscopy, *in-vitro* drug release, short-term stability and drug-excipient interactions (FTIR) indicated that all were within limits. *In-vitro* drug release studies of all the formulations were studied, out of that formulation, F9 showed 100.02 % of drug release within 20 min. and follows first order release kinetics. Short-term stability studies (40±2°C/75±5% RH for 3 months) indicated that the oral nanosuspension was stable with respect to drug content and dissolution. IR spectroscopic studies indicated that there are no drug-excipient interactions.

### 2.3 Review of literature on bioavailability enhancement of candesartan cilexetil

**Zulal NA et al (2015)** [139] formulated various solid dispersions. The different drug: carrier ratio for urea 1:2, 1:4 and 1:6, for polyethylene glycol 6000 (PEG), 1:2 and 1:4, 1:8 and mannitol 1:2, 1:4 and 1:6. Piperin and quercetin natural P-glycoprotein inhibitors were used as bioavailability enhancers. Bioavailability studies were carried out in a rat model with the SDs formulated in a suspension form and administered by the oral route. All the carriers enhanced drug dissolution in water 2 to 4-fold depending on drug/carrier ratio. Release kinetics from solid dispersions made with mannitol showed zero order drug release. Urea and PEG 6000-based solid dispersions showed 1<sup>st</sup> order drug release kinetics. FTIR studies confirmed transformation to an amorphous form of CDS in mannitol solid dispersion; this was supported by release kinetic studies. Bioavailability of the drug in the animals was enhanced by 27 and 68 % when quercetin and piperine, respectively, were incorporated. Formation of solid dispersion enhances the solubility and bioavailability of CDS when natural P-glycoprotein inhibitors such as piperine and quercetin are incorporated as enhancers.

**Beg S et al (2013)** [140] worked on formulation development and evaluation of P-SNEDDS of candesartan cilexetil, using Formulation by Design (FbD). Pseudo-ternary phase diagrams and FT-IR studies facilitated selection of constituents for P-SNEDDS viz., lauroglycol 90 (oil), tween 40 (surfactant), transcutool HP (co-surfactant) and oleylamine (cationic charge inducer). A D-optimal mixture design (three factors and two levels) was employed for optimizing P-SNEDDS employing Design Expert<sup>®</sup> software. Globule size, percent dissolution efficiency, mean dissolution time, amount permeated through intestine and emulsification time were employed as response variables to optimize the formulation. The optimized formulation was studied for *ex-vivo* permeability using everted sac technique, *in-vivo* pharmacokinetics studies and *in-situ* single pass perfusion (SPIP) studies in *Wistar* rats. The curvilinear 3-D response surface and 2-D contour plots construed remarkable diminution in globule size and consequent improvement in drug release (>90% in 15 min) with decreasing oil and increasing surfactant and co-surfactant levels. Pharmacokinetic and SPIP studies on the optimized positively charged system indicated 3-4 fold bioavailability enhancement vis-à-vis the marketed formulation (CANDESAR<sup>TM</sup>) and significant improvement as compared to conventional SEDDS. In a nutshell, the P-

SNEDDS had immense potential to significantly enhance bioavailability of poorly soluble drugs.

**Acharya A et al (2016)** [141] prepared a pro-niosomal formulation of candesartan cilexetil by a slurry method, using span 60 and tween 60 as non-ionic surfactants, maltodextrin as carrier and cholesterol and soya lecithin as stabilizers. FT-IR study showed drugs and excipients compatibility. Mean vesicles size of pro-niosome derived niosome was found in the range of 16.34-32.48  $\mu\text{m}$  and 7.25-16.45  $\mu\text{m}$  before and after shaking. An optimized formulation A3 containing a 2:1 ratio of span 60 and cholesterol showed maximum entrapment (86.17%) and *in-vitro* drug release (93.8%) compared to other formulations. *In-vitro* skin permeation studies were carried out using *Albino* rat skin and results showed that formulation A3 exhibited 88.65% drug permeation in a steady-state manner over a period of 24 h with a flux value of 1.94  $\mu\text{g}/\text{cm}^2/\text{h}$  and enhancement ratio of 3.73. *In-vivo* pharmacokinetics studies of pro-niosomal gel formulation A3 showed a significant increase in bioavailability (1.425 folds) compared with an oral formulation of candesartan cilexetil. Stability studies showed that pro-niosomal gel formulation was stable throughout its study period.

**Gurunath S et al (2014)** [142] investigated the absorption of candesartan cilexetil (CAN) by improving its solubility and inhibiting intestinal P-gp activity. A phase solubility method was used to evaluate the aqueous solubility of CAN in PVP K-30 (0.2–2%). Gibbs free energy ( $\Delta G_{\text{tro}}$ ) values were all negative. Solubility was enhanced by the freeze drying technique. FTIR spectra indicated no interaction between drug and PVP K-30. From XRD and DSC data, CAN was in the amorphous form, which explains the cumulative release of drug from its prepared systems. Enhancement of CAN absorption was noticed by improving its solubility and inhibiting the P-gp activity. The significant results ( $p < 0.05$ ) were obtained for freeze-dried solid dispersions in the presence of P-gp inhibitor than without naringin (15 mg/kg) with an absorption enhancement of 8-fold. Naringin could be employed as an excipient in the form of solid dispersions to increase CAN intestinal absorption and its oral bioavailability.

**Shaikh SM et al (2016)** [143] improved the solubility and dissolution rate and hence the permeability of candesartan cilexetil (CAN) by preparing solid dispersions/inclusion complexes. Solid dispersions were prepared using PEG 6000 [hydrophilic polymer] and

Gelucire 50/13 [Amphiphilic surfactant] by melt agglomeration (MA) and solvent evaporation (SE) methods in different drug-to-carrier ratios, while inclusion complexes were made with hydroxypropyl- $\beta$ -cyclodextrin (HP- $\beta$ -CD) [complexing agent] by grinding and spray drying method. Saturation solubility method was used to evaluate the effect of various carriers on aqueous solubility of CAN. Based on the saturation solubility data, two drug-carrier combinations, PEG 6000 (MA 1:5) and HP- $\beta$ -CD (1:1 M grinding) were selected as optimized formulations. FTIR, DSC, and XRD studies indicated no interaction of the drug with the carriers and provided valuable insight on the possible reasons for enhanced solubility. Dissolution studies showed an increase in drug dissolution of about 22 fold over the pure drug for PEG 6000 (MA 1:5) and 12 fold for HP- $\beta$ -CD (1:1 M grinding). *Ex-vivo* permeability studies indicated that the formulation having the greatest dissolution also had the best absorption through the chick ileum. Capsules containing solid dispersion/ complex exhibited better dissolution profile than the marketed product.

#### 2.4 Review of literature on bioavailability enhancement of telmisartan

**Kothawade PC et al (2013)** [144] enhanced the solubility and bioavailability of poorly water-soluble drug telmisartan by formulating solid dispersions (SDs) using spray drying method. Telmisartan was selected as a model drug due to its poor and pH-dependent solubility. Meglumine has been used as an alkalizer in SDs to increase the solubility of telmisartan. HPMC E5LV and PVP K-30 were used as polymers for preparation of solid dispersions. The prepared SDs were characterized by scanning electron microscopy (SEM), differential scanning calorimetry (DSC), powder X-ray diffraction (XRD), fourier transform infrared spectroscopy (FTIR) study, solubility study, *in-vitro* drug release study and *in-vivo* study. SEM, DSC and XRD study showed the partial conversion of crystalline telmisartan to amorphous form. The solubility of telmisartan has been found to be increased by more than 300 folds when formulated as SDs using PVP K-30. *In-vitro* drug release study showed marked enhancement in the drug release, SDs showed 100 % drug release within 30 mins while pure telmisartan showed within 120 mins. *The in-vivo* study showed significant enhancement in bioavailability of telmisartan from SDs with PVP K-30 than the plain drug. Prepared solid dispersion using spray drying technique showed significant enhancement in drug solubility, drug release, and bioavailability. This may aid in improving bioavailability to a greater extent requiring less amount of the drug.



**Patel JM et al (2014)** [145] developed nanoparticulate solid oral dosage forms of telmisartan (TLM) by converting the optimized batch of drug loaded nanosuspensions into a tablet dosage form using lyophilization technique. The TLM loaded nanosuspensions were optimized by the implementation of  $3^2$  full factorial design along with principal component analysis (PCA) with a concentration of stabilizer and amount of milling agents as factors. The optimized batch of TLM loaded nanosuspension exhibited a mean particle size of  $334.67 \pm 10.43$  nm. The results of various instrumental techniques illustrated retention of drug crystallinity after milling and lyophilization. The results of *in-vitro* drug release study of tablets containing drug nanocrystals indicated remarkable improvement in the dissolution rate as compared to the marketed tablet (Sartel<sup>®</sup> 20). The results of an *in-vivo* pharmacokinetic study on *Wister* rats indicated a 1.5-fold enhancement in oral bioavailability for tablets containing TLM nanocrystals against the marketed tablets.

**Cao Y et al (2016)** [146] prepared organic solvent-free solid dispersions (OSF-SDs) containing telmisartan (TEL) using polyvinylpyrrolidone K-30 (PVP K-30) and polyethylene glycol 6000 (PEG 6000) as hydrophilic polymers, sodium hydroxide (NaOH) as an alkalizer and poloxamer 188 as a surfactant by a lyophilization method. *In-vitro* dissolution rate and physicochemical properties of the OSF-SDs were characterized using USP-I basket method, differential scanning calorimetry (DSC), X-ray diffractometry (XRD) and Fourier transform-infrared (FT-IR) spectroscopy. In addition, the oral bioavailability of OSF-SDs in rats was evaluated by using TEL bulk powder as a reference. The dissolution rates of the OSF-SDs were significantly enhanced as compared to TEL bulk powder. The results from DSC, XRD showed that TEL was molecularly dispersed in the OSF-SDs as an amorphous form. The FT-IR results suggested that intermolecular hydrogen bonding had formed between TEL and its carriers. The OSF-SDs exhibited significantly higher  $AUC_{0-24\text{ h}}$  and  $C_{\text{max}}$ . This study demonstrated that OSF-SDs can be a promising method to enhance the dissolution rate and oral bioavailability of TEL.

**Padia N et al (2015)** [147] developed a self-micro emulsifying drug delivery system (SMEDDS), a mixture of oil, surfactant, and co-surfactant, which are emulsified in an aqueous medium under gentle digestive motility in the gastrointestinal tract, to enhance the oral bioavailability of poorly water-soluble telmisartan. Pseudoternary phase diagrams were constructed to identify the efficient self-emulsifying region. A SMEDDS were further evaluated for its percentage transmittance, emulsification time, drug content, phase

separation, globule size, zeta potential, pH, refractive index, X-ray diffraction, differential scanning calorimetry and *in-vitro* dissolution studies. Optimized formulation was also compared with the marketed product (Telma 20) in male SD rats. The pharmacokinetic study exhibited 1.54 fold increase in the oral bioavailability of telmisartan SMEDDS compared with the marketed product.

**Ahmad J et al (2011)** [148] developed, characterized self-nano emulsifying drug delivery system and its relative bioavailability was compared to the commercially available formulation. Salsol-218, tween-20, and transcitol P were chosen as oil, surfactants, and co-surfactants respectively as they show the highest solubility for telmisartan. The solubility of the drug was further improved by adding sodium hydroxide (0.67%). The droplet size of the optimized emulsion was also evaluated and was observed to be in nano range. The dissolution of the drug was rapid in simulated gastric fluid (pH 1.2) as well as in simulated intestinal fluid (pH 6.8) and was found to be pH independent. The pharmacokinetic parameters ( $AUC_{0 \rightarrow t} \pm SD$ ,  $C_{max}$ , and  $T_{max}$ ) of the optimized formulation of telmisartan after oral administration as SNEDDS were compared with oral tablet and API suspension of the drug. The results showed a 4.34-fold increase in oral bioavailability of the drug in comparison to the tablet. The results demonstrate that SNEDDS composed of sefsol-218, tween-20 and transcitol P substantially enhanced the bioavailability of telmisartan. Further, it showed highly significant fall ( $p < 0.001$ ) in mean blood pressure of hypertensive rats for 48 hours.

**Charman SA et al (1992)** [149] formulated, a lipophilic compound, WIN 54954, in a medium chain triglyceride oil/non-ionic surfactant mixture which exhibited self-emulsification under conditions of gentle agitation in an aqueous medium. The efficiency of emulsification was studied using a laser diffraction sizer to determine particle size distributions of the resultant emulsions. An optimized formulation which consisted of 25% (w/w) surfactant, 40% (w/w) oil and 35% (w/w) WIN 54954 emulsified rapidly with gentle agitation in 0.1 N HCl (37°C), producing dispersions with mean droplet diameters of less than 3 microns. The self-emulsifying preparation was compared to a polyethylene glycol 600 (PEG 600) solution formulated by administering each as prefilled soft gelatin capsules to fasted beagle dogs in a parallel crossover study. Pharmacokinetic parameters were determined and the absolute bioavailability of the drug was calculated by comparison to an i.v. injection. The SEDDS improved the reproducibility of the plasma profile in terms of

the maximum plasma concentration ( $C_{max}$ ) and the time to reach the maximum concentration ( $t_{max}$ ). There was no significant difference in the absolute bioavailability of WIN 54954 from either the SEDDS or the PEG formulations.

## 2.5 Review of literature on bioavailability enhancement of ziprasidone hydrochloride

**Miao Y et al (2016)** [150] developed self-nano emulsifying drug delivery systems (SNEDDS) in sustained-release pellets of ziprasidone to enhance the oral bioavailability and overcome the food effect of ziprasidone. Preformulation studies including a screening of excipients for solubility and pseudo-ternary phase diagrams suggested the suitability of Capmul MCM as the oil phase, Labrasol as a surfactant and PEG 400 as co-surfactant for preparation of self-nano emulsifying formulations. The preliminary composition of the SNEDDS formulations was selected from the pseudo-ternary phase diagrams. The prepared ziprasidone-SNEDDS formulations were characterized for self-emulsification time, the effect of pH and robustness to dilution, droplet size analysis, and zeta potential. The optimized ziprasidone-SNEDDS were used to prepare ziprasidone-SNEDDS sustained-release pellets via extrusion-spheronization method. The pellets were characterized by SEM, particle size, droplet size distribution, and zeta potential. *In-vitro* drug release studies indicated the ziprasidone-SNEDDS sustained-release pellets showed sustained release profiles with 90% released within 10 h. The ziprasidone-SNEDDS sustained-release pellets were administered to fasted and fed beagle dogs and their pharmacokinetics were compared to the commercial formulation of Zeldox as a control. Pharmacokinetic studies in beagle dogs showed ziprasidone with prolonged actions and enhanced bioavailability with no food effect was achieved simultaneously in ziprasidone-SNEDDS sustained-release pellets compared with Zeldox in the fed state. The results indicated a sustained release with prolonged actions of schizophrenia and bipolar disorder treatment.

**Banerjee S et al (2016)** [151] developed a stable capsule formulation of ziprasidone hydrochloride which can be administered without regards to food intake. The unstable anhydrous form of ziprasidone hydrochloride was stabilized employing hot-melt extrusion and further optimized by  $3^2$  central composite design. The formulation was optimized after establishing acceptable ranges for response variables like disintegration time, dissolution and impurity profile. A crossover fasted and fed *in-vivo* study was conducted in human

volunteers to assess the food-effect of optimized formulation vis-à-vis the marketed brand. The optimized formulation met in-house specifications for various response variables. Further, high values of correlation coefficient which for the adequate selection of experimental design and its high prognostic ability. No significant difference was observed between the  $C_{\max}$  and AUC values after administration of the optimized formulation in fasted and fed states. On the contrary, there was a statistically significant increase in the  $C_{\max}$  and AUC values after oral administration of Zeldox in fed state in comparison to the fasted state. The present study describes the successful development of a stable formulation of 20 mg of ziprasidone devoid of any food-effects.

**Thombre AG et al (2012)** [152] prepared and characterized a solid nanocrystalline dispersion (SNCD) to improve the oral absorption of ziprasidone in the fasted state, thereby reducing the food effect observed for the commercial formulation. A solution of ziprasidone hydrochloride and the polymer hydroxypropyl methylcellulose acetate succinate (HPMCAS) was spray-dried to form a solid amorphous spray-dried dispersion (SDD), which was then exposed to a controlled temperature and relative humidity (RH) to yield the ziprasidone SNCD. The SNCD was characterized using powder X-ray diffraction, thermal analysis, microscopy and *in-vitro* dissolution testing. These tools indicate the SNCD consists of a high-energy crystalline form of ziprasidone in domains approximately 100 nm in diameter but with crystal grain sizes on the order of 20 nm. The SNCD was dosed orally in capsules to beagle dogs. Pharmacokinetic studies showed complete fasted-state absorption of ziprasidone, achieving the desired improvement in the fed/fasted ratio.

**Miao Y et al (2016)** [153] worked to develop ziprasidone–phospholipid complex (ZIP-PLC) in sustained-release pellets to enhance the oral bioavailability and overcome the food effect of ziprasidone. Ziprasidone–phospholipid complex was formulated by the solvent evaporation method. The optimized ZIP-PLC was used to prepare ZIP-PLC sustained-release pellets via extrusion–spheronization method. The pellets were characterized by *in-vitro* drug-release studies and administered to fasted and fed beagle dogs and their pharmacokinetics were compared with commercial formulation Zeldox capsule as a control. The results of FTIR, SEM, DSC and PXRD studies confirmed the formation of phospholipid complex. Solubility studies showed there was a higher solubility in water for ZIP-PLC than monohydrate ziprasidone. The *in-vitro* release rate of ziprasidone from the ZIP-PLC sustained-release pellet exhibited controlled-release characteristics with over

95% total release in 12 h. Pharmacokinetic studies in beagle dogs showed ziprasidone with prolonged actions and no food effect was achieved simultaneously in ZIP-PLC sustained-release pellet compared with Zeldox capsule. The results indicated a sustained release with prolonged actions of schizophrenia and bipolar disorder treatment.

## 2.6 Review of patents related to selected project work

**Robert B et al (1999)** [154] patented drug carrier comprising particles of at least one pure active compound which is insoluble, only sparingly soluble or moderately soluble in water, aqueous media and/or organic solvents, wherein active ingredient is solid at room temperature and has an average diameter, determined by photon correlation spectroscopy (PCS) of 10 nm to 1,000 nm, the proportion of particles larger than 5  $\mu$ m in the total population being less than 0.1% (number distribution determined with a Coulter counter), and when introduced into water, aqueous media and/or organic solvents, the active compound has an increased saturation solubility and an increased rate of dissolution compared with powders of the active compound prepared using an ultrasonic probe, a ball mill or a pearl mill, the solid particles having been comminuted, without prior conversion into a melt, by using cavitation or shearing and impact forces with introduction of a high amount of energy.

**Chen MJ et al (2011)** [155] patented that compositions and methods for preparation and administration of an oral nanosuspension of a poorly soluble drug with improved bioavailability. The method was optimized through the microfluidization process with water soluble polymeric excipients in the absence of surfactants.

**Binner JGP (2010)** [156] patented a method for concentrating a nanosuspension including nanopowder particles suspended in a liquid includes reducing the liquid content of the nanosuspension and controlling the dispersion of the nanopowder particles in the liquid.

**Ferreiro MG et al (2012)** [157] patented invention relates to a method for the production of a nanoparticulate pharmaceutical composition. The method comprised the steps of a) suspending in water a poorly soluble active ingredient without the presence of a detergent, b) mechanically treating said suspension to obtain particles comprising the active ingredient with an effective average size of less than about 5000 nm, c) contacting said active ingredient or suspension with a first polyelectrolyte during, and/or before mechanically treating, d) optionally contacting said suspension with a one or more second

---

or further poly electrolytes during, before and/or after mechanically treating, e) optionally drying said suspension. The invention also pertains to the pharmaceutical compositions obtained by the method of the invention

**Amarnath S et al (2012)** [158] patented oral pharmaceutical compositions comprising candesartan or its pharmaceutically acceptable salts, esters, solvates, hydrates, enantiomers, polymorphs, or their mixtures, and processes for preparing the same are described. Also described pharmaceutical formulations comprising compositions containing candesartan or an ester thereof, processes for preparing the formulations and methods of use, treatment, and administration involving the formulations.

**Nakatani M et al (2004)** [159] patented a pharmaceutical composition comprising 3 to 50 wt. % telmisartan dispersed in a dissolving matrix comprising: (a) a basic agent in a molar ratio of basic agent: telmisartan of 1:1 to 10:1; (b) about 1 to 20 wt. % of a surfactant or emulsifier; (c) 25 to 70 wt. % of a Water-soluble diluent; and (d) 0 to 20 wt. % of one or more additional excipients and/or adjuvants; wherein the sum of all components is 100%, methods of making wherein the sum of all components are 100%, methods of making such pharmaceutical compositions, and their use.

**Shah JC et al (2008)** [160] patented pharmaceutical formulations comprising: a compound selected from the group consisting of ziprasidone, having a maximum average particle size; a carrier; and preferably at least two surface stabilizers are disclosed. The present invention also comprises methods of treating psychosis with such a formulation and processes for making such a formulation.

## 2.7 References

114. Arunkumar N, Deccaraman M, Rani C, Mohanraj KP and Venkates K, 2010, Dissolution enhancement of Atorvastatin calcium by nanosuspension technology, *Journal of Pharmacy Research*, 3(8), 1903, ISSN: 0974-6943.
115. Patel GV, Patel VB, Pathak A and Rajput SJ, 2014, Nanosuspension of efavirenz for improved oral bioavailability: formulation optimization, *in-vitro*, *in-situ* and *in-vivo* evaluation, *Drug Development and Industrial Pharmacy*, 40(1), 80–91, ISSN: 1520-5762.
116. Wahlstrom JL, Warren CJ, Wene SP, Albin LA, Smith ME, Chiang PC, Ghosh S, and Roberds SL, 2007, Pharmacokinetic evaluation of a 1, 3-dicyclohexylurea

- nanosuspension formulation to support early efficacy assessment, *Nanoscale Research Letters*, 2(6), 291–296, ISSN: 1556-276X.
117. Zhao J, Luo L, Fu Q, Guo B, Li Y, Geng Y, Wang J and Zhang T, 2016, Improved oral bioavailability of Lacidipine using nanosuspension technology: inferior *in-vitro* dissolution and superior *in-vivo* drug absorption versus Lacipil<sup>®</sup>, *Current Drug Delivery*, 13(5), 764 – 773, ISSN: 1875-5704.
118. Anju Raju, Reddy AJ, Satheesh J and Jithan AV, 2014, Preparation and characterization of nevirapine oral nanosuspensions, *Indian Journal of Pharmaceutical Sciences*, 76(1), 62–71, ISSN: 0250-474X.
119. Xia D, Quan P, Piao H, Piao H, Sun S, Yin Y and Cui F, 2010, Preparation of stable nitrendipine nanosuspensions using the precipitation–ultrasonication method for enhancement of dissolution and oral bioavailability, *European Journal of Pharmaceutical Sciences*, 40(4), 325–334, ISSN: 0928-0987
120. Liu D, Xu H, Tian B, Yuan K, Pan H, Ma S, Yang X and Pan W, 2012, Fabrication of Carvedilol Nanosuspensions through the antisolvent precipitation–ultrasonication method for the improvement of dissolution rate and oral bioavailability, *AAPS PharmSciTech*, 13(1), 295-304, ISSN: 1530-9932.
121. Sahu BP and Das MK, 2014, Formulation, optimization and *in-vitro/in-vivo* evaluation of furosemide nanosuspension for enhancement of its oral bioavailability, *Journal of Nanoparticle Research*, 16(4), 2360, ISSN: 1572-896X.
122. Thadkala K, Nanam PK, Rambabu B, Sailu C and Aukunuru J, 2014, Preparation and characterization of amorphous ezetimibe nanosuspensions intended for enhancement of oral bioavailability, *International Journal of Pharmaceutical Investigation*, 4(3), 131–137, ISSN: 2230-9713.
123. Bhalekar MR, Upadhaya PG, Reddy S, Kshirsagar SJ and Madgulkar AR, 2014, Formulation and evaluation of acyclovir nanosuspension for enhancement of oral bioavailability, *Asian Journal of Pharmaceutics*, 8(2), 110-118, ISSN: 1998-409X.
124. Natarajan J, Subramanya NM, Venkatachalam S, Kuppusamy G and Kannan E, 2013, Studies on Physico-chemical and Pharmacokinetic Properties of Olanzapine through Nanosuspension, *Journal of Pharmaceutical Sciences and Research*, 5(10), 196 – 202, ISSN: 0975-1459.
125. Sawant KK, Patel MH and Patel K, 2016, Cefdinir nanosuspension for improved oral bioavailability by media milling technique: formulation, characterization and

- in vitro-in vivo* evaluations, Drug Development and Industrial Pharmacy, 42(5), 758-68, ISSN: 1520-5762.
126. Patel Y, Poddar A, and Sawant KK, 2014, Improved oral bioavailability of cefuroxime axetil utilizing nanosuspensions developed by media milling technique, Pharmaceutical Nanotechnology, 2(2), 75-86, ISSN: 2211-7393.
127. Nagajyothi N, Dhanalakshmi M, Thenmozhi S, Natarajan R and Rajendran N, 2014, Formulation and evaluation of pitavastatin nanosuspension, International Journal of Pharmacy and Life Sciences, 5(2), 3318-3324, ISSN: 0976-7126.
128. Shah SMH, Ullah F, Khan S, Shah SMM and Sadiq A, 2016, Combinative precipitation ultrasonication approach for fabrication for stable artemisinin nanosuspension, American-Eurasian Journal of Agriculture and Environmental Sciences, 16(2), 390-401, ISSN: 1818-6769.
129. Shinde SS and Hosmani AH, 2014, Preparation and evaluation of nanosuspensions for enhancing the dissolution of lornoxicam by antisolvent precipitation technique, Indo American Journal of Pharmaceutical Research, 4(1), 398-405, ISSN: 2231-6876.
130. Sahu BP and Das MK, 2014, Nanoprecipitation with sonication for enhancement of oral bioavailability of furosemide, Acta Poloniae Pharmaceutica, 71(1), 129-137, ISSN: 0001-6837.
131. Agarwal V and Bajpai M, 2014, Preparation and optimization of esomeprazole nanosuspension using evaporative precipitation–ultrasonication, Tropical Journal of Pharmaceutical Research, 13(4), 497-503, ISSN: 1596-9827.
132. Singh C, Tiwari V, Mishra CP, Shankar R, Sharma D and Jaiswal S, 2015, Fabrication of Cefpodoxime Proxetil nanoparticles by solvent antisolvent precipitation method for enhanced dissolution, International Journal of Research in Pharmaceutical and Nano Sciences, 4(4), 217 – 235, ISSN: 2319-9563.
133. Kakran M, Sahoo GN, and Lin Li, 2015, Fabrication of nanoparticles of Silymarin, Hesperetin and Glibenclamide by evaporative precipitation of nanosuspension for fast dissolution, Pharmaceutica Analytical Acta, 6(1), 326-332, ISSN: 2153-2435.
134. Esfandi EH, Ramezania V, Vatanara A, Najafabadi AR and Moghaddam SPH, 2014, Clarithromycin dissolution enhancement by preparation of aqueous nanosuspensions using sono-precipitation technique, Iranian Journal of Pharmaceutical Research, 13(3), 809-818, ISSN: 1726-6890.



135. Ghasemian E, Rezaeian B, Alaei S, Vatanara A and Ramezani V, 2015, Optimization of Cefixime Nanosuspension to improve drug dissolution, *Pharmaceutical Sciences*, 21(Suppl 1), 136-144, ISSN: 2383-2886.
136. Zhang Z, Le Y, Wang J, Zhao H and Chen J, 2012, Irbesartan drug formulated as nanocomposite particles for the enhancement of the dissolution rate, *Particuology*, 10(4), 462–467, ISSN: 1674-2001.
137. Suthar AK, Solanki SS and Dhanwani RK, 2011, Enhancement of dissolution of poorly water-soluble raloxifene hydrochloride by preparing nanoparticles, *Journal of Advanced Pharmacy Education and Research*, 2, 189-194, ISSN: 2249-3379.
138. Vishnu Priya P, Saritha BA, and Shravani T, 2016, Formulation and evaluation of Irbesartan nanosuspension by the precipitation method, *Der Pharmacia Lettre*, 8(2), 502-510, ISSN: 0975-5071.
139. Zulal NA and Lakshmi PK, 2015, Enhancement of solubility and bioavailability of Candesartan Cilexetil using natural p-glycoprotein inhibitors, *Tropical Journal of Pharmaceutical Research*, 14(1), 21-26, ISSN: 1596-9827.
140. Beg S, Sharma G, Katare OP and Singh B, 2013, Optimized positively charged self-nano-emulsifying systems of candesartan cilexetil with enhanced bioavailability potential, *Proceedings of the 3rd International Conference on Nanotek and Expo*, OMICS Group Conferences, Hampton Inn Tropicana, Las Vegas, NV, USA, pp. 296.
141. Acharya A, Kiran Kumar GB, Ahmed MG and Paudel S, 2016, A novel approach to increase the bioavailability of Candesartan Cilexetil by proniosomal gel formulation: *in-vitro* and *in-vivo* evaluation, *International Journal of Pharmacy and Pharmaceutical Sciences*, 8(1), 241-246, ISSN: 0975-1491.
142. Gurunath S, Nanjwade BK and Patila PA, 2014, Enhanced solubility and intestinal absorption of candesartan cilexetil solid dispersions using everted rat intestinal sacs, *Saudi Pharmaceutical Journal*, 22(3), 246–257, ISSN: 1319-0164.
143. Shaikh SM and Avachat AM, 2016, Enhancement of solubility and permeability of Candesartan Cilexetil by using different pharmaceutical interventions, *Current Drug Delivery*, 13(8), 346-353, ISSN: 1875-5704.
144. Kothawade PC, Belgamwar VS, and Deshmukh SA, 2013, Solid Dispersions of Telmisartan for enhancing solubility, dissolution rate and oral bioavailability, *Indo American Journal of Pharmaceutical Research*, 3(9), 7035-7045, ISSN: 2231-6876.

- 
145. Patel JM, Dhingani A, Garala K, Raval MK and Sheth NR, 2014, Design and development of solid nanoparticulate dosage forms of telmisartan for bioavailability enhancement by integration of experimental design and principal component analysis, *Powder Technology*, 258, 331–343, ISSN: 0032-5910.
  146. Cao Y, Shi LL, Cao QR, Yang M and Cui JH, 2016, *In-Vitro* characterization and oral bioavailability of organic solvent-free solid dispersions containing telmisartan, *Iranian Journal of Pharmaceutical Research*, 15(2), 385-394, ISSN: 1726-6890.
  147. Padia N, Shukla A, and Shelat P, 2015, Development and characterization of telmisartan self-micro emulsifying drug delivery system for bioavailability enhancement, *Journal of Scientific and Innovative Research*, 4(3), 153-164, ISSN: 2320 – 4818.
  148. Ahmad J, Kohli K, and Showkat RM, 2011, Formulation of self-nano emulsifying drug delivery system for telmisartan with improved dissolution and oral bioavailability, *Journal of Dispersion Science and Technology*, 32(7), 958-968, ISSN: 0193-2691.
  149. Charman SA, Charman WN, Rogge MC, Wilson TD, Dutko FJ and Pouton CW, 1992, Self-emulsifying drug delivery systems: formulation and biopharmaceutic evaluation of an investigational lipophilic compound, *Pharmaceutical Research*, 9(1), 87-93, ISSN: 1573-904X.
  150. Miao Y and Ren L, 2016, Characterization and evaluation of self-nano emulsifying sustained-release pellet formulation of ziprasidone with enhanced bioavailability and no food effect, *Drug Delivery*, 23(7), 2163-2172, ISSN: 1521-0464.
  151. Banerjee S, Ravishankar K and Prasad RY, 2016, Formulation development and systematic optimization of stabilized ziprasidone hydrochloride capsules devoid of any food effect, *Pharmaceutical Development and Technology*, 21(7) 775-786, ISSN: 1097-9867.
  152. Thombre AG, Caldwell WB, Friesen DT, McCray SB and Sutton SC, 2012, Solid nanocrystalline dispersions of ziprasidone with enhanced bioavailability in the fasted state, *Molecular Pharmaceutics*, 9(12), 3526-3534, ISSN: 1543-8384.
  153. Miao Y, Chen G, Ren L, Ouyang P, 2016, Preparation and evaluation of ziprasidone–phospholipid complex from sustained-release pellet formulation with enhanced bioavailability and no food effect, *Journal of Pharmacy and Pharmacology*, 68(2), 185–194, ISSN: 2042-7158.
-

154. Robert B, Bernd K, Muller RH and Peters K (1999) *Pharmaceutical nanosuspensions for medicament administration as systems with increased saturation solubility and rate of solution*, US Patent 5858410.
155. Chen MJ, Hui HW, Lee T, Paul K and Surapaneni S (2011) *Nanosuspension of a poorly soluble drug via microfluidization process*, US Patent 20110124702.
156. Binner JGP L (2010) *Method for concentrating nanosuspensions*, EP1912898.
157. Ferreiro MG, Dunmann C, Kroehne L and Voigt A (2012) *Nano-particulate compositions poorly soluble compounds*, US Patent 20120058151.
158. Amarnath Suseendharnath, Venkatesh Madhavacharya Joshi, Sunil Reddy Beeram, Venkateswarlu Vobalaboina, Harshal Prabhakar Bhagwatwar and Manish Chawla (2012) *Candesartan pharmaceutical compositions*. WO2012033983 A2
159. Nakatani M, Takeshi S, Ohki T and Toyoshima K (2004) *Solid Telmisartan Pharmaceutical Formulations*. US Patent 20040110813A1.
160. Shah JC, Shah PS, Wisniecki P and Wagner DR (2008) *Injectable depot formulations and methods for providing sustained release of nanoparticle compositions*, US Patent 20080193542A1.

**EXPERIMENTAL**



## CHAPTER – 3

### Experimental

#### 3.1 List of materials used for the study

**TABLE 3.1: List of materials used for the study**

Use	Material	Grade	Manufacturer
Drugs	Candesartan Cilexetil (CC)	USP	Gift Sample from Alembic Research Centre, Vadodara
	Telmisartan (TM)	USP	Gift Sample from Alembic Research Centre, Vadodara
	Ziprasidone Hydrochloride Monohydrate (ZH)	USP	Gift Sample from Amneal Pharmaceuticals, Ahmedabad
Stabilizer	Poloxamer 188	AR Grade	Gift Sample from Astron Research Centre, Ahmedabad
	Poloxamer 407	AR Grade	Gift Sample from Astron Research Centre, Ahmedabad
	Polyvinyl alcohol	AR Grade	Loba Chemie Pvt. Ltd., Mumbai
	PVP K30	AR Grade	S. D. Fine Chemicals, Mumbai
	Sodium Lauryl Sulphate	AR Grade	Himedia Laboratories Pvt. Ltd., Mumbai
Solvent	Dichloromethane	AR Grade	Chemdyes Corporation, Rajkot
	Ethanol	AR Grade	Shree Chaltan Vibhag Khand Udyog Sahkari Mandli Ltd., Surat
	Methyl alcohol	AR Grade	Finnar Chemicals, Ahmedabad
	2-Propanol	AR Grade	ACS Chemicals, Ahmedabad
	Butanol	AR Grade	Astron Chemicals, Ahmedabad
	Ethyl Acetate	AR Grade	ACS Chemicals, Ahmedabad
	Dimethyl sulphoxide	AR Grade	Chemdyes Corporation, Rajkot
Cryoprotectant	Mannitol	AR Grade	Merck Specialities Pvt. Ltd., Mumbai

### 3.2 List of equipments used for the study

**TABLE 3.2: List of equipments used for the study**

Sr. No.	Equipments	Model/ Make
1	Digital weighing balance	Shimadzu AUX 220, Japan
2	Overhead stirrer	Remi Equipments Pvt. Ltd., India
3	Bath sonicator	Bransone Ultrasonic Corporation, USA
4	Probe sonicator	Frontline Electronics and Machinery Pvt. Ltd, India
5	UV spectrophotometer	Shimadzu UV 1800, Japan
6	Cooling microcentrifuge C24BL	Remi Equipments Pvt. Ltd., India
7	FTIR spectrophotometer	Shimadzu 8400, Japan
8	Particle sizr analysier	Zetatrac, Microtrac, USA
9	Magnetic stirrer 2 LH	Remi Equipments Pvt. Ltd., India
10	Digital Water bath	Bio-Tech, India
11	Differential scanning calorimeter	Shimadzu DSC, TA-60WS, Japan
12	Scanning electron microscope	ZEISS International, Germany
13	Lyophilizer	Thermo Scientific, Japan

### 3.3 Scanning and calibration curve preparation of drugs

#### 3.3A Scanning and calibration curve preparation of candesartan cilexetil

For estimation of drug content in candesartan cilexetil nanosuspension, a calibration curve was prepared in methanol as candesartan cilexetil is having a solubility in methanol. [81] For estimation of cumulative percentage drug release of candesartan cilexetil nanosuspension, 0.05M phosphate buffer, pH 6.5 containing 0.7% v/v polysorbate 20 was taken as dissolution media. [161]

##### 3.3A.1 Scanning and calibration curve preparation of candesartan cilexetil in methanol

A standard stock solution (100 µg/ml) of candesartan cilexetil was prepared by accurately weighing 10 mg of candesartan cilexetil and dissolved in 5 ml of methanol in a 100 ml volumetric flask. It was sonicated for 5 mins and the volume was made up to 100 ml with methanol. From the standard stock solution, candesartan cilexetil (10 µg/ml) solution was prepared in methanol and UV-scan was taken between a wavelength range of 200 - 400 nm and a wavelength showing maximum absorbance was selected as  $\lambda_{\max}$  for further analytical work.

From the standard stock solution (100 µg/ml), appropriate aliquots were taken into different volumetric flasks of 10 ml and made up to 10 ml with methanol, so as to get the concentration of 5-30 µg/ml. The absorbance of these solutions was measured at selected  $\lambda_{\max}$ . The experiment was performed in triplicate to validate the calibration curve. A calibration curve was constructed by plotting absorbance vs. concentration (µg/ml).

### **3.3A.2 Scanning and calibration curve preparation of candesartan cilexetil in 0.7% v/v polysorbate 20 in 0.05 M phosphate buffer, pH 6.5.**

A standard stock solution (100 µg/ml) of candesartan cilexetil was prepared by accurately weighing 10 mg of candesartan cilexetil and dissolved in 5 ml of 0.05M phosphate buffer, pH 6.5 containing 0.7% v/v polysorbate 20 in a 100 ml volumetric flask. It was sonicated for 5 mins and the volume was made up to 100 ml with 0.05M phosphate buffer, pH 6.5 containing 0.7% v/v polysorbate 20. From the standard stock solution, candesartan cilexetil (10 µg/ml) solution was prepared in 0.05M phosphate buffer, pH 6.5 containing 0.7% v/v polysorbate 20 and UV-scan was taken between a wavelength range of 200-400 nm and a wavelength showing maximum absorbance was selected as  $\lambda_{\max}$  for further analytical work.

From the standard stock solution (100 µg/ml), appropriate aliquots were taken into different volumetric flasks of 10 ml and made up to 10 ml with 0.05 M phosphate buffer, pH 6.5 containing 0.7% v/v polysorbate 20, so as to get the concentration of 4-16 µg/ml. The absorbance of these solutions was measured at selected  $\lambda_{\max}$ . The experiment was performed in triplicate to validate the calibration curve. A calibration curve was constructed by plotting absorbance vs. concentration (µg/ml).

### **3.3B Scanning and calibration curve preparation of telmisartan**

For estimation of drug content in telmisartan nanosuspension, a calibration curve was prepared in methanol as telmisartan is having a solubility in methanol. [93] For estimation of cumulative percentage drug release of telmisartan nanosuspension, phosphate buffer, pH 7.5 was taken as dissolution media. [162]

#### **3.3B.1 Scanning and calibration curve preparation of telmisartan in methanol**

A standard stock solution (100 µg/ml) of telmisartan was prepared by accurately weighing 10 mg of telmisartan and dissolved in 5 ml of methanol in a 100 ml volumetric flask. It

---

was sonicated for 5 mins and the volume was made up to 100 ml with methanol. From the standard stock solution, telmisartan (10 µg/ml) solution was prepared in methanol and UV-scan was taken between a wavelength range of 200- 400 nm and a wavelength showing maximum absorbance was selected as  $\lambda_{\max}$  for further analytical work.

From the standard stock solution (100 µg/ml), appropriate aliquots were taken into different volumetric flasks of 10 ml and made up to 10 ml with methanol, so as to get the concentration of 2-20 µg/ml. The absorbance of these solutions was measured at  $\lambda_{\max}$ . The experiment was performed in triplicate to validate the calibration curve. A calibration curve was constructed by plotting absorbance vs. concentration (µg/ml).

### **3.3B.2 Scanning and calibration curve preparation of telmisartan in phosphate buffer, pH 7.5.**

A standard stock solution (100 µg/ml) of telmisartan was prepared by accurately weighing 10 mg of telmisartan and dissolved in 5ml of phosphate buffer, pH 7.5 in a 100 ml volumetric flask. It was sonicated for 5 mins and the volume was made up to 100 ml with phosphate buffer, pH 7.5. From the standard stock solution, telmisartan (10 µg/ml) solution was prepared in phosphate buffer, pH 7.5 and UV-scan was taken between a wavelength range of 200-400 nm and a wavelength showing maximum absorbance was selected as  $\lambda_{\max}$  for further analytical work.

From the standard stock solution (100 µg/ml), appropriate aliquots were taken into different volumetric flasks of 10 ml and the volume was made up to 10 ml with phosphate buffer, pH 7.5, so as to get the concentration of 2-20 µg/ml. The absorbance of these solutions was measured at selected  $\lambda_{\max}$ . The experiment was performed in triplicate to validate the calibration curve. A calibration curve was constructed by plotting absorbance vs. concentration (µg/ml).

### **3.3C Scanning and calibration curve preparation of ziprasidone hydrochloride**

For estimation of drug content in ziprasidone hydrochloride nanosuspension, a calibration curve was prepared in methanol as ziprasidone hydrochloride is having a solubility in methanol. [105] For estimation of cumulative percentage drug release of ziprasidone hydrochloride nanosuspension, 0.05M sodium phosphate buffer, pH 7.5 containing 2% w/w sodium dodecyl sulfate (SDS) it was taken as dissolution media. [163]



### **3.3C.1 Scanning and calibration curve preparation of ziprasidone hydrochloride in methanol**

A standard stock solution (100  $\mu\text{g/ml}$ ) of ziprasidone hydrochloride was prepared by accurately weighing 10 mg of ziprasidone hydrochloride and dissolved in 5 ml of methanol in a 100 ml volumetric flask. It was sonicated for 5 mins and the volume was made up to 100 ml with methanol. From the standard stock solution, ziprasidone hydrochloride (10  $\mu\text{g/ml}$ ) solution was prepared in methanol and UV-scan was taken between a wavelength range of 200-400 nm and a wavelength showing maximum absorbance was selected as  $\lambda_{\text{max}}$  for further analytical work.

From the standard stock solution (100  $\mu\text{g/ml}$ ), appropriate aliquots were taken into different volumetric flasks of 10 ml and made up to 10 ml with methanol, so as to get the concentration of 10-60  $\mu\text{g/ml}$ . The absorbance of these solutions was measured at  $\lambda_{\text{max}}$ . The experiment was performed in triplicate to validate the calibration curve. A calibration curve was constructed by plotting absorbance vs. concentration ( $\mu\text{g/ml}$ ).

### **3.3C.2 Scanning and calibration curve preparation of ziprasidone hydrochloride in 0.05M sodium phosphate buffer, pH 7.5 containing 2%w/w SDS**

A standard stock solution (100  $\mu\text{g/ml}$ ) of ziprasidone hydrochloride was prepared by accurately weighing 10 mg of ziprasidone hydrochloride and dissolved in 5 ml of 0.05M sodium phosphate buffer, pH 7.5 containing 2%w/w SDS in a 100 ml volumetric flask. It was sonicated for 5 mins, the volume was made up to 100 ml with 0.05M sodium phosphate buffer, pH 7.5 containing 2%w/w SDS. From the standard stock solution, ziprasidone hydrochloride (10  $\mu\text{g/ml}$ ) solution was prepared in 0.05M sodium phosphate buffer, pH 7.5 containing 2%w/w SDS and UV-scan was taken between a wavelength range of 200-400 nm and a wavelength showing maximum absorbance was selected as  $\lambda_{\text{max}}$  for further analytical work.

From the standard stock solution (100  $\mu\text{g/ml}$ ), appropriate aliquots were taken into different volumetric flasks of 10ml and the volume was made up to 10 ml with 0.05M sodium phosphate buffer, pH 7.5 containing 2%w/w SDS, so as to get the concentration of 10-60  $\mu\text{g/ml}$ . The absorbance of these solutions was measured at selected  $\lambda_{\text{max}}$ . The experiment was performed in triplicate to validate the calibration curve. A calibration curve was constructed by plotting absorbance vs. concentration ( $\mu\text{g/ml}$ ).

### 3.4 Selection of solvent and antisolvent

The solubility of selected drugs was studied in different solvents and their combinations. Selection of good and poor solvent was done based upon the solubility of the drug in respective solvents. About 10 mg of drug was added to 10 ml of solvent in specific gravity bottles. This amount was sufficient to obtain a saturated solution. These specific gravity bottles were shaken at 100 RPM for 24 h at 25°C by keeping in a cryostatic constant temperature reciprocating shaker bath. The bottles were then opened and solutions were filtered with the help of Whatman filter paper (0.22  $\mu\text{m}$ ). The absorbance of the solution was measured at the respective  $\lambda_{\text{max}}$  of the drugs. This method was repeated for three times. [164]

### 3.5 Preparation of nanosuspension by antisolvent precipitation-ultrasonication method

Nanosuspension was prepared by the precipitation–ultrasonication method. The drug was dissolved in methanol by sonication for 5 mins at room temperature. Different stabilizers were dissolved in water to obtain a series of antisolvent. Both solutions were passed through a 0.45 $\mu\text{m}$  filter. The antisolvent was cooled to 3°C in an ice-water bath. Then, drug solution was quickly introduced by means of a syringe positioned with the needle directly into stabilizer solution into 40 ml of the pre-cooled antisolvent at different stirring speed under overhead stirrer to allow the volatile solvent to evaporate at room temperature for 4-5 hours. After precipitation of antisolvent, the sample was immediately transferred to a test tube and was treated with an ultrasonic probe at different time lengths (in mins). The probe with a tip diameter of 6 mm was immersed in the liquid, resulting in the wave traveling downwards and reflecting upwards. Batch size for preparation of nanosuspension was taken 40 ml.[119]

### 3.6 Lyophilization of nanosuspension of optimized batch

Nanosuspension was converted into the dry powder using mannitol (1:1, Total solid: Cryoprotectant) as a cryoprotectant by using lyophilizer. In lyophilization process sample was kept in the chamber and temperature maintained at -80°C for 8 h. After the 6-8 h nanosuspension was converted into the dry powder and removed from the chamber and placed in an airtight container for further work.

### 3.7 Selection of stabilizer

Different stabilizers like Polyvinyl Alcohol, PVP K-30, Sodium Lauryl Sulphate, Poloxamer 188 and Poloxamer 407 were screened by preparing nanosuspensions and measuring their saturation solubility, mean particle size, polydispersity index (PDI) and zeta potential for selection of the best one which can be utilized for further research work. [165]

### 3.8 Drug-excipient compatibility study

Studies of drug-excipient compatibility represent an important phase in the preformulation stage of the development of all dosage forms. The potential physical and chemical interactions between drugs and excipients can affect the chemical, physical, therapeutical properties and stability of the dosage form. FTIR and DSC study were selected for checking of drug-excipient compatibility study.

#### 3.8.1 Fourier transformed infrared (FTIR) spectroscopy

FTIR spectroscopy was conducted using a Shimadzu FTIR 8400 Spectrophotometer (Shimadzu, Tokyo, Japan) and the spectrum was recorded in the wavelength region of 4000–400  $\text{cm}^{-1}$ . The procedure consisted of dispersing sample (drug, stabilizer, physical mixture) by KBr pellet method. The pellet was placed in the light path and the spectrum was recorded.

#### 3.8.2 Differential scanning calorimetry (DSC)

DSC was performed using DSC-60 (Shimadzu, Tokyo, Japan) calorimeter to study the thermal behavior of the sample (drug, stabilizer, physical mixture and lyophilized nanosuspension). The instrument comprised of the calorimeter (DSC 60), flow controller (FCL60), the thermal analyzer (TA 60WS) and operating software (TA 60). The samples were heated in hermetically sealed aluminum pans under air atmosphere at a scanning rate of 10°C/min from 30°C to 330°C in an air atmosphere. Empty aluminum pan was used as a reference.

### 3.9 Plackett-Burman Design [166]

The Plackett-Burman design is suitably used to screen a large number of factors believed to be affecting important product characteristics or attributes and is generally used during the initial phase of the study. By review of the literature, five factors were selected to affect the quality of nanosuspension. To identify which factor has its prominent effect on quality, stability as well as the efficacy of the nanosuspension, the plackett-burman design was used. A total of 8 experiments (preliminary screening formulations) were generated for screening of five independent factors namely amount of drug in mg ( $X_1$ ), amount of stabilizer in mg ( $X_2$ ), solvent to antisolvent volume ratio ( $X_3$ ), stirring speed in rpm ( $X_4$ ) and sonication time in min ( $X_5$ ) for the all three drugs. Saturation solubility in  $\mu\text{g/ml}$  ( $Y_1$ ) and mean particle size in nm ( $Y_2$ ) were selected as dependent factors.

The net effect of an individual factor was calculated from the value of evaluated parameters from following equations,

$$\text{Effect of } X_1 = [(Y_1+Y_4+Y_6+Y_7)-(Y_2+Y_3+Y_5+Y_8)]/8 \quad \text{Eq...}(3.1)$$

$$\text{Effect of } X_2 = [(Y_1+Y_2+Y_5+Y_7)-(Y_3+Y_4+Y_6+Y_8)]/8 \quad \text{Eq...}(3.2)$$

$$\text{Effect of } X_3 = [(Y_1+Y_2+Y_3+Y_6)-(Y_4+Y_5+Y_7+Y_8)]/8 \quad \text{Eq...}(3.3)$$

$$\text{Effect of } X_4 = [(Y_2+Y_3+Y_4+Y_7)-(Y_1+Y_5+Y_6+Y_8)]/8 \quad \text{Eq...}(3.4)$$

$$\text{Effect of } X_5 = [(Y_1+Y_3+Y_4+Y_5)-(Y_2+Y_6+Y_7+Y_8)]/8 \quad \text{Eq...}(3.5)$$

After getting net effect of individual parameters two key parameters were identified which had maximum effect on product characteristics. These two parameters can be selected for product optimization by factorial design and other three parameters can be optimized by trial and error method.

### 3.10 Optimization of other preliminary parameters

Preliminary parameters were optimized by varying one parameter at a time while keeping others constant, so that effect of varied parameters could be evaluated. Each batch was repeated thrice ( $n=3$ ) for the confirmation of repeatability. The parameters were optimized to achieve minimum particle size and maximum saturation solubility. Optimized parameters were,

- Solvent to antisolvent volume ratio (1:4, 1:6, 1:8),
- Amount of stabilizer (30 mg, 40 mg, 50 mg),
- Stirring speed (800RPM, 1000RPM, 1200RPM),
- Sonication time (10 min, 20 min, 30 min) etc.

### 3.11 Factorial design for optimization of key parameters

A 3<sup>2</sup> factorial design was applied for optimization of key parameters of the drugs, like for candesartan cilexetil amount of drug in mg and solvent to antisolvent volume ratio, [167,168] while for telmisartan and ziprasidone hydrochloride amount of drug in mg and stirring speed. [61] Both particle size and saturation solubility, [additionally CPR at 15 mins in ziprasidone hydrochloride nanosuspension] important features of nanosuspension considered to play a significant role in the formulation performance, were taken as dependent parameters in this study. Multiple regression analysis, contour plots and 3D response surface plots were used to study the main and interaction effects of the variables on the dependent factors. The numbers of experiments required in factorial design studies were dependent on the number of independent variables selected and the number of levels at which they were studied. The response was measured for each trial and then either simple linear equation (1), or interactive equation (2) or quadratic (3) model was fitted by carrying out multiple regression analysis and F-statistics to identify statistically significant terms.

$$Y = b_0 + b_1X_1 + b_2X_2 \quad \text{Eq...}(3.6)$$

$$Y = b_0 + b_1X_1 + b_2X_2 + b_{12}X_1X_2 \quad \text{Eq...}(3.7)$$

$$Y = b_0 + b_1X_1 + b_2X_2 + b_{11}X_1^2 + b_{22}X_2^2 + b_{12}X_1X_2 \quad \text{Eq...}(3.8)$$

Where, Y is the dependent variable, while b<sub>0</sub> is the intercept, b<sub>i</sub> (b<sub>1</sub> and b<sub>2</sub>), b<sub>ij</sub> (b<sub>12</sub>) represents the regression coefficient for the second order polynomial equation and X<sub>i</sub> represents the levels of independent formulation variables. Mathematical modeling was carried out by using equation (3.8) to obtain a second order polynomial equation.[169] The values of dependent variable obtained at various levels of two independent variables (X<sub>1</sub> and X<sub>2</sub>) were subjected to multiple regressions to yield a second order polynomial equation. The main effects of X<sub>1</sub> and X<sub>2</sub> represent the average result of changing one variable at a time from its low to high value. The interaction (X<sub>1</sub>X<sub>2</sub>) shows how the particle size and saturation solubility changed when two variables were simultaneously changed.

### 3.12 Checkpoint analysis

A checkpoint analysis was performed to confirm the utility of established response surface plots and contour plots in the preparation of nanosuspension. Values of independent variables ( $X_1$  and  $X_2$ ) were selected and corresponding values of dependent variables were calculated by substituting the values in the reduced polynomial equation. Nanosuspensions were prepared experimentally by taking the amounts of the independent variables ( $X_1$  and  $X_2$ ) on the same checkpoints. Checkpoint cum optimized batch was prepared three times and mean values were determined. The difference of theoretically computed values of particle size, as well as saturation solubility and the mean values of experimentally obtained for both responses, were compared.

### 3.13 Evaluation of nanosuspensions

#### 3.13.1 Particle size and PDI

Mean particle size and size distribution (polydispersity index) of the prepared nanosuspension was determined by using Zetasizer [Zetatrak, Microtrac, Japan] which follows the principle of light diffraction, also called Photon Correlation Spectroscopy (PCS). Prior to the measurement, the samples were appropriately diluted with water to a suitable scattering intensity and re-dispersed by shaking before measurement.[129]

#### 3.13.2 Zeta potential

The Zeta potential is a measure of the electric charge at the surface of the particles, indicating the physical stability of colloidal systems. The zeta potential values higher than  $|30\text{mV}|$  indicate long-term electrostatic stability of aqueous dispersions. In this study, the Zeta Potential was assessed by determining the electrophoretic mobility of the particles using Zetasizer [Zetatrak, Microtrac, Japan].[129]

#### 3.13.3 Drug content

An aliquot (1ml) of the prepared nanosuspension was diluted in methanol and filtered with a  $0.2\ \mu\text{m}$  filter. Total drug content was determined by UV spectrophotometer at  $\lambda_{\text{max}}$  of the drug. Formula: [170]

$$\text{Total Drug Content} = \frac{(\text{Total volume of nanosuspension} \times \text{amount of drug in aliquot})}{\text{Volume of aliquot}} \quad \text{Eq...}(3.9)$$

### 3.13.4 Saturation solubility

The saturation solubility of prepared nanosuspension was performed by filling it in a vial and kept for 48 h stirring with the help of magnetic stirrer at 100 RPM to ensure saturation. Then 2 ml of nanosuspension was filled in an eppendorf tube and centrifuged at 10,000 RPM for 30 minutes. The supernatant was filtered through a 0.2 $\mu$ m syringe filter and analyzed by UV-visible spectrophotometer [UV-1800, Shimadzu, Japan] at  $\lambda_{\text{max}}$  of the drug after suitable dilution with dissolution media which was used as a blank. Triplicate analysis of each sample was carried out. By using the calibration curve, saturation solubility was calculated. [171]

### 3.13.5 *In-vitro* dissolution study

An *in-vitro* dissolution study was performed using USP 24 paddle instrument (ELECTROLAB TDT-06P). The dissolution medium was taken as per Table 3.3. To minimize foaming of the medium during the experiment, the medium was gently transferred into the dissolution vessel. Dissolution was performed at 37°C, using a paddle speed specified in following Table 3.3. Nanosuspension equivalent to a dose of the drug was added to the dissolution vessels. 5 ml samples were withdrawn at a specific time interval of 2, 4, 6, 8, 10, 15, 30, 45, 60 mins and filtered immediately through 0.2  $\mu$ m syringe filter and analyzed spectrophotometrically. Subsequently, 5 ml of fresh medium was added to the dissolution vessel. The experiments were performed in triplicate and the mean values were reported.[172]

**TABLE 3.3: Dissolution conditions for nanosuspensions [161–163]**

Dissolution Condition	Candesartan Cilexetil Nanosuspension	Telmisartan Nanosuspension	Ziprasidone Hydrochloride Nanosuspension
Dissolution media	0.05M Phosphate buffer pH 6.5, containing 0.7% v/v Polysorbate 20	Phosphate buffer pH 7.5	0.05M Sodium Phosphate buffer, pH 7.5 containing 2% w/w SDS
Volume of Dissolution media	250	900	900
Speed in RPM	50	75	75
Sampling Intervals	2, 4, 6, 8, 10, 15, 30, 45, 60mins	2, 4, 6, 8, 10, 15, 30, 45, 60mins	2, 4, 6, 8, 10, 15, 30, 45, 60mins
Dose of drug	16mg	40mg	20mg

### 3.13.6 Scanning electron microscopy (SEM)

The surface characteristics of lyophilized nanosuspensions of all three drugs were studied by Scanning electron microscopy (EVO-18, ZEISS, Germany) at 3kx to 28kx. The samples were mounted on double-sided carbon adhesive tape that has previously been secured on brass stubs and then subjected to gold coating by sputter coater, using process current of 10 mA for 4mins. The accelerating voltage was 15 kV.

### 3.13.7 Residual solvent by gas – chromatography (GC)

Residual solvents are considered as critical impurities because they may cause serious toxicity and safety issues. For the control of residual solvents, ICH Q<sub>3</sub>C guideline provides specific criteria for Class-1, Class-2, and Class-3 solvents. [173]

Residual solvent in lyophilized nanosuspension was analyzed by gas chromatography using head-space sampler. For that accurately weighed 50 mg lyophilized nanosuspension was dissolved in dimethylformamide (DMF). Subsequently, the prepared solution was analyzed using gas chromatography. GC-HS chromatograms of a standard solution of methanol and lyophilized nanosuspension were taken. Retention time for a peak corresponds to the methanol in a standard solution of methanol and sample solution of lyophilized nanosuspension were obtained and compared.

- **Method of Headspace gas chromatography**

The analysis was carried out by using Perkin Elmer's Clarus 500 gas chromatography with flame ionization detector. Dimethylformamide (DMF) was used as diluents.

- **Preparation of blank solution**

Blank solution was prepared by transferring 5 ml of diluent into a headspace vial, Polytetrafluoroethylene (PTFE) butyl septum was closed and sealed with aluminum crimp cap.

- **Preparation of standard solution**

Accurately measured 10 µl of methanol was mixed in dimethyl sulfoxide and volume was made to 5 ml with dimethyl sulfoxide. This solution was transferred into a headspace vial, PTFE butyl septum was closed and sealed with aluminum crimp cap.



---

- **Preparation of sample solution**

Accurately weighed 50 mg of lyophilized nanosuspension of candesartan cilexetil was transferred accurately into headspace vial and 5 ml of dimethyl sulfoxide was added to it. PTFE butyl septum was closed and sealed with aluminum crimp cap. It was vortexed for 5 mins.

- **Procedure for gas chromatography**

By following above-mentioned procedure, 1 vial for a blank solution, 3 vials for the standard solution, and 2 vials for the sample was prepared. These sealed vials were placed in the sample magazine and headspace analyzer was started to run. Peaks were measured and chromatograms were recorded. Amount of residual methanol was calculated by using following formula : [174,175]

$$\text{Amount of organic solvent (ppm)} = (A_T / A_S) \times (W / T) \times 10^6 \quad \text{Eq...}(3.10)$$

Where,

- $A_T$  = Average area count of peak in the sample solution chromatogram.
- $A_S$  = Average area count of the peak in the standard solution chromatogram.
- $W$  = Concentration in mg of standard sample
- $T$  = Weight in mg of test sample

**Instrument: Perkin Elmer Clarus 500**

**Column: ZB-624 30m\*0.53mm\*3um**

**Oven program**

- Initial Temp : 35°C, Hold 3.00 min
- Rate : 25 deg/min to 120°C holds for 5.00 min
- Split ratio : 20:1
- Detector : 250°C
- Injector temperature : 150°C
- Carrier gas : N<sub>2</sub>

**Headspace condition**

- Oven : 90°C
- Needle : 95°C
- Transfer Line : 100°C
- Thermostat : 30 min

**3.13.8 Accelerated Stability study as per ICH Guidelines**

Accelerated stability studies of lyophilized nanosuspension were conducted at  $25 \pm 2^\circ\text{C}$  and  $60 \pm 5\%$  RH for 6 months as per ICH guidelines. Lyophilized nanosuspension was encapsulated in hard gelatin capsules. At periodic time intervals (0, 1, 3 and 6 months), the samples were withdrawn and analyzed for particle size, saturation solubility, % CPR at 2 min and % w/w of drug content. [176]

**3.14 Bioavailability study****3.14.1 Study objective**

- ✓ To study the oral bioavailability study of poorly water-soluble selected drugs after converting it into nanosuspension
- ✓ To study possible pharmacokinetic parameters of drugs formulated in nanosuspension dosage form.
- ✓ To compare the bioavailability of optimized batch of nanosuspensions with available marketed preparation.

**3.14.2 Experimental procedure**

The total study protocol was divided into three parts each for one selected drug.

- ✓ **Part –A: Candesartan Cilxetil Nanosuspension**
- ✓ **Part –B: Telmisartan Nanosuspension**
- ✓ **Part –C: Ziprasidone Hydrochloride Nanosuspension**

**3.14.3 Selection of animals**

*Wister* rats of either sex with an average weight of  $200 \pm 20$  gm or age ~ 10 weeks (on the day of study) were procured in order to investigate the pharmacokinetic behavior of nanosuspensions. The study was approved by Institutional Ethics Committee of Department of Pharmaceutical Sciences, Saurashtra University, Rajkot, Gujarat, India

(CPCSEA No: IAEC/DPS/SU/1508, Dated: 04/06/2015) and the guidelines were followed throughout the study. All the rats were acclimatized to a temperature ( $20 \pm 2^\circ\text{C}$ ) and relative humidity ( $45 \pm 15\% \text{RH}$ ), with a 12 hr light/dark cycle over a period of 5 days prior to administration of the drug. During this acclimatization period, the animals were carefully observed to ensure their good health and suitability for inclusion in the study. For all rats, a standard laboratory diet (Pranav Agromart Ltd, Baroda, India) and domestic mains tap water were available ad libitum. The animals were disconnected from the diet at least 12 h before dosing. During study periods, rats were housed singly in polypropylene and stainless steel cages. [177,178] One group of rats for optimized nanosuspension formulation and one group of rats for marketed formulation were taken.

- ✓ Group-I: 6 Rats for the optimized nanosuspension formulation
- ✓ Group-II: 6 Rats for the marketed formulation

#### 3.14.4 Dosing Details

**TABLE 3.4: Dosing details for bioavailability study**

Group	Treatment	Animals Per group	Blood collection time points (h)	Dose (mg/kg) [179]	Route of administration
1	Candesartan Cilexetil Nanosuspension (CCNS)	6	0.25,0.5,1,2, 4, 6,8,12,24	1.65mg/kg	Oral
2	Marketed formulation of Candesartan Cilexetil (Atacand®) (CCMKT)	6	0.25,0.5,1,2, 4,6,8,12,24	1.65mg/kg	Oral
3	Telmisartan Nanosuspension (TMNS)	6	0.25,0.5,1,2, 4,6,8,12,24	4.11 mg/kg	Oral
4	Marketed formulation of Telmisartan (Inditel® 40) (TMMKT)	6	0.25,0.5,1,2, 4,6,8,12,24	4.11 mg/kg	Oral
5	Ziprasidone Hydrochloride Nanosuspension (ZHNS)	6	0.25,0.5,1,2, 4,6,8,12	2.05mg/kg	Oral
6	Marketed formulation of Ziprasidone Hydrochloride (Zipsydon® 20) (ZHMKT)	6	0.25,0.5,1,2, 4,6,8,12	2.05mg/kg	Oral

#### 3.14.4 Collection of blood samples

A blood sample was collected from the retro-orbital plexus of anesthetized rats with diethyl ether. For zero time analysis, a blood sample was withdrawn before administration of the drug and after administration, blood samples were collected at the specific intervals. Samples were collected as per above-mentioned Table 3.4 for each group. Blood was

collected in such a quantity to get 0.5 ml plasma from it at each time point. The collected sample was analyzed by the suitable analytical method. Maximum blood concentration ( $C_{max}$ ) and time to achieve  $C_{max}$  ( $T_{max}$ ) was calculated from concentration-time curve data. The area under the concentration-time curve ( $AUC_{0-24}$ ) was calculated to the last blood concentration. These parameters and other pharmacokinetic parameters were calculated by Microsoft Excel<sup>®</sup> version 2013 (Microsoft Corporation, Washington, USA). Reduction of dose to reach  $C_{max}$  of the marketed formulation was also calculated.

#### 3.14.6A Bioanalytical method for candesartan cilexetil nanosuspension

A Liquid Chromatograph Mass Spectroscopy (LC/MS/MS) system equipped with Shimadzu LC SOLUTION (5.53 SP3C) was employed for the present investigation. The system consisted of Shimadzu LC-20ADvp as a binary solvent delivery system, Shimadzu SIL-20AC Auto Sampler, Shimadzu HPLC-ESI-MS/MS injector and MS/MS 8030 detector as a source of detection.

- **Chromatographic conditions**

Mobile phase	: Methanol and Acetonitrile (5 mM Ammonium Acetate in Water: Acetonitrile 10:90 % v/v)
Column	: Zodiac CN <sup>®</sup> C18 (5 $\mu$ m*250 mm*4.6 mm)
Flow rate	: 0.5 ml/min
Injection volume	: 10 $\mu$ l
Runtime	: 7 min

- **Preparation of mobile phase**

For preparing a mobile phase, in measuring cylinder 900 ml of HPLC grade acetonitrile and 100 ml of 5 mM ammonium acetate in water was taken, then transferred into a reagent bottle and mixed the contents thoroughly and stored at ambient temperature. This solution was used within 3 days from the date of preparation.

- **Preparation of Internal Standard (ISTD) solutions**

Carbamazepine was weighed accurately equivalent to 2 mg of carbamazepine and the appropriate volume of methanol was added to make a final concentration of carbamazepine equivalent to 0.1 mg/ml accounting for its potency and the actual amount weighed. The

solution was stored in a refrigerator at  $5 \pm 3^\circ\text{C}$  and equilibrated to room temperature prior to use. The solution was used within 7 days from the date of preparation.

10.0  $\mu\text{l}$  of ISTD stock solution, 0.1 mg/ml was pipetted out in 10.0 ml volumetric flask and made up the volume to 10.0ml with methanol. The solution was stored in a refrigerator at  $5 \pm 3^\circ\text{C}$  and equilibrated to room temperature prior to use. The solution was used within 7 days from the date of preparation.

- **Sample preparation**

500  $\mu\text{l}$  of respective spiking solution was spiked into a tube containing 9500  $\mu\text{l}$  of rat plasma and vortex to mix. The required number of calibration curve standards were retrieved from the deep freezer, thawed them at room temperature and the tubes were vortexed to mix. 0.2 ml of sample were transferred into the pre-labeled tube. 50  $\mu\text{l}$  of ISTD dilution was added to all the samples except standard blank and vortexed for about 15 seconds. 1.2 ml of ethyl acetate was added to the tubes, capped and vortexed all the samples on cyclo mixer, for 10 minutes. Extracted samples were centrifuged at 10,000 RPM, at  $10 \pm 2^\circ\text{C}$  for 10 mins. 1.0 ml of supernatant was transferred into pre-labeled tubes and evaporated to dryness under vacuum by using a vacuum oven set at  $40 \pm 5^\circ\text{C}$ . After drying, samples were reconstituted with 100  $\mu\text{l}$  of reconstitution solution and vortexed for about 30 seconds. Reconstituted samples were transferred into pre-labeled autosampler vials, arranged in the autosampler and injected by using HPLC-ESI-MS/MS.

- **Procedure for aqueous sample preparation**

400  $\mu\text{l}$  of reconstitution solution was taken in pre-labeled tubes. 500  $\mu\text{l}$  of ISTD dilution was added and vortexed to mix. 100  $\mu\text{l}$  of respective spiking solution was added and vortexed to mix. The appropriate volume of samples transferred into pre-labeled autosampler vials and injected by HPLC-ESI-MS/MS.

- **Construction of calibration curve**

The chromatograms were acquired by using Lab Solution Software 5.60 SP2D supplied by Shimadzu. The calibration curve was plotted as the peak area ratio (Drug/ISTD) on Y-axis vs. the nominal concentration of Drug on the X-axis. The concentrations of the unknown samples were calculated by using linear regression equation with a  $1/C^2$  weighting factor,

performed for each set of data using Microsoft Excel® version 2013 (Microsoft Corporation, Washington, USA).

- **Pharmacokinetic studies**

The applicability of the developed LCMS method for candesartan cilexetil in rat plasma was demonstrated by the results obtained from pharmacokinetic studies conducted on *Wister* rats (n=6). Each rat was treated with oral nanosuspension of candesartan cilexetil at a dose of 1.65 mg/kg in a single dose by curved gastric gavage tubes directly into the stomach. Serial blood samples were collected from retro-orbital venous plexus with hematocrit over a period 24 h. Blood samples from each group were collected at predetermined time intervals into heparinized plastic tubes. All these samples of blood were kept in refrigerated cold conditions (2-8°C) until separation of plasma. Each sample was processed further by the method as mentioned under sample preparation and subjected to LCMS analysis for the estimation of drug content by a bioanalytical method. The pharmacokinetic calculations were performed on the basis of plasma concentration-time data. Reduction of a dose of candesartan cilexetil after conversion into nanosuspension to reach  $C_{max}$  of the marketed formulation was also calculated.

### 3.14.6B Bioanalytical method for telmisartan nanosuspension [180]

A High-Performance Liquid Chromatographic System (HPLC) equipped with Shimadzu LC SOLUTION was employed for the present investigation. The system consisted of Shimadzu UFLC 20-AD as a binary solvent delivery system, Shimadzu 7D Rheodyne injector loop injector and Photo Diode Array (PDA) detector as a source of detection.

- **Chromatographic conditions**

Mobile phase	: Methanol and Acetonitrile (70:30 %v/v)
Column	: Phenomenex Luna® C8 column (300 mm*4.6 mm + pore size 100 Å)
Flow rate	: 1 ml/min
Injection volume	: 20 µl
Run time	: 10 min

- **Preparation of mobile phase**

For preparing a mobile phase, HPLC grade methanol and acetonitrile were filtered through a 0.2  $\mu\text{m}$  membrane filter and subjected to degassing in an ultrasonic bath for a period of 15 mins.

- **Standard solutions**

A primary stock solution (1 mg/ml) was prepared by dissolving 10 mg of telmisartan in 10 ml of HPLC grade methanol. The stock solution was suitably diluted with HPLC grade methanol to obtain a working range of standard solutions. The working standard solutions were used to prepare a calibration curve. Plasma used in the study was isolated from rat's blood by centrifugation at 10000 RPM for a period of 15 min at 4°C, using a laboratory centrifuge. The calibration curve samples were prepared by spiking 500  $\mu\text{l}$  of drug-free rat plasma with 100  $\mu\text{l}$  of previously diluted working standard solution in order to obtain final concentrations of 10, 25, 50, 75, 100, 250, 500, 750 and 1000 ng/ml. All samples were stored in refrigerated cold conditions (2-8°C) and equilibrated to room temperature prior to use.

- **Sample preparation**

Prior to sample analysis, 100  $\mu\text{l}$  of each solution was extracted using 300  $\mu\text{l}$  of diethyl ether: dichloromethane (60:40% v/v) for protein precipitation. Further, each of the mixtures was vortexed for a period of 5 min in a vortex mixer with subsequent centrifugation at 10,000 RPM, for a period of 10 mins at 4°C using a centrifuge. For each sample, an aliquot of a supernatant was isolated and subjected to dryness. The residue was reconstituted in 100  $\mu\text{l}$  of mobile phase and subsequently centrifuged at 10,000 RPM for 10 min at 4°C in a laboratory centrifuge. The supernatant was finally collected and directly injected into the HPLC system.

- **Construction of calibration curve**

The values of peak areas were plotted against their respective concentrations in order to construct the calibration curve for telmisartan. Linear regression analysis was performed for each set of data using Microsoft Excel<sup>®</sup> version 2013 (Microsoft Corporation, Washington, USA).

- **Pharmacokinetic studies**

The applicability of the developed HPLC method for telmisartan in rat plasma was demonstrated by the results obtained from pharmacokinetic studies conducted on *Wister* rats (n=6). Each rat was treated with oral nanosuspension of telmisartan at a dose of 4.11 mg/kg in a single dose by curved gastric gavage tubes directly into the stomach. Serial blood samples were collected from retro-orbital venous plexus with hematocrit over a period 24 h. Blood samples from each group were collected at predetermined time intervals into heparinized plastic tubes. All these samples of blood were kept in refrigerated cold conditions (2-8°C) until separation of plasma. Each sample was processed further by the method as mentioned under sample preparation and subjected to HPLC analysis for the estimation of drug content by a bioanalytical method. The pharmacokinetic calculations were performed on the basis of plasma concentration-time data.

### **3.14.6C Bioanalytical method for ziprasidone hydrochloride [181]**

The integrated high-performance liquid chromatography system (LC 2010C, Shimadzu Corporation, Tokyo, Japan) was equipped with a quaternary pump, a degasser, an autosampler, an injector with a 100 µl loop, a column oven, a Fluorescence detector and a data system (LC solution software version 1.21).

- **Chromatographic conditions**

Mobile phase	: 10mM Potassium dihydrogen phosphate buffer (pH: 2.5): Acetonitrile (70: 30)
Column	: Hypersil gold C-18 (150 mm* 4.6 mm* 5 µ)
Flow rate	: 1 ml/min
Injection volume	: 20 µl
Runtime	: 10 min

- **Standard solutions**

A standard stock solution of ziprasidone hydrochloride (1 mg /ml) was prepared in Milli Q water and the Prazosin Internal Standard (1 mg/ml) was separately prepared in methanol. Spiking solutions were prepared by appropriate dilution in methanol: water (50:50). The Internal Standard working solution (75ng/ml) was prepared by diluting its stock solution



with methanol: water (50:50). Spiking solutions (0.2 ml) were added to drug-free human serum (9.8 mL) as a bulk, to obtain ziprasidone hydrochloride spiking concentration levels of 1.5 ng/ml to 200 ng/ml.

- **Sample preparation**

A 400  $\mu$ l volume of serum was transferred to a 4 ml vial, and then 50  $\mu$ l of Internal standard working solution (75 ng/ml) was spiked. After vortexing for the 30s, add 100  $\mu$ l of 0.05 M sodium hydroxide in vials. Then 2.5 ml aliquot of the extraction solvent, methyl-tertbutyl ether was added using hand step (Brand Eppendorf, Germany). The sample was vortex-mixed for 10 min using a multi-pulse vortexer (Heidolph, Germany). The sample was then centrifuged at RPM 1891  $\pm$  100 for 5 minutes at 10°C using Multifuge 3S-R (Kendro Lab, Heraeus, Germany). The organic layer (2.0 ml) was quantitatively transferred to a 4 ml glass tube and evaporated to dryness using a TurboVap LV Evaporator (Speedoap, India) at 40°C under a stream of nitrogen. Then, the dried extract was reconstituted in 250  $\mu$ l of Mobile phase and a 20  $\mu$ l aliquot was injected into the chromatographic system.

- **Construction of calibration curve**

The chromatograms were acquired by using Lab Solution Software supplied by Shimadzu. The calibration curve was plotted as the peak area ratio (Drug/ISTD) on Y-axis vs. the nominal concentration of drug on the X-axis. The concentrations of the unknown samples were calculated by using linear regression equation with a  $1/C^2$  weighting factor. Linear regression analysis was performed for each set of data using Microsoft Excel® version 2013 (Microsoft Corporation, Washington, USA).

- **Pharmacokinetic studies**

The applicability of the developed HPLC method for ziprasidone hydrochloride in rat plasma was demonstrated by the results obtained from pharmacokinetic studies conducted on *Wister* rats (n=6). Each rat was treated with oral nanosuspension of ziprasidone hydrochloride at a dose of 2.05 mg/kg in a single dose by curved gastric gavage tubes directly into the stomach. Serial blood samples were collected from retro-orbital venous plexus with hematocrit over a period 12 h. Blood samples from each group were collected at predetermined time intervals into heparinized plastic tubes. All these samples of blood

were kept in refrigerated cold conditions (2-8°C) until serum separation. Each sample was processed further by the method as mentioned under sample preparation and subjected to HPLC analysis for the estimation of drug content by a bioanalytical method. The pharmacokinetic calculations were performed on the basis of serum concentration-time data.

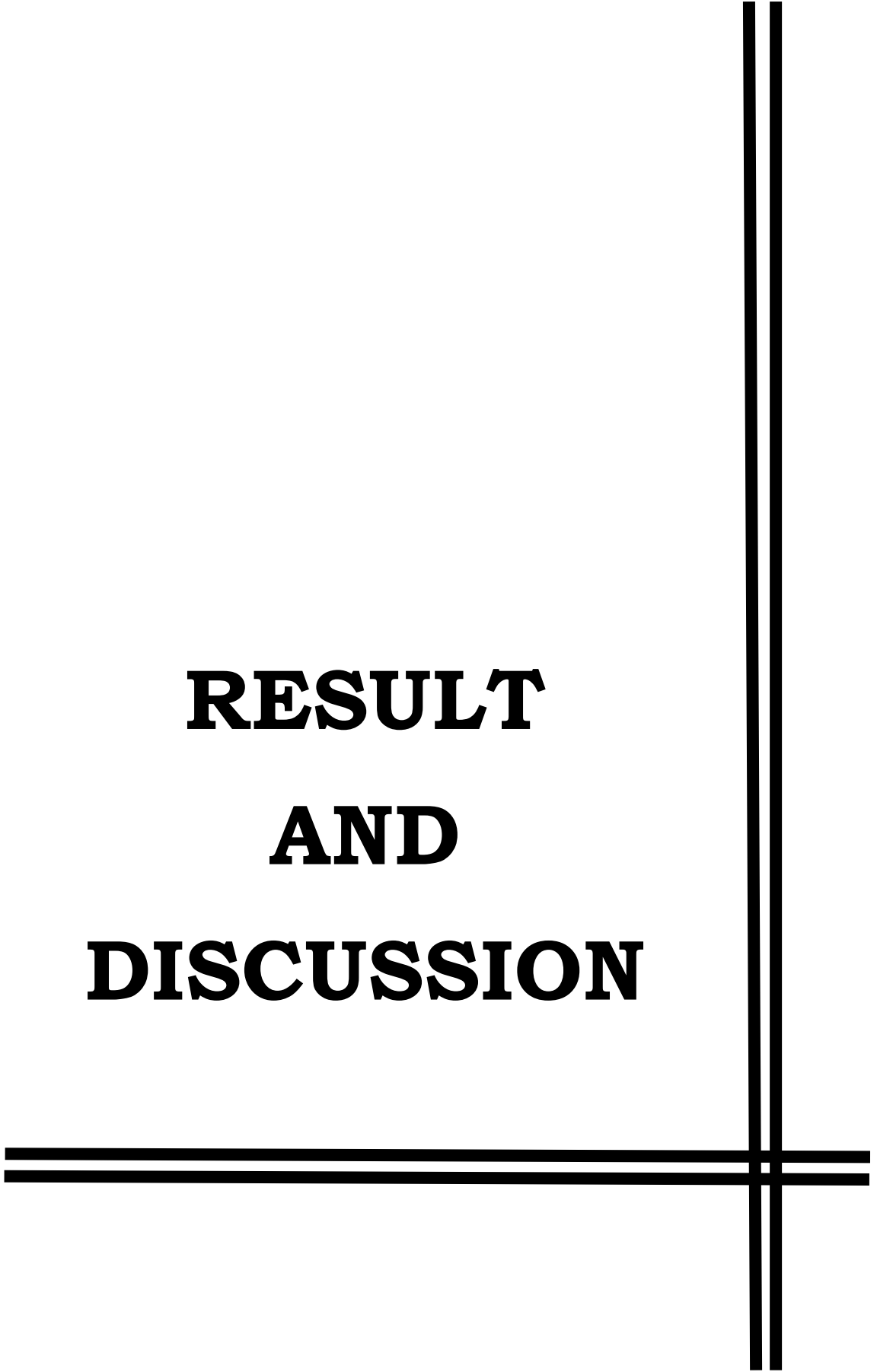
### 3.15 References

161. <http://www.accessdata.fda.gov/scripts/cder/dissolution/candesartancilexetil> (Accessed 1 March 2011)
162. <http://www.accessdata.fda.gov/scripts/cder/dissolution/telmisartan> (Accessed 13 March 2011)
163. [http://www.accessdata.fda.gov/scripts/cder/dissolution/ziprasidone\\_hydrochloride](http://www.accessdata.fda.gov/scripts/cder/dissolution/ziprasidone_hydrochloride) (Accessed 30 March 2012)
164. Shivakumar HG, Ramalingaraju G, and Siddaramaiah, 1999, Influence of solvents on crystal habit and properties of paracetamol crystals, *Indian Journal of Pharmaceutical Sciences*, 61(2), 100-104, ISSN: 0250-474X.
165. Pandya VM, Patel JK and Patel DJ, 2011, Formulation, optimization and characterization of Simvastatin Nanosuspension prepared by nanoprecipitation technique, *Der Pharmacia Lettre*, 3(2), 129-140, ISSN: 0975-5071.
166. Gacula MC (1993) Product Optimization. In: *Design and Analysis of Sensory Optimization*, Food and Nutrition Press, Trumbull: Connecticut USA, pp. 105-236.
167. Kakran M, Sahoo NG, Li L, Judeh Z, Wang Y, Chong K and Loh L, 2010, Fabrication of drug nanoparticles by evaporative precipitation of nanosuspension, *International Journal of Pharmaceutics*, 383(1-2), 285–292, ISSN: 0378-5173.
168. Das S and Suresh PK, 2011, Nanosuspension: a new vehicle for the improvement of the delivery of drugs to the ocular surface: Application to amphotericin B, *Nanomedicine: Nanotechnology, Biology, and Medicine*, 7(2), 242–247, ISSN: 1549-9634.
169. Armstrong NC and James KC (1996) *Pharmaceutical experimental design and interpretation*, Second Edition, CRC Press, USA, pp. 131-192.
170. Shid RL, Dhole SN, Kulkarni N and Shid SL, 2014, Formulation and evaluation of nanosuspension formulation for drug delivery of simvastatin, *International Journal of Pharmaceutical Sciences and Nanotechnology*, 7(4), 2650-2665, ISSN: 0974-3278.

- 
171. Muller RH, Jacobs C, and Kayser O, 2001, Nanosuspensions as particulate drug formulations in therapy rationale for development and what we can expect for the future, *Advanced Drug Delivery Reviews*, 47(1), 3–19, ISSN: 0169-409X.
  172. Li W, Yang Y, Tian Y, Xu X, Chen Y, Mu L, Zhang Y and Fang L, 2011, Preparation and *in-vitro/in-vivo* evaluation of Revaprazan Hydrochloride nanosuspension, *International Journal of Pharmaceutics*, 408(1-2), 157–162, ISSN: 0378-5173.
  173. ICH Harmonised Tripartite Guideline, Guideline for Residual Solvents, Q<sub>3</sub>C(R6).  
[http://www.ich.org/fileadmin/Public\\_Web\\_Site/ICH\\_Products/Guidelines/Quality/Q3C/Q3C\\_R6\\_\\_Step\\_4.pdf](http://www.ich.org/fileadmin/Public_Web_Site/ICH_Products/Guidelines/Quality/Q3C/Q3C_R6__Step_4.pdf)
  174. Reddy PB and Reddy MS, 2009, Residual Solvents Determination by HS-GC with Flame Ionization Detector in Omeprazole, Pharmaceutical formulations, *International Journal of PharmTech Research*, 1(2), 230-234, ISSN: 0974-4304.
  175. Paul SD, Mazumder R, Bhattacharya S and Jha AK, 2013, Method development and validation for the determination of residual solvents in ophthalmic nanoparticle suspension, *World Journal of Pharmacy and Pharmaceutical Sciences*, 2(6), 5802-5810, ISSN: 2278-4357.
  176. ICH Harmonised Tripartite Guideline, Stability Testing of New Drug Substances and Products, Q1A (R2).  
[http://www.ich.org/fileadmin/Public\\_Web\\_Site/ICH\\_Products/Guidelines/Quality/Q1A\\_R2/Step4/Q1A\\_R2\\_\\_Guideline.pdf](http://www.ich.org/fileadmin/Public_Web_Site/ICH_Products/Guidelines/Quality/Q1A_R2/Step4/Q1A_R2__Guideline.pdf)
  177. Zhang H, Jiang Y, Wen J, Zhou T, Fan G and Wu Y, 2009, Rapid determination of telmisartan in human plasma by HPLC using a monolithic column with fluorescence detection and its application to a bioequivalence study, *Journal of Chromatography B : Analytical Technologies in the Biomedical and Life Sciences*, 877(29), 3729-3733. ISSN: 1570-0232.
  178. Balakrishnan P, Lee B, Hoon DO, Kim JO, Hong MJ, Jee J, Kim JA, Yoo BK, Woo JS, Yong CS and Choi H, 2009, Enhanced oral bioavailability of dexibuprofen by a novel solid self-emulsifying drug delivery system (SEDDS), *European Journal of Pharmaceutics and Biopharmaceutics*, 72(3), 539-545, ISSN: 1929-8857.
-

179. Jang-Woo S, In-Chan S, and Chang-Gue S, 2010, Interpretation of animal dose and human equivalent dose for drug development, *The Journal of Korean Oriental Medicine*, 31(3), 1-7, ISSN: 1011-8934.
180. Patel JM, Dhingani AP, Garala KC, Raval MK and Sheth NR, 2012, Development and validation of bioanalytical HPLC method for estimation of Telmisartan in rat plasma: application to pharmacokinetic studies, *Dhaka University Journal of Pharmaceutical Sciences*, 11(2), 121-127, ISSN: 1816-1839.
181. Tripathi P and Pandey Y, 2012, High performance liquid chromatographic estimation of ziprasidone in human serum, *Journal of Pharmaceutical and Bioanalytical Science*, 1(1), 8-15, ISSN: 0731-7085.

**RESULT  
AND  
DISCUSSION**



## CHAPTER – 4

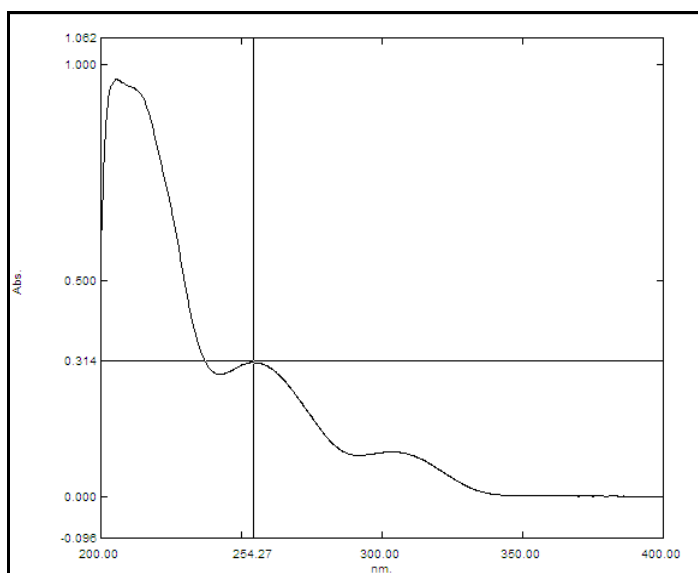
### Result and Discussion

#### **4A. Result and discussion of candesartan cilexetil nanosuspension**

##### **4A.1 Scanning and calibration curve preparation**

##### **4A.1.1 Scanning and calibration curve preparation of candesartan cilexetil in methanol**

The standard stock solution of candesartan cilexetil was prepared in methanol as per the method described in experimental section and scanned by UV Visible spectrophotometer between 200 to 400 nm. The UV absorption spectrum of candesartan cilexetil showed  $\lambda_{\max}$  at 254 nm [182] as shown in Figure 4.1.



**FIGURE 4.1: Scanning of candesartan cilexetil in methanol**

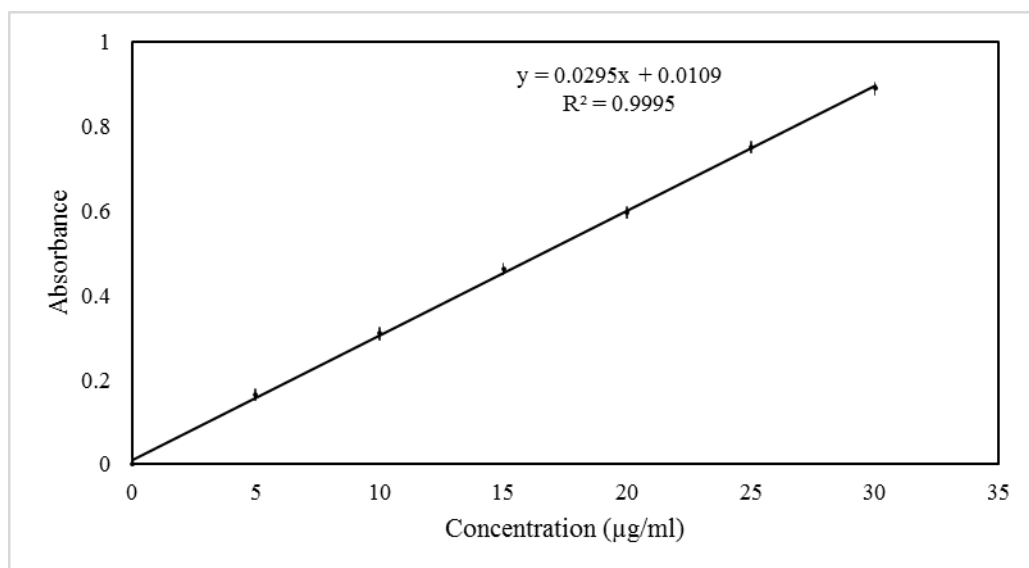
A calibration curve was prepared in methanol in the range of 5-30  $\mu\text{g/ml}$  by UV-Visible spectrophotometer. The absorbance of these solutions was measured at 254 nm. This procedure was performed in triplicate to validate the calibration curve. The data is given in Table 4.1.

**TABLE 4.1: Calibration curve data of candesartan cilexetil in methanol**

Sr. No.	Concentration ( $\mu\text{g/ml}$ )	Absorbance at 254 nm* (Mean $\pm$ SD)
1	0	0.000 $\pm$ 0.000
2	5	0.164 $\pm$ 0.012
3	10	0.309 $\pm$ 0.015
4	15	0.463 $\pm$ 0.015
5	20	0.596 $\pm$ 0.015
6	25	0.751 $\pm$ 0.010
7	30	0.889 $\pm$ 0.018

\*Indicates average of three determinations

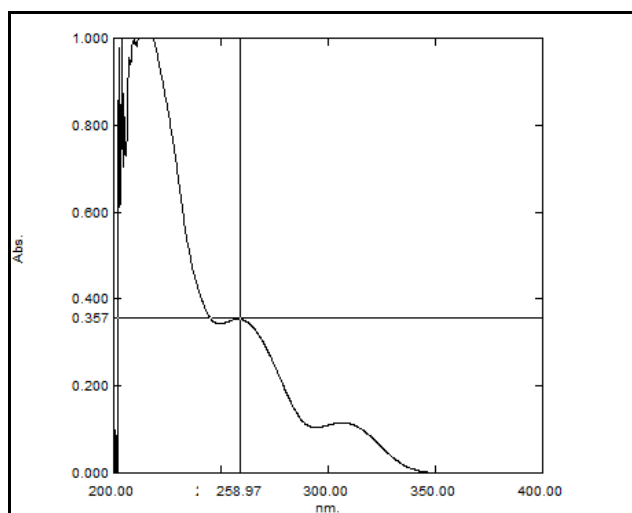
A calibration curve was constructed by plotting absorbance vs. concentration in  $\mu\text{g/ml}$  as shown in Figure 4.2 and a regression equation was found to be  $Y = 0.0295X + 0.0109$  with regression coefficient 0.9995.



**FIGURE 4.2: Calibration curve of candesartan cilexetil in methanol**

#### **4.1A.2 Scanning and calibration curve preparation of candesartan cilexetil in 0.05 M phosphate buffer, pH 6.5 containing 0.7% v/v polysorbate 20.**

The standard stock solution of candesartan cilexetil (10 µg/ml) was prepared in 0.05 M phosphate buffer, pH 6.5 containing 0.7% v/v polysorbate 20 and scanned by UV Visible spectrophotometer between 200 to 400 nm. The UV absorption spectrum of candesartan cilexetil showed  $\lambda_{\max}$  at 259 nm [183] as shown in Figure 4.3.



**FIGURE 4.3: Scanning of candesartan cilexetil in 0.05 M phosphate buffer, pH 6.5 containing 0.7% v/v polysorbate 20**

A calibration curve was prepared in 0.05 M phosphate buffer, pH 6.5 containing 0.7% v/v polysorbate 20 [172] in the range of 4-16 µg/ml by UV-Visible spectrophotometer. The



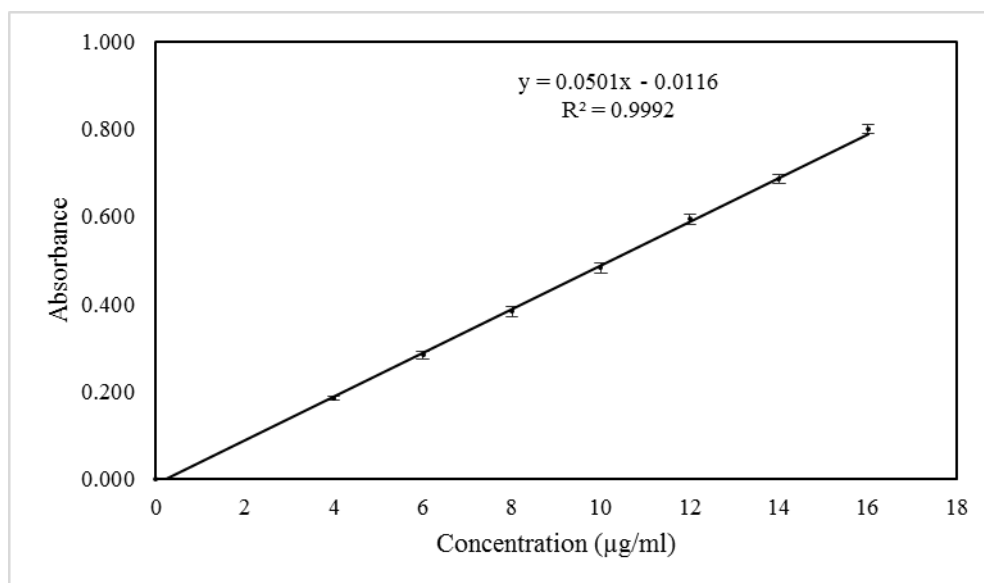
absorbance of these solutions was measured at 259 nm. This procedure was performed in triplicate to validate the calibration curve. The data is given in Table 4.2.

**TABLE 4.2: Calibration curve data of candesartan cilexetil in 0.05 M phosphate buffer, pH 6.5 containing 0.7% v/v polysorbate 20**

Sr. No.	Concentration ( $\mu\text{g/ml}$ )	Absorbance at 259 nm* (Mean $\pm$ SD)
1	0	0.000 $\pm$ 0.000
2	4	0.184 $\pm$ 0.005
3	6	0.284 $\pm$ 0.008
4	8	0.383 $\pm$ 0.012
5	10	0.482 $\pm$ 0.012
6	12	0.595 $\pm$ 0.012
7	14	0.686 $\pm$ 0.010
8	16	0.800 $\pm$ 0.010

\*Indicates average of three determinations

A calibration curve was prepared in 0.05 M phosphate buffer, pH 6.5 containing 0.7% v/v polysorbate 20 in the range of 4-16  $\mu\text{g/ml}$  as shown in Figure 4.4 and regression equation was found to be  $Y = 0.0501X - 0.0116$  with regression coefficient 0.9992.



**FIGURE 4.4: Calibration curve of candesartan cilexetil in 0.05 M phosphate buffer, pH 6.5 containing 0.7% v/v polysorbate 20**

#### 4A.2 Selection of solvent and antisolvent

Selection of solvent and antisolvent was performed on the basis of solubility of candesartan cilexetil in different solvents and their combinations. [164] Results indicated that drug had the highest solubility (5.31mg/ml) in methanol and least solubility (0.00119 mg/ml) in water, so they were selected as solvent and antisolvent respectively as shown in Table 4.3.

**TABLE 4.3: Results of selection of solvents for CCNS**

Drug	Solvents	Solubility (mg/ml) (Mean $\pm$ SD)*
Candesartan Cilexetil	Water	<b>0.00119 <math>\pm</math> 0.0001</b>
	Methanol	<b>5.31 <math>\pm</math> 0.54</b>
	Alcohol	2.51 $\pm$ 0.21
	Iso-propanol	0.33 $\pm$ 0.012
	N-Butanol	0.13 $\pm$ 0.052
	Alcohol:2-Propanol (1:1)	0.55 $\pm$ 0.034
	Alcohol: Butanol (1:1)	0.17 $\pm$ 0.029
	Ethyl Acetate	0.34 $\pm$ 0.038

\* Indicates average of three determinations

#### 4A.3 Selection of stabilizer

Different stabilizers like polyvinyl alcohol, PVP K-30, sodium lauryl sulfate, poloxamer 188 and poloxamer 407 were screened by preparing nanosuspensions with bellow mentioned formulating and processing parameters as shown in Table 4.4 [184]

**TABLE 4.4: Formulating and processing parameters for selection of stabilizer for CCNS**

Batch Code	Stabilizers	Amount of Stabilizers (mg)	Amount of Candesartan Cilexetil (mg)	Stirring Speed (RPM)	Stirring Time (h)	Sonication Time (min)	Solvent : Antisolvent Volume Ratio
CF1	Polyvinyl Alcohol	30	10	800	4	20	1:20
CF2	PVP K30	30					
CF3	Sodium Lauryl Sulphate	4					
CF4	Poloxamer 188	30					
CF5	Poloxamer 407	30					

The prepared nanosuspensions (CF1 to CF5) were evaluated by measuring their saturation solubility, mean particle size, polydispersity index (PDI) and zeta potential for selection of the best stabilizer which can be utilized for further research work, as shown in Table 4.5.

**TABLE 4.5: Results for selection of stabilizer for CCNS**

Batch Code	Stabilizer Used	Saturation Solubility ( $\mu\text{g/ml}$ ) (Mean $\pm$ SD)*	Mean Particle Size (nm) (Mean $\pm$ SD)*	PDI (Mean $\pm$ SD)*	Zeta Potential (mV) (Mean $\pm$ SD)*
CF1	Polyvinyl Alcohol	54.26 $\pm$ 1.28	512.0 $\pm$ 4.2	1.093 $\pm$ 0.11	31.22 $\pm$ 1.02
<b>CF2</b>	<b>PVP K-30</b>	<b>80.13 <math>\pm</math> 2.01</b>	<b>243.3 <math>\pm</math> 5.4</b>	<b>0.298 <math>\pm</math> 0.04</b>	<b>-32.89 <math>\pm</math> 0.89</b>
CF3	Sodium Lauryl Sulphate	51.39 $\pm$ 0.98	436.0 $\pm$ 9.3	0.732 $\pm$ 0.02	-30.79 $\pm$ 0.92
CF4	Poloxamer 188	60.81 $\pm$ 0.57	320.0 $\pm$ 8.8	0.553 $\pm$ 0.03	-31.17 $\pm$ 1.25
CF5	Poloxamer 407	57.21 $\pm$ 0.87	598.0 $\pm$ 5.8	1.089 $\pm$ 0.15	20.53 $\pm$ 1.10

\* Indicates average of three determinations

Table 4.5 indicated that PVP K-30 showing highest saturation solubility and lowest mean particle size. It also showed minimum PDI showing uniformity in particle size of nanosuspension and highest zeta potential indicating greater stability, so PVP K-30 was selected as a stabilizer for further studies.

#### 4A.4 Drug-excipient compatibility study

Studies of drug-excipient compatibility represent an important phase in the preformulation stage of the development of all dosage forms. The potential physical and chemical interactions between drugs and excipients can affect the chemical, physical, therapeutical properties and stability of the dosage form. Fourier transformed infrared (FTIR) spectroscopy and differential scanning calorimetry (DSC) were selected for checking of drug-excipient compatibility. [185]

##### 4A.4.1 Fourier transformed infrared (FTIR) spectroscopy

FTIR spectroscopy was conducted using a Shimadzu FTIR 8400 spectrophotometer (Shimadzu, Tokyo, Japan) and the spectrum was recorded in the wavelength region of 4000–400  $\text{cm}^{-1}$  as shown in Figure 4.5 [A, B, C].

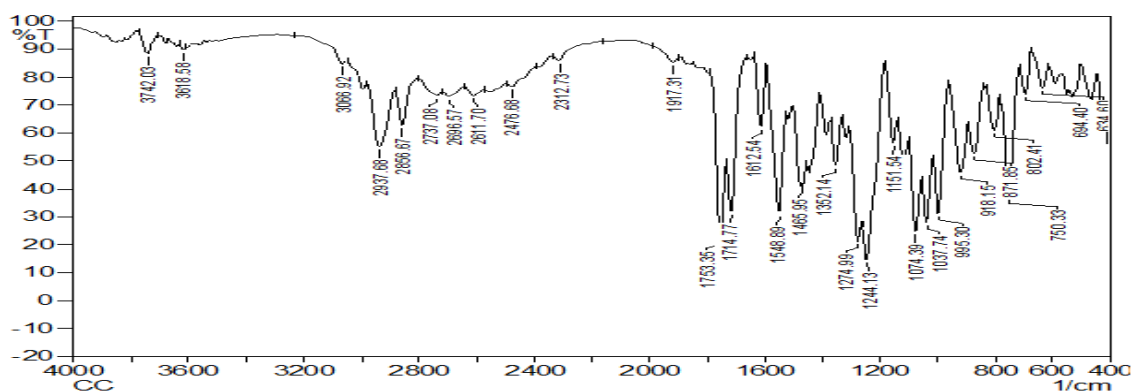


FIGURE 4.5 [A]: FT-IR spectra of candesartan cilexetil

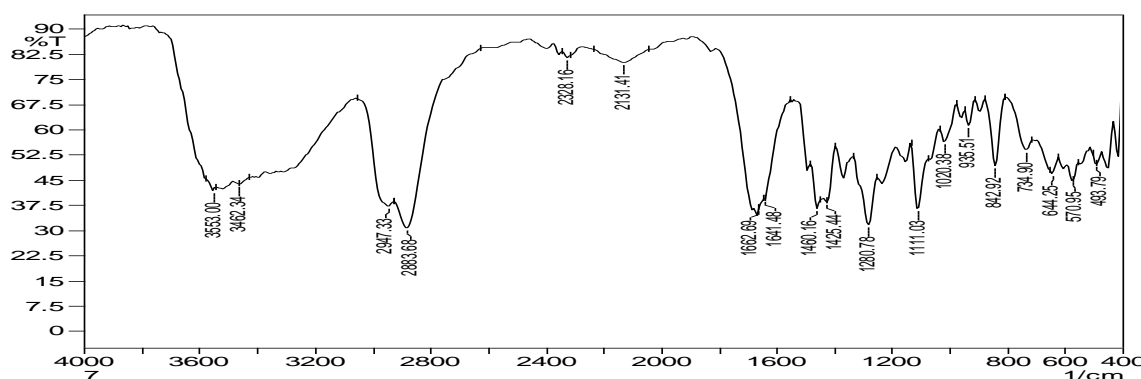
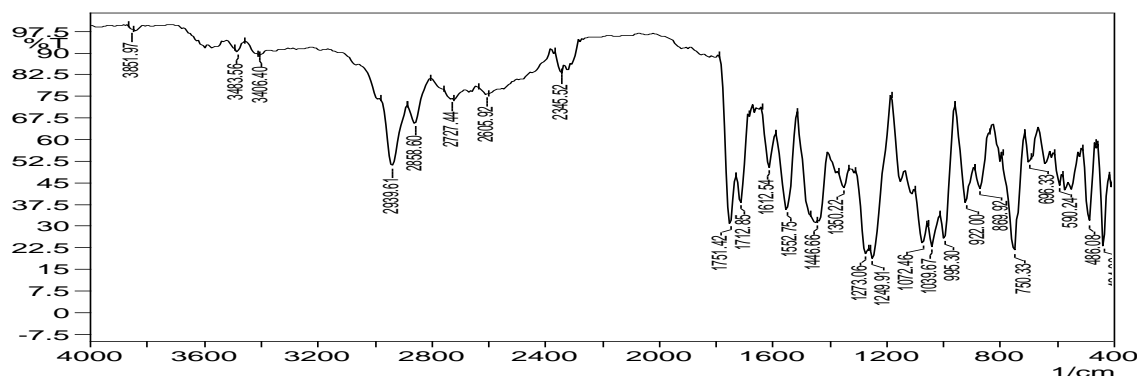


FIGURE 4.5 [B]: FT-IR spectra of PVP K-30



**FIGURE 4.5 [C]: FT-IR spectra of a physical mixture of candesartan cilexetil and PVP K-30**

Candesartan cilexetil, PVP K-30, and its physical mixture were subjected to FTIR studies and characteristic bands were identified and presented in Table 4.6.

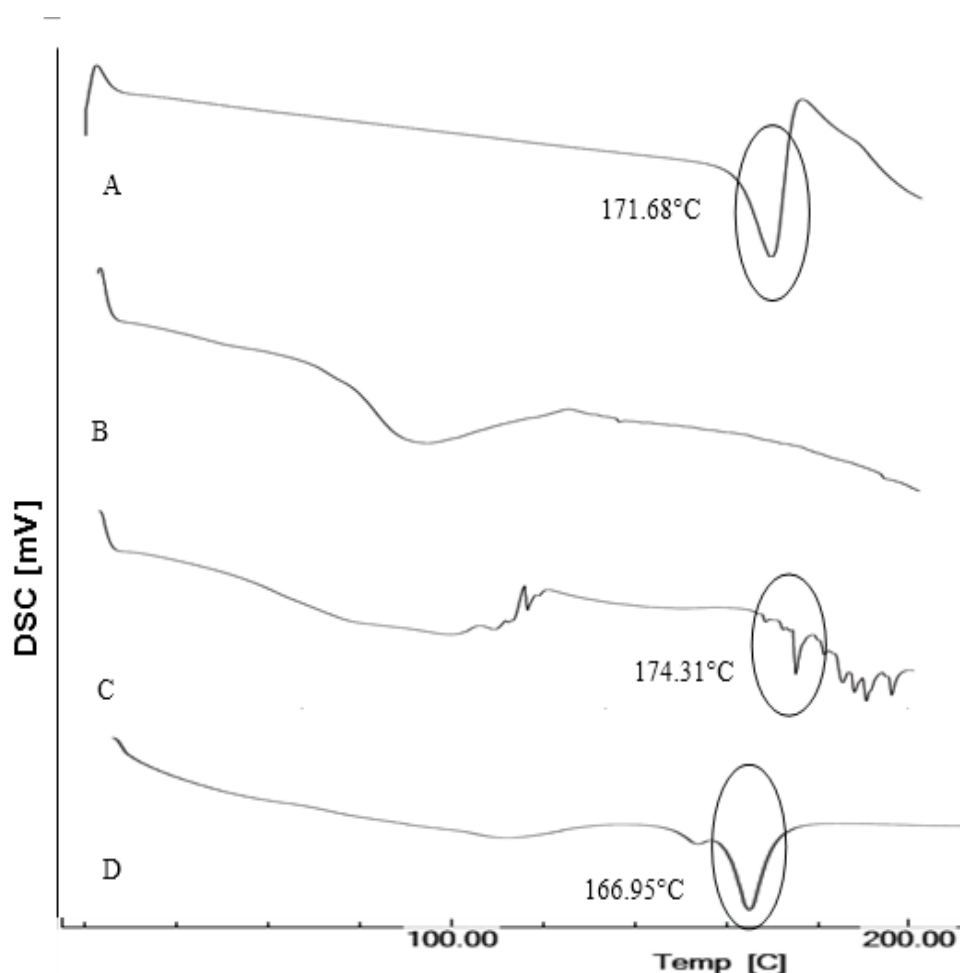
**TABLE 4.6: Comparison of characteristic bands between candesartan cilexetil and its physical mixture.**

Characteristic bands [186–188]	Peak Value, cm <sup>-1</sup>	
	Candesartan Cilexetil	Physical Mixture
Aromatic –C-H stretching	3066.92	3066.92
Aliphatic – C-H stretching	2937.68	2939.61
-N=N stretching	1612.54	1612.54
-C=N-N stretching	1548.89	1552.75
-C-N stretching	1274.99	1273.06
-C-O stretching of ether	1244.13	1249.91
-C-N stretching	1037.74	1039.67

Table 4.6 indicates that the bands were similar for both pure drug and physical mixture and therefore there was no incompatibility between candesartan cilexetil and PVP K-30.

#### 4A.4.2 Differential scanning calorimetry (DSC)

DSC was performed using DSC-60 (Shimadzu, Tokyo, Japan) calorimeter to study the thermal behavior of samples (candesartan cilexetil, PVP K-30, physical mixture and lyophilized nanosuspension). Information of thermal analysis by DSC can be seen in Figure 4.6.



**FIGURE 4.6: DSC thermograms of [A] Candesartan cilexetil [B] PVP K-30 [C] Physical mixture of candesartan cilexetil and PVP K-30 [D] Lyophilized nanosuspension of candesartan cilexetil**

In DSC measurements, candesartan cilexetil showed the melting endotherm at 171.68°C, while the melting endotherm of lyophilized nanosuspension was recorded at 166.95°C. The decrease of the melting endotherm of candesartan cilexetil nanosuspension may be due to the effect of particle size reduction by antisolvent precipitation followed by ultrasonication.

#### 4A.5 Plackett-Burman Design (PB)

Most common screening design is Plackett–Burman (PB) design that screens a large number of factors and identifies critical one in a minimal number of running with a good degree of accuracy. Generally, a number of runs needed to investigate the main effects are in multiples of 4 in PB designs. [189,190] It is used during the initial phase of the study. Provided the interaction effects are nil or negligible, the Plackett-Burman design is

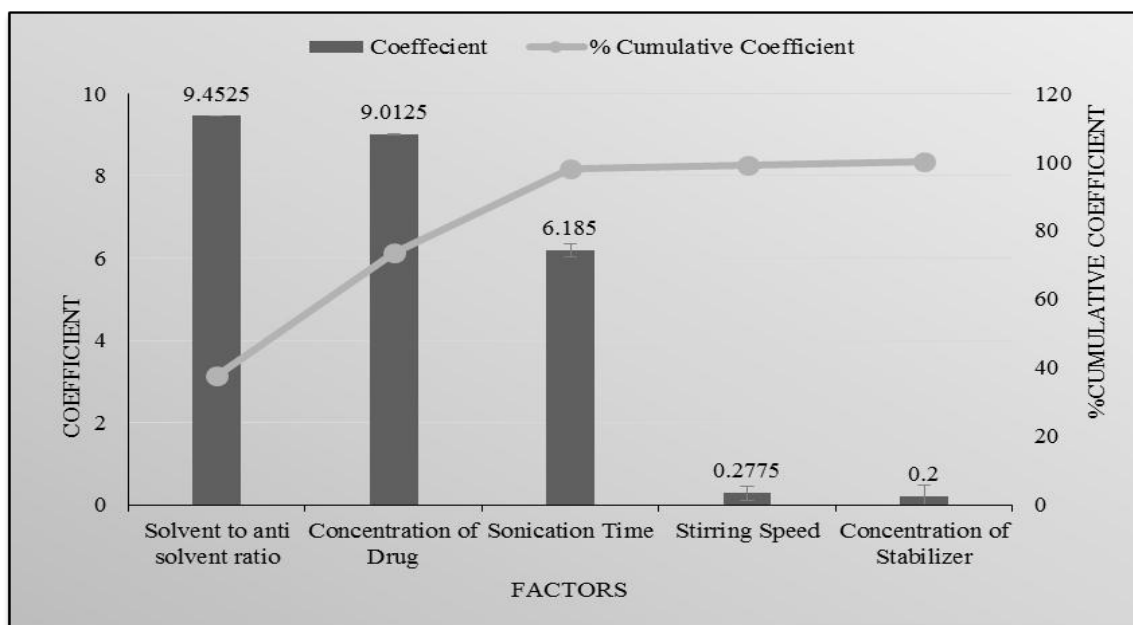
effective for measuring main effects. As shown in Table 4.7 the selected response parameters showed a wide variation suggesting that the independent variables had a significant effect on the response parameters chosen.

**TABLE 4.7: Layout and observed responses of Plackett-Burman design batches for CCNS (Preliminary Screening Formulations)**

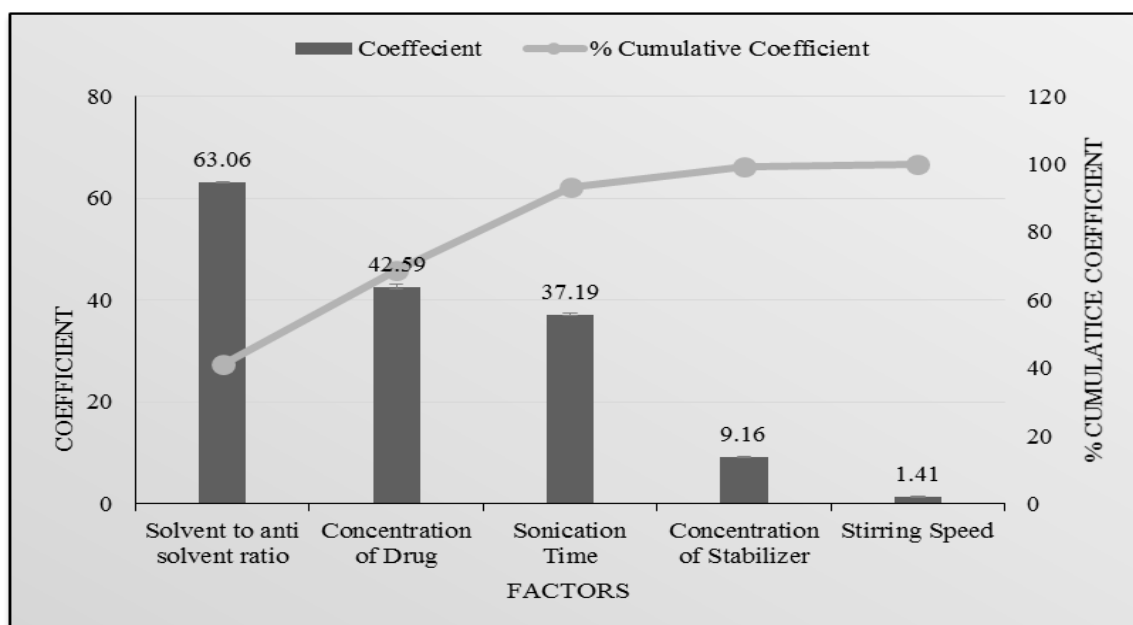
Batch Code	Amount of Candesartan Cilexetil (mg) X <sub>1</sub>	Amount of PVP K-30 (mg) X <sub>2</sub>	Solvent: antisolvent Volume Ratio X <sub>3</sub>	Stirring Speed (RPM) X <sub>4</sub>	Sonication Time (Min) X <sub>5</sub>	Saturation Solubility (µg/ml) (Mean ± SD)* Y <sub>1</sub>	Mean Particle Size (nm) (Mean ± SD)* Y <sub>2</sub>
CF6	20	50	1:20	800	30	95.13 ± 2.1	259.0 ± 4.6
CF7	10	50	1:20	1200	10	89.34 ± 1.8	272.1 ± 3.9
CF8	10	30	1:20	1200	30	88.14 ± 1.7	370.0 ± 6.1
CF9	20	30	1:10	1200	30	100.43 ± 2.0	257.0 ± 5.1
CF10	10	50	1:10	800	30	93.13 ± 0.9	337.0 ± 4.1
CF11	20	30	1:20	800	10	117.29 ± 0.7	218.4 ± 4.5
CF12	20	50	1:10	1200	10	75.29 ± 0.8	467.0 ± 5.8
CF13	10	30	1:10	800	10	45.43 ± 1.3	563.0 ± 6.1

\* Indicates average of three determinations

Figure 4.7 and Figure 4.8 indicates the amount of candesartan cilexetil and solvent to antisolvent volume ratio had maximum effect on mean particle size and saturation solubility as compared to other parameters like amount of PVP K-30, stirring speed and sonication time.



**FIGURE 4.7:** Pareto chart of the effect of independent variables on saturation solubility of CCNS



**FIGURE 4.8:** Pareto chart of the effect of independent variables on mean particle size of CCNS

#### 4A.6 Optimization of other preliminary parameters [191–193]

Candesartan cilexetil nanosuspension was prepared using PVP K-30 as a stabilizer. The three different amounts of PVP K-30 viz. 30 mg, 40 mg, and 50 mg were selected. Nanosuspensions were prepared according to the procedure given in experimental section. Prepared nanosuspensions were evaluated with different evaluation parameters like mean



particle size and saturation solubility to select amount of PVP K-30 for further formulation work. As shown in Table 4.8, 50 mg PVP K-30 was selected which was showing minimum mean particle size and maximum saturation solubility.

Stirring speed is important processing parameter for preparation of nanosuspension. For the optimization of stirring speed 800 RPM, 1000 RPM and 1200 RPM were selected. Nanosuspensions were prepared according to the procedure given in experimental section. Prepared nanosuspensions were evaluated with different evaluation parameters like mean particle size and saturation solubility to select the stirring speed for further formulation work, as shown in Table 4.8, 1200 RPM stirring speed was selected which was showing minimum mean particle size and maximum saturation solubility.

Once the precipitation of drug particle had occurred in suspension, to convert into the uniform nanosized particles probe sonicator was used. 10 mins, 20 mins and 30 mins periods were screened for sonication time. Nanosuspension was prepared according to the procedure given before. Prepared nanosuspensions were evaluated with different evaluation parameters like mean particle size and saturation solubility to select the optimized time period of sonication for further formulation work. As shown in Table 4.8, 30 mins sonication time was selected which was showing minimum mean particle size and maximum saturation solubility.

**TABLE 4.8: Results of optimization of other preliminary parameters for CCNS**

Batch Code	Preliminary Parameters		Mean Particle Size (nm) (Mean $\pm$ SD)*	Saturation Solubility ( $\mu$ g/ml) (Mean $\pm$ SD)*
CF14	Amount of Stabilizer (mg)	30	328.5 $\pm$ 5.1	85.07 $\pm$ 1.11
CF15		40	301.1 $\pm$ 8.2	92.15 $\pm$ 1.21
<b>CF16</b>		<b>50</b>	<b>293.5 <math>\pm</math> 7.7</b>	<b>95.67 <math>\pm</math> 1.14</b>
CF17	Stirring Speed (RPM)	800	389.8 $\pm$ 6.7	88.01 $\pm$ 0.98
CF18		1000	342.2 $\pm$ 9.8	91.32 $\pm$ 1.29
<b>CF19</b>		<b>1200</b>	<b>251.0 <math>\pm</math> 4.6</b>	<b>102.22 <math>\pm</math> 1.02</b>
CF20	Sonication Time (min)	10	382.8 $\pm$ 3.8	79.71 $\pm$ 1.1 9
CF21		20	319.0 $\pm$ 9.4	87.24 $\pm$ 1.31
<b>CF22</b>		<b>30</b>	<b>244.5 <math>\pm</math> 6.2</b>	<b>95.3 <math>\pm</math> 1.14</b>

\*Indicates average of three determinations

### 4A.7 3<sup>2</sup> Factorial Design

Various formulations were prepared the varying amount of candesartan cilexetil and solvent: antisolvent volume ratio. [167,168] As shown in Table 4.9 a 3<sup>2</sup> full factorial design was used to evaluate the effect of both independent variables on the predetermined dependent variables viz., mean particle size and saturation solubility.

**TABLE 4.9: Layout and observed responses of 3<sup>2</sup> factorial design for CCNS**

Batch Code	Level of Amount of Candesartan Cilexetil X <sub>1</sub>	Level of Solvent : Antisolvent Volume Ratio X <sub>2</sub>	Mean Particle Size (nm) (Mean ± SD)* Y <sub>1</sub>	Saturation Solubility (µg/ml) (Mean ± SD)* Y <sub>2</sub>
CFD1	-1	-1	434.0 ± 9.1	72.91 ± 2.14
CFD2	-1	0	342.0 ± 6.0	95.12 ± 2.03
CFD3	-1	1	375.0 ± 8.7	85.67 ± 1.67
CFD4	0	-1	406.0 ± 7.0	35.88 ± 0.61
CFD5	0	0	309.0 ± 11.0	50.94 ± 0.91
CFD6	0	1	353.7 ± 5.9	38.03 ± 1.11
CFD7	1	-1	335.7 ± 7.6	94.90 ± 1.54
<b>CFD8</b>	<b>1</b>	<b>0</b>	<b>240.7 ± 8.2</b>	<b>113.92 ± 2.50</b>
CFD9	1	1	308.0 ± 9.0	101.24 ± 1.32
<b>Translation of Coded Levels in Actual Units</b>				
<b>Variables Level</b>		<b>Low (-1)</b>	<b>Medium (0)</b>	<b>High (1)</b>
X <sub>1</sub>		10 mg	15 mg	20 mg
X <sub>2</sub>		1:10	1:15	1:20

\*Indicates average of three determinations

Some other parameters were also evaluated like, cumulative percentage released (CPR) at 2 minutes, zeta potential, PDI and % w/w drug content etc. as shown in Table 4.10.

**Table 4.10: Other evaluation parameters of factorial batches of CCNS**

Batch Code	CPR at 2mins (% w/w) (Mean ± SD)*	PDI (Mean ± SD)*	Zeta Potential (mV) (Mean ± SD)*	Drug Content (%w/w) (Mean ± SD)*
CFD1	91.45 ± 3.84	0.539 ± 0.051	18.88 ± 1.52	93.29 ± 1.21
CFD2	99.79 ± 1.02	0.514 ± 0.059	-29.41 ± 2.12	94.81 ± 2.14
CFD3	97.11 ± 1.43	0.654 ± 0.071	16.55 ± 1.24	95.39 ± 1.33
CFD4	95.40 ± 2.01	0.734 ± 0.084	-24.36 ± 0.98	92.74 ± 0.54
CFD5	98.36 ± 3.87	0.855 ± 0.095	-10.51 ± 0.57	99.33 ± 0.86
CFD6	98.92 ± 0.83	0.866 ± 0.101	18.74 ± 1.65	99.43 ± 1.52
CFD7	99.63 ± 1.44	0.521 ± 0.085	17.17 ± 1.88	98.22 ± 1.43
<b>CFD8</b>	<b>97.13 ± 1.91</b>	<b>0.343 ± 0.042</b>	<b>25.98 ± 1.85</b>	<b>101.1 ± 1.57</b>
CFD9	93.90 ± 2.11	0.987 ± 0.058	22.14 ± 2.12	98.94 ± 1.29

\*Indicates average of three determinations

#### 4A.8 Statistical analysis

A full model was derived after putting the values of regression coefficients in the equation (3.8). Regression analysis was carried out using Microsoft Excel<sup>®</sup> version 2013 (Microsoft Corporation, Washington, USA); the fitted results are shown in Table 4.11, Table 4.12, equation (4.1) and (4.2).

**TABLE 4.11: Results of regression analysis of mean particle size for CCNS**

	Mean Particle Size (nm) (Y <sub>1</sub> )		
	Coefficient	Std. Error	P- value
b <sub>0</sub>	308.3333	5.35182	1.15E-05
b <sub>1</sub>	-44.6667	2.931312	0.000614
b <sub>2</sub>	-23.1667	2.931312	0.004223
b <sub>11</sub>	-17	5.077182	0.044114
b <sub>22</sub>	71.5	5.077182	0.000776
b <sub>12</sub>	8	3.59011	0.007058
	<b>R<sup>2</sup> = 0.994142</b>		

For mean particle size (nm) (Y<sub>1</sub>)

$$Y_1 = 308.3333 - 44.6667X_1 - 23.1667X_2 - 17X_1^2 + 71.5X_2^2 + 8.701X_1X_2 \quad \text{Eq...}(4.1)$$

**TABLE 4.12: Results of regression analysis of saturation solubility for CCNS**

	Saturation Solubility ( $\mu\text{g/ml}$ ) ( $Y_2$ )		
	Coefficient	Std. Error	P- value
$b_0$	51.7644	1.914023	0.000111
$b_1$	9.3933	1.048354	0.002934
$b_2$	3.5416	1.048354	0.043145
$b_{11}$	52.3431	1.815802	9.17E-05
$b_{22}$	-15.2217	1.815802	0.00356
$b_{12}$	-1.605	1.283966	0.299919
	<b><math>R^2 = 0.996992</math></b>		

For **saturation solubility ( $\mu\text{g/ml}$ ) ( $Y_2$ )**

$$Y_2 = 51.76444 + 9.3933X_1 + 3.5416X_2 + 52.3431X_1^2 - 15.2217X_2^2 - 1.605X_1X_2 \quad \text{Eq...}(4.2)$$

The coefficients in Table 4.11 and Table 4.12 represent the respective quantitative effect of independent variables ( $X_1$  and  $X_2$ ) and their interactions on the various responses. It was seen that all the independent variables had a significant effect on the response ( $p < 0.05$ ). The negative sign of the coefficient indicated that increase in the value of independent variable decreases the value of response and vice versa. The absolute value of the coefficient indicates the magnitude of the effect of the independent variable on the response; higher the value higher the magnitude.

**TABLE 4.13: ANOVA for a full model for CCNS**

Source of variation	DF	SS	MS	F	F significant
<b>Mean Particle Size (nm)</b>					
Regression	5	26249.33	5249.867	101.8293	0.001514
Residual	3	154.6667	51.55556	-	-
Total	8	26404	-	-	-
<b>Saturation Solubility (<math>\mu\text{g/ml}</math>)</b>					
Regression	5	6558.02	1311.604	198.9006	0.000558
Residual	3	19.78281	6.59427	-	-
Total	8	6577.803	-	-	-

The results of ANOVA for full model suggested that  $F_{cal}$  value for mean particle size was 101.8293.  $F_{tab}$  value at (5, 3) was 9.0 for  $Y_1$ . So,  $F_{cal}$  value for  $Y_1$  was higher than  $F_{tab}$ .

The results of ANOVA for full model suggested that  $F_{cal}$  value for saturation solubility was 198.9006.  $F_{tab}$  value at (5, 3) was 9.0 for  $Y_2$ . So,  $F_{cal}$  value for  $Y_2$  was higher than  $F_{tab}$ .

All dependent variables were found  $F_{cal}$  value significantly higher than  $F_{tab}$ . Therefore, selected factors have a significant effect on all dependent variables.

All the determination coefficients  $R^2$  are larger than 0.99, indicating that over 99% of the variation in the response could be explained by the model and the goodness of fit of the model was confirmed. The F-ratio was found to be far greater than the theoretical value with a very low probability of less than 0.0001 for each regression model, indicating that the regression model was significant with a confidence level of 95%. The observed responses showed a wide variation suggesting that the selected both independent variables had a significant effect on resultant particle size and saturation solubility.

#### 4A.9 Contour plots

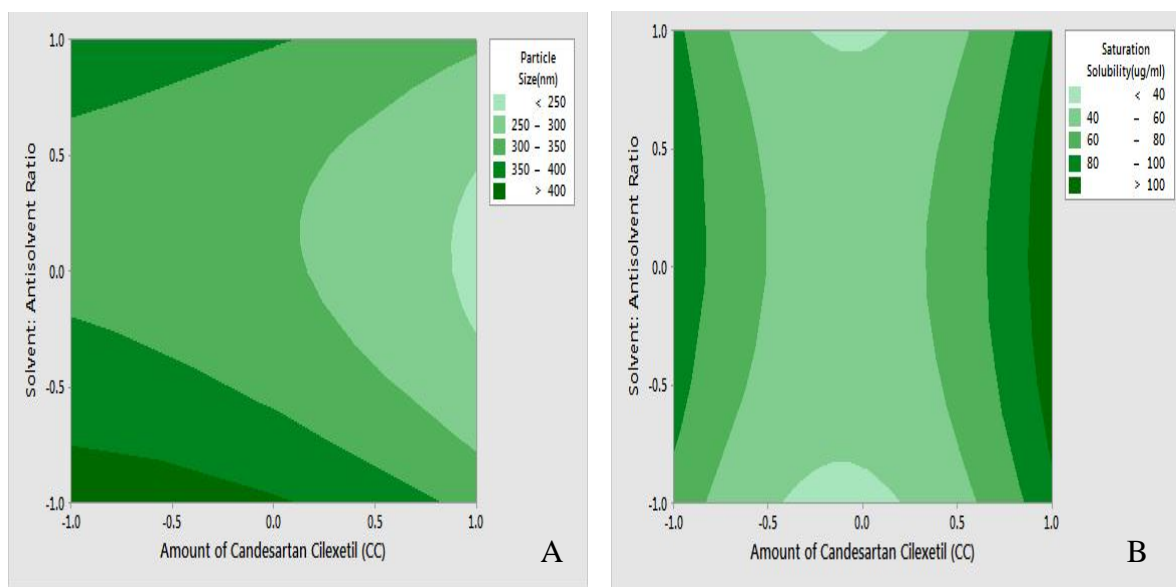
Two-dimensional contour plots were established using statistical software Minitab 17 (Minitab Inc., USA) to examine the relationship between independent and dependent variables as shown in Figure 4.9.

Figure 4.9 [A] shows contour plot for mean particle size (nm) at prefixed values between 250 to 400 nm. The contour plot was found to be non-linear. So the relationship between independent variables and particle size was not linear. The minimum (light green part) is clearly evidence from contour plot which specifies the solvent: antisolvent volume ratio and amount of candesartan cilexetil for lowest mean particle size. Their respective values are approximate 1:15 (coded value 0) solvent: antisolvent ratio and 20 mg (coded value +1) amount of candesartan cilexetil.

Figure 4.9 [B] shows contour plot for saturation solubility ( $\mu\text{g/ml}$ ) at prefixed values between 40 to 100  $\mu\text{g/ml}$ . The contour plot was found to be non-linear. So the relationship between independent variables and dependent variables was not linear. The maximum (dark green part) is clearly evidence from contour plot which specifies the solvent: antisolvent volume ratio and amount of candesartan cilexetil for maximum saturation

solubility. Their respective values are approximate 1:15 (coded value 0) solvent: antisolvent ratio and 20 mg (coded value +1) amount of candesartan cilexetil.

The maxima of saturation solubility and minima of particle size are seemed to be overlapping. So, there exists a direct relation between saturation solubility and particle size. The batch showing lowest particle size is also having highest saturation solubility.



**FIGURE 4.9: Contour plot of CCNS for effect on [A] Mean particle size and [B] Saturation solubility**

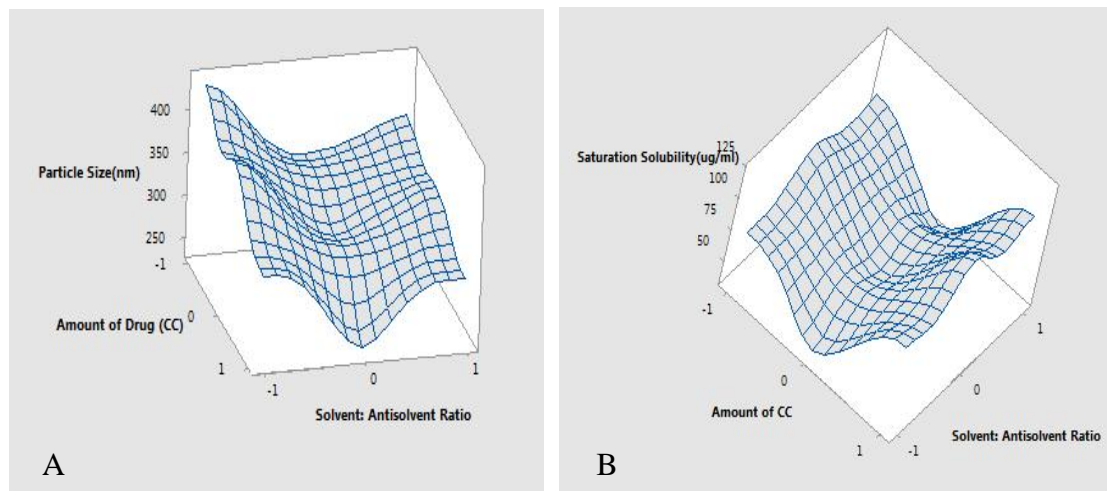
#### 4A.10 Surface plots

To find out main and interaction effect of the independent variables, response surface plots are very helpful.

Figure 4.10 [A] shows the response surface plot of mean particle size as a function of independent variables. Mean particle size decreases as the plot comes toward central part. The center of the plot indicates the minimum particle size which was obtained by intermediate solvent: antisolvent volume ratio (coded value 0) and highest amount of candesartan cilexetil (coded value +1).

Figure 4.10 [B] shows the response surface plot of saturation solubility respectively as a function of solvent: antisolvent volume ratio and amount of candesartan cilexetil using statistical software Minitab 17. (Minitab Inc., USA) Saturation solubility increases as the

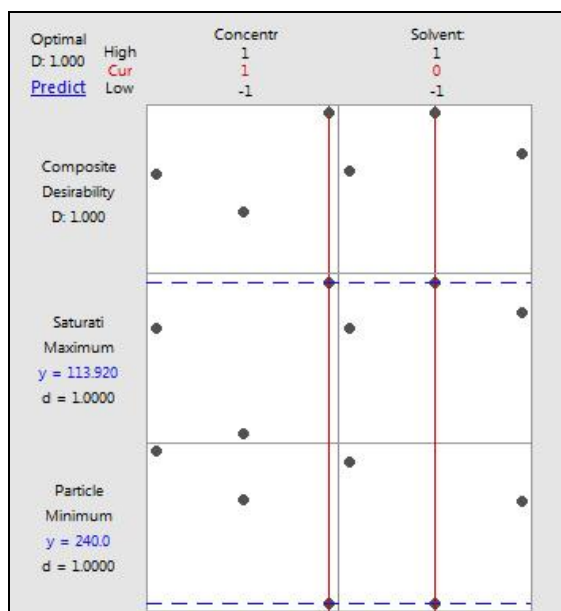
plot come toward central part. The center of the plot indicates the highest saturation solubility which was obtained by intermediate solvent: antisolvent volume ratio (coded value 0) and highest amount of candesartan cilexetil (coded value +1).



**FIGURE 4.10: Response surface plot of CCNS for effect on [A] Mean particle size and [b] Saturation solubility**

#### **4A.11 Optimization of candesartan cilexetil nanosuspension by desirability function of Minitab17.0**

The optimum formulation was selected based on the criteria of attaining the minimum mean particle size ( $Y_1$ ) and the maximum saturation solubility ( $Y_2$ ). An overall desirability function dependent on all investigated formulation variables was used to predict the ranges of the variable where the optimum formulation might occur. The desirable ranges are from zero to one (least to most desirable, respectively). The optimized batch composition is presented in below Figure 4.11.



**FIGURE 4.11: Optimized plot of factorial design form Minitab 17 for CCNS**

#### 4A.12 Checkpoint cum optimized batch analysis

From the above Minitab data optimized batch was CFD-8. The desirability of the optimized batch was 1.0. Formulation and process parameters for the optimized batch are shown in Table 4.14. The optimized lyophilized formulation was filled in hard gelatin capsules and kept in the tightly closed container.

**TABLE 4.14: Formulation and process parameters for an optimized batch of CCNS**

Amount of Candesartan Cilexetil	20 mg
Amount of PVP K-30	50 mg
Solvent : Antisolvent Volume Ratio	1:15
Stirring Speed	1200 RPM
Stirring Time	4 h
Sonication Time	30 mins
Amount of lyophilizer (1:1, Total Solid: Mannitol)	70 mg

#### 4A.13 Checkpoint batch cum optimized batch validation

To evaluate model a checkpoint batch cum optimized batch CFD-8 was prepared at  $X_1=+1$  and  $X_2=0$  levels. Dependent parameters were determined and compared with predicted values as shown in Table 4.15.



**TABLE 4.15: Composition of checkpoint batch cum optimized batch of CCNS**

Amount of Candesartan Cilexetil (mg) (X <sub>1</sub> )		Solvent: Antisolvent Volume Ratio (X <sub>2</sub> )	
Coded value	Decoded value	Coded value	Decoded value
+1	20 mg	0	1:15

**TABLE 4.16: Comparison of calculated data with experimental data of CCNS**

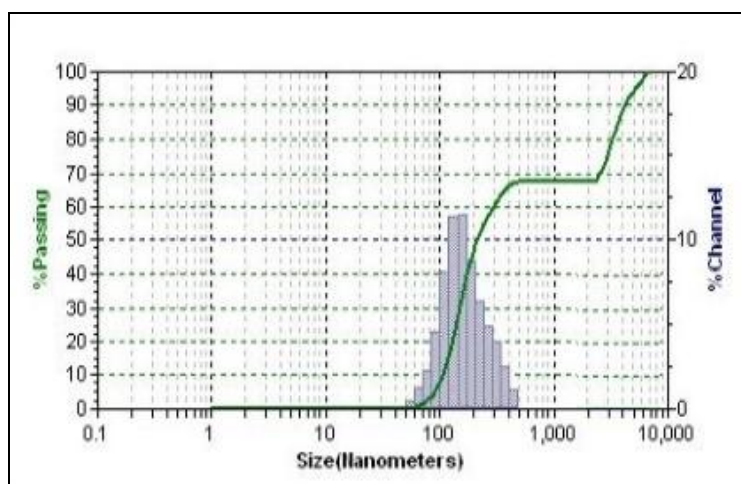
Response	Predicted	Observed	% Bias
Mean Particle Size (Y <sub>1</sub> )	246.66 nm	242.9 nm	- 1.52%
Saturation Solubility (Y <sub>2</sub> )	113.50 µg/ml	109.8 µg/ml	- 3.26%

When the batch CFD-8 was prepared using defined level of the amount of candesartan cilexetil and solvent: antisolvent volume ratio using Minitab17 (Minitab Inc., USA), the results obtained with checkpoint cum optimized batch (CFD-8) were close to predicted values. Thus, it can be concluded that the statistical model is mathematically valid.

#### 4A.14 Evaluation of optimized batch of candesartan cilexetil nanosuspension

##### 4A.14.1 Particle size and PDI

Particle size distribution of the optimized batch is shown in Figure 4.12. The mean particle size of the optimized batch was  $242.9 \pm 10.0$  nm and PDI was 0.343. Candesartan cilexetil nanosuspension based final formulation was intended for oral administration for which PDI and particle size above 5µm is not critical. The mean particle size of a nanosuspension is around 200-1000 nm. [80] From the Table 4.9, it was found that mean particle sizes of all formulations were in the nanometer range. It indicated that all formulations fulfill the requirements of a nanosuspension.



**Figure 4.12: Particle size graph for CCNS**

#### **4A.14.2 Zeta potential**

PVP K-30 is a well-known efficient polymeric stabilizer forming adsorption layers of drug nanoparticles. [165] In general, zeta potential value of  $\pm 30\text{mV}$  is sufficient for the stability of nanosuspension. [171] Zeta potential of optimized formulation was observed  $25.98 \pm 1.85\text{mV}$  which complies with the requirement of zeta potential.

#### **4A.14.3 Drug content**

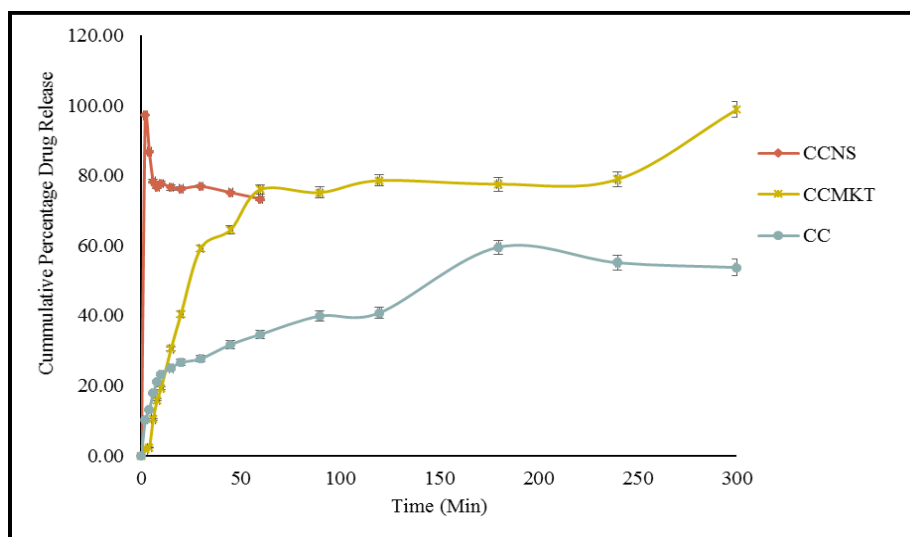
An aliquot (1 ml) of the prepared nanosuspension was diluted in methanol and filtered with a  $0.2 \mu\text{m}$  filter. Total drug content was determined by UV-Visible spectrophotometer at 254 nm and was found to be 101.01 % w/w of the candesartan cilexetil.

#### **4A.14.4 Saturation solubility**

Saturation solubility of an optimized batch of candesartan cilexetil nanosuspension and the pure drug was found to be  $109.8 \mu\text{g/ml}$  and  $1.192 \mu\text{g/ml}$  respectively it indicates that saturation solubility of nanosuspension was 100 times than that of pure drug. This drastic increase in saturation solubility was a result of a reduction in particle size and subsequent increase in surface area. So, it can be assumed that this increase in saturation solubility may increase bioavailability.

#### 4A.14.5 *In-vitro* dissolution study

The dissolution profile of nanosuspension, un-milled (pure drug) suspension and marketed formulation (ATACAND<sup>®</sup> Tablet) are presented in Figure 4.13. In nanosuspension, more than 97.13% drug was released within 2 mins, while cumulative percentage release of un-milled suspension and marketed formulation showed 34.63% and 75.97% at 60 min respectively. So, nanosuspension enhanced the rate of dissolution of candesartan cilexetil to a great extent.



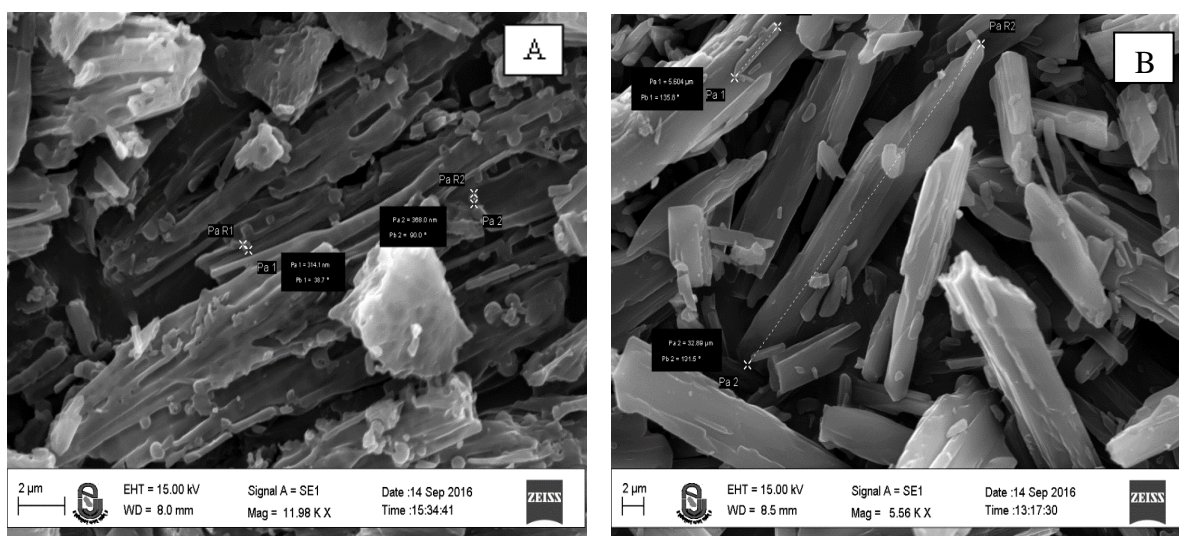
**FIGURE 4.13: Comparison of *in-vitro* dissolution of candesartan cilexetil nanosuspension with marketed formulation**

**TABLE 4.17: Evaluation parameters of an optimized batch of CCNS**

Evaluation Parameters	Results
Mean Particle Size	242.9 nm
PDI	0.343
Zeta Potential	25.98 mV
Drug Content	101.01 % w/w
Saturation Solubility	109.8 µg/ml
CPR at 2 mins	97.13 % w/w

#### 4A.14.6 Scanning electron microscopy (SEM)

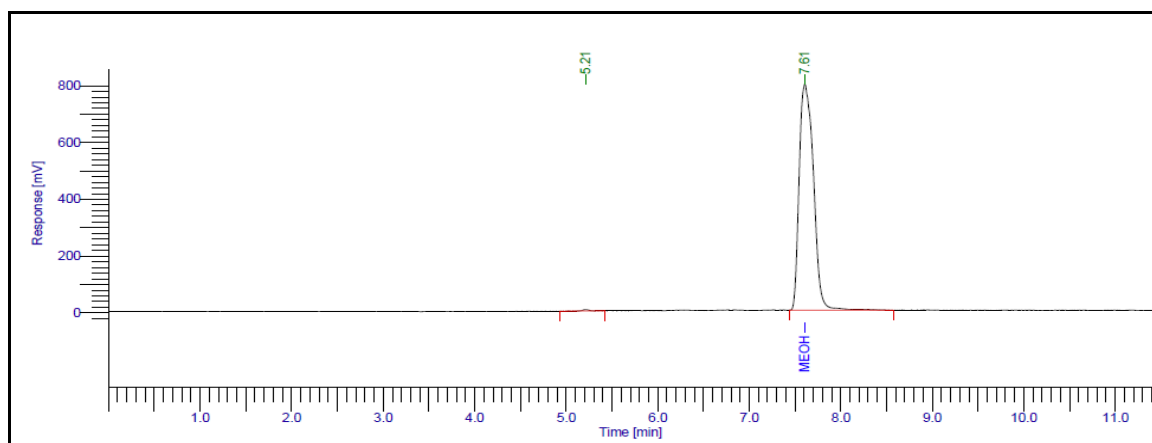
The surface characteristics of candesartan cilexetil and its lyophilized nanosuspension were studied by scanning electron microscopy (EVO-18, ZEISS, Germany) at 3kx to 28kx. The samples were mounted on double-sided carbon adhesive tape that has previously been secured on brass stubs and then subjected to gold coating by sputter coater, using process current of 10 mA for 4 mins. The accelerating voltage was 15 kV. The surface topology as measured by scanning electron microscopy of candesartan cilexetil was found to be long, thin and flat with particles larger (5-32 $\mu$ m) in size, as shown in Figure 4.14. However, after conversion to lyophilized nanosuspension, particles became smaller (about 300nm) which were adsorbed on the surface of mannitol used as cryoprotectant may be by hydrophobic interaction.



**FIGURE 4.14: Scanning electron microscopy of [A] Candесartan cilexetil and [B] CCNS**

#### 4A.14.7 Residual solvent by gas – chromatography (GC)

Methanol is included in Class 3 solvents, may be regarded as less toxic and of low risk to human health. According to ICH guidelines, it is considered that amounts of these residual solvents of 3000 ppm per day would be acceptable without justification. [173] Amount of methanol was evaluated for residual solvent content in lyophilized nanosuspension of candesartan cilexetil by gas chromatography using head-space sampler. Results of GC indicated that 171.87 ppm methanol was present in the sample which is the far lesser amount of class 3 solvents. Figure 4.15 indicates gas chromatograph of methanol in lyophilized candesartan cilexetil nanosuspension.



**FIGURE 4.15: Gas-chromatograph of methanol in the lyophilized candesartan cilexetil nanosuspension**

#### 4A.14.8 Accelerated stability study

The accelerated stability study indicated that lyophilized candesartan cilexetil nanosuspension was physically and chemically stable when stored at the  $25 \pm 2^\circ\text{C}$  and  $60 \pm 5\%$  RH for a period of 6 months. [176] Table 4.18 shows results of mean particle size, saturation solubility, cumulative percentage release at 2 mins and %w/w of drug content indicated that there was a slight change in all parameters which had  $< \pm 5\%$  bias which was insignificant. The negligible difference was observed in results obtained from the optimized batch before and after the stability study according to ICH guideline.

**TABLE 4.18: Results of accelerated stability study of CCNS**

Sr. No.	Storage condition for stability study	Time Period (months)	Evaluation Parameters			
			Mean Particle Size (nm) (Mean $\pm$ SD)*	Saturation Solubility ( $\mu\text{g}/\text{ml}$ ) (Mean $\pm$ SD)*	CPR at 2mins (%w/w) (Mean $\pm$ SD)*	Drug Content (%w/w) (Mean $\pm$ SD)*
1	$25^\circ\text{C} \pm 2^\circ\text{C}$ and $60\% \pm 5\%$ RH	0	242.7 $\pm$ 4.5	111.85 $\pm$ 1.5	97.13 $\pm$ 0.61	101.01 $\pm$ 0.35
2		1	259.1 $\pm$ 5.1	110.52 $\pm$ 0.9	96.85 $\pm$ 2.95	100.85 $\pm$ 0.52
3		3	265.1 $\pm$ 8.1	109.82 $\pm$ 0.8	95.92 $\pm$ 1.12	99.87 $\pm$ 0.47
4		6	281.2 $\pm$ 7.9	109.05 $\pm$ 1.9	95.14 $\pm$ 1.81	97.17 $\pm$ 0.89

\*Indicates average of three determinations

#### 4A.15 Bioavailability Study

For bioavailability study, each *Wistar* rat was treated with oral nanosuspension of candesartan cilexetil at a dose of 1.65 mg/kg in a single dose. Blood samples were

collected from retro-orbital venous plexus over a period 24 h. Each sample was analyzed by LCMS for the estimation of drug content by a bioanalytical method. The pharmacokinetic calculations were performed on the basis of plasma concentration-time data, as shown in Table 4.19.

**TABLE 4.19: Results of bioavailability study of candesartan cilexetil nanosuspension and marketed formulation**

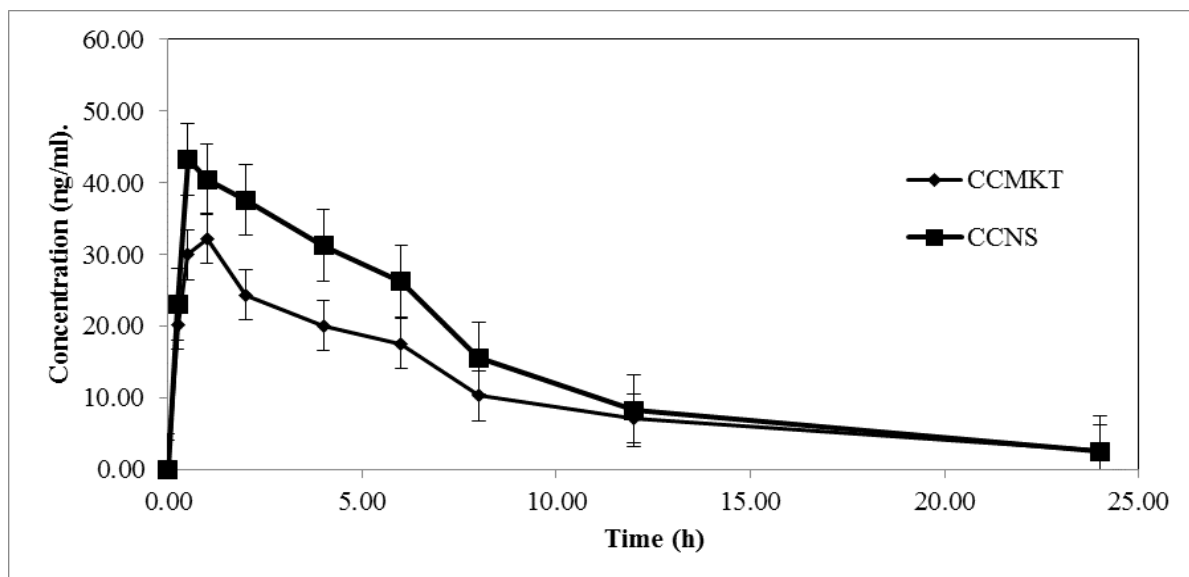
Sr. No.	Time (h)	CCNS (ng/ml) (Mean ± SD)*	CCMKT (ng/ml) (Mean ± SD)*	AUC(CCNS) (ng/ml).h	AUC(CCMKT) (ng/ml).h
1	0.00	0.00 ± 0.000	0.00 ± 0.000	0.0000	0.0000
2	0.25	23.00 ± 2.464	20.21 ± 3.029	2.8755	2.5263
3	0.5	43.29 ± 3.414	29.94 ± 4.588	10.8233	6.2690
4	1.00	40.48 ± 2.420	32.24 ± 4.758	20.2393	15.5465
5	2.00	37.61 ± 2.481	24.36 ± 2.744	37.6123	28.3027
6	4.00	31.24 ± 2.782	20.08 ± 2.371	62.4796	44.4366
7	6.00	26.23 ± 2.901	17.54 ± 2.855	78.6897	37.6117
8	8.00	15.56 ± 3.209	10.29 ± 3.434	62.2418	27.8307
9	12.00	8.24 ± 2.531	7.13 ± 2.014	49.4358	34.8453
10	24.00	2.48 ± 1.462	2.70 ± 1.988	29.7812	58.9919
Total				354.1785	256.3607

\*Indicates average of 6 determinations

CCNS – Candesartan Cilexetil Nanosuspension,

CCMKT – Candesartan Cilexetil Marketed Formulation

Figure 4.16 shows the mean plasma concentration ( $\mu\text{g/ml}$ ) vs. Time (h) in rats after administration of optimized nanosuspension of candesartan cilexetil and its marketed formulation (Atacand<sup>®</sup>). It is evident that the area under curve (AUC) values, for the optimized formulation containing candesartan cilexetil was higher than the corresponding values of the marketed formulation of candesartan cilexetil (Table 4.19). The increase AUC values could be attributed to the improved dissolution of candesartan cilexetil from the optimized nanosuspension formulation as compared to its marketed formulation.



**FIGURE 4.16: Plasma concentration vs. time profile of candesartan cilexetil nanosuspension and marketed formulation**

The values of all major pharmacokinetic parameters like maximum plasma concentration ( $C_{max}$ ), the time required for maximum plasma concentration ( $T_{max}$ ), the area under the curve ( $AUC_{0 \rightarrow 24}$ ), terminal half-life ( $T_{1/2}$ ), elimination rate constant ( $K_E$ ) and absorption rate constant ( $K_a$ ) have been summarized in Table 4.20.

**TABLE 4.20: Results of pharmacokinetic parameters of candesartan cilexetil nanosuspension and marketed formulation**

Pharmacokinetic Parameters	Candesartan Cilexetil Nanosuspension (CCNS)	Candesartan Cilexetil Marketed Formulation (CCMKT)
$C_{max}$ (ng/ml)	43.29	32.24
$T_{max}$ (h)	0.5	1.0
$AUC_{0-24}$ (ng/ml)*h	354.18	256.36
$t_{1/2E}$ (h)	7.689	8.431
$K_E$ ( $h^{-1}$ )	0.090	0.082
$K_a$ ( $h^{-1}$ )	0.281	0.169

The calculation was performed for the equivalent dose of test product (CCNS) required attaining same  $C_{max}$  as of marketed product. [194]

F-Ratio was calculated from the following equation,

$$F_r = \frac{[AUC]_{test}[D]_{std}}{[AUC]_{std}[D]_{test}} \quad \text{Eq...}(4.3)$$

Where,  $F_r$  = Relative bioavailability (F-Ratio)  
 $[AUC]_{test}$  = AUC of candesartan cilexetil nanosuspension  
 $[AUC]_{std}$  = AUC of candesartan cilexetil marketed formulation  
 $[D]_{test}$  = Dose of candesartan cilexetil nanosuspension  
 $[D]_{std}$  = Dose of candesartan cilexetil marketed formulation

Using above equation, bioavailability fraction obtained from candesartan cilexetil nanosuspension was **1.39**.

Volume of distribution was calculated by following equation,

$$V_d = \frac{FD}{C_{max}} \quad \text{Eq...}(4.4)$$

Where,  $V_d$  = Volume of distribution  
 $F$  = F-Ratio  
 $D$  = Dose of the product  
 $C_{max}$  = Maximum plasma concentration

Using above equation, the volume of distribution obtained from candesartan cilexetil nanosuspension was **26.136 lit**.

From the following equation amount of candesartan cilexetil to be administered to attain the same plasma concentration of marketed product was calculated

$$C = \frac{K_a F X_0}{V_d(K_a - K_e)} [e^{-K_e t} - e^{-K_a t}] \quad \text{Eq...}(4.5)$$

Where  $C$  =  $C_{max}$  of candesartan cilexetil marketed formulation  
 $K_a$  = Absorption rate constant of candesartan cilexetil nanosuspension  
 $F$  = F- Ratio



- $X_0$  = Amount of candesartan cilexetil administered by nanosuspension  
 $V_d$  = Volume of distribution of candesartan cilexetil nanosuspension  
 $K_e$  = Elimination rate constant of candesartan cilexetil nanosuspension  
 $t$  = Time required for maximum plasma concentration by candesartan cilexetil nanosuspension

AUC was higher by 1.38 times and  $C_{max}$  by 1.34 time higher for candesartan cilexetil nanosuspension as compared to marketed formulation shows quite a good rise in bioavailability.  $T_{max}$  was half as compared to marketed formulation indicates a substantial improvement in absorption of the drug from nanosuspension.

Using above equation, amount of candesartan cilexetil should be administered by nanosuspension ( $X_0$ ) was found to be **0.412mg/day** for rats, which was further converted to human equivalent dose, which was 9.9 mg/day.

The reported usual dose of candesartan cilexetil is 8 mg / 16 mg once daily in the management of **hypertension**. Lower initial doses should be considered in patients with intravascular volume depletion. In **heart failure**, candesartan cilexetil is given in an initial dose of 4 mg once daily; should be doubled at intervals of not less than two weeks up to 32 mg once daily if tolerated. The study was conducted with 16mg/day dose of candesartan cilexetil nanosuspension. Results suggested that by converting candesartan cilexetil into nanosuspension form dose can be reduced from 16 to 9.9mg/day which was 61.87% of the regular dose that indicated 38.13% dose reduction. **The improvement in bio-availability due to conversion from drug to nanosuspension was 38.13%.**

#### 4A.16 Conclusion

Plackett - Burman design was effectively employed to identify formulating and processing key parameters, affecting the quality of the candesartan cilexetil nanosuspension.  $3^2$  factorial design was employed for optimization of the formulation of nanosuspension. All the predetermined independent variables were found to affect the dependent variables from the resultant nanosuspension. The optimum formulation prepared by response optimizer by desirability function provided a final formulation with  $D = 1.000$  which released 97.13% of candesartan cilexetil within 2mins. The *in-vivo* studies confirmed that nanosuspension loaded candesartan cilexetil showed a significantly better AUC as compared to marketed formulation and dose of candesartan cilexetil was reduced about 38.13% to reach plasma

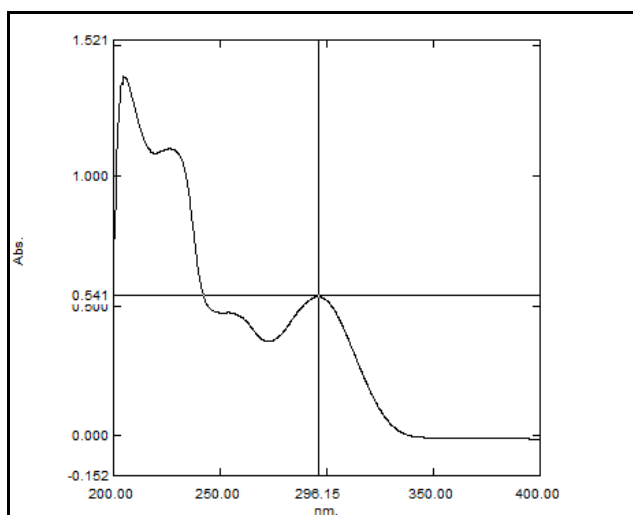
concentration of marketed formulation. The improved formulation could offer improved drug delivery strategy which might allow concomitant use of candesartan cilexetil in nanosuspension form. The nanosuspension of candesartan cilexetil exhibited 38.13% improvement in bio-availability.

## 4B. Result and discussion of telmisartan nanosuspension

### 4B.1 Scanning and calibration curve preparation of telmisartan

#### 4B.1.1 Scanning and calibration curve preparation of telmisartan in methanol

The standard stock solution of telmisartan was prepared in methanol as per the method described in experimental section and scanned by UV-Visible spectrophotometer between 200 to 400 nm. The UV absorption spectrum of telmisartan showed  $\lambda_{\max}$  at 296 nm [195] as shown in Figure 4.1.



**FIGURE 4.17: Scanning of telmisartan in methanol**

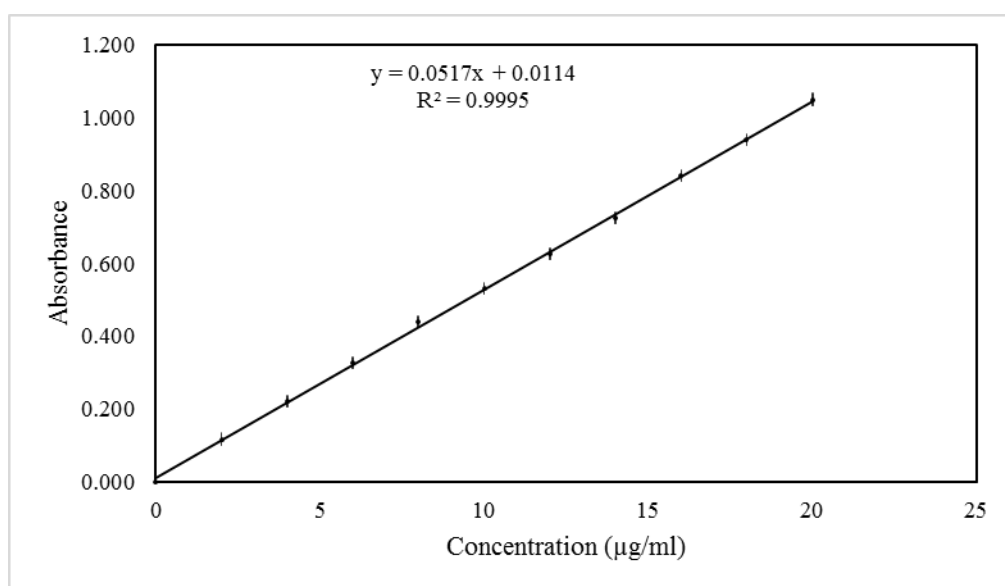
A calibration curve was prepared in methanol in the range of 2-20  $\mu\text{g/ml}$  by UV-Visible spectrophotometer. The absorbance of these solutions was measured at 296 nm. This procedure was performed in triplicate to validate the calibration curve. The data is given in Table 4.21.

**TABLE 4.21: Calibration curve data of telmisartan in methanol**

Sr. No.	Concentration (µg/ml)	Absorbance at 296nm* (Mean ± SD)
1	0	0.000 ± 0.000
2	2	0.117 ± 0.008
3	4	0.221 ± 0.008
4	6	0.327 ± 0.009
5	8	0.440 ± 0.018
6	10	0.532 ± 0.013
7	12	0.625 ± 0.015
8	14	0.724 ± 0.010
9	16	0.842 ± 0.017
10	18	0.939 ± 0.009
11	20	1.050 ± 0.015

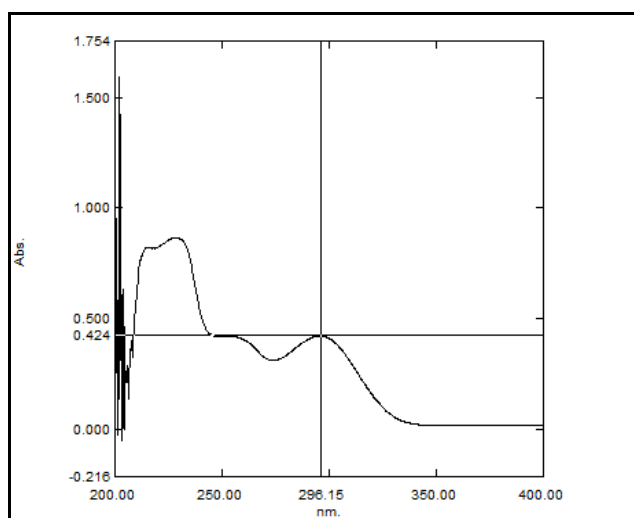
\*Indicates average of three determinations

A calibration curve was constructed by plotting absorbance vs. concentration in µg/ml as shown in Figure 4.18 and regression equation was found to be  $Y = 0.051X + 0.011$  with regression coefficient 0.999.

**FIGURE 4.18: Calibration curve of telmisartan in methanol**

#### 4.1B.2 Scanning and calibration curve preparation of telmisartan in phosphate buffer, pH 7.5.

The standard stock solution of telmisartan (10  $\mu\text{g/ml}$ ) was prepared in phosphate buffer, pH 7.5, scanned by UV-Visible spectrophotometer between 200 to 400 nm. The UV absorption spectrum of telmisartan showed  $\lambda_{\text{max}}$  at 296 nm [196] as shown in Figure 4.19.



**FIGURE 4.19: Scanning of telmisartan in phosphate buffer, pH 7.5**

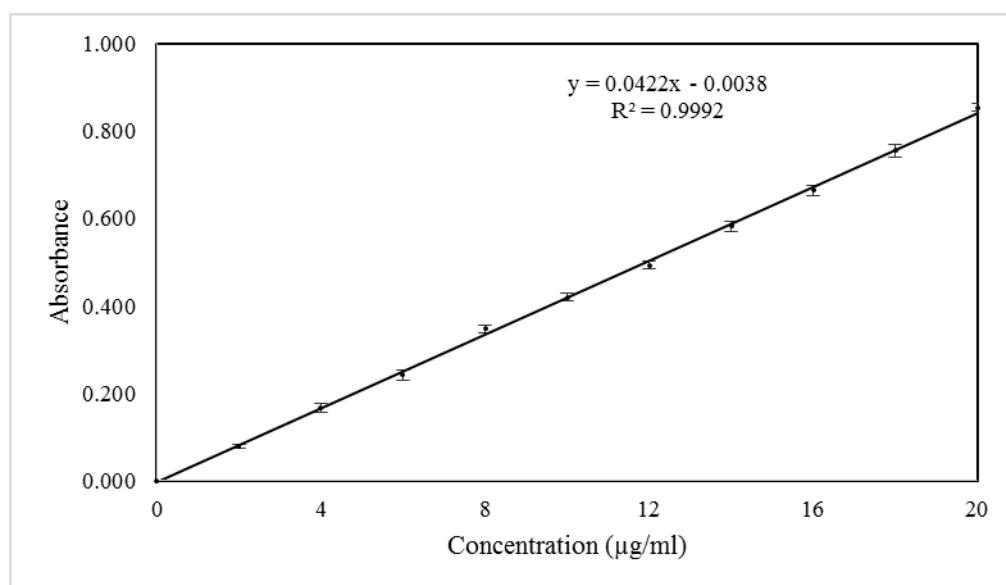
A calibration curve was prepared in phosphate buffer, pH 7.5 [172] in the range of 2-20  $\mu\text{g/ml}$  by UV-Visible spectrophotometer. The absorbance of these solutions was measured at 296 nm. This procedure was performed in triplicate to validate the calibration curve. The data is given in Table 4.22.

**TABLE 4.22: Calibration curve data of telmisartan in phosphate buffer, pH 7.5**

Sr. No.	Concentration ( $\mu\text{g/ml}$ )	Absorbance at 296nm* (Mean $\pm$ SD)
1	0	0.000 $\pm$ 0.000
2	2	0.079 $\pm$ 0.004
3	4	0.167 $\pm$ 0.011
4	6	0.242 $\pm$ 0.012
5	8	0.348 $\pm$ 0.009
6	10	0.420 $\pm$ 0.009
7	12	0.494 $\pm$ 0.008
8	14	0.582 $\pm$ 0.012
9	16	0.664 $\pm$ 0.012
10	18	0.755 $\pm$ 0.015
11	20	0.854 $\pm$ 0.0100

\*Indicates average of three determinations

A calibration curve was prepared in phosphate buffer, pH 7.5 in the range of 2-20  $\mu\text{g/ml}$  as shown in Figure 4.20 and regression equation was found to be  $Y = 0.042X - 0.003$  with regression coefficient 0.999.

**FIGURE 4.20: Calibration curve of telmisartan in phosphate buffer, pH 7.5**

#### 4B.2 Selection of solvent and antisolvent for telmisartan nanosuspension (TMNS)

Selection of solvent and antisolvent was performed on the basis of solubility of telmisartan in different solvents and their combinations. [164] Results indicated that drug had the highest solubility (3.329 mg/ml) in methanol and least solubility (0.012 mg/ml) in water, so they were selected as solvent and antisolvent respectively as shown in Table 4.23.

**TABLE 4.23: Results of selection of solvents for TMNS**

Drug	Solvents	Solubility (mg/ml) (Mean $\pm$ SD)*
Telmisartan	Water	0.012 $\pm$ 0.0041
	Methanol	3.329 $\pm$ 0.23
	Alcohol	0.877 $\pm$ 0.052
	Iso-propanol	0.094 $\pm$ 0.0021
	N-Butanol	1.975 $\pm$ 0.18
	Alcohol:2-Propanol (1:1)	0.609 $\pm$ 0.033
	Alcohol: Butanol (1:1)	1.235 $\pm$ 0.095
	Ethyl Acetate	0.562 $\pm$ 0.046

\* Indicates average of three determinations

#### 4B.3 Selection of stabilizer

Different stabilizers like polyvinyl alcohol, PVP K-30, sodium lauryl sulfate, poloxamer 188 and poloxamer 407 were screened by preparing nanosuspensions with bellow mentioned formulating and processing parameters as shown in Table 4.24. [184]

**TABLE 4.24: Formulating and processing parameters for selection of stabilizer for TMNS**

Batch Code	Stabilizers	Amount of Stabilizers (mg)	Amount of Telmisartan (mg)	Stirring Speed (RPM)	Stirring Time (h)	Sonication Time (min)	Solvent : Antisolvent Volume Ratio
TF1	Polyvinyl Alcohol	30	10	800	4	20	1:8
TF2	PVP K30	30					
TF3	Sodium Lauryl Sulphate	4					
TF4	Poloxamer 188	30					
TF5	Poloxamer 407	30					

The prepared nanosuspensions (TF1 to TF5) were evaluated by measuring their saturation solubility, mean particle size, polydispersity index (PDI) and zeta potential for selection of the best stabilizer which can be utilized for further research work, as shown in Table 4.25.

**TABLE 4.25: Results for selection of stabilizer for TMNS**

Batch Code	Stabilizer Used	Saturation Solubility ( $\mu\text{g/ml}$ ) (Mean $\pm$ SD)*	Mean Particle Size (nm) (Mean $\pm$ SD)*	PDI (Mean $\pm$ SD)*	Zeta Potential (mV) (Mean $\pm$ SD)*
TF1	Polyvinyl Alcohol	58.46 $\pm$ 2.55	214.8 $\pm$ 5.1	0.742 $\pm$ 0.21	17.60 $\pm$ 1.25
TF2	PVP K-30	39.51 $\pm$ 1.47	360.0 $\pm$ 3.8	1.077 $\pm$ 0.14	19.85 $\pm$ 1.38
TF3	Sodium Lauryl Sulphate	36.09 $\pm$ 0.84	85.60 $\pm$ 4.8	1.255 $\pm$ 0.34	-16.68 $\pm$ 1.41
TF4	Poloxamer 188	48.61 $\pm$ 0.97	380.0 $\pm$ 6.4	1.423 $\pm$ 0.41	-15.34 $\pm$ 0.97
<b>TF5</b>	<b>Poloxamer 407</b>	<b>76.38 <math>\pm</math> 1.02</b>	<b>276.5 <math>\pm</math> 5.1</b>	<b>0.673 <math>\pm</math> 0.11</b>	<b>-22.82 <math>\pm</math> 1.02</b>

\* Indicates average of three determinations

Table 4.25 indicated that poloxamer 407 showing highest saturation solubility. It also showed minimum PDI showing uniformity in particle size of nanosuspension and highest zeta potential indicating greater stability, so poloxamer 407 was selected as a stabilizer for further studies.

#### 4B.4 Drug-excipient compatibility study

Studies of drug-excipient compatibility represent an important phase in the preformulation stage of the development of all dosage forms. The potential physical and chemical interactions between drugs and excipients can affect the chemical, physical, therapeutical properties and stability of the dosage form. Fourier transformed infrared (FTIR) spectroscopy and differential scanning calorimetry (DSC) were selected for checking of drug-excipient compatibility. [197]

##### 4B.4.1 Fourier transformed infrared (FTIR) spectroscopy

FTIR spectroscopy was conducted using a Shimadzu FTIR 8400 spectrophotometer (Shimadzu, Tokyo, Japan) and the spectrum was recorded in the wavelength region of 4000–400  $\text{cm}^{-1}$  as shown in Figure 4.21 [A, B, C].



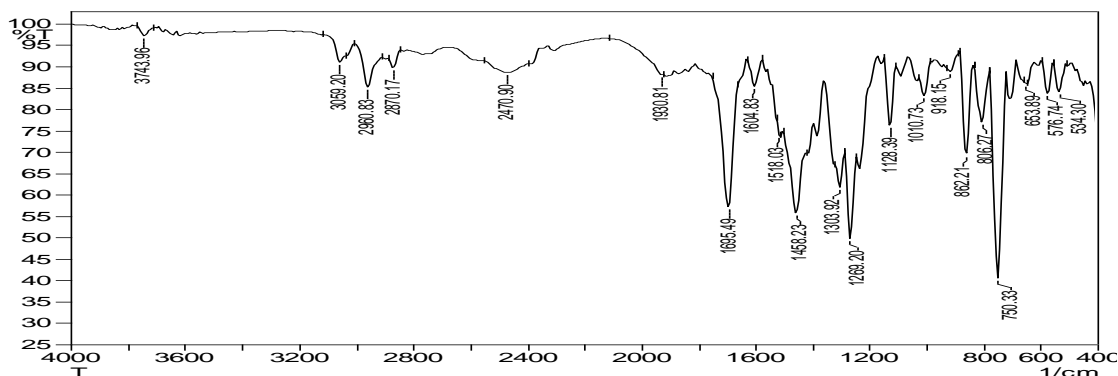


FIGURE 4.21 [A]: FT-IR spectra of telmisartan

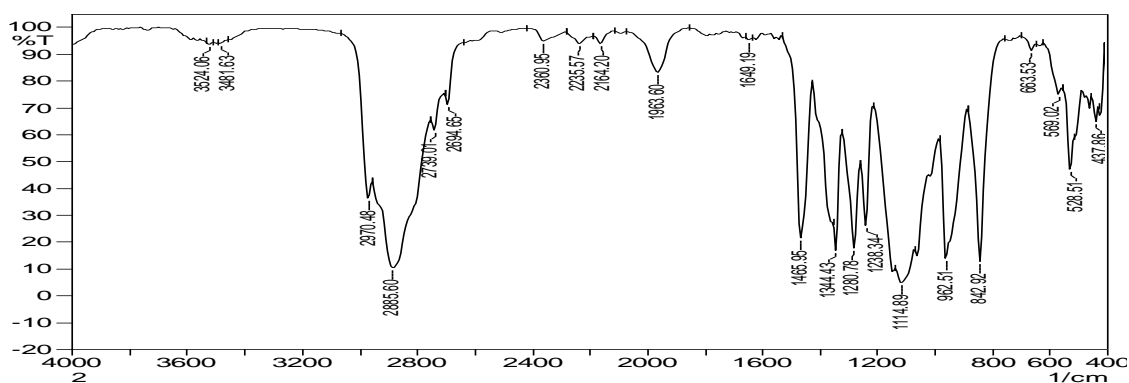


FIGURE 4.21 [B]: FT-IR spectra of poloxamer 407

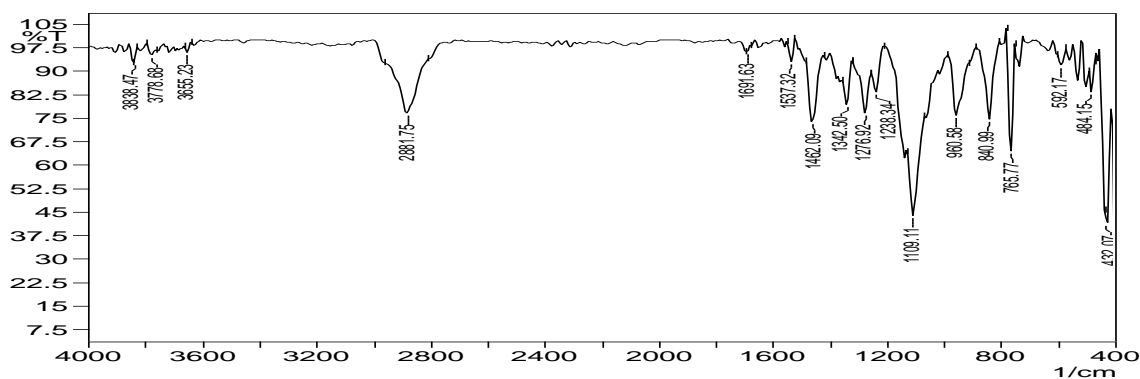


FIGURE 4.21 [C]: FT-IR spectra of a physical mixture of telmisartan and poloxamer 407

Telmisartan, poloxamer 407 and its physical mixture were subjected to FTIR studies and characteristic bands were identified and given in Table 4.26.

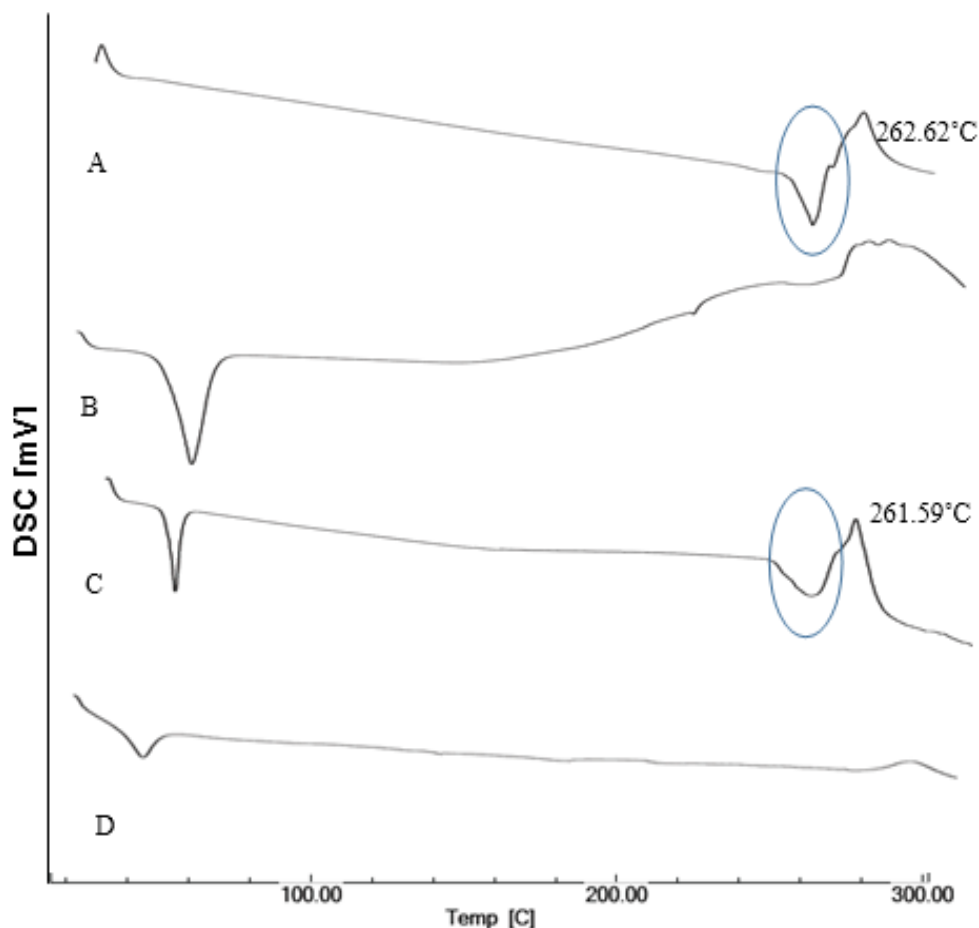
**TABLE 4.26: Comparison of characteristic bands between telmisartan and its physical mixture**

Characteristic bands [187,188]	Peak Value, cm <sup>-1</sup>	
	Telmisartan	Physical Mixture
-OH stretching of -COOH	1518.03	1517.32
-COOH stretching	1695.49	1691.63
Aliphatic C-H stretching	2880.17	2881.75

Table 4.26 indicates that the bands were similar for both pure drug and physical mixture and therefore there was no incompatibility between telmisartan and poloxamer 407.

#### **4B.4.2 Differential scanning calorimetry (DSC)**

DSC was performed using DSC-60 (Shimadzu, Tokyo, Japan) calorimeter to study the thermal behavior of samples (telmisartan, poloxamer 407, physical mixture and lyophilized nanosuspension). Information of thermal analysis by DSC can be seen in Figure 4.22.



**FIGURE 4.22: DSC thermograms of [A] Telmisartan [B] Poloxamer 407 [C] Physical mixture of telmisartan and poloxamer 407 [D] Lyophilized nanosuspension of telmisartan**

In DSC measurements, telmisartan showed the melting endotherm at 262.62°C, while the melting endotherm of the physical mixture was observed at 261.59°C. However, no endotherm was observed in the DSC curve for lyophilized nanosuspension. This result indicated that telmisartan no longer presents as a crystalline form when processed by antisolvent precipitation followed by ultrasonication, but exists in the amorphous state.

#### **4B.5 Plackett - Burman Design (PB)**

Most common screening design is Plackett–Burman (PB) design that screens a large number of factors and identifies critical one in a minimal number of running with a good degree of accuracy. Generally, a number of runs needed to investigate the main effects are multiple of 4 in PB designs.[189,190] It is used during the initial phase of the study.

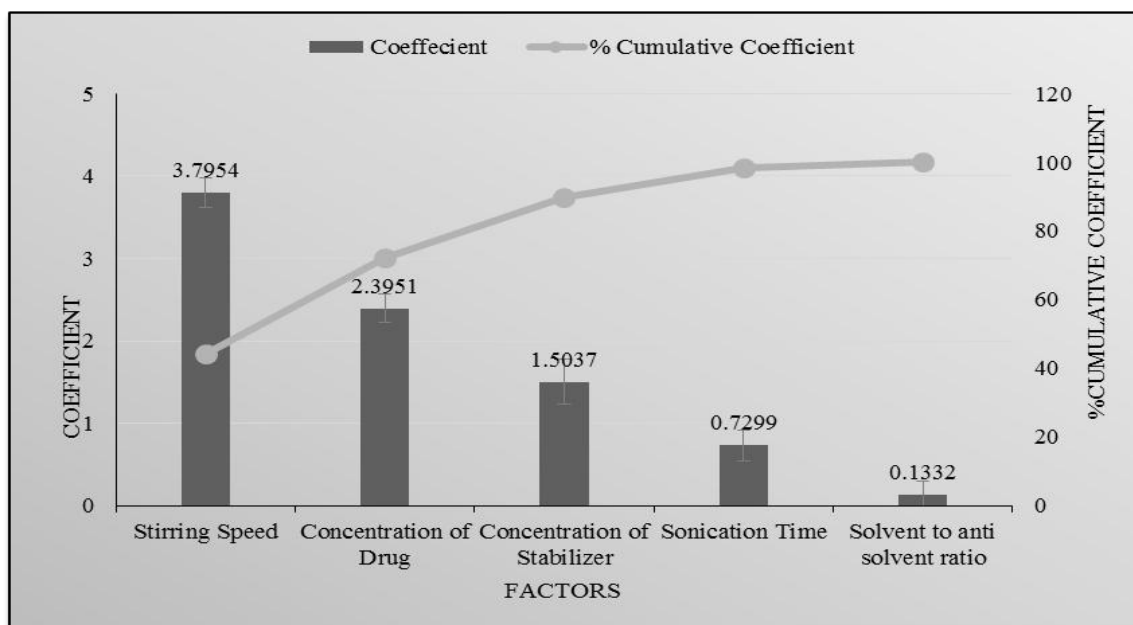
Provided the interaction effects are nil or negligible, the Plackett-Burman design is effective for measuring main effects. As shown in Table 4.27, the selected response parameters showed a wide variation suggesting that the independent variables had a significant effect on the response parameters chosen.

**TABLE 4.27: Layout and observed responses of Plackett - Burman design batches for TMNS (Preliminary Screening Formulations)**

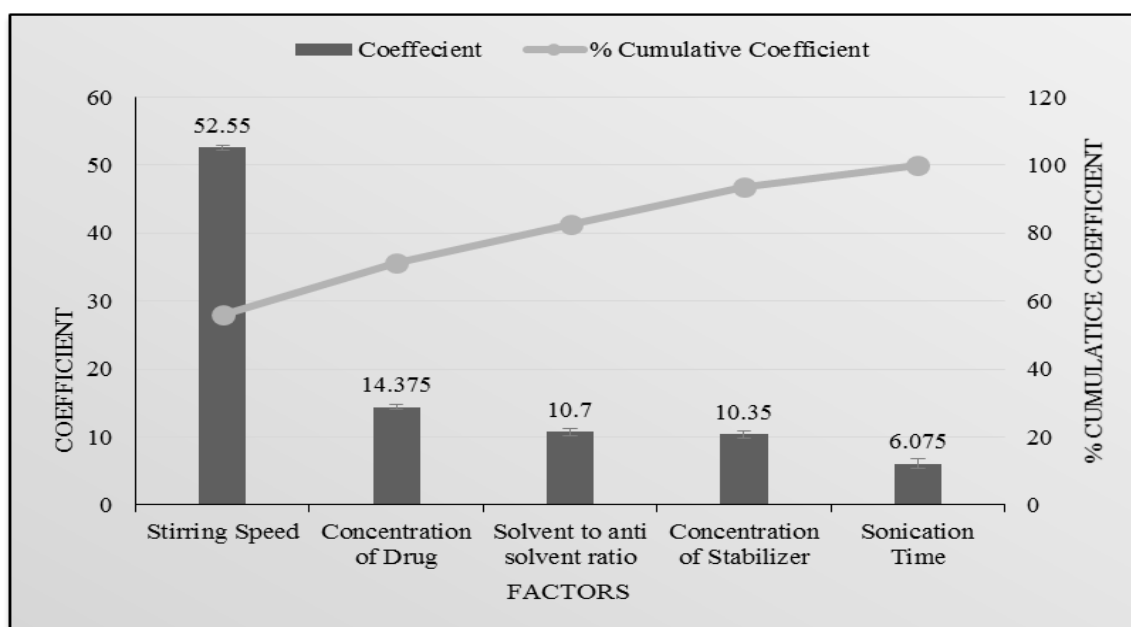
Batch Code	Amount of Telmisartan (mg) X <sub>1</sub>	Amount of Poloxamer 407 (mg) X <sub>2</sub>	Solvent : Antisolvent Volume Ratio X <sub>3</sub>	Stirring Speed (RPM) X <sub>4</sub>	Sonication Time (Min) X <sub>5</sub>	Saturation Solubility (µg/ml) (Mean ± SD)* Y <sub>1</sub>	Mean Particle Size (nm) (Mean ± SD)* Y <sub>2</sub>
TF6	20	50	1:8	800	30	70.21 ± 2.14	373.3 ± 9.8
TF7	10	50	1:8	1200	10	84.50 ± 1.98	130.1 ± 6.4
TF8	10	30	1:8	1200	30	78.19 ± 2.05	215.5 ± 6.8
TF9	20	30	1:5	1200	30	87.48 ± 1.14	112.8 ± 5.1
TF10	10	50	1:5	800	30	86.29 ± 0.97	123.8 ± 5.7
TF11	20	30	1:8	800	10	86.88 ± 1.85	125.0 ± 4.2
TF12	20	50	1:5	1200	10	84.26 ± 2.51	132.5 ± 4.5
TF13	10	30	1:5	800	10	60.69 ± 1.21	389.2 ± 7.1

\* Indicates average of three determinations

Figure 4.23 and Figure 4.24 indicated stirring speed and amount of telmisartan had maximum effect on mean particle size and saturation solubility as compared to other parameters like amount of poloxamer 407, the solvent to antisolvent volume ratio and sonication time.



**FIGURE 4.23: Pareto chart of the effect of independent variables on saturation the solubility of TMNS**



**FIGURE 4.24: Pareto chart of the effect of independent variables on mean particle size of TMNS**

#### 4B.6 Optimization of other preliminary parameters [191–193]

Telmisartan nanosuspension was prepared using poloxamer 407 as a stabilizer. The three different amounts of poloxamer 407 viz. 30, 40 and 50 mg were selected. Nanosuspension was prepared according to the procedure given in experimental section. Prepared nanosuspensions were evaluated with different evaluation parameters like mean particle

size and saturation solubility to select amount of poloxamer 407 for further formulation work. As shown in Table 4.28, 50mg poloxamer 407 was selected which was showing minimum mean particle size and maximum saturation solubility.

Solvent: antisolvent volume ratio is important formulation parameter for preparation of nanosuspension. For the optimization of solvent: antisolvent volume ratio 1:4, 1:6 and 1:8 were selected. Nanosuspensions were prepared according to the procedure given in experimental section. Prepared nanosuspensions were evaluated with different evaluation parameters like mean particle size and saturation solubility to select solvent: antisolvent volume ratio for further formulation work, as shown in Table 4.28, 1:8 solvent: antisolvent volume ratio was selected which was showing minimum mean particle size and maximum saturation solubility.

Once the precipitation of drug particle had occurred in suspension, to convert into the uniform nanosized particles probe sonicator was used. 10 mins, 20 mins, and 30 mins period were selected for sonication. Nanosuspension was prepared according to the procedure given before. Prepared nanosuspensions were evaluated with different evaluation parameters like mean particle size and saturation solubility to select the optimized time period of sonication for further formulation work. As shown in Table 4.28, 30 mins sonication time was selected which was showing minimum mean particle size and maximum saturation solubility.

**TABLE 4.28: Results of optimization of other preliminary parameters for TMNS**

Batch Code	Preliminary Parameters		Mean Particle Size (nm) (Mean $\pm$ SD)*	Saturation Solubility ( $\mu\text{g/ml}$ ) (Mean $\pm$ SD)*
TF14	Amount of Poloxamer 407 (mg)	30	304.5 $\pm$ 5.2	64.36 $\pm$ 1.15
TF15		40	228.0 $\pm$ 9.2	77.22 $\pm$ 1.52
<b>TF16</b>		<b>50</b>	<b>152.4 <math>\pm</math> 7.4</b>	<b>82.17 <math>\pm</math> 1.29</b>
TF17	Solvent to Antisolvent Volume Ratio	1:4	312.0 $\pm$ 3.9	79.71 $\pm$ 1.21
TF18		1:6	289.8 $\pm$ 8.4	77.24 $\pm$ 1.32
<b>TF19</b>		<b>1:8</b>	<b>254.2 <math>\pm</math> 11.2</b>	<b>91.3 <math>\pm</math> 1.51</b>
TF20	Sonication Time (min)	10	365.5 $\pm$ 9.0	62.27 $\pm$ 1.09
TF21		20	222.3 $\pm$ 6.7	69.22 $\pm$ 1.26
<b>TF22</b>		<b>30</b>	<b>180.2 <math>\pm</math> 5.8</b>	<b>83.31 <math>\pm</math> 1.35</b>

\* Indicates average of three determinations

### 4B.7 3<sup>2</sup> Factorial Design

Various formulations were prepared the varying amount of telmisartan and stirring speed. [61] As shown in Table 4.29 a 3<sup>2</sup> full factorial design was used to evaluate the effect of both independent variables on the predetermined dependent variables viz., particle size and saturation solubility.

**TABLE 4.29: Layout and observed responses of 3<sup>2</sup> factorial design for TMNS**

Batch Code	Level of Amount of Telmisartan X <sub>1</sub>	Level of Stirring Speed X <sub>2</sub>	Mean Particle Size (nm) (Mean ± SD)* Y <sub>1</sub>	Saturation Solubility (µg/ml) (Mean ± SD)* Y <sub>2</sub>
TFD1	-1	-1	465.0 ± 8.9	63.15 ± 0.98
TFD2	-1	0	384.0 ± 4.8	71.42 ± 0.85
TFD3	-1	1	365.0 ± 8.1	84.93 ± 1.05
TFD4	0	-1	430.0 ± 7.2	83.51 ± 1.12
TFD5	0	0	344.0 ± 6.7	86.59 ± 1.08
<b>TFD6</b>	<b>0</b>	<b>1</b>	<b>325.6 ± 6.4</b>	<b>102.60 ± 1.32</b>
TFD7	1	-1	405.0 ± 5.9	74.27 ± 0.97
TFD8	1	0	334.0 ± 8.0	83.31 ± 1.21
TFD9	1	1	314.0 ± 9.1	93.05 ± 1.16
<b>Translation of Coded Levels in Actual Units</b>				
<b>Variables Level</b>		<b>Low (-1)</b>	<b>Medium (0)</b>	<b>High (1)</b>
X <sub>1</sub>		10 mg	15 mg	20 mg
X <sub>2</sub>		800 RPM	1000 RPM	1200 RPM

\* Indicates average of three determinations

Some other parameters were also evaluated like, CPR at 2 minutes, zeta potential, PDI, and %w/w drug content etc. as shown in Table 4.30.

**Table 4.30: Other evaluation parameters of factorial batches of TMNS**

Batch Code	CPR at 2mins (% w/w) (Mean ± SD)*	PDI (Mean ± SD)*	Zeta Potential (mV) (Mean ± SD)*	Drug Content (%w/w) (Mean ± SD)*
TFD1	92.17 ± 1.84	0.529 ± 0.049	17.38 ± 1.82	95.24 ± 1.02
TFD2	101.27 ± 2.25	0.919 ± 0.112	-28.10 ± 2.06	97.52 ± 1.11
TFD3	88.64 ± 1.56	0.784 ± 0.082	-15.33 ± 1.48	100.95 ± 1.84
TFD4	97.92 ± 1.91	0.963 ± 0.101	-18.08 ± 1.09	99.81 ± 0.54
TFD5	93.32 ± 1.42	0.845 ± 0.062	27.76 ± 2.15	96.00 ± 0.29
<b>TFD6</b>	<b>98.24 ± 1.38</b>	<b>0.459 ± 0.038</b>	<b>-29.96 ± 1.87</b>	<b>99.54 ± 0.81</b>
TFD7	96.25 ± 2.05	0.419 ± 0.051	-18.22 ± 1.55	94.00 ± 0.73
TFD8	93.28 ± 1.09	0.716 ± 0.068	-19.04 ± 1.61	92.10 ± 0.58
TFD9	91.27 ± 1.19	0.645 ± 0.043	19.27 ± 1.72	93.24 ± 0.69

\* Indicates average of three determinations

#### 4B.8 Statistical analysis

A full model was derived after putting the values of regression coefficients in the equation (3.8). Regression analysis was carried out using Microsoft Excel<sup>®</sup> version 2013 (Microsoft Corporation, Washington, USA); the fitted results are shown in Table 4.31, Table 4.32, equation (4.6) and (4.7).

**TABLE 4.31: Results of regression analysis of mean particle size for TMNS**

	Mean Particle Size (nm) (Y <sub>1</sub> )		
	Coefficient	Std. Error	P- value
b <sub>0</sub>	346.3333	3.115572	1.605E-06
b <sub>1</sub>	-26.8333	1.706469	0.000559056
b <sub>2</sub>	-49.3333	1.706469	9.08819E-05
b <sub>11</sub>	11.5	2.955691	0.030105281
b <sub>22</sub>	30	2.955691	0.00203757
b <sub>12</sub>	2.25	2.089989	0.360540266
	<b>R<sup>2</sup> = 0.997511</b>		

For mean particle size (nm) (Y<sub>1</sub>)

$$Y_1 = 346.33 - 26.83X_1 - 49.33X_2 - 11.5X_1^2 + 30X_2^2 + 2.25X_1X_2$$

Eq...(4.6)



**TABLE 4.32: Results of regression analysis of saturation solubility for TMNS**

	Saturation Solubility ( $\mu\text{g/ml}$ ) ( $Y_2$ )		
	Coefficient	Std. Error	P- value
$b_0$	90.47	0.853323206	1.84994E-06
$b_1$	5.188333333	0.467384369	0.001566266
$b_2$	9.941666667	0.467384369	0.000227337
$b_{11}$	-13.545	0.809533473	0.000464816
$b_{22}$	2.145	0.809533473	0.077015288
$b_{12}$	-0.75	0.572426609	0.281413408
<b><math>R^2 = 0.996541</math></b>			

For saturation solubility ( $\mu\text{g/ml}$ ) ( $Y_2$ )

$$Y_2 = 90.47 + 5.1883X_1 + 9.941X_2 - 13.545X_1^2 + 2.145X_2^2 - 0.75X_1X_2 \quad \text{Eq...}(4.7)$$

The coefficients in Table 4.31 and Table 4.32 represent the respective quantitative effect of independent variables ( $X_1$  and  $X_2$ ) and their interactions on the various responses. It was seen that all the independent variables had a significant effect on the response ( $p < 0.05$ ). The negative sign of the coefficient indicated that increase in the value of independent variable decreases the value of response and vice versa. The absolute value of the coefficient indicates the magnitude of the effect of the independent variable on the response; higher the value higher the magnitude.

**TABLE 4.33: ANOVA for a full model for TMNS**

Source of variation	DF	SS	MS	F	F significant
<b>Mean Particle Size (nm)</b>					
Regression	5	21007.58333	4201.516667	240.4683625	0.000420651
Residual	3	52.41666667	17.47222222	-	-
Total	8	21060	-	-	-
<b>Saturation Solubility (<math>\mu\text{g/ml}</math>)</b>					
Regression	5	1132.919333	226.5838667	172.8738746	0.000688496
Residual	3	3.932066667	1.310688889	-	-
Total	8	1136.8514	-	-	-

The results of ANOVA for full model suggested that  $F_{cal}$  value for mean particle size was 240.46.  $F_{tab}$  value at (5, 3) was 9.0 for  $Y_1$ . So,  $F_{cal}$  value for  $Y_1$  was higher than  $F_{tab}$ .

The results of ANOVA for full model suggested that  $F_{cal}$  value for saturation solubility was 172.87.  $F_{tab}$  value at (5, 3) was 9.0 for  $Y_2$ . So,  $F_{cal}$  value for  $Y_2$  was higher than  $F_{tab}$ .

All dependent variables were found  $F_{cal}$  value significantly higher than  $F_{tab}$ . Therefore, selected factors have a significant effect on all three dependent variables.

All the determination coefficients  $R^2$  are larger than 0.99, indicating that over 99% of the variation in the response could be explained by the model and the goodness of fit of the model was confirmed. The F-ratio was found to be far greater than the theoretical value with a very low probability of less than 0.0001 for each regression model, indicating that the regression model is significant with a confidence level of 95%. The observed responses showed a wide variation suggesting that the selected both independent variables had a significant effect on resultant particle size and saturation solubility.

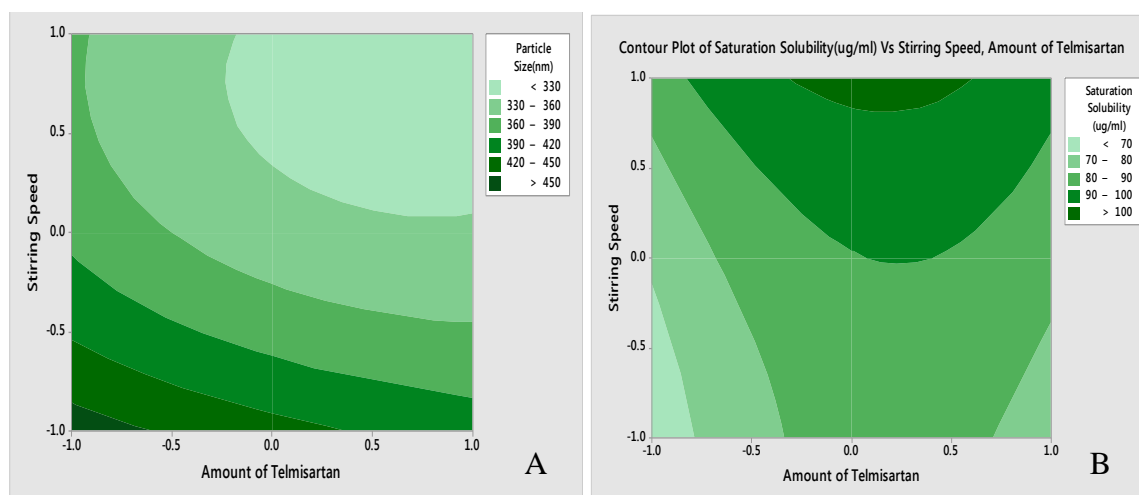
#### 4B.9 Contour plots

Two-dimensional contour plots were established using statistical software Minitab 17 (Minitab Inc., USA) to examine the relationship between independent and dependent variables as shown in the figure.

Figure 4.25 [A] shows contour plot for particle size (nm) at prefixed values between 330 to 450 nm. The contour plot was found to be non-linear. So the relationship between independent variables and particle size is not linear. The minimum (Light Green part) is clearly evidence from contour plot which specifies the stirring speed and amount of telmisartan for lowest particle size. Their respective values are approx. 1200rpm (coded value +1) stirring speed and 15 mg (coded value 0) amount of telmisartan.

Figure 4.25 [B] shows contour plot for saturation solubility ( $\mu\text{g}/\text{ml}$ ) at prefixed values between 70 to 100  $\mu\text{g}/\text{ml}$ . The contour plot was found to be non-linear. So the relationship between independent variables and dependent variables were not linear. The maximum (Dark Green part) is clearly evidence from contour plot which specifies the stirring speed and amount of telmisartan for maximum saturation solubility. Their respective values are approx. 1200rpm (coded value +1) stirring speed and 15 mg (coded value 0) amount of telmisartan.

The maxima of saturation solubility and minima of particle size are seemed to be overlapping. So, there exists a direct relation between saturation solubility and particle size. The batch showing lowest particle size is also having highest saturation solubility.



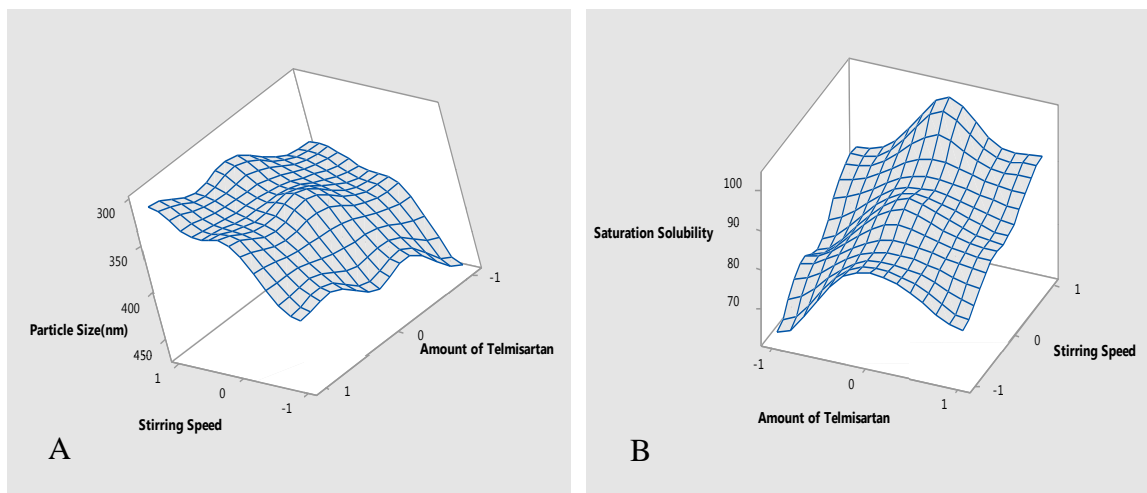
**FIGURE 4.25: Contour plot of TMNS for effect on [A] Mean particle size and [B] Saturation solubility**

#### 4B.10 Surface plots

To find out main and interaction effect of the independent variables, response surface plots are very helpful.

Figure 4.26 [A] shows the response surface plot of particle size as a function of stirring speed and drug concentration using statistical software Minitab 17 (Minitab Inc., USA). Particle size decreases as the plot comes toward central part. The center of the plot indicates the minimum particle size which was obtained by highest stirring speed and an intermediate amount of telmisartan.

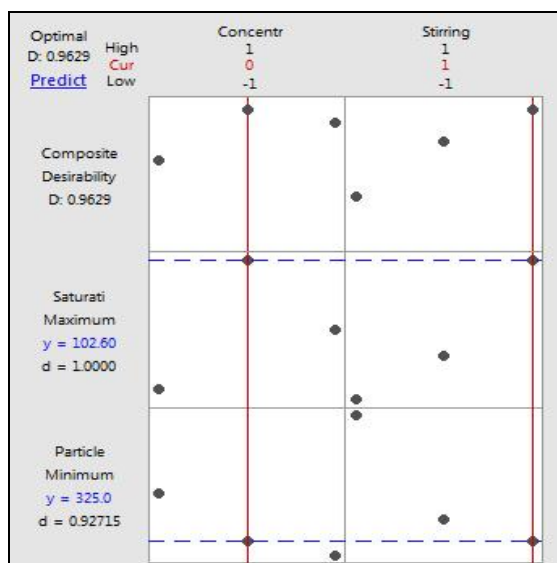
Figure 4.26 [B] shows the response surface plot of saturation solubility respectively as a function of stirring speed and drug concentration using statistical software Minitab 17 (Minitab Inc., USA). Saturation solubility increases as the plot come toward central part. The center of the plot indicates the highest saturation solubility which was obtained by highest stirring speed and an intermediate amount of telmisartan.



**FIGURE 4.26: Response surface plot of TMNS for effect on [A] Mean particle size and [B] Saturation solubility**

**4B.11 Optimization of nanosuspension by desirability function of Minitab17.0**

The optimum formulation was selected based on the criteria of attaining the minimum mean particle size ( $Y_1$ ) and the maximum saturation solubility ( $Y_2$ ). An overall desirability function dependent on all investigated formulation variables was used to predict the ranges of the variable where the optimum formulation might occur. The desirable ranges are from zero to one (least to most desirable, respectively). The optimized batch composition is presented in below Figure 4.27.



**FIGURE 4.27: Optimized plot of factorial design form Minitab 17 for TMNS**

#### 4B.12 Checkpoint cum optimized batch analysis

From the above Minitab data optimized batch was TFD-6. The desirability of the optimized batch was 0.9629. Formulation and process parameters for the optimized batch are shown in Table 4.34. The optimized lyophilized formulation was filled in hard gelatin capsules and kept in the tightly closed container.

**TABLE 4.34: Formulation and process parameters for an optimized batch of TMNS**

Amount of Telmisartan	15 mg
Amount of Poloxamer 407	50 mg
Solvent: Antisolvent Volume Ratio	1:8
Stirring Speed	1200 RPM
Stirring Time	4 h
Sonication Time	30 mins
Amount of lyophilizer (1:1, Total Solid: Mannitol)	65 mg

#### 4B.13 Checkpoint batch cum optimized batch validation

To evaluate model a checkpoint batch cum optimized batch TFD-6 was prepared at  $X_1 = 0$  and  $X_2 = +1$  levels. Dependent parameters were determined and compared with predicted values as shown in Table 4.35.

**TABLE 4.35: Composition of checkpoint batch cum optimized batch of TMNS**

Amount of Drug ( $X_1$ )		Solvent-Antisolvent Volume Ratio ( $X_2$ )	
Coded value	Decoded value	Coded value	Decoded value
0	15 mg	+1	1:8

**TABLE 4.36: Comparison of calculated data with experimental data of TMNS**

Response	Predicted	Observed	% Bias
Mean Particle Size ( $Y_1$ )	327.0 nm	328.0 nm	+ 0.305%
Saturation Solubility ( $Y_2$ )	102.55 $\mu\text{g/ml}$	100.16 $\mu\text{g/ml}$	- 2.330%

When the batch TFD-6 was prepared using defined level of the amount of telmisartan and stirring speed using Minitab17 (Minitab Inc., USA), the results obtained with checkpoint cum optimized batch (TFD-6) were close to predicted values. Thus, it can be concluded that the statistical model is mathematically valid.

#### 4B.14 Evaluation of optimized batch of telmisartan nanosuspension

##### 4B.14.1 Particle size and PDI

Particle size distribution of the optimized batch is shown in Figure 4.28. The mean particle size of the optimized batch is  $328.0 \pm 9.6$  nm. Telmisartan nanosuspension based final formulation was intended for oral administration for which PDI and particle size above  $5 \mu\text{m}$  is not critical. The particle size of a nanosuspension is around 200-1000 nm. [80] From the Table 4.29, it was found that mean particle sizes of all formulations were in the nanometer range. It shows that all formulations fulfill the requirements of a nanosuspension.

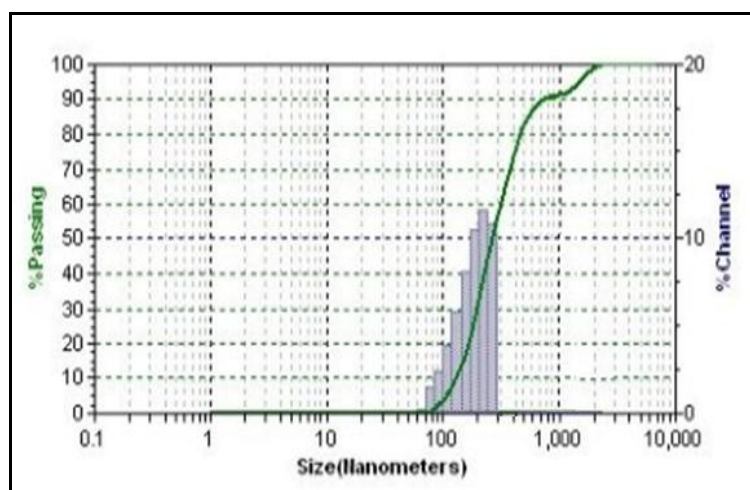


Figure 4.28: Particle size graph for TMNS

##### 4B.14.2 Zeta potential

Poloxamer 407 is a well-known efficient polymeric stabilizer forming a substantial mechanical and thermodynamic barrier at the interface of drug nanoparticles. [198] In general, zeta potential value of  $\pm 30\text{mV}$  is sufficient for the stability of nanosuspension. [171] Zeta potential of optimized formulation was observed  $-30.36 \pm 2.51\text{mV}$  which complies with the requirement of zeta potential.

##### 4B.14.3 Drug content

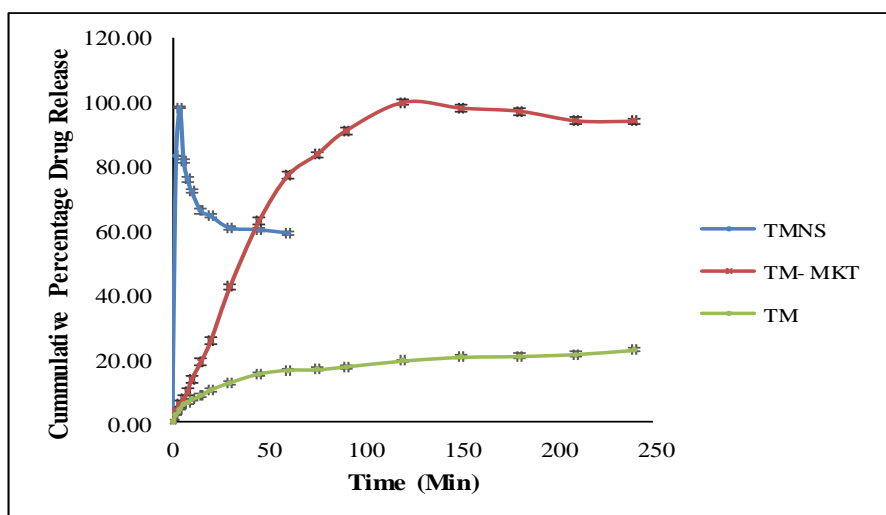
An aliquot (1 ml) of the prepared nanosuspension was diluted in methanol and filtered with a  $0.2 \mu\text{m}$  filter. Total drug content was determined by UV-Visible spectrophotometer at 296 nm and was found to be 99.54% w/w of the telmisartan.

#### 4B.14.4 Saturation solubility

Saturation solubility of an optimized batch of telmisartan nanosuspension and the pure drug was found to be 100.16  $\mu\text{g/ml}$  and 3.51  $\mu\text{g/ml}$  respectively. It indicates that saturation solubility of nanosuspension was 30-35 times than that of pure drug. This drastic increase in saturation solubility is as a result of a reduction in particle size and subsequent increase in surface area. So, it can be assumed that this increase in saturation solubility may increase bioavailability.

#### 4B.14.5 *In-vitro* dissolution study

The dissolution profile of nanosuspension, un-milled (pure drug) suspension and marketed formulation (Inditel 40 Tablet) are presented in Figure 4.29. In nanosuspension, more than 102.60 % drug was released within 2 mins, while cumulative percentage drug release of un-milled suspension, marketed formulated showed 16.41% and 77.08% at 60 mins respectively. So, nanosuspension enhanced the rate of dissolution of telmisartan to great extent.



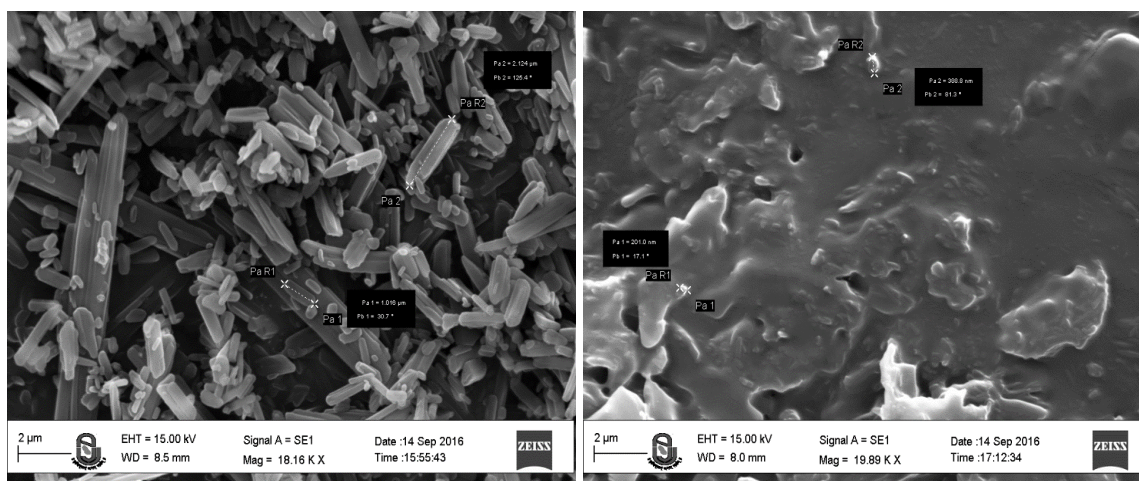
**FIGURE 4.29: Comparison of *in-vitro* dissolution of telmisartan nanosuspension with marketed formulation**

**TABLE 4.37: Evaluation parameters of an optimized batch of TMNS**

Evaluation Parameters	Results
Mean Particle Size	328.0 nm
PDI	0.477
Zeta Potential	-30.36 mV
Drug Content	99.54 % w/w
Saturation Solubility	100.16 µg/ml
CPR at 2 mins	102.60 % w/w

#### 4B.14.6 Scanning electron microscopy (SEM)

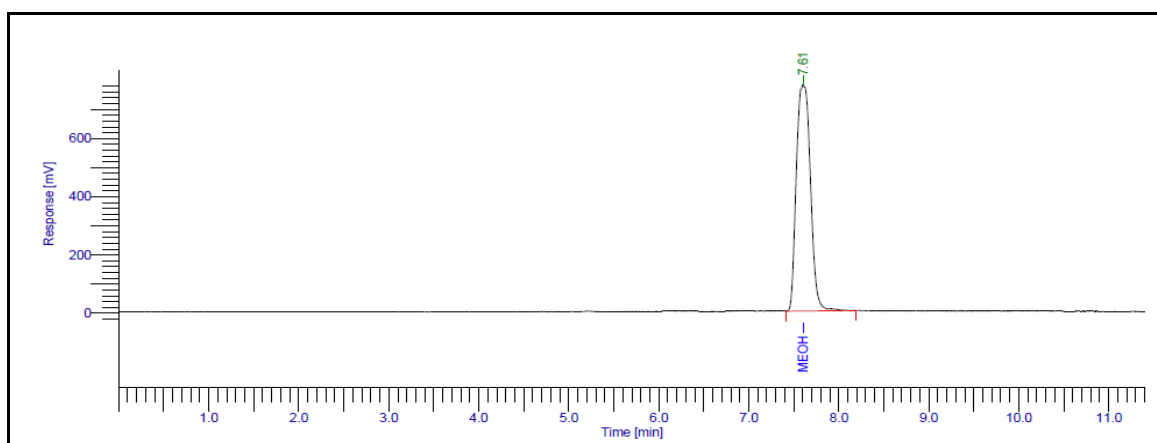
The surface characteristics of telmisartan and its lyophilized nanosuspension were studied by scanning electron microscopy (EVO-18, ZEISS, Germany) at 13kx to 28kx. The samples were mounted on double-sided carbon adhesive tape that has previously been secured on brass stubs and then subjected to gold coating by sputter coater, using process current of 10 mA for 4 mins. The accelerating voltage was 15 kV. The surface topology as measured by scanning electron microscopy of telmisartan was found to be long, thin and flat with particles larger (1-20 µm) in size, as shown in Figure 4.30. However, after conversion to lyophilized nanosuspension, particles became smaller (about 200-390 nm) which were adsorbed on the surface of mannitol used as cryoprotectant may be by hydrophobic interaction.

**FIGURE 4.30: Scanning electron microscopy of [a] telmisartan [B] TMNS**



#### 4B.14.7 Residual solvent by gas – chromatography (GC)

Methanol is included in Class 3 solvent, may be regarded as less toxic and of low risk to human health. According to ICH guidelines, it is considered that amount of these residual solvents of 3000 ppm per day would be acceptable without justification. [173] Amount of methanol was evaluated for residual solvent content in lyophilized nanosuspension of telmisartan by gas chromatography using head-space sampler. Results of GC indicated that 192.27 ppm methanol was present in the sample which is the far lesser amount of class 3 solvents. Figure 4.31 indicates gas chromatograph of methanol in lyophilized telmisartan nanosuspension.



**FIGURE 4.31: Gas chromatograph of methanol in the lyophilized telmisartan nanosuspension**

#### 4B.14.8 Accelerated stability study

The accelerated stability study indicated that lyophilized telmisartan nanosuspension was physically and chemically stable when stored at the  $25 \pm 2^\circ\text{C}$  and  $60 \pm 5\%$  RH for a period of 6 months. [176] Table 4.38 shows results of mean particle size, saturation solubility, cumulative percentage release at 2 mins and %w/w of drug content indicated that there was a slight change in all parameters which had  $< \pm 5\%$  bias which was insignificant. The negligible difference was observed in results obtained from the optimized batch before and after the stability study according to ICH guideline.

**TABLE 4.38: Results of accelerated stability study of TMNS**

Sr. No.	Storage condition for stability study	Time Period (months)	Evaluation Parameters			
			Mean Particle Size (nm) (Mean $\pm$ SD)*	Saturation Solubility ( $\mu$ g/ml) (Mean $\pm$ SD)*	CPR at 2mins (%w/w) (Mean $\pm$ SD)*	Drug Content (%w/w) (Mean $\pm$ SD)*
1	25°C $\pm$ 2°C and 60% $\pm$ 5% RH	0	328.0 $\pm$ 5.4	100.16 $\pm$ 2.1	98.24 $\pm$ 0.85	99.54 $\pm$ 0.53
2		1	339.1 $\pm$ 4.8	99.27 $\pm$ 1.80	97.98 $\pm$ 0.79	98.85 $\pm$ 0.52
3		3	356.1 $\pm$ 8.2	98.76 $\pm$ 1.65	97.12 $\pm$ 0.87	97.67 $\pm$ 0.47
4		6	385.2 $\pm$ 9.7	98.15 $\pm$ 1.71	96.54 $\pm$ 0.46	96.97 $\pm$ 0.89

\* Indicates average of three determinations

#### 4B.15 Bioavailability study

For bioavailability study, each rat was treated with oral nanosuspension of telmisartan at a dose of 4.11 mg/kg in a single dose. Blood samples were collected from retro-orbital venous plexus over a period 24 h. Each sample was analyzed by HPLC for the estimation of drug content by a bioanalytical method. The pharmacokinetic calculations were performed on the basis of plasma concentration-time data, as shown in Table 4.39.

**TABLE 4.39: Results of bioavailability study of telmisartan nanosuspension and marketed formulation**

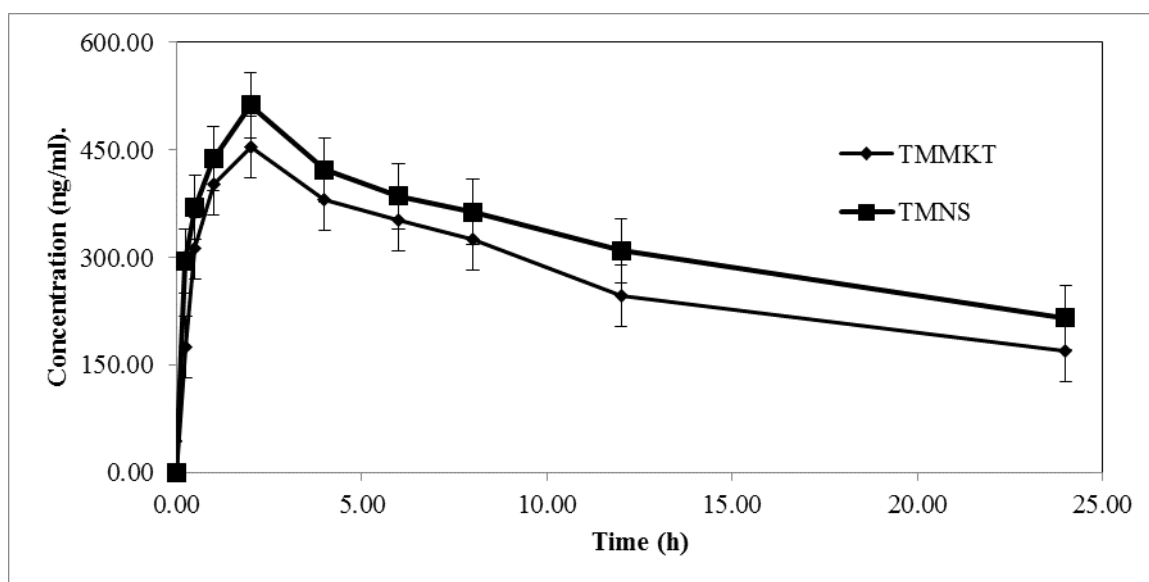
Sr. No.	Time (h)	TMNS (ng/ml)* (Mean $\pm$ SD)	TMMKT (ng/ml)* (Mean $\pm$ SD)	AUC(TMNS) (ng/ml).h	AUC(TMMKT) (ng/ml).h
1	0.00	0.00 $\pm$ 0.00	0.00 $\pm$ 0.00	0.0000	0.0000
2	0.25	294.42 $\pm$ 37.23	175.25 $\pm$ 30.78	36.8025	21.9063
3	0.5	370.24 $\pm$ 20.08	312.37 $\pm$ 36.14	83.0825	60.9525
4	1.00	437.59 $\pm$ 55.75	401.84 $\pm$ 37.28	201.9575	178.5525
5	2.00	512.51 $\pm$ 22.07	453.19 $\pm$ 39.93	475.0500	427.5150
6	4.00	422.36 $\pm$ 39.10	380.22 $\pm$ 47.65	934.8700	833.4100
7	6.00	385.47 $\pm$ 31.75	351.78 $\pm$ 38.60	807.8300	732.0000
8	8.00	363.42 $\pm$ 33.27	325.54 $\pm$ 21.68	748.8900	677.3200
9	12.00	309.34 $\pm$ 37.05	246.89 $\pm$ 36.02	1345.5200	1144.8600
10	24.00	215.62 $\pm$ 35.15	169.12 $\pm$ 17.72	3149.7600	2496.0600
Total				7783.7625	6572.5763

\*Indicates average of 6 determinations

TMNS – Telmisartan Nanosuspension,

TMMKT – Telmisartan Marketed Formulation

Figure 4.32 shows the mean plasma concentration ( $\mu\text{g/ml}$ ) vs. Time (h) in rats after administration of optimized nanosuspension of telmisartan and its marketed formulation (Inditel 40 Tablet). It is evident that the area under curve (AUC) values for the optimized formulation containing telmisartan was higher than the corresponding values of the marketed formulation of telmisartan (Table 4.39). The increase AUC values could be attributed to the improved dissolution of telmisartan from the optimized nanosuspension formulation as compared to its marketed formulation.



**FIGURE 4.32: Plasma concentration vs. time profile of telmisartan nanosuspension and marketed formulation**

The values of all major pharmacokinetic parameters like maximum plasma concentration ( $C_{\max}$ ), the time required for maximum plasma concentration ( $T_{\max}$ ), the area under the curve ( $AUC_{0\rightarrow 24}$ ), terminal half-life ( $T_{1/2}$ ), elimination rate constant ( $K_E$ ) and absorption rate constant ( $K_a$ ) have been summarized in Table 4.40.

**TABLE 4.40: Results of pharmacokinetic parameters of telmisartan nanosuspension and marketed formulation**

Pharmacokinetic Parameters	Telmisartan Nanosuspension (TMNS)	Telmisartan Cilexetil Marketed Formulation (TMMKT)
C <sub>max</sub> (ng/ml)	542.51	453.19
T <sub>max</sub> (h)	1.0	2.0
AUC <sub>0-24</sub> (ng/ml)*h	7783.763	6572.576
t <sub>1/2E</sub> (h)	23.526	20.684
K <sub>E</sub> (h <sup>-1</sup> )	0.029	0.034
K <sub>a</sub> (h <sup>-1</sup> )	0.387	0.127

The calculation was performed for the equivalent dose of test product (TMNS) required attaining same C<sub>max</sub> of the marketed product. [194]

F-Ratio was calculated from the following equation,

$$F_r = \frac{[AUC]_{test}[D]_{std}}{[AUC]_{std}[D]_{test}} \quad \text{Eq...(4.3)}$$

- Where, Fr = Relative bioavailability (F-Ratio)  
 [AUC]<sub>test</sub> = AUC of telmisartan nanosuspension  
 [AUC]<sub>std</sub> = AUC of telmisartan marketed formulation  
 [D]<sub>test</sub> = Dose of telmisartan nanosuspension  
 [D]<sub>std</sub> = Dose of telmisartan marketed formulation

Using above equation, bioavailability fraction obtained from telmisartan nanosuspension was **1.184**.

Volume of distribution was calculated by following equation,

$$V_d = \frac{FD}{C_{max}} \quad \text{Eq...(4.4)}$$

- Where, V<sub>d</sub> = Volume of distribution  
 F = F-Ratio  
 D = Dose of the product  
 C<sub>max</sub> = Maximum plasma concentration

Using above equation, the volume of distribution obtained from telmisartan nanosuspension was **1.898 lit.**

From the following equation amount of drug to be administered to attain the same plasma concentration of marketed product was calculated

$$C = \frac{K_a F X_0}{V_d (K_a - K_e)} [e^{-K_e t} - e^{-K_a t}] \quad \text{Eq... (4.5)}$$

- Where, C = C<sub>max</sub> of telmisartan marketed formulation  
 K<sub>a</sub> = Absorption rate constant of telmisartan nanosuspension  
 F = F-Ratio  
 X<sub>0</sub> = Amount of telmisartan administered by nanosuspension  
 V<sub>d</sub> = Volume of distribution of telmisartan nanosuspension  
 K<sub>e</sub> = Elimination rate constant of telmisartan nanosuspension  
 t = Time required for maximum plasma concentration by telmisartan nanosuspension

AUC was higher by 1.184 times and C<sub>max</sub> by 1.197 times higher for telmisartan nanosuspension as compared to marketed formulation shows quite a good rise in bio-availability. T<sub>max</sub> was half as compared to marketed formulation indicates a substantial improvement in absorption of the drug from nanosuspension.

Using above equation, amount of telmisartan should be administered by nanosuspension (X<sub>0</sub>) was found to be **0.672 mg/day** for rats, which was further converted to human equivalent dose, which was **32.7 mg/day**.

The reported usual dose of telmisartan is 40 mg / 80 mg once daily in the management of **hypertension**. Lower initial doses should be considered in patients with hepatic or renal impairment. The study was conducted with 40 mg/day dose of telmisartan nanosuspension. Results suggested that by converting telmisartan into nanosuspension form dose can be reduced from 40 to 32.7 mg/day which was **81.75%** of the regular dose that indicated **18.25% dose reduction**. The improvement in bioavailability due to conversion from drug to nanosuspension was 18.25%.

**4B.16 Conclusion**

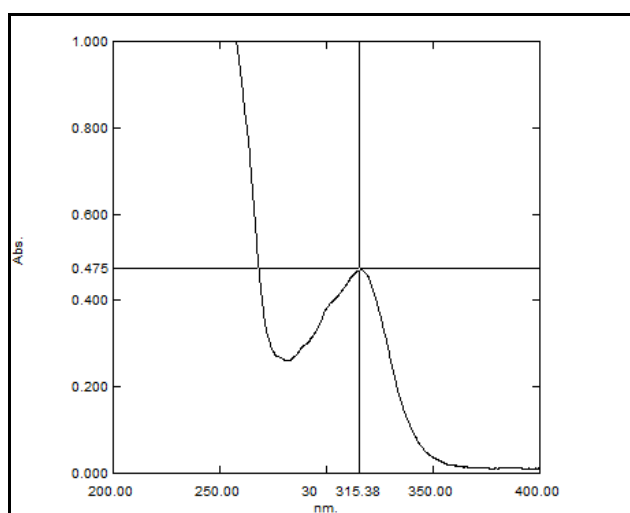
Plackett - Burman design was effectively employed to identify formulating and processing key parameters that are affecting the quality of the telmisartan nanosuspension.  $3^2$  factorial design was employed for optimization of the formulation of nanosuspension. All the predetermined independent variables were found to affect the dependent variables from the resultant nanosuspension. The optimum formulation prepared by response optimizer by desirability function provided a final formulation with  $D = 0.9629$  which released 102.60% of telmisartan within 2 mins. The *in-vivo* studies confirmed that nanosuspension loaded telmisartan showed a significantly better AUC as compared to marketed formulation and dose of telmisartan was reduced about 18.25% to reach plasma concentration of marketed formulation. The improved formulation could offer improved drug delivery strategy which might allow concomitant use of telmisartan in nanosuspension form. The nanosuspension of drug exhibited 18.25% improvement in bioavailability.

## 4C. Result and discussion of ziprasidone hydrochloride nanosuspension

### 4C.1 Scanning and calibration curve preparation of ziprasidone hydrochloride

#### 4C.1.1 Scanning and calibration curve preparation of ziprasidone hydrochloride in methanol

The standard stock solution of ziprasidone hydrochloride was prepared in methanol as per the method described in experimental section and scanned by UV-Visible spectrophotometer between 200 to 400 nm. The UV absorption spectrum of ziprasidone hydrochloride showed  $\lambda_{\max}$  at 315 nm [199] as shown in Figure 4.33.



**FIGURE 4.33: Scanning of ziprasidone hydrochloride in methanol**

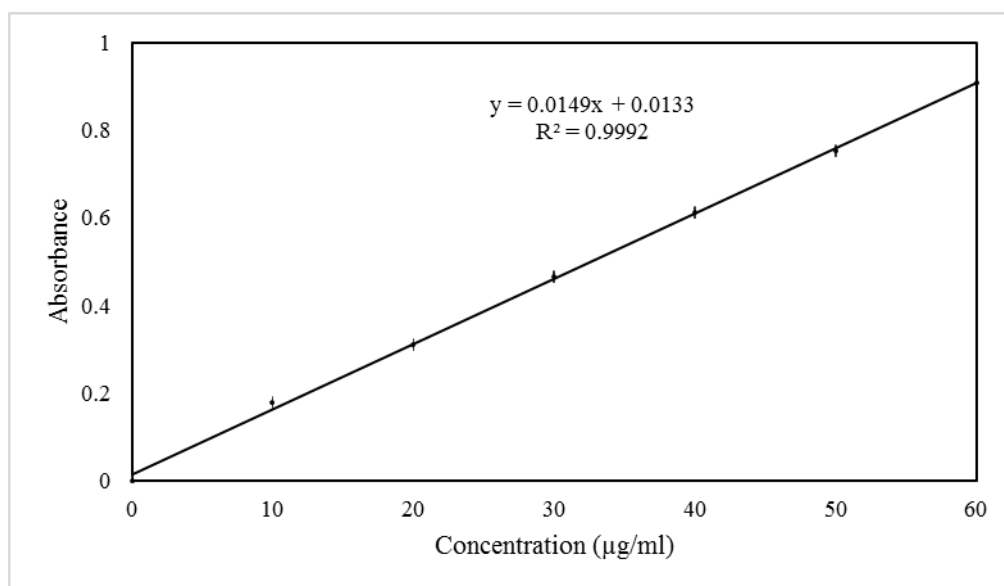
A calibration curve was prepared in methanol in the range of 10-60  $\mu\text{g/ml}$  by UV-Visible spectrophotometer. The absorbance of these solutions was measured at 315 nm. This procedure was performed in triplicate to validate the calibration curve. The data is given in Table 4.41.

**TABLE 4.41: Calibration curve data of ziprasidone hydrochloride in methanol**

Sr. No.	Concentration ( $\mu\text{g/ml}$ )	Absorbance at 315nm* (Mean $\pm$ SD)*
1	0	0.000 $\pm$ 0.000
2	10	0.178 $\pm$ 0.007
3	20	0.31 $\pm$ 0.008
4	30	0.465 $\pm$ 0.006
5	40	0.612 $\pm$ 0.012
6	50	0.753 $\pm$ 0.001
7	60	0.909 $\pm$ 0.011

\*Indicates average of three determinations

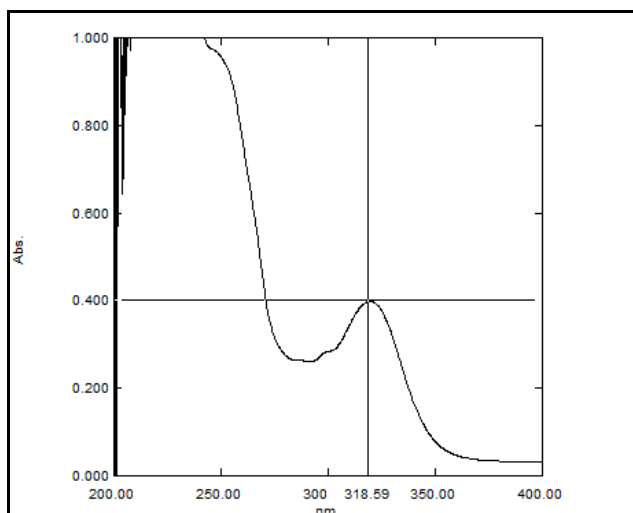
A calibration curve was constructed by plotting absorbance vs. concentration in  $\mu\text{g/ml}$  as shown in Figure 4.34 and regression equation was found to be  $Y = 0.0149X + 0.0133$  with regression coefficient 0.999.

**FIGURE 4.34: Calibration curve of ziprasidone hydrochloride in methanol**



#### 4C.1.2 Scanning and calibration curve preparation of ziprasidone hydrochloride in 0.05M sodium phosphate buffer, pH 7.5 containing 2% w/w SDS

The standard stock solution of ziprasidone hydrochloride (10  $\mu\text{g/ml}$ ) was prepared in 0.05M sodium phosphate buffer, pH 7.5 containing 2% w/w SDS and scanned by UV-Visible spectrophotometer between 200 to 400 nm. The UV absorption spectrum of ziprasidone hydrochloride showed  $\lambda_{\text{max}}$  at 318 nm [200] as shown in Figure 4.35.



**Figure 4.35: Scanning of ziprasidone hydrochloride in 0.05M sodium phosphate buffer, pH 7.5 containing 2% SDS**

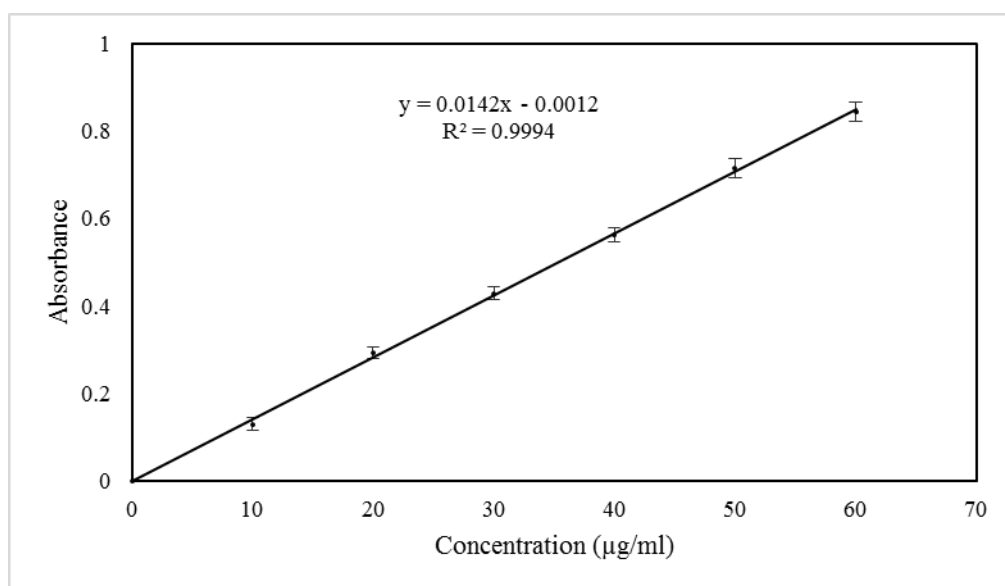
A calibration curve was prepared in 0.05 M sodium phosphate buffer, pH 7.5 containing 2 %w/w SDS in the range of 10-60  $\mu\text{g/ml}$  by UV-Visible spectrophotometer. The absorbance of these solutions was measured at 318 nm. This procedure was performed in triplicate to validate the calibration curve. The data is given in Table 4.42.

**Table 4.42: Calibration curve data of ziprasidone hydrochloride in 0.05M sodium phosphate buffer, pH 7.5 containing 2% SDS**

Sr. No.	Concentration (µg/ml)	Absorbance at 318nm (Mean ± SD)*
1	0	0.000 ± 0.000
2	10	0.129 ± 0.006
3	20	0.293 ± 0.009
4	30	0.429 ± 0.011
5	40	0.563 ± 0.011
6	50	0.715 ± 0.009
7	60	0.845 ± 0.005

\*Indicates average of three determinations

A calibration curve was prepared in 0.05 M sodium phosphate buffer, pH 7.5 containing 2% w/w SDS in the range of 10-60µg/ml as shown in Figure 4.35 and regression equation was found to be  $Y = 0.0142X - 0.0012$  with regression coefficient 0.9994.



**Figure 4.36: Calibration curve of ziprasidone hydrochloride in 0.05M sodium phosphate buffer, pH 7.5 containing 2% SDS**

#### 4C.2 Selection of solvent and antisolvent for ziprasidone hydrochloride nanosuspension (ZHNS)

Selection of solvent and antisolvent was performed on the basis of solubility of ziprasidone hydrochloride in different solvents and their combinations. [163] Results showed that drug had the highest solubility (2.443mg/ml) in methanol and least solubility (0.022 mg/ml) in water, so they were selected as solvent and antisolvent respectively as shown in Table 4.43.

**TABLE 4.43: Results of selection of solvents for ZHNS**

Drug	Solvents	Solubility (mg/ml) (Mean $\pm$ SD)*
Ziprasidone Hydrochloride	Water	0.022 $\pm$ 0.0013
	Methanol	2.443 $\pm$ 0.052
	Alcohol	0.375 $\pm$ 0.033
	Iso-propanol	0.82 $\pm$ 0.0023
	N-Butanol	0.120 $\pm$ 0.010
	Alcohol:2-Propanol (1:1)	0.138 $\pm$ 0.025
	Alcohol: Butanol (1:1)	0.158 $\pm$ 0.034
	Ethyl Acetate	0.044 $\pm$ 0.018

\* Indicates average of three determinations

#### 4C.3 Selection of stabilizer

Different stabilizers like polyvinyl alcohol, PVP K-30, sodium lauryl sulfate, poloxamer 188 and poloxamer 407 were screened by preparing nanosuspensions with bellow mentioned formulating and processing parameters as shown in Table 4.44 [184]

**TABLE 4.44: Formulating and processing parameters for selection of stabilizer for ZHNS**

Batch Code	Stabilizers	Amount of Stabilizers (mg)	Amount of Ziprasidone Hydrochloride* (mg)	Stirring Speed (RPM)	Stirring Time (h)	Sonication Time (min)	Solvent : Antisolvent Volume Ratio
ZF1	Polyvinyl Alcohol	30	11.3	1000	5	20	1:8
ZF2	PVP K30	30					
ZF3	Sodium Lauryl Sulphate	4					
ZF4	Poloxamer 188	30					
ZF5	Poloxamer 407	30					

\* 11.3 mg of Ziprasidone Hydrochloride is equivalent to 10 mg of Ziprasidone Base [106]

The prepared nanosuspensions (ZF1 to ZF5) were evaluated by measuring their saturation solubility, mean particle size, polydispersity index (PDI) and zeta potential for selection of the best stabilizer which can be utilized for further research work, as shown in Table 4.45.

**TABLE 4.45: Results for selection of stabilizer for ZHNS**

Batch Code	Stabilizer Used	Saturation Solubility ( $\mu\text{g/ml}$ ) (Mean $\pm$ SD)*	Mean Particle Size (nm) (Mean $\pm$ SD)*	PDI (Mean $\pm$ SD)*	Zeta Potential (mV) (Mean $\pm$ SD)*
ZF1	Polyvinyl Alcohol	29.64 $\pm$ 2.78	336.8 $\pm$ 5.1	1.27 $\pm$ 0.15	-21.56 $\pm$ 1.12
ZF2	PVP K-30	42.49 $\pm$ 1.08	234.0 $\pm$ 4.7	0.84 $\pm$ 0.11	27.85 $\pm$ 0.32
ZF3	Sodium Lauryl Sulphate	34.03 $\pm$ 0.81	333.5 $\pm$ 7.3	1.09 $\pm$ 0.05	-29.11 $\pm$ 0.72
ZF4	Poloxamer 188	31.27 $\pm$ 1.74	318.0 $\pm$ 6.8	0.75 $\pm$ 0.06	-31.41 $\pm$ 1.15
<b>ZF5</b>	<b>Poloxamer 407</b>	<b>45.58 <math>\pm</math> 1.62</b>	<b>210.4 <math>\pm</math> 5.9</b>	<b>0.40 <math>\pm</math> 0.03</b>	<b>32.53 <math>\pm</math> 0.90</b>

\*Indicates average of three determinations

Table 4.45 indicated that poloxamer 407 showing highest saturation solubility and lowest mean particle size. It also showed minimum PDI showing uniformity in particle size of nanosuspension and highest zeta potential indicating greater stability, so poloxamer 407 was selected as a stabilizer for further studies.

#### 4C.4 Drug-excipient compatibility study

Studies of drug-excipient compatibility represent an important phase in the preformulation stage of the development of all dosage forms. The potential physical and chemical interactions between drugs and excipients can affect the chemical, physical, therapeutical properties and stability of the dosage form. Fourier transformed infrared (FTIR) spectroscopy and differential scanning calorimetry (DSC) were selected for checking of drug-excipient compatibility. [201,202]

##### 4C.4.1 Fourier transformed infrared (FTIR) spectroscopy

FTIR spectroscopy was conducted using a Shimadzu FTIR 8400 spectrophotometer (Shimadzu, Tokyo, Japan) and the spectrum was recorded in the wavelength region of  $4000\text{--}400\text{ cm}^{-1}$  as shown in Figure 4.37 [A, B, C].

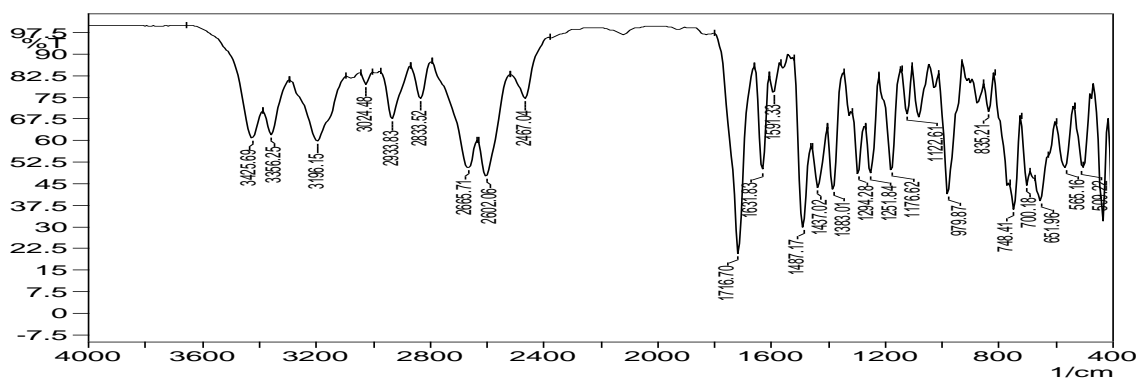


FIGURE 4.37 [A]: FT-IR spectra of ziprasidone hydrochloride

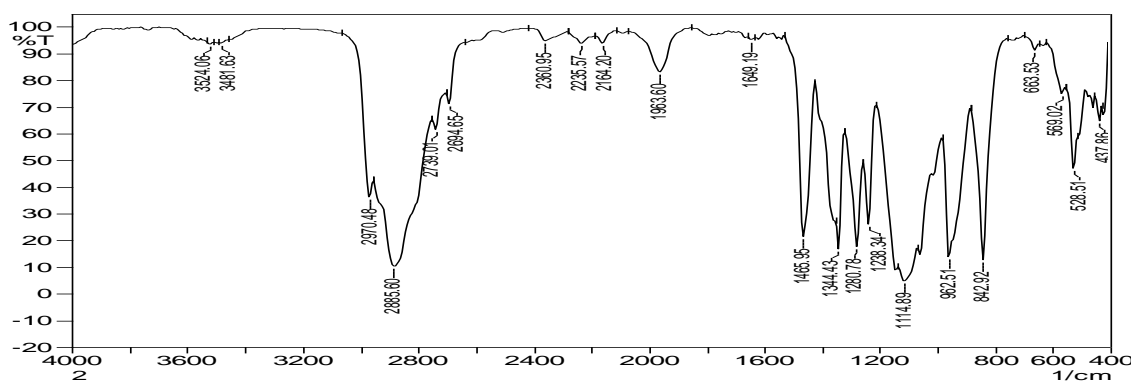
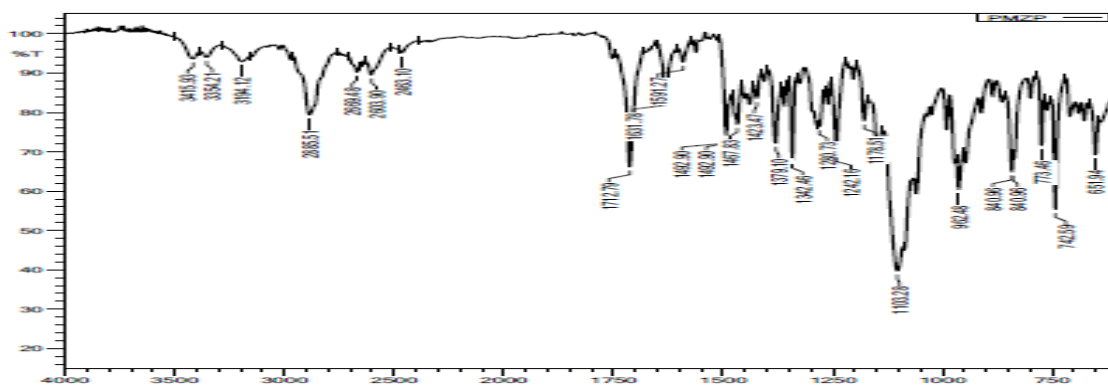


FIGURE 4.37 [B]: FT-IR spectra of poloxamer 407



**FIGURE 4.37 [C]: FT-IR spectra of a physical mixture of ziprasidone hydrochloride and poloxamer 407**

Ziprasidone hydrochloride, poloxamer 407 and its physical mixture were subjected to FTIR studies and characteristic bands were identified and given in Table 4.46.

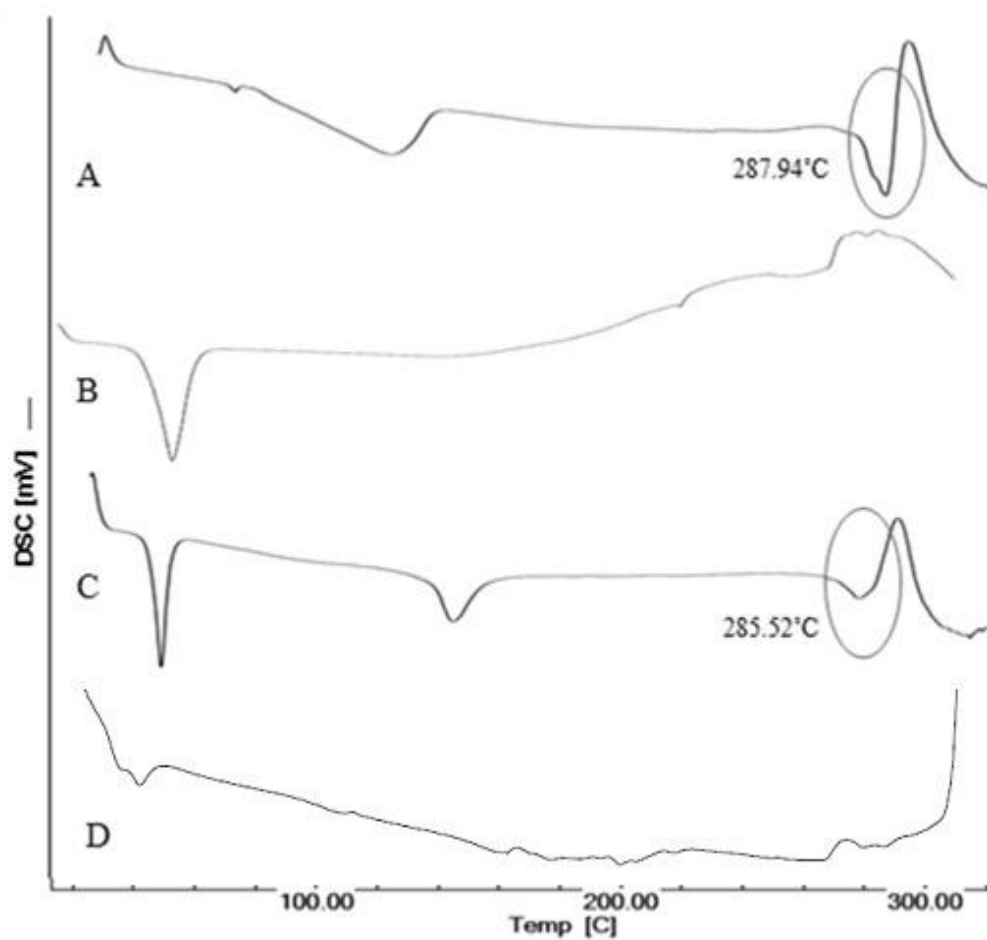
**TABLE 4.46: Comparison of characteristic bands between ziprasidone hydrochloride and its physical mixture.**

Characteristic bands [187,188]	Peak Value, cm <sup>-1</sup>	
	Ziprasidone Hydrochloride	Physical Mixture
Piperazinyl-N-H stretching	3356.25	3354.21
	3425.69	3415.93
Aromatic –C-H stretching	3196.15	3194.12
Aliphatic –C-H stretching	2883.52	2885.51
-C-H Stretching	1631.83	1631.78
-CH bending of -CH <sub>2</sub>	1487.17	1492.90
-C-Cl stretching	651.96	651.94

Table 4.46 indicates that the bands were similar for both pure drug and physical mixture and therefore there was no incompatibility between ziprasidone hydrochloride and poloxamer 407.

#### 4C.4.2 Differential scanning calorimetry (DSC)

DSC was performed using DSC-60 (Shimadzu, Tokyo, Japan) calorimeter to study the thermal behavior of the sample (ziprasidone hydrochloride, poloxamer 407, physical mixture and lyophilized nanosuspension). Information of thermal analysis by DSC can be seen in Figure 4.38.



**FIGURE 4.38: DSC thermograms of [A] Ziprasidone hydrochloride [B] Poloxamer 407 [C] Physical mixture of ziprasidone hydrochloride and poloxamer 407 [D] Lyophilized nanosuspension of ziprasidone hydrochloride**

In DSC measurements, the melting endotherm of ziprasidone hydrochloride was observed at 287.94°C, while the melting endotherm of physical mixture was recorded at 285.52°C. However, no endotherm was observed in the DSC curve for lyophilized nanosuspension. This result indicated that ziprasidone hydrochloride no longer presents as a crystalline form when processed by antisolvent precipitation followed by ultrasonication, but exists in the amorphous state.

#### **4C.5 Plackett - Burman Design (PB)**

Most common screening design is Plackett-Burman (PB) design that screens a large number of factors and identifies critical one in a minimal number of running with a good degree of accuracy. Generally, a number of runs needed to investigate the main effects are

multiple of 4 in PB designs. [189,190] It is used during the initial phase of the study. Provided the interaction effects are nil or negligible, the Plackett-Burman design is effective for measuring main effects. As shown in Table 4.47 the selected response parameters showed a wide variation suggesting that the independent variables had a significant effect on the response parameters chosen.

**TABLE 4.47: Layout and observed responses of Plackett - Burman design batches for ZHNS (Preliminary Screening Formulations)**

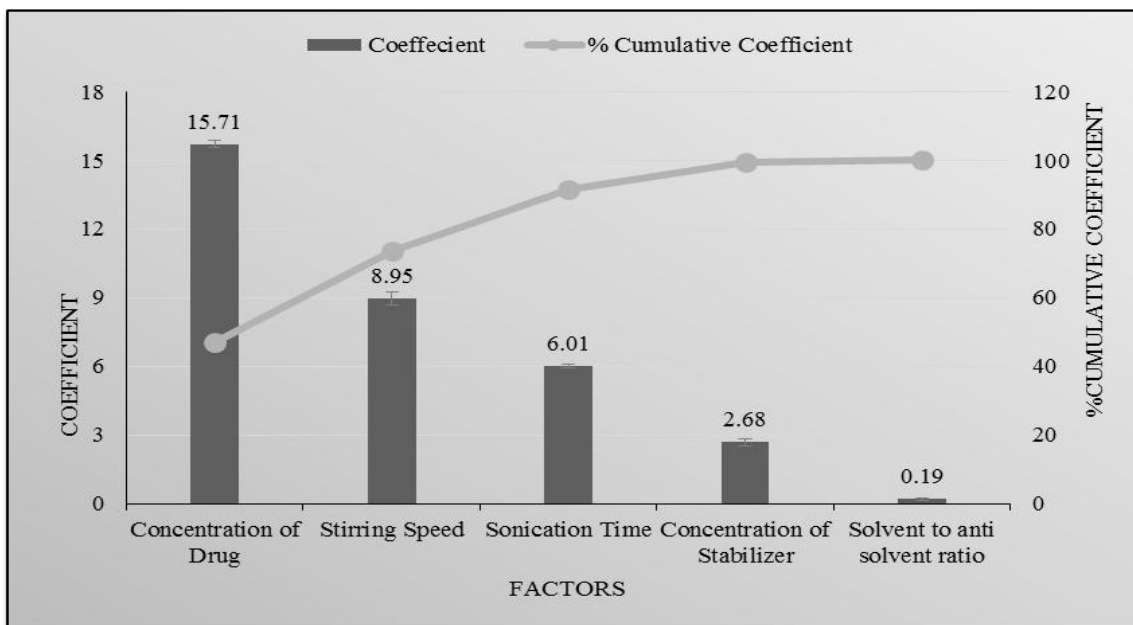
Batch Code	Amount of Ziprasidone HCl (mg) X <sub>1</sub> **	Amount of Poloxamer 407 (mg) X <sub>2</sub>	Solvent : Anti-solvent Volume Ratio X <sub>3</sub>	Stirring Speed (RPM) X <sub>4</sub>	Sonication Time (Min) X <sub>5</sub>	Saturation Solubility (µg/ml) (Mean ± SD)* Y <sub>1</sub>	Mean Particle Size (nm) (Mean ± SD)* Y <sub>2</sub>
ZF6	22.6	50	1:8	800	30	89.46 ± 1.8	325.5 ± 4.6
ZF7	11.3	50	1:8	1200	10	45.01 ± 1.0	395.2 ± 6.1
ZF8	11.3	30	1:8	1200	30	95.74 ± 2.4	318 ± 7.2
ZF9	22.6	30	1:5	1200	30	82.69 ± 2.1	348.7 ± 6.9
ZF10	11.3	50	1:5	800	30	63.92 ± 0.97	378.3 ± 5.3
ZF11	22.6	30	1:8	800	10	78.33 ± 1.7	354.9 ± 7.8
ZF12	22.6	50	1:5	1200	10	120.11 ± 2.2	298.4 ± 5.1
ZF13	11.3	30	1:5	800	10	40.28 ± 2.1	410.5 ± 4.8

\* Indicates average of three determinations

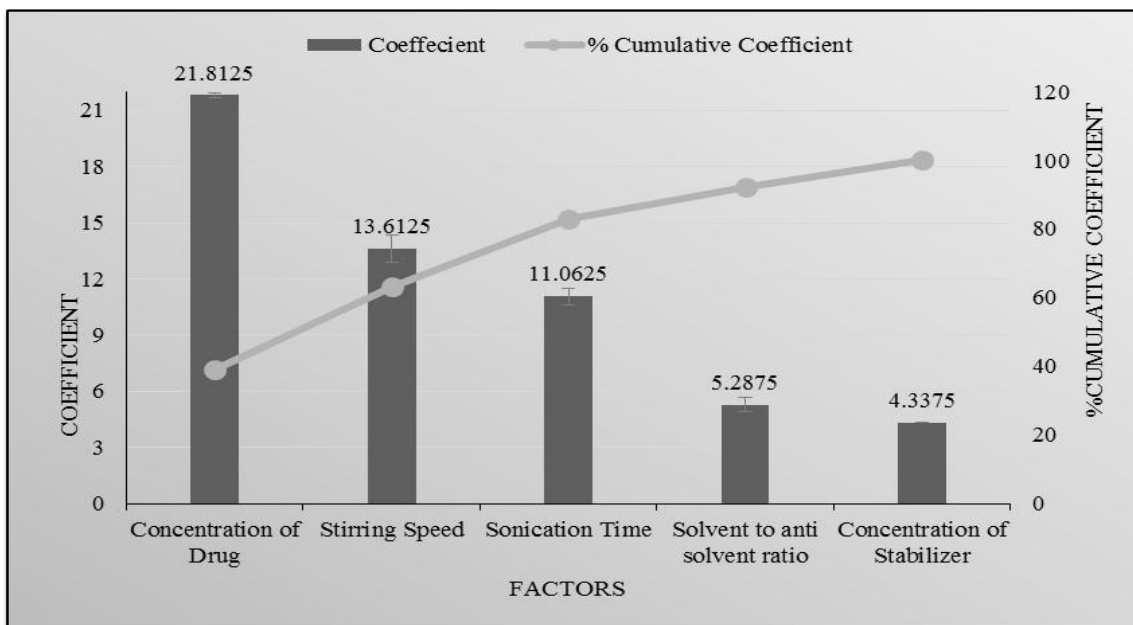
\*\* 11.3 mg of Ziprasidone Hydrochloride is equivalent to 10 mg of Ziprasidone Base[106]

Figure 4.39 and Figure 4.40 indicates the amount of ziprasidone hydrochloride and stirring speed had maximum effect on mean particle size and saturation solubility as compared to other parameters like solvent: antisolvent volume ratio, amount of poloxamer 407 and sonication time.





**FIGURE 4.39: Pareto chart of the effect of independent variables on saturation the solubility of ZHNS**



**FIGURE 4.40: Pareto chart of the effect of independent variables on mean particle size of ZHNS**

**4C.6 Optimization of other preliminary parameters [191–193]**

Ziprasidone hydrochloride nanosuspension was prepared using Poloxamer 407 as a stabilizer. The three different amounts of poloxamer 407 viz. 30 mg, 40 mg, and 50 mg were selected. Nanosuspension was prepared according to the procedure given in experimental section. Prepared nanosuspensions were evaluated with different evaluation parameters like mean particle size and saturation solubility to select amount of poloxamer 407 for further formulation work. As shown in Table 4.48, 50 mg poloxamer 407 was selected which was showing minimum mean particle size and maximum saturation solubility.

Solvent: antisolvent volume ratio is important formulation parameter for preparation of nanosuspension. For the optimization of solvent: antisolvent volume ratio 1:4, 1:6 and 1:8 were selected. Nanosuspensions were prepared according to the procedure given in experimental section. Prepared nanosuspensions were evaluated with different evaluation parameters like mean particle size and saturation solubility to select solvent: antisolvent volume ratio for further formulation work, as shown in Table 4.48, 1:8 solvent: antisolvent volume ratio was selected which was showing minimum mean particle size and maximum saturation solubility.

Once the precipitation of drug particle had occurred in suspension, to convert into the uniform nanosized particles probe sonicator was used. 10 mins, 20 mins, and 30 mins period were selected for sonication. Nanosuspension was prepared according to the procedure given before. Prepared nanosuspensions were evaluated with different evaluation parameters like mean particle size and saturation solubility to select the optimized time period of sonication for further formulation work. As shown in Table 4.48, 30 mins sonication time was selected which was showing minimum mean particle size and maximum saturation solubility.

**TABLE 4.48: Results of optimization of other preliminary parameters for ZHNS**

Batch Code	Preliminary Parameters		Mean Particle Size (nm) (Mean ± SD)*	Saturation Solubility (µg/ml) (Mean ± SD)*
ZF14	Amount of Poloxamer 407 (mg)	30	361.6 ± 6.5	49.21 ± 0.95
ZF15		40	342.0 ± 7.1	57.15 ± 1.02
<b>ZF16</b>		<b>50</b>	<b>231.7 ± 5.8</b>	<b>62.78 ± 1.22</b>
ZF17	Solvent to Antisolvent Volume Ratio	1:4	355.8 ± 6.8	41.52 ± 0.59
ZF18		1:6	321.0 ± 4.6	49.22 ± 1.28
<b>ZF19</b>		<b>1:8</b>	<b>250.6 ± 5.1</b>	<b>62.50 ± 1.72</b>
ZF20	Sonication Time (min)	10	346.5 ± 7.8	47.72 ± 0.79
ZF21		20	320.0 ± 5.9	59.33 ± 1.11
<b>ZF22</b>		<b>30</b>	<b>252.0 ± 8.2</b>	<b>65.23 ± 1.53</b>

\*Indicates average of three determinations

#### 4C.7 3<sup>2</sup> Factorial Design

Various formulations were prepared the varying amount of ziprasidone hydrochloride and stirring speed. [61] As shown in Table 4.49 a 3<sup>2</sup> full factorial design was used to evaluate the effect of both independent variables on the predetermined dependent variables viz., particle size and saturation solubility and cumulative percentage release (CPR) at 15 mins.

**TABLE 4.49: Layout and observed responses of 3<sup>2</sup> factorial design for ZHNS**

Batch Code	Level of Amount of Ziprasidone Hydrochloride X <sub>1</sub>	Level of Stirring Speed X <sub>2</sub>	Mean Particle Size (nm) (Mean ± SD)* Y <sub>1</sub>	Saturation Solubility (µg/ml) (Mean ± SD)* Y <sub>2</sub>	CPR at 15 mins (%w/w) (Mean ± SD)* Y <sub>3</sub>
ZFD1	-1	-1	421.2 ± 5.8	45.32 ± 0.59	71.25 ± 1.65
ZFD2	-1	0	296.4 ± 6.4	64.84 ± 0.84	77.62 ± 2.14
ZFD3	-1	1	219.8 ± 8.1	59.68 ± 1.05	86.6 ± 1.89
ZFD4	0	-1	418.2 ± 9.5	69.94 ± 1.24	83.51 ± 3.14
ZFD5	0	0	302.5 ± 6.9	81.74 ± 0.68	88.15 ± 2.11
<b>ZFD6</b>	<b>0</b>	<b>1</b>	<b>220.0 ± 4.8</b>	<b>72.99 ± 1.84</b>	<b>95.33 ± 0.99</b>
ZFD7	1	-1	408.3 ± 8.5	57.75 ± 1.22	83.61 ± 1.24
ZFD8	1	0	286.5 ± 4.1	66.41 ± 1.06	84.65 ± 1.89
ZFD9	1	1	214.0 ± 6.2	52.07 ± 0.87	91.34 ± 2.31
<b>Translation of Coded Levels in Actual Units</b>					
<b>Variables Level</b>			<b>Low (-1)</b>	<b>Medium (0)</b>	<b>High (1)</b>
X <sub>1</sub> **			11.3 mg	16.95 mg	22.6 mg
X <sub>2</sub>			800 RPM	1000 RPM	1200 RPM

\*Indicates average of three determinations

\*\* 11.3 mg of Ziprasidone Hydrochloride is equivalent to 10 mg of Ziprasidone Base[106]

Some other parameters were also evaluated for zeta potential, PDI and % w/w drug content etc. as shown in Table 4.50.

**Table 4.50: Other evaluation parameters of factorial batches of ZHNS**

Batch Code	PDI (Mean ± SD)*	Zeta Potential (mV) (Mean ± SD)*	Drug Content (%w/w) (Mean ± SD)*
ZFD1	0.530 ± 0.072	20.5 ± 2.51	95.49 ± 2.01
ZFD2	0.819 ± 0.056	-19.8 ± 1.21	99.52 ± 1.51
ZFD3	0.752 ± 0.062	-29.4 ± 1.68	96.93 ± 0.87
ZFD4	0.652 ± 0.049	17.5 ± 1.53	97.73 ± 1.85
ZFD5	0.591 ± 0.034	-18.5 ± 2.95	96.95 ± 0.64
<b>ZFD6</b>	<b>0.425 ± 0.051</b>	<b>-31.4 ± 1.45</b>	<b>99.12 ± 1.24</b>
ZFD7	0.694 ± 0.039	25.3 ± 2.11	96.34 ± 1.33
ZFD8	0.561 ± 0.043	27.0 ± 2.60	95.53 ± 0.95
ZFD9	0.489 ± 0.052	-23.9 ± 2.15	97.38 ± 0.95

\*Indicates average of three determinations

#### 4C.8 Statistical analysis

A full model was derived after putting the values of regression coefficients in the equation (3.8). Regression analysis was carried out using Microsoft Excel<sup>®</sup> version 2013 (Microsoft Corporation, Washington, USA); the fitted results are shown in Table 4.51, Table 4.52, Table 4.53 equation (4.8), (4.9) and (4.10).

**TABLE 4.51: Results of regression analysis of mean particle size for ZHNS**

	Mean Particle Size (nm) (Y <sub>1</sub> )		
	Coefficient	Std. Error	P- value
b <sub>0</sub>	298.6667	2.165954	8.40962E-07
b <sub>1</sub>	-4.66667	1.186342	0.029258979
b <sub>2</sub>	-99	1.186342	3.79289E-06
b <sub>11</sub>	-6	2.054805	0.061496845
b <sub>22</sub>	22	2.054805	0.001741971
b <sub>12</sub>	2	1.452966	0.262413056
	<b>R<sup>2</sup> = 0.9995</b>		

For mean particle size (nm) (Y<sub>1</sub>)

$$Y_1 = 298.6667 - 4.66X_1 - 99X_2 - 6.0X_1^2 + 22.0X_2^2 + 2.0 X_1X_2 \quad \text{Eq...}(4.8)$$

**TABLE 4.52: Results of regression analysis of saturation solubility for ZHNS**

	Saturation Solubility (µg/ml) (Y <sub>2</sub> )		
	Coefficient	Std. Error	P- value
b <sub>0</sub>	82.47020344	0.607532	8.81E-07
b <sub>1</sub>	1.065	0.332759	0.049312
b <sub>2</sub>	1.954319249	0.332759	0.009847
b <sub>11</sub>	-17.21030516	0.576355	8.25E-05
b <sub>22</sub>	-11.37234742	0.576355	0.000284
b <sub>12</sub>	-5.01	0.407545	0.001159
	<b>R<sup>2</sup> = 0.9979</b>		

For saturation solubility ( $\mu\text{g/ml}$ ) ( $Y_2$ )

$$Y_2 = 82.4702 + 1.065X_1 + 1.9543X_2 - 17.2103X_1^2 - 11.3723X_2^2 - 5.01X_1X_2 \quad \text{Eq...}(4.9)$$

**TABLE 4.53: Results of regression analysis of CPR at 15 mins for ZHNS**

	CPR at 15 mins (%w/w) ( $Y_3$ )		
	Coefficient	Std. Error	P- value
$b_0$	87.79667	0.446627	2.90289E-07
$b_1$	4.021667	0.244627	0.000489794
$b_2$	5.816667	0.244627	0.000163007
$b_{11}$	-6.485	0.423707	0.000605765
$b_{22}$	1.8	0.423707	0.023897733
$b_{12}$	-1.905	0.299606	0.007871496
	<b><math>R^2 = 0.9973</math></b>		

For CPR at 15 mins ( $Y_3$ )

$$Y_3 = 87.79667 + 4.021667X_1 + 5.8166X_2 - 6.485X_1^2 + 1.8X_2^2 - 1.905X_1X_2 \quad \text{Eq...}(4.10)$$

The coefficients in Table 4.51, Table 4.52 and Table 4.53 represent the respective quantitative effect of independent variables ( $X_1$ ,  $X_2$ , and  $X_3$ ) and their interactions on the various responses. It was seen that all the independent variables had a significant effect on the response ( $p < 0.05$ ). The negative sign of the coefficient indicated that increase in the value of independent variable decreases the value of response and vice versa. The absolute value of the coefficient indicates the magnitude of the effect of the independent variable on the response; higher the value higher the magnitude.

**TABLE 4.54: ANOVA for a full model for ZHNS**

Source of variation	DF	SS	MS	F	F <sub>significant</sub>
<b>Mean Particle Size (nm)</b>					
Regression	5	59992.66667	11998.53333	1420.878947	2.94327E-05
Residual	3	25.33333333	8.444444444	-	-
Total	8	60018	-	-	-
<b>Saturation Solubility (µg/ml)</b>					
Regression	5	981.1717116	196.2343423	295.3688168	0.000309346
Residual	3	1.99311164	0.664370547	-	-
Total	8	983.1648233	-	-	-
<b>CPR at 15 mins (%w/w)</b>					
Regression	5	405.1510333	81.03020667	225.6759585	0.000462499
Residual	3	1.077166667	0.359055556	-	-
Total	8	406.2282	-	-	-

The results of ANOVA for full model suggested that  $F_{cal}$  value for mean particle size was 1420.87.  $F_{tab}$  value at (5, 3) was 9.0 for  $Y_1$ . So,  $F_{cal}$  value for  $Y_1$  was higher than  $F_{tab}$ .

The results of ANOVA for full model suggested that  $F_{cal}$  value for saturation solubility was 295.36.  $F_{tab}$  value at (5, 3) was 9.0 for  $Y_2$ . So,  $F_{cal}$  value for  $Y_2$  was higher than  $F_{tab}$ .

The results of ANOVA for full model suggested that  $F_{cal}$  value for CPR at 15 mins was 225.67.  $F_{tab}$  value at (5, 3) was 9.0 for  $Y_3$ . So,  $F_{cal}$  value for  $Y_3$  was higher than  $F_{tab}$ .

All dependent variables were found  $F_{cal}$  value significantly higher than  $F_{tab}$ . Therefore, selected factors have a significant effect on all three dependent variables.

All the determination coefficients  $R^2$  are larger than 0.99, indicating that over 99% of the variation in the response could be explained by the model and the goodness of fit of the model was confirmed. The F-ratio was found to be far greater than the theoretical value with a very low probability of less than 0.0001 for each regression model, indicating that the regression model is significant with a confidence level of 95%. The observed responses showed a wide variation suggesting that the selected both independent variables had a significant effect on resultant mean particle size, saturation solubility and CPR at 15 mins.

#### 4C.9 Contour plots

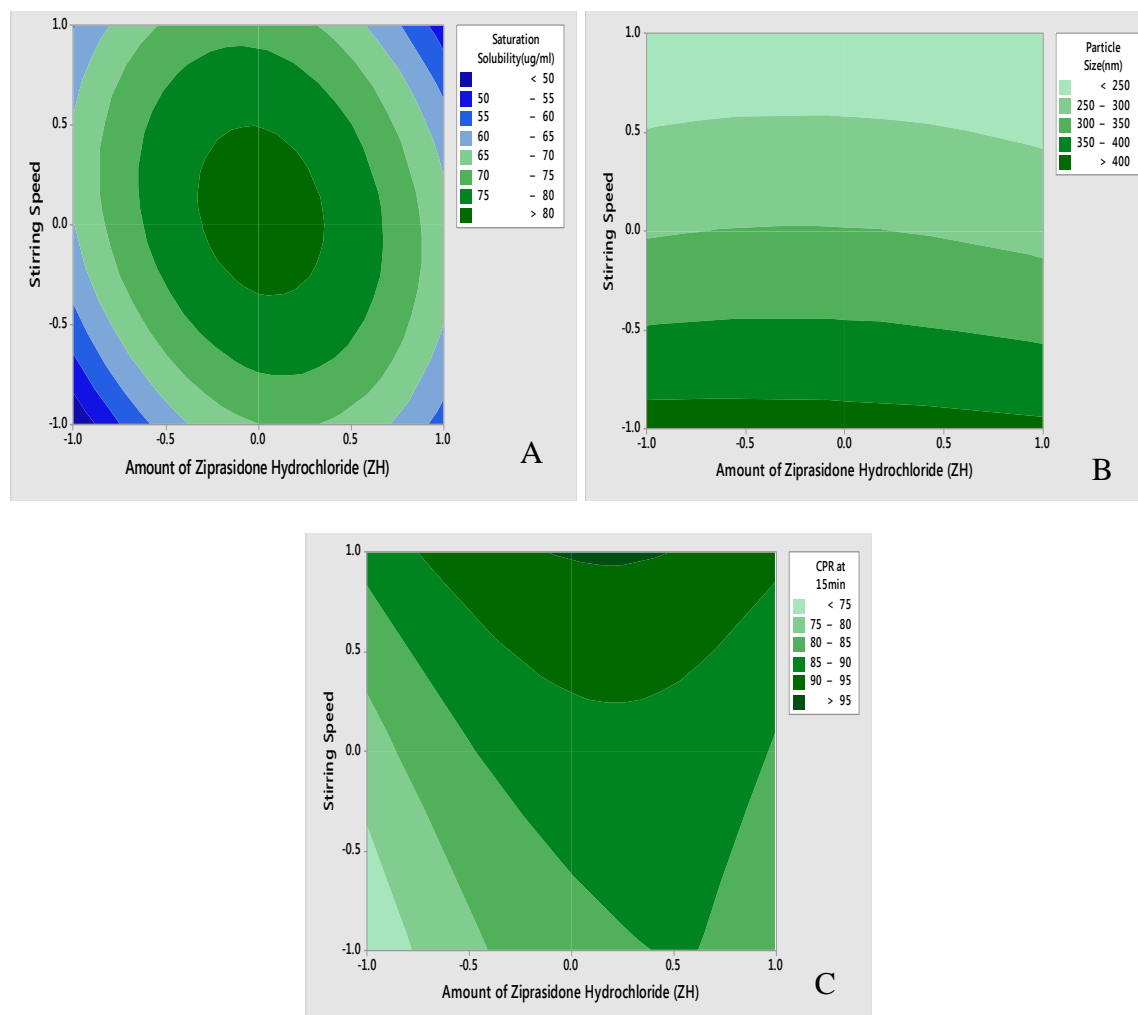
Two-dimensional contour plots were established using statistical software Minitab 17 (Minitab Inc., USA) to examine the relationship between independent and dependent variables as shown in figure 4.41.

Figure 4.41 [A] indicates contour plot for mean particle size (nm) at prefixed values between 250 to 400 nm. The contour plot was found to be non-linear. So the relationship between independent variables and mean particle size is not linear. The minimum (Light Green part) is clearly evidence from contour plot which specifies the stirring speed and amount of ziprasidone hydrochloride for lowest mean particle size. Their respective values are approx. 1200 RPM (coded value +1) stirring speed and 16.95 mg (coded value 0) amount of ziprasidone hydrochloride.

Figure 4.41 [B] and [C] shows contour plot for saturation solubility ( $\mu\text{g/ml}$ ) and cumulative percentage release (CPR) at 15 mins at prefixed values between 50 to 80  $\mu\text{g/ml}$  and 75 to 95 respectively. The contour plot was found to be non-linear. So the relationship between independent variables and dependent variables were not linear. The maximum (Dark Green part) is clearly evidence from contour plot which specifies the stirring speed and amount of ziprasidone hydrochloride for maximum saturation solubility and cumulative percentage release (CPR) at 15 mins. Their respective values are approx. 1200 RPM (coded value +1) stirring speed and 16.95 mg (coded value 0) amount of ziprasidone hydrochloride.

The maxima of saturation solubility and minima of mean particle size are seemed to be overlapping. So, there exists a direct relation between saturation solubility and mean particle size. The batch showing lowest mean particle size is also having highest saturation solubility and cumulative percentage release (CPR) at 15 mins.





**FIGURE 4.41: Contour plot of ZHNS for effect on [A] Mean particle size, [B] Saturation solubility and [C] CPR at 15 mins**

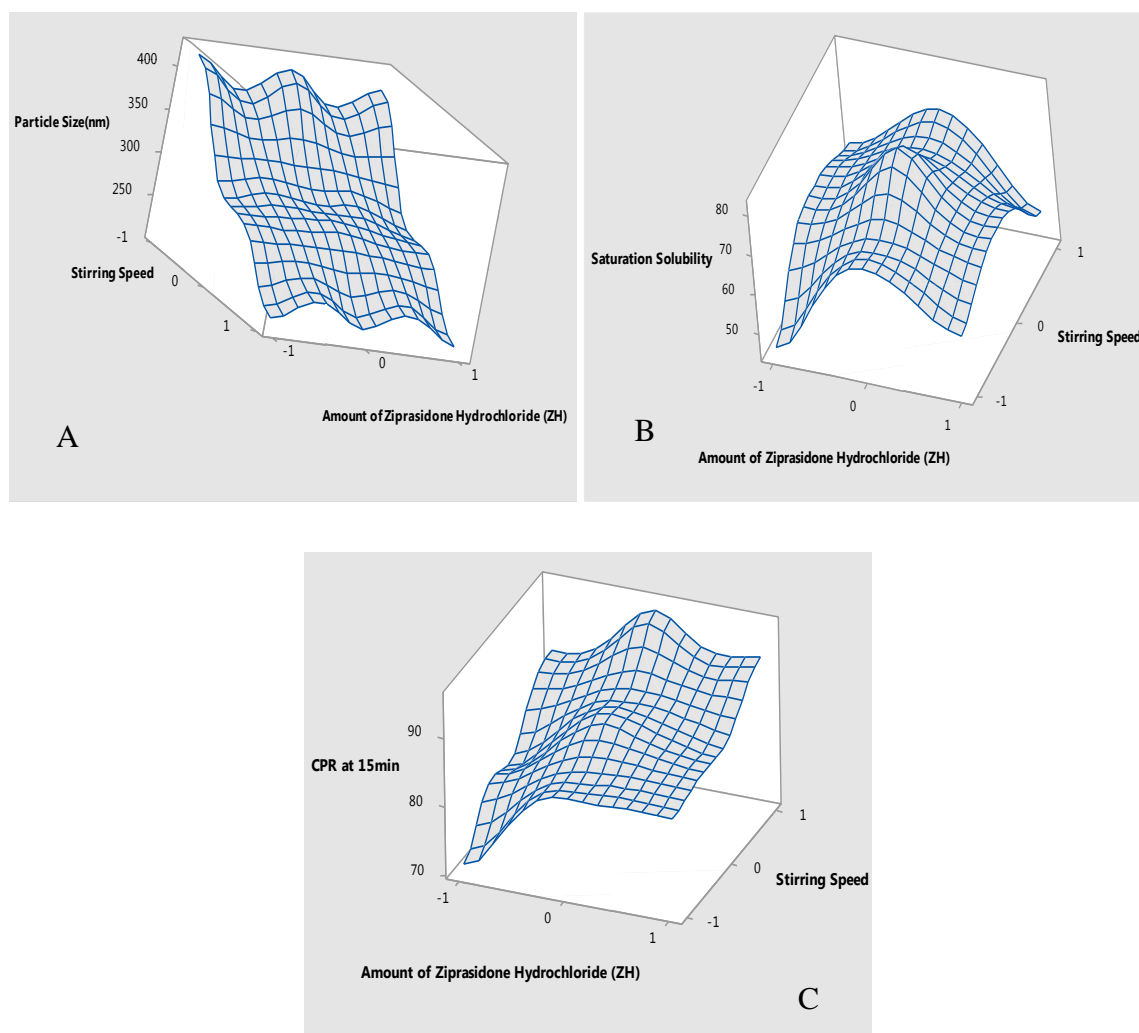
#### 4C.10 Surface plots

To find out main and interaction effect of the independent variables, response surface plots are very helpful.

Figure 4.42[A] shows the response surface plot of mean particle size as a function of independent variables. Mean particle size decreases as the plot comes toward central part. The center of the plot indicates the minimum particle size which was obtained by highest stirring speed and an intermediate amount of ziprasidone hydrochloride.

Figure 4.42[B] and [C] shows the response surface plot of saturation solubility ( $\mu\text{g/ml}$ ) and cumulative percentage release (CPR) at 15 mins respectively as a function of stirring speed and amount of ziprasidone hydrochloride using Minitab 17 (Minitab Inc., USA) software.

Saturation solubility ( $\mu\text{g/ml}$ ) and cumulative percentage release (CPR) at 15 mins increases as the plot comes toward central part. The center of the plot indicates the highest saturation solubility ( $\mu\text{g/ml}$ ) and cumulative percentage release (CPR) at 15 mins which were obtained by highest stirring speed and an intermediate amount of ziprasidone hydrochloride.

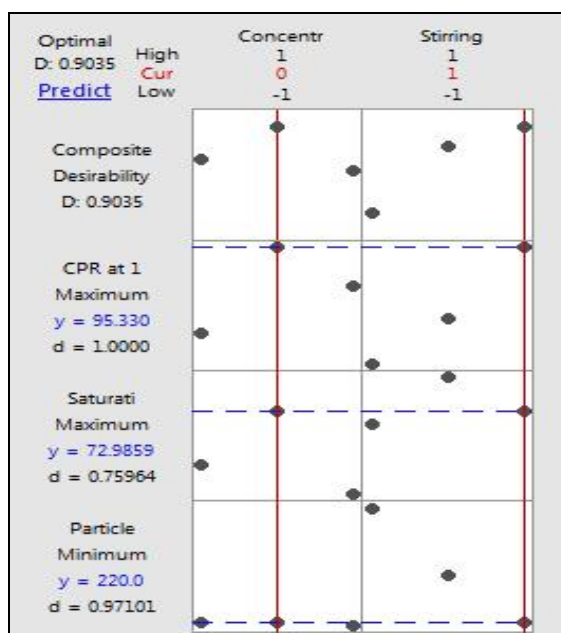


**FIGURE 4.42: Response surface plot of ZHNS for effect on [A] Mean particle size, [B] Saturation solubility and [C] CPR at 15 mins.**

#### 4C.11 Optimization of nanosuspension by desirability function of Minitab17.0

The optimum formulation was selected based on the criteria of attaining the minimum mean particle size ( $Y_1$ ), the maximum saturation solubility ( $Y_2$ ) and maximum cumulative percentage release ( $Y_3$ ). An overall desirability function dependent on all investigated formulation variables was used to predict the ranges of the variable where the optimum

formulation might occur. The desirable ranges are from zero to one (least to most desirable, respectively). The optimized batch composition is presented in below Figure 4.43.



**FIGURE 4.43: Optimized plot of factorial design form Minitab 17 for ZHNS**

#### 4C.12 Checkpoint cum optimized batch analysis

From the above Minitab data optimized batch was ZFD-6. The desirability of the optimized batch was 0.9035. Formulation and process parameters for the optimized batch are shown in Table 4.55. The optimized lyophilized formulation was filled in hard gelatin capsules and kept in the tightly closed container.

**TABLE 4.55: Formulation and process parameters for an optimized batch of ZHNS**

Amount of Ziprasidone Hydrochloride (Equivalent to 15 mg of Ziprasidone Base)	16.95 mg
Amount of Poloxamer 407	50 mg
Solvent: Antisolvent Volume Ratio	1:8
Stirring Speed	1200 RPM
Stirring Time	5 h
Sonication Time	30 mins
Amount of lyophilizer (1:1, Total Solid: Mannitol)	66.95 mg

### 4C.13 Checkpoint batch cum optimized batch validation

To evaluate model a checkpoint batch cum optimized batch ZFD-6 was prepared at  $X_1 = 0$  and  $X_2 = +1$  levels. Dependent parameters were determined and compared with predicted values as shown in Table 4.56.

**TABLE 4.56: Composition of checkpoint batch cum optimized batch of ZHNS**

Amount of Drug ( $X_1$ )		Stirring Speed ( $X_2$ )	
Coded value	Decoded value	Coded value	Decoded value
0	16.95 mg	+1	1200 RPM

**TABLE 4.57: Comparison of calculated data with experimental data of ZHNS**

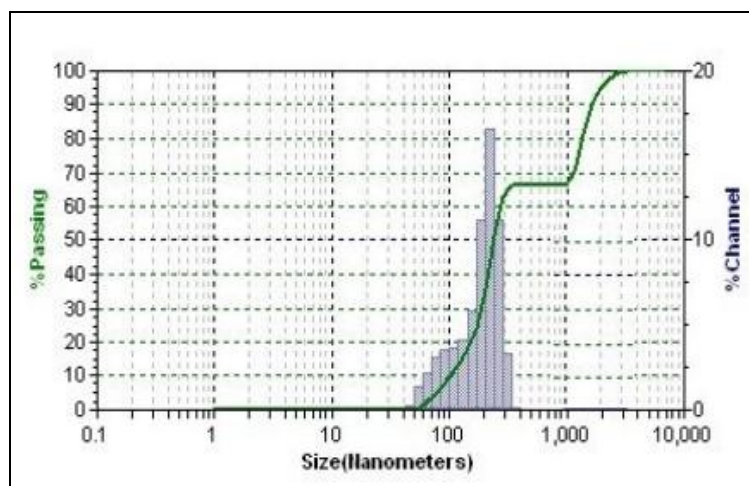
Response	Predicted	Observed	% Bias
Mean Particle Size ( $Y_1$ )	221.66 nm	220.0 nm	-0.7488
Saturation Solubility ( $Y_2$ )	73.05 $\mu\text{g/ml}$	72.99 $\mu\text{g/ml}$	-0.0821
CPR at 15 mins ( $Y_3$ )	95.41 % w/w	95.33 % w/w	-0.0838

When the batch ZFD-6 was prepared using defined level of the amount of ziprasidone hydrochloride and stirring speed using Minitab17 (Minitab Inc., USA), the results obtained with checkpoint cum optimized batch (ZFD-6) were close to predicted values. Thus, it can be concluded that the statistical model is mathematically valid.

### 4C.14 Evaluation of optimized batch of ziprasidone hydrochloride nanosuspension

#### 4C.14.1 Particle size and PDI

Particle size distribution of the optimized batch is shown in Figure 4.44. The mean particle size of the optimized batch is  $242.9 \pm 10$  nm. Ziprasidone hydrochloride nanosuspension based final formulation is intended for oral administration for which PDI and particle size above  $5 \mu\text{m}$  is not critical. The particle size of a nanosuspension is around 200-1000 nm. [80] From the Table 4.49, it was found that mean particle sizes of all formulations were in the nanometer range. It shows that all formulations fulfill the requirements of a nanosuspension.



**Figure 4.44: Particle size graph for ZHNS**

#### **4C.14.2 Zeta potential**

Poloxamer 407 is a well-known efficient polymeric stabilizer forming a substantial mechanical and thermodynamic barrier at the interface of drug nanoparticles. [198] In general, zeta potential value of  $\pm 30$  mV is sufficient for the stability of nanosuspension. [171] Zeta potential of optimized formulation was observed  $-32.1 \pm 3.18$  mV, which complies with the requirement of zeta potential.

#### **4C.14.3 Drug content**

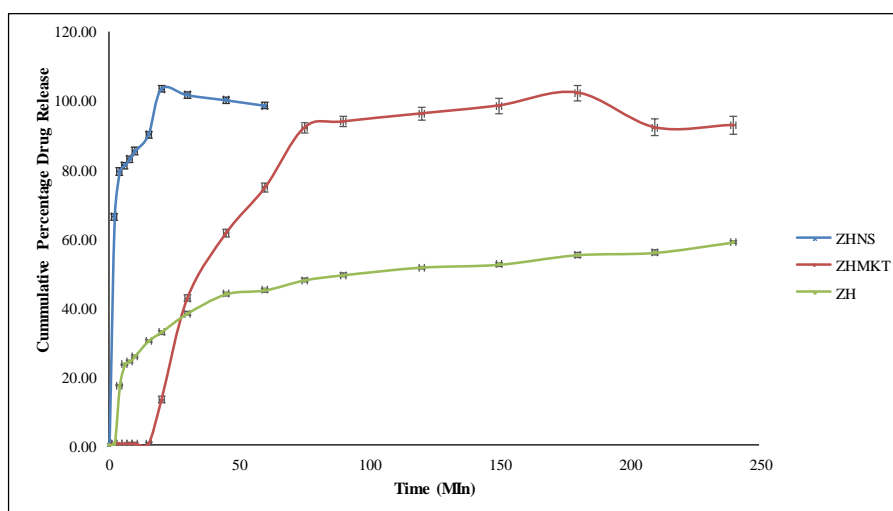
An aliquot (1ml) of the prepared nanosuspension was diluted in methanol and filtered with a  $0.2 \mu\text{m}$  filter. Total drug content was determined by UV-Visible spectrophotometer at 315 nm and was found to be 100.46 %w/w of the ziprasidone hydrochloride.

#### **4C.14.4 Saturation solubility**

Saturation solubility of an optimized batch of ziprasidone hydrochloride nanosuspension and the pure drug was found to be  $76.25 \mu\text{g/ml}$  and  $7.18 \mu\text{g/ml}$  respectively. It indicates that saturation solubility of nanosuspension was 10 times than that of pure drug. This drastic increase in saturation solubility is as a result of a reduction in particle size and subsequent increase in surface area. So, it can be assumed that this increase in saturation solubility may increase bioavailability.

#### 4C.14.5 *In-vitro* dissolution

The dissolution profile of nanosuspension, un-milled (pure drug) suspension and marketed formulation (Zipsydon<sup>®</sup> 20 Capsule) are presented in Figure 4.45. In nanosuspension, more than 96.61 % drug was released within 15 mins, while cumulative percentage drug release of un-milled suspension, marketed formulated showed 44.93% and 74.80% at 60 mins respectively. So, nanosuspension enhanced the rate of dissolution of ziprasidone hydrochloride to great extent.



**FIGURE 4.45: Comparison of *in-vitro* dissolution of ziprasidone hydrochloride nanosuspension with marketed formulation**

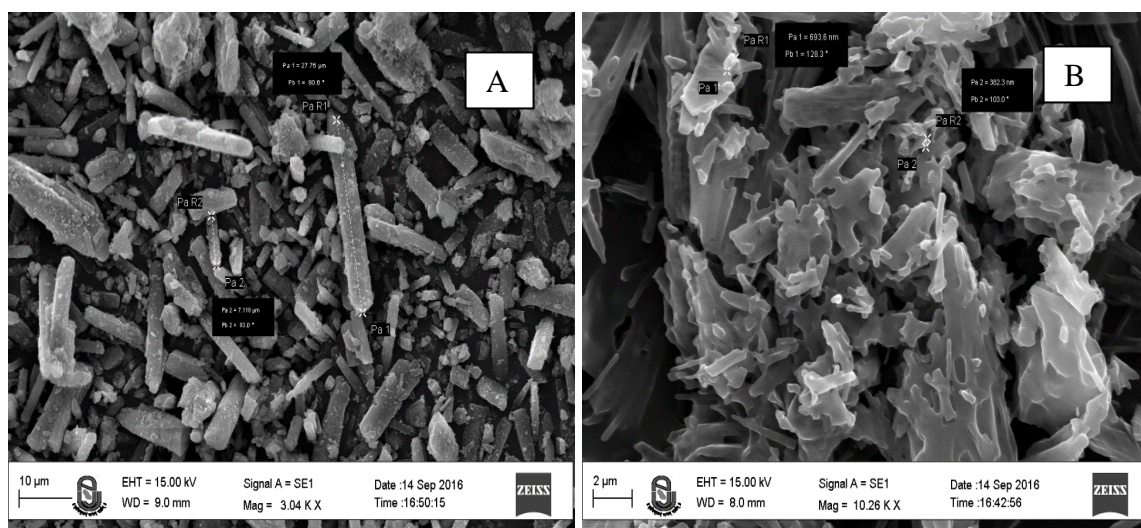
**TABLE 4.58: Evaluation parameters of an optimized batch of ZHNS**

Evaluation Parameters	Results
Mean Particle Size	218.0 nm
PDI	0.456
Zeta Potential	-32.1 mV
Drug Content	100.46 % w/w
Saturation Solubility	76.25 µg/ml
CPR at 15 mins	96.61 % w/w

#### 4C.14.6 Scanning electron microscopy (SEM)

The surface characteristics of ziprasidone hydrochloride and its lyophilized nanosuspension were studied by scanning electron microscopy (EVO-18, ZEISS,

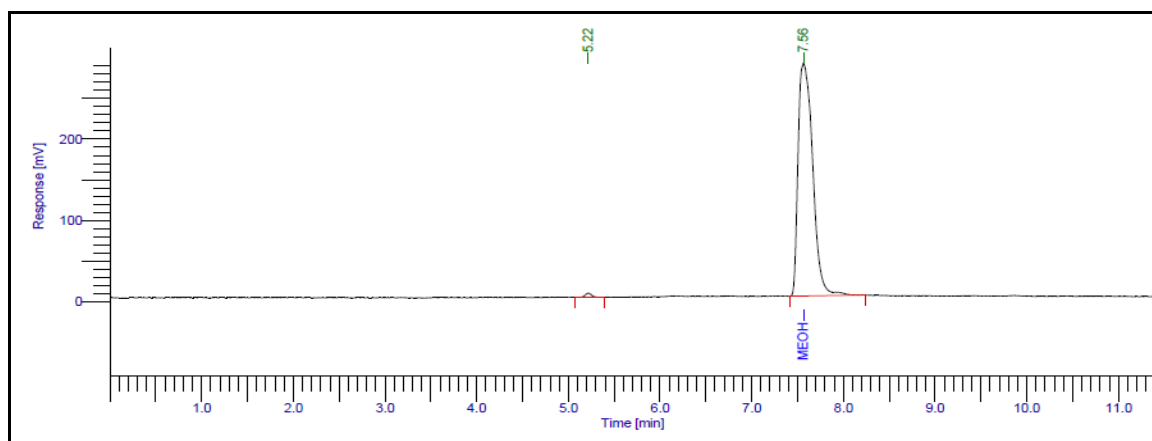
Germany) at 3kx to 16kx. The samples were mounted on double-sided carbon adhesive tape that has previously been secured on brass stubs and then subjected to gold coating by sputter coater, using process current of 10 mA for 4 mins. The accelerating voltage was 15 kV. The surface topology as measured by scanning electron microscopy of ziprasidone hydrochloride was found to be long, thin and flat with particles larger (2-27 $\mu\text{m}$ ) in size, as shown in Figure 4.46. However, after conversion to lyophilized nanosuspension, particles became smaller (about 230-300 nm) which were adsorbed on the surface of mannitol used as cryoprotectant may be by hydrophobic interaction.



**FIGURE 4.46: Scanning electron microscopy of [A] Ziprasidone hydrochloride and [B] ZHNS**

#### 4C.14.7 Residual solvent by gas – chromatography (GC)

Methanol is included in Class 3 solvent, may be regarded as less toxic and of low risk to human health. According to ICH guidelines, it is considered that amount of these residual solvents of 3000 ppm per day would be acceptable without justification. [173] Amount of methanol was evaluated for residual solvent content in lyophilized nanosuspension of ziprasidone hydrochloride by gas-chromatography using head-space sampler. Results of GC revealed that 73.53 ppm methanol was present in the sample which is the far lesser amount of class 3 solvents. Figure 4.47 indicates gas chromatograph of methanol in lyophilized ziprasidone hydrochloride nanosuspension.



**FIGURE 4.47: Gas chromatograph of methanol in lyophilized ziprasidone hydrochloride nanosuspension**

#### 4C.14.8 Accelerated stability study

The accelerated stability study indicated that lyophilized ziprasidone hydrochloride nanosuspension was physically and chemically stable when stored at the  $25 \pm 2^\circ\text{C}$  and  $60 \pm 5\%$  RH for a period of 6 months. [176] Table 4.59 shows results of mean particle size, saturation solubility, cumulative percentage drug release at 15 mins and % w/w of drug content indicated that there was a slight change in all parameters which had  $< \pm 5\%$  bias which was insignificant. The negligible difference was observed in results obtained from the optimized batch before and after the stability study according to ICH guideline.

**TABLE 4.59: Results of accelerated stability study of ZHNS**

Sr. No.	Storage condition for stability study	Time Period (months)	Evaluation Parameters			
			Mean Particle Size (nm) (Mean $\pm$ SD)*	Saturation Solubility ( $\mu\text{g/ml}$ ) (Mean $\pm$ SD)*	CPR at 15 mins (%w/w) (Mean $\pm$ SD)*	Drug Content (%w/w) (Mean $\pm$ SD)*
1	$25^\circ\text{C} \pm 2^\circ\text{C}$ and $60\% \pm 5\%$ RH	0	$218.0 \pm 5.4$	$76.25 \pm 1.5$	$96.61 \pm 0.85$	$100.46 \pm 1.7$
2		1	$245.2 \pm 8.1$	$76.07 \pm 0.7$	$96.06 \pm 0.75$	$99.49 \pm 0.82$
3		3	$292.1 \pm 6.4$	$75.59 \pm 0.6$	$95.86 \pm 0.77$	$98.91 \pm 0.34$
4		6	$310.2 \pm 7.5$	$74.71 \pm 0.9$	$95.44 \pm 0.61$	$98.17 \pm 0.91$

\*Indicates average of three determinations

#### 4C.15 Bioavailability study

For bioavailability study, each rat was treated with oral nanosuspension of ziprasidone hydrochloride at a dose of 2.31 mg/kg in a single dose. Blood samples were collected from retro-orbital venous plexus over a period 12 h. Each sample was analyzed by HPLC for the



estimation of drug content by a bioanalytical method. The pharmacokinetic calculations were performed on the basis of serum concentration-time data, as shown in Table 4.60.

**TABLE 4.60: Results of bioavailability study of ziprasidone hydrochloride nanosuspension and marketed formulation**

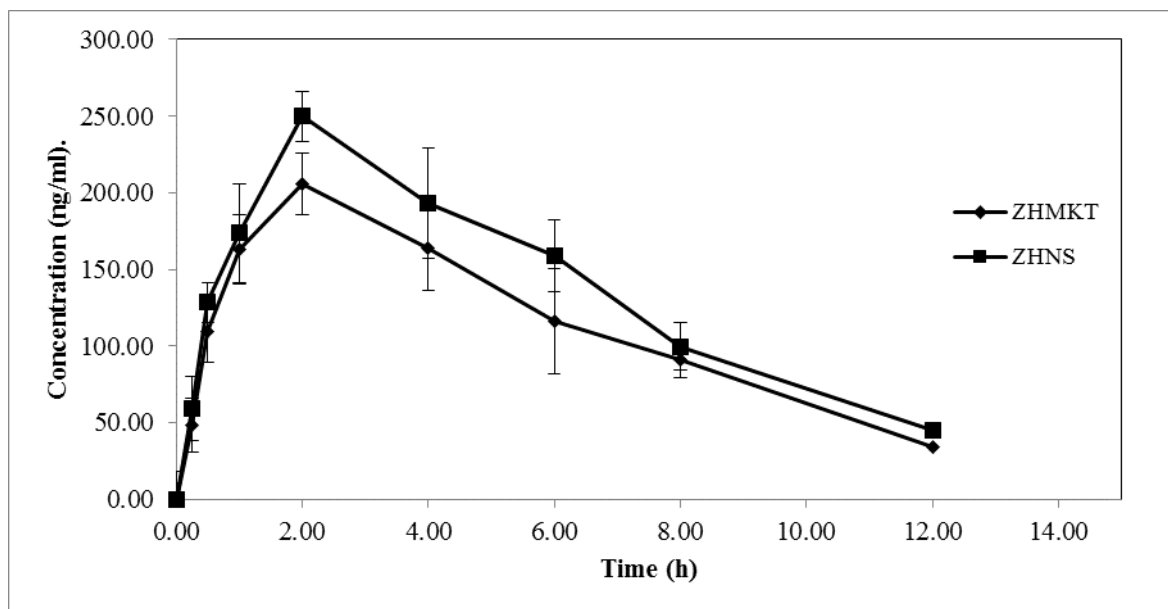
Sr. No.	Time (h)	ZHNS (ng/ml) (Mean ± SD)*	ZHMKT (ng/ml) (Mean ± SD)*	AUC(ZHNS) (ng/ml).h	AUC(ZHMKT) (ng/ml).h
1	0.00	0.00 ± 0.00	0.00 ± 0.00	0.0000	0.0000
2	0.25	59.08 ± 18.054	48.22 ± 10.556	7.3850	6.0275
3	0.5	128.44 ± 20.617	109.53 ± 17.921	32.1100	19.7188
4	1.00	173.55 ± 13.018	162.78 ± 19.870	86.7750	68.0775
5	2.00	249.71 ± 31.965	205.54 ± 22.768	249.7100	184.1600
6	4.00	192.85 ± 16.424	163.80 ± 20.122	385.7000	369.3400
7	6.00	158.43 ± 35.978	115.91 ± 27.195	475.2900	279.7100
8	8.00	99.61 ± 23.414	90.73 ± 34.177	398.4400	206.6400
9	12.00	44.82 ± 15.239	34.34 ± 11.085	268.9200	250.1400
Total				1904.3300	1383.8138

\*Indicates average of 6 determinations

ZHNS – Ziprasidone Hydrochloride Nanosuspension,

ZHMKT – Ziprasidone Hydrochloride Marketed Formulation

Figure 4.48 shows the mean serum concentration ( $\mu\text{g/ml}$ ) vs. Time (h) in rats after administration of optimized nanosuspension of ziprasidone hydrochloride and its marketed formulation (Zipsydon<sup>®</sup> 20 Capsule). It is evident that the area under curve (AUC) values, for the optimized formulation containing ziprasidone hydrochloride was higher than the corresponding values of the marketed formulation of ziprasidone hydrochloride (Table 4.60). The increase AUC values could be attributed to the improved dissolution of ziprasidone hydrochloride from the optimized nanosuspension formulation as compared to its marketed formulation.



**FIGURE 4.48: Serum concentration vs. time profile of ziprasidone hydrochloride nanosuspension and marketed formulation**

The values of all major pharmacokinetic parameters like maximum serum concentration ( $C_{max}$ ), the time required for maximum serum concentration ( $T_{max}$ ), the area under the curve ( $AUC_{0 \rightarrow 12}$ ), terminal half-life ( $T_{1/2}$ ), elimination rate constant ( $K_E$ ) and absorption rate constant ( $K_a$ ) have been summarized in Table 4.61.

**TABLE 4.61: Results of pharmacokinetic parameters of ziprasidone hydrochloride nanosuspension and marketed formulation**

Pharmacokinetic Parameters	Ziprasidone Hydrochloride Nanosuspension (ZHNS)	Ziprasidone Hydrochloride Marketed Formulation (ZHMKT)
$C_{max}$ (ng/ml)	249.71	205.54
$T_{max}$ (h)	2.0	2.0
$AUC_{0-12}$ (ng/ml)*h	1904.33	1383.81
$t_{1/2E}$ (h)	7.049	7.226
$K_E$ ( $h^{-1}$ )	0.098	0.096
$K_a$ ( $h^{-1}$ )	0.622	0.409

The calculation was performed for the equivalent dose of test product (ZHNS) required attaining same  $C_{max}$  of the marketed product. [194]

F-Ratio was calculated from following equation,

$$F_r = \frac{[AUC]_{test}[D]_{std}}{[AUC]_{std}[D]_{test}} \quad \text{Eq...}(4.3)$$

Where,  $F_r$  = Relative Bioavailability (F-Ratio)  
 $[AUC]_{test}$  = AUC of ziprasidone hydrochloride nanosuspension  
 $[AUC]_{std}$  = AUC of ziprasidone hydrochloride marketed formulation  
 $[D]_{test}$  = Dose of ziprasidone hydrochloride nanosuspension  
 $[D]_{std}$  = Dose of ziprasidone hydrochloride marketed formulation

Using above equation, bioavailability fraction obtained from ziprasidone hydrochloride nanosuspension was **1.38**

The volume of distribution was calculated by the following equation,

$$V_d = \frac{FD}{C_{max}} \quad \text{Eq...}(4.4)$$

Where,  $V_d$  = Volume of distribution  
 $F$  = F-Ratio  
 $D$  = Dose of the product  
 $C_{max}$  = Maximum plasma concentration

Using above equation, the volume of distribution obtained from ziprasidone hydrochloride nanosuspension was **2.54 lit.**

From the following equation amount of drug to be administered to attain the same plasma concentration of marketed product was calculated

$$C = \frac{K_a F X_0}{V_d(K_a - K_e)} [e^{-K_e t} - e^{-K_a t}] \quad \text{Eq...}(4.5)$$

Where,  
 $C$  =  $C_{max}$  of ziprasidone hydrochloride marketed formulation  
 $K_a$  = Absorption rate constant of ziprasidone hydrochloride nanosuspension

- F = F-Ratio  
 $X_0$  = Amount of ziprasidone hydrochloride administered by nanosuspension  
 $V_d$  = Volume of distribution of ziprasidone hydrochloride nanosuspension  
 $K_e$  = Elimination rate constant of ziprasidone hydrochloride nanosuspension  
t = Time required for maximum plasma concentration by ziprasidone hydrochloride nanosuspension

AUC was higher by 1.38 time and  $C_{max}$  by 1.21 time higher for ziprasidone hydrochloride nanosuspension as compared to marketed formulation indicates a substantial improvement in absorption of the drug from nanosuspension.

Using above equation, amount of ziprasidone hydrochloride should be administered by nanosuspension ( $X_0$ ) was found to be **0.31 mg/twice a day** for rats, which was further converted to human equivalent dose, which was **15.16 mg/ twice a day**.

The reported usual dose of ziprasidone is 20 mg / 40 mg twice a day (Equivalent to 22.6mg / 45.2 mg twice a day dose of ziprasidone hydrochloride) in management schizophrenia with food. Doses may be increased if necessary at intervals of not less than 2 days up to 80 mg twice daily. For maintenance, doses as low as 20 mg twice daily may be effective. The study was conducted with 22.6 mg/ twice a day dose of ziprasidone hydrochloride nanosuspension (Equivalent to 20mg/twice a day dose of ziprasidone base)[106].

Results suggested that by converting ziprasidone hydrochloride into nanosuspension form dose can be reduced from 22.6 to 15.16 mg/ twice a day which was **67.0%** of the regular dose that indicated **33.0% dose reduction**. The improvement in bioavailability due to the conversion of drug nanosuspension was 33.0%.

#### 4C.16 Conclusion

Plackett - Burman Design was effectively employed to identify formulating and processing key parameters that are affecting the quality of the ziprasidone hydrochloride nanosuspension.  $3^2$  factorial design was employed for optimization of the formulation of nanosuspension. All the predetermined independent variables were found to affect the dependent variables from the resultant nanosuspension. The optimum formulation prepared by response optimizer by desirability function provided a final formulation with  $D = 0.9035$  which released 96.61% of ziprasidone hydrochloride within 15 mins. The *in-vivo* studies confirmed that nanosuspension loaded ziprasidone hydrochloride showed a

significantly better AUC as compared to marketed formulation and dose of ziprasidone hydrochloride was reduced about 33.0 % to reach plasma concentration of marketed formulation. The improved formulation could offer improved drug delivery strategy which might allow concomitant use of ziprasidone hydrochloride in nanosuspension form. The nanosuspension of drug exhibited 33% improvement in bioavailability.

#### 4C.17 References

182. Pradhan KK, Mishra US, Pattnaik S, Panda CK, and Sahu KC, 2011, Development and validation of a stability-indicating UV Spectroscopic method for Candesartan in bulk and formulations, *Indian Journal of Pharmaceutical Sciences*, 73(6), 693–696, ISSN: 0250-474X.
183. Muszalska I, Sobczak A, Dolhan A and Jelinska A, 2014, Analysis of Sartans: A Review, *Journal of Pharmaceutical Sciences*, 103(1), 2–28, ISSN: 1520-6017.
184. Pandya VM, Patel JK, and Patel DJ, 2010, Effect of different stabilizer on the formulation of Simvastatin Nanosuspension prepared by nanoprecipitation technique, *Research Journal of Pharmaceutical, Biological, and Chemical Sciences*, 1(4), 910 -917, ISSN: 0975-8585.
185. Kamalakkannan V, Puratchikody A, and Ramanathan L, 2013, Development and characterization of controlled release polar lipid microparticles of Candesartan Cilexetil by solid dispersion, 8(2), 125–136, ISSN: 1735-9414.
186. Anonymous (2016) Infrared Reference Spectra – Candesartan Cilexetil. In: *The Japanese Pharmacopoeia*, 17<sup>th</sup> Edition, The Ministry of Health, Labour and Welfare, Japan, pp. 1804.
187. Silverstein RM and Webster FX (2010) Infrared Spectroscopy. In: *Spectrometric identification of an organic compound*, 6<sup>th</sup> Edition, John Wiley and Sons Inc, New Delhi, pp. 71-143.
188. Kamp W. (1991) Infrared Spectroscopy. In: *Organic Spectroscopy*, 3<sup>rd</sup> Edition, Macmillan Press Ltd., London, pp. 19-100.
189. Shah SR, Parikh RH, Chavda JR and Sheth NR, 2013, Application of Plackett–Burman screening design for preparing glibenclamide nanoparticles for dissolution enhancement, *Powder Technology*, 235, 405–411, ISSN: 0032-5910.
190. Rahman Z, Zidan A, Habib MJ and Khan MA, 2010, Understanding the quality of protein loaded PLGA nanoparticles variability by Plackett–Burman design, *International Journal of Pharmaceutics*, 389(1-2), 186–194, ISSN: 0378-5173.

191. Patel DJ and Patel JK, 2010, Optimization of formulation parameters on famotidine nanosuspension using factorial design and the desirability function, *International Journal of PharmTech Research*, 2(1), 155-161, ISSN: 0974-4304.
192. Raval AJ and Patel MM, 2011, Preparation and characterization of nanoparticles for solubility and dissolution rate enhancement of Meloxicam, *International Research Journal of Pharmaceuticals*, 1(2), 42-49, ISSN: 2048-4143.
193. Patel DJ, Patel JK, Pandya VM and Jivani RR, 2010, Effect of Formulation variables on Nanosuspension containing Famotidine prepared by Solvent Evaporation Technique, *International Journal of Pharmaceutical Sciences and Nanotechnology*, 2(4), 707-713, ISSN: 0974-3278.
194. Moschwitz J, Achleitner G, Pomper H and Muller RH, 2004, Development of an intravenously injectable chemically stable aqueous Omeprazole formulation using nanosuspension technology, *European Journal of Pharmaceutics and Biopharmaceutics*, 58(3), 615-9, ISSN: 0939-641.
195. Wagner JG (1993) *Pharmacokinetics for Pharmaceutical Scientist*. Technomic Publishing Co. Inc., Lancaster.
196. Patel K, Patel A, Dave J and Patel C, 2012, Absorbance correction method for estimation of Telmisartan and Metoprolol succinate in combined tablet dosage form, *Pharmaceutical Methods*, 3(2), 106-111, ISSN: 2229-4716.
197. Patel PA and Patravale VB, 2010, Commercial Telmisartan Tablets: A Comparative evaluation with Innovator Brand Micardis, *International Journal of Pharma Sciences and Research*, 1(8), 282-292, ISSN: 0975-9492.
198. Patel B, Parikh RH, and Swarnkar D, 2012, Enhancement of dissolution of Telmisartan through use of solid dispersion technique - surface solid dispersion, *Journal of Pharmacy and Bioallied Sciences*, 4 (Suppl 1), S64-S68, ISSN: 0975-7406.
199. Thakkar HP, Patel BV, and Thakkar SP, 2011, Development and characterization of nanosuspensions of Olmesartan Medoxomil for bioavailability enhancement, *Journal of Pharmacy and Bioallied Sciences*, 3(3), 426-434, ISSN: 0975-7406.
200. H. Ramanathan, 2011, USP Pending Monograph Draft 1 — For Public Comment USP,  
[www.usp.org/sites/default/files/usp\\_pdf/EN/USPNF/./m5431draft\\_ziprasidone.pdf](http://www.usp.org/sites/default/files/usp_pdf/EN/USPNF/./m5431draft_ziprasidone.pdf)
201. Anandkumar Y, Anitha M, Hemanth A and Srinivas S, 2010, Development of rapid UV Spectrophotometric method for the estimation of Ziprasidone

- hydrochloride in bulk and formulations, Digest Journal of Nanomaterials and Biostructures, 5(1), 279 – 283, ISSN: 1842-3582.
202. Latha MM, Sundar VD, Nandhakumar S, and Dhana Raju MD, 2014, Design and evaluation of sustained release tablets containing a solid dispersion of Ziprasidone Hydrochloride, International Journal of PharmTech Research, 6(3), 959-968, ISSN: 0974-4304.
203. Jadhav KS and Erande KB, 2016, Solubility enhancement and formulation of fast dissolving tablet of Ziprasidone Hydrochloride, International Journal of Research in Pharmacy and Chemistry, 6(4), 675-683, ISSN: 2231-2781.

**SUMMARY  
AND  
CONCLUSION**





## CHAPTER – 5

### Summary and Conclusion

Bioavailability enhancement is nowadays a great challenge to the pharmaceutical industries. The drug specifically from BCS class II and IV are always considered to have a dissolution rate limited bioavailability. Various approaches have been used to enhance the rate of dissolution of such types of drugs in order to get better bioavailability. Nanosuspension is one of those approaches which can tremendously enhance the effective surface area of drug particles as well as also shows vapor pressure effect and thereby increases the rate of dissolution and hence bioavailability. Telmisartan and candesartan cilexetil, antihypertensive agents - angiotensin II inhibitors as well as ziprasidone hydrochloride, an atypical antipsychotic drug are BCS class II drugs which are poorly soluble in water. Hence, dissolution is a rate-limiting step for enhancement of bioavailability of selected drugs.

The first part of the research work included the formulation of candesartan cilexetil nanosuspension by antisolvent precipitation followed by ultrasonication technique for improvement of oral bioavailability. PVP K-30 was found to be the most suitable stabilizer of candesartan cilexetil. Compatibility study was carried out using FTIR and DSC studies and showed drug- excipient compatibility. Plackett - Burman Design was effectively employed to identify formulating and processing key parameters that are affecting the quality of the candesartan cilexetil nanosuspension.  $3^2$  factorial design was employed to

optimize and evaluate the main effects, interaction effects and quadratic effects on the formulation of nanosuspension. The optimum formulation prepared by response optimizer by desirability function provided a final formulation with  $D = 1.000$  which released 97.13% of candesartan cilexetil within 2 mins. The *in-vivo* studies confirmed that nanosuspension loaded candesartan cilexetil showed a significantly better AUC as compared to marketed formulation exhibiting improved bioavailability and dose of candesartan cilexetil was reduced about 38.13.0% to reach peak plasma concentration of marketed formulation.

The second part of the research work included the formulation of telmisartan nanosuspension for improvement of oral bioavailability. Poloxamer 407 was found to be the most suitable stabilizer of telmisartan. Preliminary and compatibility study was carried out using FTIR and DSC studies and showed drug- excipient compatibility. Plackett - Burman Design was effectively employed to identify formulating and processing key parameters that are affecting the quality of the telmisartan nanosuspension.  $3^2$  factorial design was employed to optimize and evaluate the main effects, interaction effects and quadratic effects on the formulation of nanosuspension. The optimum formulation prepared by response optimizer by desirability function provided a final formulation with  $D = 0.9629$  which released 102.60% of telmisartan within 2 mins. The *in-vivo* studies confirmed that nanosuspension loaded telmisartan showed a significantly better AUC as compared to marketed formulation exhibiting improved bioavailability and dose of telmisartan was reduced about 18.25% to reach peak plasma concentration of marketed formulation.

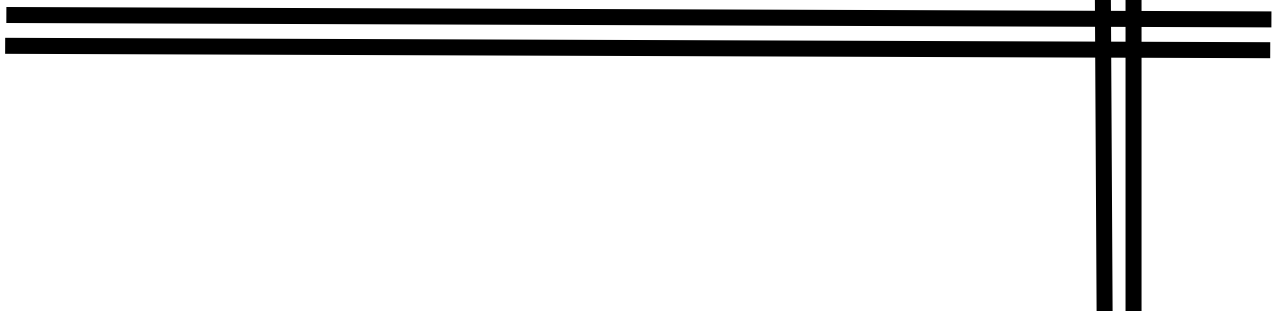
If the case of a salt of a weak acid like candesartan cilexetil ( $pK_a - 4.45$ ) is considered, at any given pH of the bulk of the solution, the pH of the diffusion layer of the salt form of a weak acid will be higher than the observable with the free acid form of telmisartan ( $pK_a - 6$ ). Owing to the increased pH of the diffusion layer, the solubility, and dissolution rate of a weak acid salt form is promoted, which may reflect in bioavailability too. It was supported by the results of bioavailability of both the drugs. Bioavailability improvement in candesartan cilexetil was 38.13% whereas that of telmisartan was found to 18.25%.

The third part of the research work included the formulation of ziprasidone hydrochloride nanosuspension for improvement of oral bioavailability. Poloxamer 407 was found to be the most suitable stabilizer of ziprasidone hydrochloride. Preliminary and compatibility

---

study was carried out using FTIR and DSC studies and showed drug- excipient compatibility. Plackett - Burman Design was effectively employed to identify formulating and processing key parameters that are affecting the quality of the ziprasidone hydrochloride nanosuspension.  $3^2$  factorial design was employed to optimize and evaluate the main effects, interaction effects and quadratic effects on the formulation of nanosuspension. The optimum formulation prepared by response optimizer by desirability function provided a final formulation with  $D = 0.9035$  which released 96.61% of ziprasidone hydrochloride within 15 mins. The *in-vivo* studies confirmed that nanosuspension loaded ziprasidone hydrochloride showed a significantly better AUC as compared to marketed formulation exhibiting improved bioavailability and dose of ziprasidone hydrochloride was reduced about 33.0 % to reach peak serum concentration of marketed formulation.

# **BIBLIOGRAPHY**



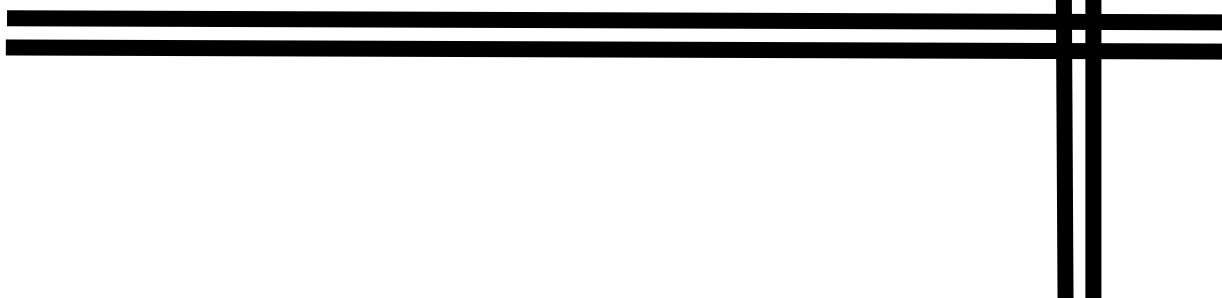
**BIBLIOGRAPHY**

- Chingunpitak J, Puttipipatkachorn S, Chavalitshewinkoon-Petmitr P, Tozuka Y, Moribe K and Yamamoto K, 2008, Formation, Physical stability and in-vitro antimalarial activity of dihydro-artemisinin nanosuspensions obtained by the co-grinding method, *Drug Development, and Industrial Pharmacy*, 34(3), 31422, ISSN: 1520-5762.
- Sutradhar KB, Khatun S and Luna IP, 2013, Increasing Possibilities of Nanosuspension, *Journal of Nanotechnology*, Volume 2013 (2013), 1-12, ISSN: 1687-9511.
- Samar AA, Maha AH, Ali SA and Kadria AE, 2015, Nanosuspension: An Emerging Trend for Bioavailability Enhancement of Etodolac, *International Journal of Polymer Science*, Volume 2015 (2015), 1-16, ISSN: 1687-9430.
- Peters K, Muller RH, and Craig DQM, 1999, An investigation into the distribution of lecithins in nanosuspension systems using low-frequency dielectric spectroscopy, *International Journal of Pharmaceutics*, 184, 53–61, ISSN: 0378-5173.
- Komasa T, Fujimura H, Tagawa T, Sugiyama A and Kitano Y, 2014, Practical method for preparing nanosuspension formulations for toxicology studies in the discovery stage: formulation optimization and *in vitro/in vivo* evaluation of nanosized poorly water-soluble compounds, *Chemical and Pharmaceutical Bulletin*, 62(11), 1073-1082, ISSN: 1347-5223.
- Talat M, Upadhyay P, Omray P, Koteswara KB and Srivastava ON, 2014, Preparation and Characterization of Nanosuspension of Tamoxifen Citrate for Intra-Venous Administration in Drug-Resistant Breast Cancer Cells, *Advanced Science Letters*, 20(7-9), 1483-1489, ISSN: 1936-7317.
- Muthu MS and Singh S, 2009, Poly (D, L-Lactide) Nanosuspensions of Risperidone for Parenteral Delivery: Formulation and *In-Vitro* Evaluation, *Current Drug Delivery*, 6, 62-68, ISSN: 1875-5704.
- Shakeel F, Ramadan W and Shafiq S, 2009, Solubility and Dissolution Improvement of Aceclofenac using Different Nanocarriers, *Journal of Bioequivalence and Bioavailability*, 1(2), 39-43, ISSN:0975-0851.
- Nakarani M, Misra AK, Patel JK and Vaghani SS, 2010, Itraconazole nanosuspension for oral delivery: Formulation, characterization and *in vitro* comparison with the

- marketed formulation, *DARU Journal of Pharmaceutical Sciences*, 18(2), 84-90, ISSN: 2008-2231.
- Pandya VM, Patel JK and Patel DJ, 2011, Formulation and Optimization of Nanosuspensions for Enhancing Simvastatin Dissolution Using Central Composite Design, *Dissolution Technologies*, 18(3), 40-45, ISSN: 1521-298X.
  - Kumar A, Sahoo SK, Padhee K, Singh Kochar PP, Satapathy A and Pathak N, 2011, Review on solubility enhancement techniques for hydrophobic drugs, *Pharmacie Globale International Journal of Comprehensive Pharmacy*, 3(3), 1-7, ISSN 0976-8157.
  - Lee J, Lee SJ, Choi JY, Yoo JY, Ahn CH, 2005, Amphiphilic amino acid copolymers as stabilizers for the preparation of nanocrystal dispersion, *European Journal of Pharmaceutical Sciences*, 24 (5) 441–449, ISSN: 0928-0987.
  - Eerdenbrugh BV, Froyen L, Humbeeck JV, Martens JA, Augustijns P, Mooter GV, 2008, Drying of crystalline drug nanosuspensions—The importance of surface hydrophobicity on dissolution behavior upon redispersion, *European Journal of Pharmaceutical Sciences*, 35(2), 127–135, ISSN: 0928-0987.
  - Savjani KT, Gajjar AK, and Savjani JK, 2012, Drug Solubility: Importance and Enhancement Techniques, *International Scholarly Research Network Pharmaceutics*, Volume 2012, 1-10, ISSN: 2356-7872.
  - Chaudhary A, Nagaich U, Gulati N, Sharma VK and Khosa RL, 2012, Enhancement of solubilization and bioavailability of poorly soluble drugs by physical and chemical modifications: A recent review, *Journal of Advanced Pharmacy Education and Research*, 2(1), 32-67, ISSN 2249-3379.
  - Liu P (2013) Nanocrystal formulation of poorly soluble drugs. Ph.D. Thesis. Division of Pharmaceutical Technology, Faculty of Pharmacy, University of Helsinki, Finland.
  - Modesto-Lopez LB and Biswas P, 2010, Role of the effective electrical conductivity of nanosuspensions in the generation of TiO<sub>2</sub> agglomerates with electrospray, *Journal of Aerosol Science*, 41(8), 790–804, ISSN: 0021-8502.
  - Verma S, Lan Y, Gokhale R, Burgess DJ, 2009, Quality by design approach to understand the process of nanosuspension preparation, *International Journal of Pharmaceutics*, 377(1-2), 185–198, ISSN: 0378-5173.

- Ali HSM, York P, and Blagden N, 2009, Preparation of hydrocortisone nanosuspension through a bottom-up nanoprecipitation technique using microfluidic reactors, *International Journal of Pharmaceutics*, 375(1-2), 107–113, ISSN: 0378-5173.
- Gao L, Liu G, Wang X, Liu F, Xu Y and Ma J, 2011, Preparation of a chemically stable quercetin formulation using nanosuspension technology, *International Journal of Pharmaceutics*, 404(1-2), 231–237, ISSN: 0378-5173.
- Bajaj S, Singla D and Sakhuja N, 2012, Stability Testing of Pharmaceutical Products, *Journal of Applied Pharmaceutical Science*, 2(3), 129-138, ISSN: 2231-3354.

# **APPENDICES**





## Appendix A - IAEC Approval letter



Re-Accredited  
Grade B by N A A C  
(CGPA 2.93)

**SAURASHTRA UNIVERSITY**  
Department of Pharmaceutical Sciences  
Rajkot - 360 005

Phone : Office : +91-281-2578501-10 Ext.-492/ 493  
Fax : + 91-281-2585083  
E-mail : headpharmacy@gmail.com, info@sudps.org  
Website : www.saurashtrauniversity.edu, www.sudps.org

Ref. No. SU/ DPS/147 / 2015

Date : 4 \ 6 \ 15

CERTIFICATE

This is certify that the project proposal number IAEC/DPS/SU/1508 with title “Design, development and evaluation of nanosuspensions for enhancement of oral bioavailability of poorly soluble drugs” has been approved by the IAEC at the meeting held on 6<sup>th</sup> May, 2015.

Name of Chairman IAEC:  
(Dr. Mihir Raval)

Name of CPCSEA Link nominee:  
(Dr. V. P. Vadodaria)

Signature with date

Chairman of IAEC:

CPCSEA Link nominee:

## Appendix B - GUJCOST Minor Research Project Sanction Letter

### GUJARAT COUNCIL ON SCIENCE AND TECHNOLOGY



सत्यमेव जयते

Department of Science & Technology, Government of Gujarat

Block: B, 7th Floor, M.S. Building, Nr.Pathikashram, Sector-11  
Gandhinagar, Gujarat-382011.  
Phone: (079) 23259362-65 Fax: (079) 23259363  
E-mail: sciof-gujcost@gujarat.gov.in  
URL: www.gujcost.gujarat.gov.in



**Dr. Narottam Sahoo**

Advisor & Member Secretary

No: GUJCOST/ MRP/ 2014-15/

30th March, 2015

**Ms. Jalpa S. Paun**

Department of Pharmaceutics  
B.K.ModyGovt.Pharmacy College,  
Polytechnic Campus,  
Near AjiDam,Rajkot

Sub: Award of GUJCOST Minor Research Project Grant for the proposal on "Development and evaluation of Ziprasidone Hydrochloride loaded Nanosuspension for bioavailability enhancement" By Ms. Jalpa S. Paun

Dear Madam,

Warm Greetings from Gujarat Council on Science and Technology (GUJCOST), Gandhinagar.

With reference to your project proposal on Development and evaluation of Ziprasidone Hydrochloride loaded Nanosuspension for bioavailability enhancement and subsequent presentation before the Expert Committee, GUJCOST is pleased to inform you that your proposal has been sanctioned for an amount of Rs. 4,75,000/- for two years' time period.

As per the GUJCOST guidelines and for the disbursement of the grant, a Memorandum of Understanding (M.O.U) has to be signed between the Principal/ Head of the Institute, Principal Investigator of the project and GUJCOST on Rs. 100/- stamp paper with Notary registration. A draft MOU has been enclosed herewith for your reference.

We request you to please send us the signed copy of the MOU at the earliest so that necessary financial assistance may be released.

Tanking you and with best regards.

Yours sincerely,

(Narottam Sahoo)

Encl.: As above

**Appendix C - List of Publications**

- **Paun JS and Tank HM**, 2012, Nanosuspension: An Emerging Trend for Bioavailability Enhancement of Poorly Soluble Drugs, Asian Journal of Pharmacy and Technology, 2(4), 158-169, ISSN: 2231-5705.
- **Paun JS and Tank HM**, 2016, Screening of Formulating and Processing Parameters on Candesartan Cilexetil Nanosuspension Prepared by Nanoprecipitation-Ultrasonication Technique, International Journal of Pharmaceutical Research, 8(4), 8-13, ISSN 0975-2366.
- **Paun JS and Tank HM**, 2016, Screening of formulating and processing parameters for Ziprasidone Hydrochloride nanosuspension prepared by nanoprecipitation-ultrasonication technique, Journal of Pharmaceutical Science and Bioscientific Research, 6(6), 766-772, ISSN 2277-3681.

ISSN- 2231-5705 (Print)  
ISSN- 2231-5713 (Online)

www.asianpharmaonline.org



### REVIEW ARTICLE

## **Nanosuspension: An Emerging Trend for Bioavailability Enhancement of Poorly Soluble Drugs**

**Paun J.S.<sup>1\*</sup> and Tank H.M.<sup>2</sup>**

<sup>1</sup>Department of Pharmaceutics, S.J. Thakkar Pharmacy College, Rajkot

<sup>2</sup>Department of Pharmaceutics, Matushree V.B. Manvar College of Pharmacy, Dumiyani

\*Corresponding Author E-mail: [jalpa\\_paun@rediffmail.com](mailto:jalpa_paun@rediffmail.com)

### **ABSTRACT:**

Drug effectiveness is influenced by a crucial factor like solubility of drug, independence of the route of administration. Most of the newly discovered drugs coming out from High-throughput screening are failing due to their poor water solubility which is major problem for dosage form design. Now a day, nanoscale systems for drug delivery have gained much interest as a way to improve the solubility problems. Nanosuspension technology is a unique and economical approach to overcome poor bioavailability that is related with the delivery of hydrophobic drugs, including those that are poorly soluble in aqueous media. Design and development of nanosuspension of such drugs is an attractive alternative to solve this problem. Preparation of nanosuspension is simple and applicable to all poorly soluble drugs. A nanosuspension not only solves the problem of solubility and bioavailability but also alters pharmacokinetic profile of the drug which may also improve safety and efficacy. This review article takes account of introduction, advantages, properties, formulation consideration, preparation, characterization and application of the nanosuspensions.

**KEYWORDS:** Nanosuspensions, Poorly soluble drugs, Drug Delivery, Bioavailability, Solubility enhancement.

### **INTRODUCTION:**

Bioavailability is defined as the rate and extent to which the active ingredient is absorbed from a drug product and becomes available at the site of action.<sup>1</sup> From a pharmacokinetic perspective, bioavailability data for a given formulation provide an estimate of the relative fraction of the orally administered dose that is absorbed into the systemic circulation when compared to the bioavailability data for a solution, suspension or intravenous dosage form. In addition, bioavailability studies provide other useful pharmacokinetic information related to distribution, elimination, effects of nutrients on absorption of the drug, dose proportionality and linearity in pharmacokinetics of the active and inactive moieties. Bioavailability data can also provide information indirectly about the properties of a drug substance before entry into the systemic circulation, such as permeability and the influence of pre-systemic enzymes and/or transporters.

Bioavailability of a drug is largely determined by the properties of the dosage form, rather than by the drug's physicochemical properties, which determine absorption potential. Differences in bioavailability among formulations of a given drug can have clinical significance; thus, knowing whether drug formulations are equivalent is essential.

Poorly water soluble drugs are increasingly becoming a problem in terms of obtaining satisfactory dissolution within the gastrointestinal tract that is necessary for good oral bioavailability. It is not only existing drugs that cause problems but it is the challenge to ensure that new drugs are not only active pharmacologically but have enough solubility to ensure fast enough dissolution at the site of administration, often the gastrointestinal tract.<sup>2</sup>

### **FACTORS AFFECTING BIOAVAILABILITY:**

Low bioavailability is most common with oral dosage forms of poorly water-soluble, slowly absorbed drugs. Solid drugs need to dissolve before they are exposed to be absorbed. If the drug does not dissolve readily or cannot penetrate the epithelial membrane (eg, if it is highly ionized

Received on 28.10.2012      Accepted on 12.11.2012  
© Asian Pharma Press All Right Reserved  
Asian J. Pharm. Tech. 2(4): Oct. - Dec. 2012; Page 158-169

## Screening of Formulating and Processing Parameters of Candesartan Cilexetil Nanosuspension Prepared by Nanoprecipitation-Ultrasonication Technique.

JALPA S. PAUN<sup>\*\*1</sup>, HEMRAJ M. TANK<sup>2</sup>

<sup>1</sup>B. K. Mody Govt. Pharmacy College, Rajkot-360003, Gujarat, India.,<sup>2</sup>Matushree V. B. Manvar College of Pharmacy, Dumiyani-360440, Gujarat, India.

### ABSTRACT

Low oral bioavailability of poorly water-soluble drugs poses a great challenge during drug development. Poor water solubility and low dissolution rate are issues for the majority of upcoming and existing biologically active compounds. Candesartan Cilexetil is BCS class-II drug having low solubility and high permeability. The aim of the present investigation was to identify critical formulating and processing parameters which influences on quality of the nanosuspension. Nanosuspension formulation of a poorly soluble drug was developed using nanoprecipitation-ultrasonication technique. Key factors affecting formulation of nanosuspension were identified by Plackett and Burman Design of experiments to optimize nanosuspension and evaluation was done by measurement of saturation solubility, mean particle size, poly dispersity index and zeta potential. The obtained results showed that nanosuspension prepared with the PVPK-30 has improved saturation solubility as compare to all other stabilizers. Result also revealed that solvent: anti-solvent ratio as well as amount of drug were found to be promising formulating parameters having prominent effect on quality of Candesartan Cilexetil nanosuspension.

**KEYWORDS:** Candesartan Cilexetil, Nanosuspension, Nanoprecipitation-ultrasonication, Plackett and Burman design.

### INTRODUCTION

In pharmaceutical field, formulation of poorly water-soluble drug has always been a challenging problem and it is a major issue for the development of new dosage form. Around 10% of the present drugs, 40% of the research drugs and 60% of drugs coming directly from synthesis have low solubility about 1–10 µg/ml.[1-3] If drug solubility cannot be improved, the drug cannot be absorbed through GI tract upon oral administration and cannot exert its pharmacological action on the target tissue.[4] It is due to the phospholipidic nature of cell membranes, thus certain degree of lipophilicity is required for those drug compounds, while in terms of permeability high lipophilicity is beneficial. In most cases it translates into poor aqueous solubility.[5] This creates delivery problems such as low oral bioavailability and erratic absorption. Drug solubility can be enhanced using traditional approaches such as co-solvents, salt formation, complexation, or delivery through carriers like liposome, solid-dispersions or micronization.[6] However, in many cases they cannot solve the bioavailability problem. For example, micronization of poorly soluble drugs has been applied for many years to improve dissolution velocity of poorly soluble

drugs, but reducing the drug to micron size does not increase the saturation solubility of the drug, and at such a low saturation solubility, as generally observed in the BCS class II drugs, the increment in the dissolution characteristics does not help to a great extent, nanonization has been employed for treating the BCS class II drugs. When the drug being reduced to nanosized level, there is an increase in the saturation solubility assisted by improvement in dissolution characteristics, which could be attributed to the effective increase in the particle surface area, according to Ostwald-Freundlich equation and Noyes-Whitney equation. Ostwald-Freundlich equation expresses how particle size influences on saturation solubility ( $C_s$ ), a compound-specific constant relying only on temperature in a given solvent. Accordingly,  $C_s$  of the drug increases substantially with a decrease of particle size.[2,7] Nanosuspensions have emerged as a promising strategy for an efficient delivery of hydrophobic drugs because of their versatile features such as very small particle size.[8] Candesartan cilexetil is an ester prodrug that is hydrolyzed during absorption from the gastrointestinal tract to the active form

\* Address For Correspondence:

Jalpa S. Paun, B.K. Mody Govt. Pharmacy College, Bhavnagar Road, Rajkot-360003

(M) 9428232292, Email :[jalpa\\_paun@rediffmail.com](mailto:jalpa_paun@rediffmail.com)

R = 18.06.16, R = 30.06.16, A = 20.07.16

8 | *International Journal of Pharmaceutical Research* | Oct – Dec 2016 | Vol 8 | Issue 4



## JOURNAL OF PHARMACEUTICAL SCIENCE AND BIOSCIENTIFIC RESEARCH (JPSBR)

(An International Peer Reviewed Pharmaceutical Journal that Encourages Innovation and Creativities)

### Screening of Formulating and Processing Parameters for Ziprasidone Hydrochloride Nanosuspension Prepared by Nanoprecipitation-Ultrasonication Technique

J. S. Paun<sup>\*1</sup>, H. M. Tank<sup>2</sup>

<sup>1</sup>B. K. Mody Govt. Pharmacy College, Rajkot-360003, Gujarat, India.

<sup>2</sup>Matushree V. B. Manvar College of Pharmacy, Dumiyani-360440, Gujarat, India.

#### Article history:

Received 07 Aug 2016

Accepted 30 Aug 2016

Available online 01 Nov 2016

#### Citation:

Paun J. S., Tank H. M. Screening of Formulating and Processing Parameters for Ziprasidone Hydrochloride Nanosuspension Prepared by Nanoprecipitation-Ultrasonication Technique *J Pharm Sci Bioscientific Res.* 2016. 6(6): 766-772

#### \*For Correspondence:

Jalpa S. Paun

B. K. Mody Govt. Pharmacy College,  
Rajkot-360003, Gujarat, India.

([www.jpsbr.org](http://www.jpsbr.org))

#### ABSTRACT:

Low oral bioavailability of poorly water-soluble dosage form poses a great challenge during formulation development. Poor water solubility and low dissolution rate are issues for the majority of upcoming and existing biologically active compounds. Ziprasidone Hydrochloride (ZH) is BCS class-II drug having low solubility and high permeability. The aim of the present investigation was to identify critical formulating and processing parameters which influences on quality of the nanosuspension. Nanosuspension formulation of a poorly soluble drug was developed using nanoprecipitation-ultrasonication technique. A total of 8 experiments were generated for screening 5 independent factors namely the amount of Ziprasidone Hydrochloride (mg) ( $X_1$ ), amount of stabilizer (mg) ( $X_2$ ), solvent to anti-solvent volume ratio ( $X_3$ ), stirring speed (rpm) ( $X_4$ ) and sonication time (min) ( $X_5$ ). Mean particle size (nm) ( $Y_1$ ) and Saturation solubility ( $\mu\text{g/ml}$ ) ( $Y_2$ ) were selected as dependent factors. The obtained results showed that nanosuspension prepared with the Poloxamer 407 has improved saturation solubility as compare to all other stabilizers. Result also revealed that concentration of drug and stirring speed were found to be promising formulating and processing parameters having prominent effect on quality of Ziprasidone Hydrochloride nanosuspension.

**KEY WORDS:** Ziprasidone Hydrochloride, Nanosuspension, Nanoprecipitation-ultrasonication, Plackett and Burman design.

#### INTRODUCTION:

In pharmaceutical field, formulation of poorly water-soluble drug has always been a challenging problem and it is a major issue for the development of new dosage form. Around 10% of the present drugs, 40% of the research drugs and 60% of drugs coming directly from synthesis have low solubility about 1–10  $\mu\text{g/ml}$ .<sup>[1-3]</sup> If drug solubility cannot be improved, the drug cannot be absorbed through GI tract upon oral administration and cannot exert its pharmacological action on the target tissue.<sup>[4]</sup> It

is due to the phospholipidic nature of cell membranes, thus certain degree of lipophilicity is required for those drug compounds, while in terms of permeability high lipophilicity is beneficial. In most of the cases it translates into poor aqueous solubility.<sup>[5]</sup> This creates delivery problems such as low oral bioavailability and erratic absorption. Drug solubility can be enhanced using traditional approaches such as co-solvents, salt formation, complexation, micronization or delivery through carriers like liposome, solid-dispersions.<sup>[6]</sup> However, in many cases they cannot solve the bioavailability problem. For

**Appendix D - Poster Presentation of Research Work in National Level Seminar**

**Jalpa S. Paun, Hemraj M. Tank**, Application of Plackett-Burman screening design for optimizing formulating and processing parameters of Ziprasidone Hydrochloride Nanosuspension, poster presented in SERB sponsored Two Days National Seminar on Bioavailability Enhancement: An Industry Desire and Regulatory Constraints at Department of Pharmaceutical Sciences, Saurashtra University, Rajkot, 30th – 31<sup>st</sup> July 2016.



Accredited grade "A" by  
NAAC

SERB Sponsored Two Days National Seminar On  
"Bioavailability Enhancement: An Industry Desire and Regulatory Constrains"



Department of Science & Technology  
Govt. of India

**PP-22**

**APPLICATION OF PLACKETT–BURMAN SCREENING DESIGN FOR OPTIMIZING  
FORMULATING AND PROCESSING PARAMETERS OF ZIPRASIDONE  
HYDROCHLORIDE NANOSUSPENSION**

**Jalpa S. Paun<sup>\*1</sup>, Hemraj M. Tank<sup>2</sup>**

<sup>1</sup>B. K. Mody Govt. Pharmacy College, Rajkot-360003, Gujarat, India.


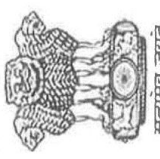



<sup>2</sup>Matushree V. B. Manvar College of Pharmacy, Dumiyani-360440, Gujarat, India.

Email address: jalpa\_paun@rediffmail.com

**ABSTRACT**

Low oral bioavailability of poorly water-soluble drugs poses a great challenge during drug development. Poor water solubility and low dissolution rate are issues for the majority of upcoming and existing biologically active compounds. Ziprasidone Hydrochloride (ZH) is BCS class-II drug having low solubility and high permeability. The aim of the present investigation was to identify critical formulating and processing parameters which influences on quality of the nanosuspension. Nanosuspension formulation of a poorly soluble drug was developed using nanoprecipitation-ultrasonication technique. A total of 8 experiments were generated for screening 5 independent factors namely the amount of Ziprasidone Hydrochloride (mg) ( $X_1$ ), amount of stabilizer (mg) ( $X_2$ ), solvent to anti-solvent volume ratio( $X_3$ ), stirring speed (rpm) ( $X_4$ ) and sonication time (min) ( $X_5$ ). Mean particle size (nm) ( $Y_1$ ), saturation solubility ( $\mu\text{g/ml}$ ) ( $Y_2$ ) and CPR at 15 min (%) ( $Y_3$ ) were selected as dependent factors. The obtained results showed that nanosuspension prepared with the Poloxamer 407 has improved saturation solubility as compare to all other stabilizers. Result also revealed that concentration of drug and stirring speed were found to be promising formulating and processing parameters having prominent effect on quality of Ziprasidone Hydrochloride nanosuspension.



 <p>SAURASHTRA UNIVERSITY Accredited Grade "A" by NAAC</p>	 <p>Science and Engineering Research Board (SERB), DST, Govt. of India</p>
<h1>CERTIFICATE</h1>	
<p><i>This is to certify that</i></p>	
<p><b>Dr./Mr./Mrs./Ms./</b> <u>JALPA S. PAUN</u></p>	
<p><i>Has Participated as Delegate / Presenter of a paper in Poster Session at</i> <b>SERB Sponsored Two Days National Seminar</b></p>	
<p>On</p>	
<p><b>"Bioavailability Enhancement : An Industry Desire and Regulatory Constrains"</b></p>	
<p>Organized by</p>	
<p><b>Department of Pharmaceutical Sciences, Saurashtra University, Rajkot</b> <b>During 30<sup>th</sup> - 31<sup>st</sup> July-2016</b></p>	
 <p>Dr. Mihir K. Raval Convener</p>	
 <p>Ms. Priya V. Patel Coordinator</p>	